




**TURUN
YLIOPISTO
UNIVERSITY
OF TURKU**



**THE ROLE OF MELANOCORTIN 1
RECEPTOR IN THE REGULATION
OF CHOLESTEROL AND
FATTY ACID METABOLISM
IN THE LIVER**

Keshav Thapa



**TURUN
YLIOPISTO**
UNIVERSITY
OF TURKU

THE ROLE OF MELANOCORTIN 1 RECEPTOR IN THE REGULATION OF CHOLESTEROL AND FATTY ACID METABOLISM IN THE LIVER

Keshav Thapa

University of Turku

Faculty of Medicine
Institute of Biomedicine
Pharmacology, Drug Development and Therapeutics
Drug Research Doctoral Programme

Supervised by

Docent Petteri Rinne, PhD
Institute of Biomedicine
University of Turku
Turku, Finland

Professor Eriika Savontaus, MD, PhD
Institute of Biomedicine
University of Turku
Turku, Finland

Reviewed by

Docent Kaija Autio, PhD
Faculty of Biochemistry and
Molecular Medicine
University of Oulu
Oulu, Finland

Docent Panu Luukkonen, MD, PhD
Department of Internal Medicine
University of Helsinki
Helsinki, Finland

Opponent

Professor Jukka Hakkola, MD, PhD
Research Unit of Biomedicine and
Internal Medicine
Faculty of Medicine
University of Oulu
Oulu, Finland

The originality of this publication has been checked in accordance with the University of Turku quality assurance system using the Turnitin OriginalityCheck service.

Cover Image: Sebastian Kaulitzki

ISBN 978-951-29-9963-7 (PRINT)
ISBN 978-951-29-9964-4 (PDF)
ISSN 0355-9483 (Print)
ISSN 2343-3213 (Online)
Painosalama, Turku, Finland 2024

*“In the midst of winter, I found there was, within me, an invincible summer”
-Albert Camus*

UNIVERSITY OF TURKU

Faculty of Medicine

Institute of Biomedicine

Pharmacology, Drug Development and Therapeutics

KESHAV THAPA: The role of melanocortin 1 receptor in the regulation of cholesterol and fatty acid metabolism in the liver

Doctoral Dissertation, 193 pp.

Drug Research Doctoral Programme

November 2024

ABSTRACT

The melanocortins are a family of neuropeptide hormones consisting of melanocyte-stimulating hormones, α -, β -, and γ -MSH, and adrenocorticotrophic hormone (ACTH) as well as five different melanocortin receptors (MC1R - MC5R). These peptides are widely expressed in the body and are involved in a diverse number of physiological functions including pigmentation, steroidogenesis, exocrine function, energy homeostasis, inflammation, and immunomodulation. MC1R is abundantly expressed in the melanocytes, and leukocytes where it regulates skin pigmentation and inflammatory responses respectively. MC1R is also expressed in the liver and white adipose tissue but its functional role in these metabolic tissues remain elusive. Therefore, the main aim of this thesis was to elucidate the regulatory role of MC1R signaling in cholesterol, bile acid, and fatty acid metabolism, particularly in the liver.

To address this objective, hepatocyte-specific MC1R knockout (Mc1r LKO), and global MC1R deficient (Mc1r^{e/c}) mice were fed either a chow or a Western-type diet, and characterized for body weight and composition, lipid metabolism, and liver morphology. First, MC1R was found to be expressed in hepatocytes as well as in other cell types in the mouse liver, and downregulated in mice fed a Western-type diet, and in patients with metabolic dysfunction-associated steatotic liver disease (MASLD). Mc1r LKO mice on a chow diet showed increased liver weight, elevated levels of cholesterol in the plasma and liver, and perturbed bile acid metabolism. Secondly, pharmacological activation of MC1R reduced the cellular cholesterol content, and increased the uptake of LDL and HDL particles in cultured hepatocytes. Lastly, in terms of adiposity and fatty acid metabolism, Mc1r^{e/c} mice on a Western diet showed increased white adipose tissue mass, adipocyte hypertrophy and plasma triglycerides (TG) concentration. This phenotype was recapitulated in Mc1r LKO mice, indicating a dependency of the phenotype on dysfunctional MC1R in the liver. Mc1r LKO mice also showed upregulation of markers of de novo lipogenesis (DNL), apoptosis, and inflammation as well as increased liver TG accumulation and fibrosis.

In conclusion, the results from this thesis identify a novel function of hepatic MC1R signaling in the regulation of cholesterol and fatty acid metabolism in the liver, suggesting that MC1R could be a promising therapeutic target for the management of metabolic diseases such as, MASLD.

KEYWORDS: Melanocortin 1 receptor, liver, cholesterol, triglycerides, fibrosis, adipocyte, animal model

TURUN YLIOPISTO

Lääketieteellinen tiedekunta

Biolääketieteen laitos

Farmakologia, lääkekehitys ja lääkehoito

KESHAV THAPA : Melanokortiini 1 reseptorin merkitys maksan

kolesteroli- ja rasvahappoaineenvaihdunnan säätelyssä

Väitöskirja, 193 s.

Lääkekehityksen tohtoriohjelma

Marraskuu 2024

TIIVISTELMÄ

Melanokortiinit ovat neuropeptidejä, joihin lukeutuvat α -, β -, ja γ -melanosyyttejä stimuloiva hormoni (MSH) sekä adrenokortikotropiini (ACTH). Ne säätelevät elimistön fysiologisia toimintoja aktivoimalla melanokortiinireseptoreja, joita on tunnistettu 5 eri alatyyppeä (MC1R - MC5R). MC1R alatyyppeä ilmennetään erityisesti melanosyyteissä sekä veren valkosoluissa, joissa se säätelee ihon pigmentaatiota ja tulehdusvasteita. Kyseistä reseptorialatyyppeä on löydetty myös maksasta ja rasvakudoksesta, mutta sen fysiologinen merkitys näissä kudoksissa on jäänyt epäselväksi. Tämän väitöskirjatyön tavoitteena oli selvittää MC1R:n roolia erityisesti maksan kolesteroli- ja rasvahappoaineenvaihdunnassa.

Ensimmäinen osatyö osoitti, että maksassa MC1R alatyyppeä ilmenee maksasoluissa mutta myös muissa maksan solutyypeissä, ja että sen määrä laskee korkearasvaisen ruokavalion myötä hiirillä sekä rasvamaksataudissa ihmisillä. Maksasoluihin kohdennettu MC1R:n geneettinen puutos (Mc1r LKO) lisäsi maksan painoa, kohotti verenkierron ja maksan kolesterolitasaaja sekä häiritsi sappiaineenvaihduntaa tavallista rehua syöville nuorilla hiirillä. MC1R:n farmakologinen aktivaatio puolestaan pienensi solunsisäistä kolesterolimäärää sekä tehosti lipoproteiinipartikkelien soluunottoa viljellyissä maksasoluissa. Toisessa osatyössä tutkittiin MC1R:n merkitystä rasva-aineenvaihdunnassa hyödyntämällä Mc1r^{e/e}-hiirimallia, jossa MC1R:n puutos ilmenee koko kehossa. Tavallista tai korkearasvaista rehua syöneet Mc1r^{e/e} hiiret olivat normaalipainoisia mutta alttiimpia kehon rasvamassan lisääntymiselle ja rasvasolujen koon kasvulle. Tämä ilmiö havaittiin myös korkearasvaista rehua saaneilla Mc1r LKO hiirillä, mikä osoittaa vaikutusten johtuvan häiriöstä maksasolujen MC1R signaloinnissa. MC1R:n puutos maksasoluissa johti myös triglyseridipitoisuuksien kohoamiseen, maksan rasvoittumiseen ja sidekudoksen määrän lisääntymiseen sekä muutoksiin maksan rasvahapposynteesiä säätelevien geenien ilmenemisessä.

Väitöskirjatyön löydökset osoittavat MC1R:n säätelevän maksan kolesteroli- ja rasvahappoaineenvaihduntaa, ja sen puutoksen altistavan rasvamassan lisääntymiselle ja maksan rasvoittumiselle. MC1R on siten mahdollinen lääkekehityskohde metabolisten häiriöiden kuten rasvamaksataudin hoidossa.

AVAINSANAT: Melanokortiini 1 reseptori, maksa, kolesteroli, triglyseridi, fibroosi, rasvasolu, hiirimalli

Table of Contents

Abbreviations	9
List of Original Publications.....	10
1 Introduction	11
2 Review of the Literature	13
2.1 Pro-opiomelanocortin and melanocortins	13
2.2 Melanocortin receptors.....	16
2.2.1 Melanocortin 1 receptor.....	17
2.2.2 Melanocortin 2 receptor.....	20
2.2.3 Melanocortin 3 receptor.....	21
2.2.4 Melanocortin 4 receptor.....	21
2.2.5 Melanocortin 5 receptor.....	22
2.3 Synthetic ligands for melanocortin receptors	22
2.4 Physiological functions and therapeutic potential of melanocortin 1 receptor.....	24
2.5 Melanocortin 1 receptor signaling pathways.....	27
2.6 The liver	29
2.6.1 Liver anatomy	29
2.6.2 The microscopic architecture and functions of the liver	29
2.6.3 Liver energy metabolism	32
2.6.3.1 Hepatic lipid metabolism.....	33
2.6.3.1.1 Fatty acid metabolism in the liver	33
2.6.3.1.2 Fatty acid uptake and transport in the liver.....	35
2.6.3.1.3 De novo lipogenesis	37
2.6.3.1.4 Fatty acid oxidation	40
2.6.3.1.5 Lipoprotein metabolism and secretion	41
2.6.3.1.6 Triglyceride metabolism	43
2.6.3.1.7 Cholesterol metabolism.....	45
2.6.3.2 Bile acid metabolism.....	48
2.6.3.3 Carbohydrate metabolism.....	50
2.6.3.3.1 Glucose uptake in the liver	50
2.6.3.3.2 Glycogen synthesis in the liver	53
2.6.3.3.3 Glycogenolysis in the liver	53
2.6.3.3.4 Gluconeogenesis in the liver	54

2.7	Liver diseases	56
2.7.1	Metabolic dysfunction-associated steatotic liver disease.....	56
2.7.1.1	Metabolic dysfunction-associated steatohepatitis.....	59
2.7.1.2	Cirrhosis and hepatocellular carcinoma	60
2.8	Adipose tissue.....	61
2.8.1	The lipid droplets.....	62
2.8.2	Adipose tissue lipolysis.....	63
2.8.3	Liver-adipose tissue crosstalk.....	64
3	Aims	66
4	Materials and Methods.....	67
4.1	Animals and animal models.....	67
4.2	Ethical considerations	68
4.3	In vivo experiments	68
4.3.1	Body weight and body composition measurement.....	68
4.3.2	Food intake	68
4.3.3	Glucose and insulin tolerance tests	69
4.3.4	Feces collection for bile acid analysis.....	69
4.3.5	Tissue collection.....	69
4.4	Ex vivo and in vitro assays	70
4.4.1	Blood parameters	70
4.4.2	Hepatic lipid analysis	70
4.4.3	Measurement of bile acids.....	70
4.4.4	Histology, immunohistochemistry, and immunofluorescence staining	71
4.4.5	Cell culture and treatment	71
4.4.5.1	Primary mouse hepatocyte isolation and treatment	72
4.4.5.2	Cyclic AMP determination	73
4.4.5.3	Fluorescently labelled LDL and HDL uptake assay.....	73
4.4.5.4	Filipin staining for cellular free cholesterol.....	73
4.4.5.5	Enzyme-linked immunosorbent assay.....	74
4.4.5.6	Flow cytometry analysis of cell surface LDLR expression	74
4.4.5.7	Gene expression analysis	75
4.4.5.8	Protein extraction and Western blot analysis.....	75
4.5	Transcriptome analysis	76
4.6	Statistical analysis	77
5	Results	78
5.1	The effects of MC1R on cholesterol and bile acid metabolism.....	78
5.1.1	MC1R expression in the liver.....	78
5.1.2	Characterization of hepatocyte-specific MC1R knock-out mouse model	80

5.1.3	The effects of hepatocyte-specific MC1R deficiency on cholesterol, triglycerides, fibrosis, and bile acids	81
5.1.4	The effects of MC1R activation on cholesterol and lipid handling in HepG2 cells	85
5.1.5	The effects of pharmacological activation of MC1R on intracellular signaling pathways in HepG2 cells	87
5.2	The effects of hepatocyte-specific MC1R deficiency on fatty acid metabolism	88
5.2.1	Adipose tissue and liver phenotype in global MC1R deficient mice	88
5.2.2	Liver and adipose tissue phenotype in Western diet-fed hepatocyte-specific MC1R deficient mice	91
5.2.3	Hepatic transcriptome analysis of hepatocyte-specific MC1R deficient mice	93
5.2.4	The effects of pharmacological activation of MC1R in HepG2 cells and primary mouse hepatocytes.....	97
6	Discussion.....	100
6.1	Implication of MC1R signaling in the regulation of cholesterol and bile acid metabolism.....	100
6.2	Liver and adipose tissue phenotype of global and hepatocyte-specific MC1R deficient mouse models	105
6.3	Study limitations.....	110
6.4	Therapeutic perspectives	111
7	Summary/Conclusions	113
	Acknowledgements.....	115
	References	118
	Appendices	142
	Original Publications.....	149

Abbreviations

ACTH	Adrenocorticotrophic hormone
AMPK	AMP-activated protein kinase
ATGL	Adipose triglyceride lipase
ChREBP	Carbohydrate response element-binding protein
CVD	Cardiovascular disease
DEGs	Differentially expressed genes
DHCR7	7-dehydrocholesterol reductase
DNL	De novo lipogenesis
ER	Endoplasmic reticulum
FA	Fatty acid
FAO	Fatty acid oxidation
FASN	Fatty acid synthase
FFA	Free fatty acid
GPCR	G protein-coupled receptors
HDL	High density lipoprotein
HMGCR	3-hydroxy-3-methylglutaryl-CoA reductase
HSL	hormone sensitive lipase
JNK	c-Jun amino-terminal kinase
MASLD	Metabolic dysfunction-associated steatotic liver disease
MASH	Metabolic dysfunction-associated steatohepatitis
MGL	Monoglyceride lipase
POMC	Pro-opiomelanocortin
PPARA	Peroxisome proliferation-activated receptor alpha
SCD1	Stearoyl-CoA desaturase 1
SR-BI	Scavenger receptor BI
SREBP1c	Sterol regulatory element binding protein 1c
SREBP2	Sterol regulatory element binding protein 2
TG	Triglycerides
VLDL	Very-low-density lipoprotein
WAT	White adipose tissue

List of Original Publications

This dissertation is based on the following original publications, which are referred to in the text by their Roman numerals:

- I Thapa K, Kadiri JJ, Saukkonen K, Pennanen I, Ghimire B, Cai M, Savontaus E, Rinne P. Melanocortin 1 receptor regulates cholesterol and bile acid metabolism in the liver. *elife*, 2023; 12: e84782.
- II Thapa K, Ghimire B, Pokharel P, Cai M, Savontaus E, Rinne P. Hepatocyte-specific loss of melanocortin 1 receptor disturbs fatty acid metabolism and promotes adipocyte hypertrophy. *International Journal of Obesity*, 2024; 48, 1625-1637.

The original publications have been reproduced with the permission of the copyright holders.

1 Introduction

Metabolic dysfunction-associated steatotic liver disease (MASLD) is the most prevalent chronic liver condition, closely linked to obesity and type 2 diabetes (Than and Newsome, 2015). It is characterized by excessive lipid accumulation in hepatocytes (steatosis) without significant alcohol consumption or other liver injury causes, such as viral hepatitis. Elevated plasma levels of low-density lipoprotein cholesterol (LDL-c) are a common risk factor, increasing the likelihood of cardiovascular disease (CVD) in MASLD patients. Clinically, MASLD is often associated with an atherogenic lipoprotein phenotype, a form of dyslipidemia characterized by higher levels of small, dense low-density lipoprotein (LDL) particles, decreased high-density lipoprotein cholesterol (HDL-c), and elevated triglycerides (TG) in the blood (Targher et al., 2024). MASLD encompasses a wide range of liver damage, from simple steatosis to more severe conditions like metabolic dysfunction-associated steatohepatitis (MASH), fibrosis, cirrhosis, and hepatocellular carcinoma (HCC) (Bessone et al., 2018). MASH, is characterized by hepatic inflammation and hepatocyte apoptosis, which can lead to liver fibrosis and eventually cirrhosis (Magee et al., 2016). While MASLD progression is generally slow, approximately 20-30% of patients with MASLD progress from simple steatosis to MASH, and around 9-25% of those with MASH develop cirrhosis (Heyens et al., 2021; Yu et al., 2016). Despite increasing understanding of the mechanisms driving MASLD progression, there are currently no specific therapeutic options, highlighting the urgent need for novel, safe, and effective pharmacological interventions for managing MASLD.

The melanocortin family consists of structurally similar peptides, including α -, β -, and γ -melanocyte stimulating hormones (α -, β -, and γ -MSH) and adrenocorticotrophic hormone (ACTH). These peptides are derived from the common precursor molecule, pro-opiomelanocortin (POMC), via post-translational processing (Smith and Funder, 1988). Melanocortins exert their effects by binding with five distinct receptor subtypes (MC1R - MC5R), each characterized by unique binding affinities (Kim et al., 2002). These melanocortin receptors (MCRs) are widely expressed across various tissues and regulate diverse physiological processes, such as melanogenesis, steroidogenesis, exocrine secretion, sexual function,

inflammation, and energy homeostasis (Cone, 1999; Fan et al., 1997; Kim et al., 2000). Due to these diverse functions, MCRs have become a promising targets for therapeutic intervention in inflammatory, metabolic, and CVD (Cai et al., 2009). Several MCR-targeted drugs are currently under clinical investigation, and a few have been approved for treating conditions like skin disorders, sexual dysfunction, and genetic obesity (Montero-Melendez et al., 2022).

MC1R is a well-characterized receptor for α -MSH, predominantly expressed in melanocytes, where it plays a critical role in regulating skin pigmentation (Nagui et al., 2017; Park et al., 2019). Additionally, MC1R expression has been identified in various cell types, including monocytes and macrophages, dendritic cells, neutrophils, endothelial cells, fibroblasts, and goblet cells of the duodenum (Becher et al., 1999; Catania et al., 1996; Colombo et al., 2002; Hartmeyer et al., 1997; Reichrath et al., 2005; Star et al., 1995). Evidence also supports its role as an anti-inflammatory and immunomodulatory regulator in leukocytes (Catania, 2007). Furthermore, MC1R expression has also been reported in the liver and adipose tissue of both humans and mice (Boston and Cone, 1996; Gatti et al., 2006; Hoch et al., 2007; Møller et al., 2015). However, these studies primarily focused on characterizing the expression of MC1R without exploring its functional significance in these metabolic tissues. Consequently, the functional role of MC1R, particularly in the liver, remains poorly understood.

The primary aim of this thesis was to investigate the role of MC1R in the regulation of cholesterol and fatty acid (FA) metabolism using MC1R signaling-deficient mouse models (in vivo) and liver cell culture models (in vitro). The development and characterization of a hepatocyte-specific MC1R deficient mouse model revealed that functional MC1R is expressed in the liver, and its deficiency leads to disturbances in cholesterol, bile acid, and FA metabolism. These findings highlight a novel role of hepatic MC1R signaling in lipid metabolism, opening new avenues for further investigation into MC1R biology and its therapeutic potentials. Even though the direct translation of the results of this thesis into human biology are unclear in this moment, these findings suggest that activating MC1R signaling in the liver could serve as a protective mechanism against MASLD and associated metabolic complications such as hyperlipidemia.

2 Review of the Literature

2.1 Pro-opiomelanocortin and melanocortins

Melanocortins are a group of small peptide hormones derived via the post-translational cleavage of the common precursor molecule POMC. This family of hormones include α -, β -, and γ -MSH, as well as ACTH. Melanocortin peptides play key roles in regulating a wide array of physiological processes, including energy homeostasis, adrenal function, sexual behavior, thermoregulation, immune response, and skin pigmentation (Böhm and Grässel, 2012). The *POMC* gene is predominantly expressed in the anterior and intermediate lobes of the pituitary gland as well as in the hypothalamus (Bumaschny et al., 2007). It is present in peripheral tissues, including the skin (Slominski et al., 2000). The *POMC* gene is located on the short arm of chromosome 2p23.3 and encodes a 267 amino-acid polypeptide precursor called pre-opiomelanocortin (pre-POMC). The synthesis of POMC involves the removal of a 26-amino-acid signal peptide sequence (Harno et al., 2018; Toda et al., 2017). The human POMC sequence consists of 241 amino acids, whereas in mice and rats, it is composed of 209 amino acids. Structurally, POMC includes a highly conserved N-terminal peptide domain (known as the 16K fragment or pro- γ -MSH), which contains the first (γ) MSH sequence; a central ACTH (1-39) sequence that encompasses the α -MSH sequence; and a C-terminus region that contains (β -LPH), β -endorphin, and the third (β) MSH sequence (Bicknell, 2008) (Fig. 2.1). The successful cloning of the *POMC* gene was accomplished by Nakanishi et al. in 1979, and the term “*POMC*” was introduced by Michael Chrétien and colleagues in the same year (Chrétien et al., 1979; Nakanishi et al., 1979). Notably, there exist only a single functional copy of the *POMC* gene, and its overall structure has remained conserved across different species, except in salmon, which lacks the γ -MSH sequence (Kawauchi et al., 1981). Despite some variations in peptide length among organisms, the *POMC* gene structure is highly conserved, particularly in regions encoding biologically active peptides such as ACTH, α -MSH, and β -endorphin (Bumaschny et al., 2007).

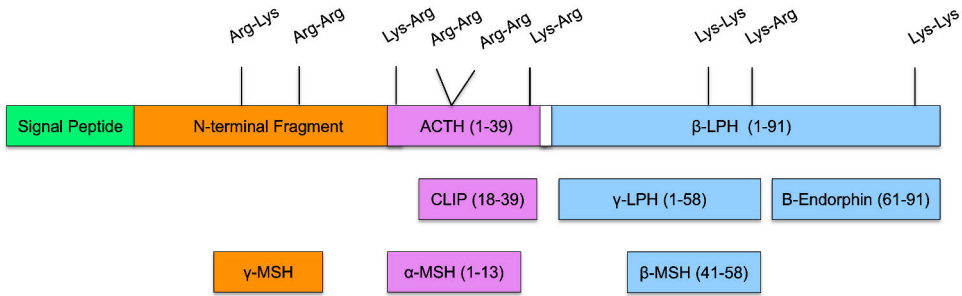


Figure 2.1. Schematic structure of the pro-opiomelanocortin (POMC) precursor protein. The *POMC* gene encodes a hormone precursor that is cleaved at dibasic amino acid sites during post-translational modification to produce melanocortin peptides.

ACTH is well-known for its essential role in stimulating steroidogenesis in the adrenal cortex, where it promotes the production of corticosteroids. Unlike other melanocortin peptides ACTH uniquely activates all five MCR subtypes, making it a central player in a wide range of physiological processes (Yuan and Tao, 2022). In mammals, α -MSH is primarily recognized for its involvement in skin pigmentation, and is highly conserved across species (Catania et al., 2000). In contrast, β -MSH and γ -MSH have been less extensively studied. Notably, β -MSH lacks an N-terminal cleavage site and is absent in rodents (Bennett, 1986). γ -MSH is composed of two cleavage products, gamma-1 and gamma-3, and features a critical N-terminal lysine residue (Roselli-Reh fuss et al., 1993). Interestingly, while all MSH peptides share a conserved core sequence of amino acids (MEHFRW), γ -MSH differs slightly by

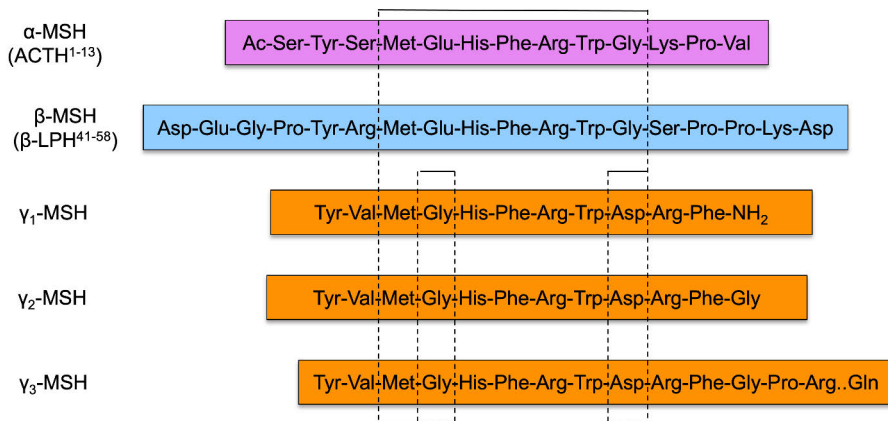


Figure 2.2. Conserved core amino acid sequences of melanocyte-stimulating hormones (MSH). All the three peptides— α -MSH, β -MSH, and γ -MSH—share a conserved core heptapeptide sequence (indicated by dotted lines). Figure adapted from (Humphreys, 2004).

having a glycine residue substituted for glutamic acid, illustrating subtle but significant variations among these peptides. This diverse array of MSH peptides, each with unique structural characteristics and receptor-binding properties, plays vital roles in various physiological functions, including energy homeostasis and immune regulation.

The processing of POMC into its biologically active peptides is primarily facilitated by subtilisin-like endoproteases known as prohormone convertases (PCs) specially PC1/3 and PC2. These enzymes cleave POMC at dibasic amino acid residue pairs (Arg-Lys, Arg-Arg, Lys-Arg or Lys-Lys), which flank all bioactive peptides within POMC sequence (Fig. 2.2) (Humphreys, 2004). In the anterior pituitary, PC1/3 predominantly processes the POMC precursor into larger peptides with higher molecular weight, including ACTH, β -LPH, and the N-terminal fragment (Fig. 2.3). PC2 in conjunction with other processing enzymes like carboxypeptidase E (CPE) and α -amidating monooxygenase (PAM), is responsible for the cleavage of smaller peptides, including β -endorphin, and α -, β -, and γ -MSH hormones (Wardlaw, 2011). The production of α -MSH involves further modification, where it undergoes acetylation by the N-acetyltransferase (N-AT) enzyme, resulting in a mature α -MSH peptide. This acetylation enhances its resistance to proteolytic degradation, thereby prolonging its biological activity.

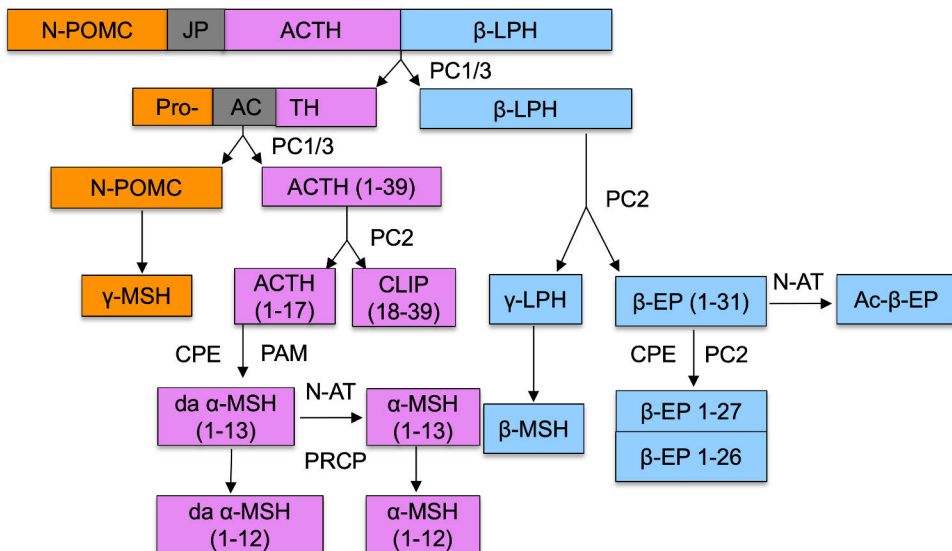


Figure 2.3. Schematic of melanocortin synthesis via the processing of the common pro-opiomelanocortin (POMC) precursor. The POMC molecule is cleaved by the serine proteases pro-protein convertase 1 (PC1) and pro-protein convertase 2 (PC2) into functional peptide fragments. Key abbreviations: ACTH – adrenocorticotrophic hormone; CLIP – corticotropin-like intermediate peptide; β -LPH – β -lipotropic hormone; β -EP – β -endorphin; PC1 – pro-protein convertase 1; PC2 – pro-protein convertase 2. Figure adapted from (Wardlaw, 2011).

However, both acetylated and non-acetylated forms of α -MSH have relatively short half-lives due to enzymatic degradation. For instance, prolyl carboxypeptidase (PRCP) is one of the enzymes that inactivates α -MSH, contributing to its rapid turnover (Wallingford et al., 2009).

2.2 Melanocortin receptors

Melanocortins mediate their biological functions via a family of five closely related MCR subtypes, MC1R - MC5R, named in order of their discovery. These receptors are broadly distributed across various tissues, and their diverse functions are determined by their unique tissue-specific expression and ligand-binding profiles. As members of the G protein-coupled receptor (GPCR) superfamily, MCRs are characterized by a seven-transmembrane domain structure, allowing them to transduce extracellular signals into intracellular responses (Schiöth, 2001). This structural configuration enables MCRs to play crucial roles in a range of physiological processes. The specificity of receptor subtypes and their affinity for different ligands add complexity to melanocortins at both cellular and systemic levels. A comparison of the MCR subtypes reveals a significant sequence homology, ranging from 38% to 60% at the amino acid level. For example, melanocortin 4 receptor (MC4R) and melanocortin 5 receptor (MC5R) share about 60% sequence homology, whereas MC2R and MC4R exhibit around 38% sequence identity (Yang, 2011). The successful cloning of these receptors has spurred extensive research into their physiological functions, continually uncovering new roles and highlighting their evolving importance in cellular regulation and systemic processes (Tatro, 1996).

Melanocortins exhibit varying binding affinities to different MCR subtypes. For instance, ACTH and α -MSH bind to MC1R with equal affinity, but only ACTH can activate MC2R. While ACTH can also bind to MC3R, MC4R and MC5R, γ -MSH predominantly binds to MC3R, and α -MSH shows a preference for MC5R. The binding affinities of POMC-derived peptides to MCR subtypes are summarized in Table 2.1. Ligand stimulation of MCRs typically activates the classical signaling pathway involving the stimulatory G protein (G_s), leading to the activation of adenylate cyclase (AC) and an increase in intracellular cyclic adenosine 3',5-monophosphate (cAMP) levels (Cone et al., 1996). MCRs may also couple with other G proteins (G_i/o , and G_q) and engage additional signaling pathways, such as PI3 kinase, which subsequently activates mitogen-activated protein kinases (MAPKs) like extracellular signal-regulated kinases 1 and 2 (ERK1/2) and c-Jun amino-terminal kinase (JNK) (Chai et al., 2007; Konda et al., 1994).

The wide-ranging physiological functions of MCRs include roles in melanogenesis, cardiovascular regulation, exocrine secretion, sexual function,

energy homeostasis, as well as anti-inflammatory and immunomodulatory actions (Cone, 2006; Tao, 2017; Wang et al., 2019). MC1R, primarily known as the α -MSH receptor, is mainly expressed in the skin and plays a crucial role in skin and hair pigmentation (Jackson et al., 2007). It is also found in leukocytes, where it exerts anti-inflammatory effects. MC2R, or the ACTH receptor, is predominantly expressed in the adrenal cortex and adipose tissue (Cone et al., 1996). MC3R and MC4R are mainly localized in the central nervous system (CNS) and are involved in regulating body weight, energy homeostasis, feeding behavior, and sexual function. MC5R is expressed in exocrine glands and other peripheral tissues such as adipose tissue, kidney, and leukocytes (Gong, 2014). Overall, MCR subtypes are widely expressed throughout the body and are implicated in a various diseases including obesity, sexual dysfunction, cancer, skin disorders, diabetes, and metabolic and inflammatory conditions (Do Carmo et al., 2013; Hadley, 2005; Roberts et al., 1983).

Table 2.1. Binding affinities of proopiomelanocortin (POMC)-derived peptides to their respective melanocortin receptors. Table adapted from (Yuan and Tao, 2022).

Peptide receptor	Sites of expression	Natural Ligand and affinity	Function
MC1R	Integumentary system, endothelial cells, immune system	α -MSH > β -MSH > γ 3-MSH > ACTH > γ 1-MSH > γ 2-MSH	Pigmentation and anti-inflammation
MC2R	Adrenal cortex	ACTH	Steroidogenesis
MC3R	Central nervous system (CNS), digestive system, immune cells	γ 1-MSH > γ 3-MSH > β -MSH > γ 2-MSH > α -MSH > ACTH	Energy homeostasis and anti-inflammation
MC4R	Central nervous system (CNS), heart, pancreas	β -MSH > α -MSH > ACTH > γ 1-MSH > γ 3-MSH > γ 2-MSH	Energy homeostasis, blood pressure regulation, sexual function
MC5R	Exocrine glands	α -MSH > β -MSH > ACTH > γ 1-MSH > γ 2-MSH = γ 3-MSH	Synthesis and secretion of exocrine gland products

2.2.1 Melanocortin 1 receptor

MC1R is a well-recognized regulator of melanin production, playing a crucial role in determining skin phenotype and sensitivity to ultraviolet (UV) light-induced damage. Although initially identified in melanocytes, MC1R is also expressed in various other cell types, including monocytes, macrophages, dendritic cells, neutrophils, endothelial cells, fibroblasts, and goblet cells in the duodenum (Becher et al., 1999; Catania et al., 1996; Colombo et al., 2002; Hartmeyer et al., 1997; Reichrath et al., 2005; Star et al.,

1995). The human *MC1R* gene was first cloned 1992 by two independent research groups (Chhajlani and Wikberg, 1992; Mountjoy et al., 1992), with the murine homolog of *MC1R* also identified and mapped in the same year (Mountjoy et al., 1992). Subsequent cloning of *MC1R* from other mammalian and non-mammalian species followed swiftly. The human *MC1R* gene, which is intron-less, is mapped to chromosome 16q24.3 and gives rise to three protein-coding splice variants (Gantz et al., 1994). Structurally, MC1R is an integral membrane protein comprising 317 amino acids, characterized by typical GPCR features such as an extracellular N-terminus, 7 transmembrane segments, and an intracellular C-terminal domain (Fig. 2.4). MC1R belongs to class A of GPCR family, with rhodopsin serving as the prototype (Gether, 2000). Despite the crystallization challenges posed by GPCRs, initial insights into their secondary and tertiary structures have been derived from low-resolution electron microscopy of bacteriorhodopsin and the crystal structure of rhodopsin (Palczewski et al., 2000; Subramaniam and Henderson, 1999). Most recently, Ma et al. revealed high-resolution cryo-electron microscopy structures of active MC1R-Gs complexes bound to different ligands: the endogenous agonist α -MSH, the stable α -MSH analogue afamelanotide, and the partial agonist SHU9119 (Ma et al., 2021). The binding models observed in these studies were consistent with those of MC4R-Gs complex (Israeli et al., 2021), supporting a conserved ligand recognition mechanism among MCRs. Additionally, the discovery of a conserved calcium-binding site in the MC1R-Gs complex highlights the pivotal role of calcium ions in ligand recognition and MC1R activation.

Beyond its role in pigmentation, MC1R is integral to inflammation and immune modulation. Activation of MC1R by α -MSH exerts anti-inflammatory effects by reducing pro-inflammatory cytokines production while simultaneously enhancing anti-inflammatory cytokines levels (Catania et al., 2004). MC1R activation has also been associated with anti-carcinogenic and tumor-suppressive effects in skin melanocytes (Eves et al., 2003; Kokot et al., 2009). Moreover, MC1R plays a functional role in the intestinal immune system and has been implicated in the pathophysiology of inflammatory bowel disease (Maaser et al., 2006).

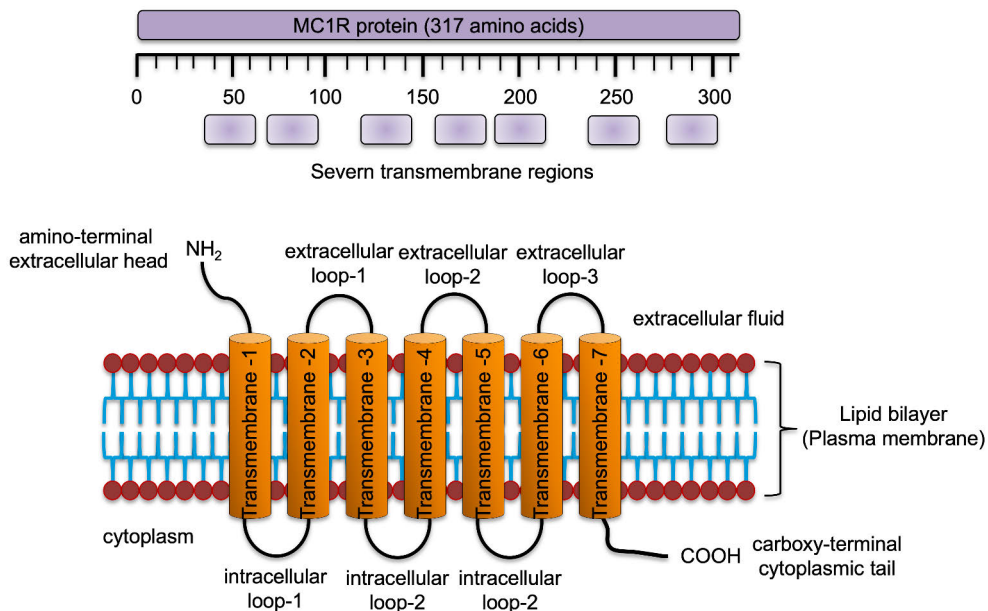


Figure 2.4. Structure of the mature melanocortin 1 receptor (MC1R) protein. The human *MC1R* gene encodes a seven-transmembrane protein that is highly polymorphic. The transmembrane domains traverse the cell membrane seven times. The extracellular N-terminus interacts with ligands, while the intracellular C-terminus initiates signaling pathways, such as the activation of adenylyl cyclase (AC). Figure adapted from (Wolf Horrell et al., 2016).

MC1R activity is intricately regulated by melanocortins, the agonist agouti signaling protein (ASIP), and β -defensin 3 (β D3). A distinctive feature of MCRs is their interaction with both naturally occurring agonists and antagonists. For MC1R, melanocortins such as α -MSH serve as agonists, stimulating receptor activity. Conversely, ASIP acts as an inverse agonist that directly inhibits MC1R, reducing its basal signaling activity and suppressing eumelanogenesis. Additionally, β D3 functions as a natural antagonist, dampening the signaling response induced by agonists without affecting the receptor's basal activity. The binding of α -MSH to MC1R leads to an increase in cAMP synthesis, initiating downstream signaling pathways. ASIP competes with α -MSH for binding to MC1R, which diminishes receptor activity and lowers cAMP production (Fig. 2.5). In contrast, β D3 binding does not alter basal cAMP levels but disrupts the interaction of both α -MSH and ASIP with MC1R, thereby modulating the receptor's response without direct activation or inhibition. This complex regulation by both agonists and antagonists highlights the dynamic control of MC1R signaling and its role in various physiological processes.

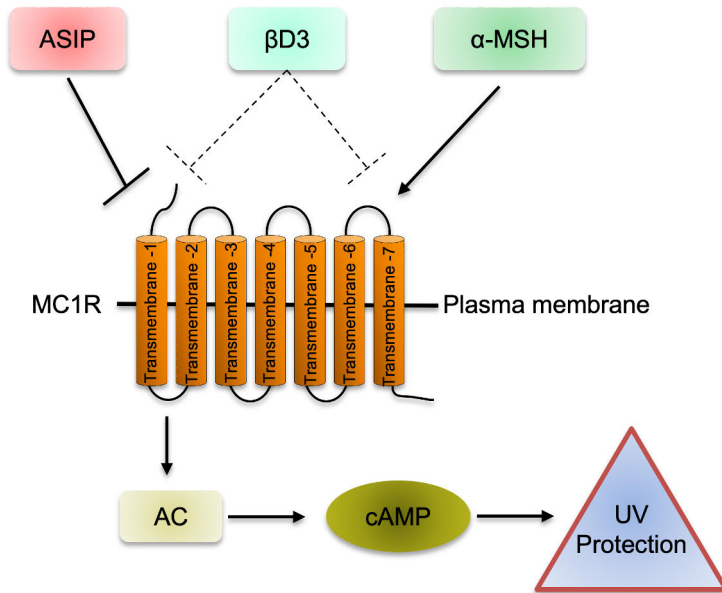


Figure 2.5. Melanocortin 1 receptor (MC1R) and its three main ligands. MC1R is activated when α -MSH binds to it, leading to an increase in cyclic adenosine monophosphate (cAMP) levels and the production of eumelanin, which provides protection against UV radiation. β -defensin 3 (β D3) acts as a neutral antagonist of MC1R, blocking the effects of both α -MSH and agouti signaling protein (ASIP). Key abbreviations: cAMP – cyclic adenosine monophosphate; UV – ultraviolet; β D3 – β -defensin 3; ASIP – agouti signaling protein; AC – adenylate cyclase. Figure adapted from (Wolf Horrell et al., 2016).

2.2.2 Melanocortin 2 receptor

The human *MC2R*, also known as the ACTH receptor, was the second MCR subtype to be cloned. The *MC2R* gene encodes a protein comprising 325 amino acid residues and is mapped to chromosome 18p11.2. As a unique MCR subtype, *MC2R* is specifically activated by ACTH, earning it the designation of the ACTH receptor. It is primarily expressed in the zona fasciculata and zona reticularis of the adrenal glands, where it plays a key role in regulating steroidogenesis (Ruggiero and Lalli, 2016). This function has been further supported by human genetic studies, which have linked mutations in the *MC2R* gene to familial glucocorticoid deficiency (Lin et al., 2007). Additionally, *MC2R* expression has been detected in human skin and murine adipocytes. In rodents, activation of *MC2R* by its canonical ligand, ACTH, facilitates lipolysis in white adipose tissue (WAT) (Møller et al., 2011). However, human WAT lacks *MC2R* expression (Møller et al., 2015), highlighting species-specific differences in *MC2R* expression profiles.

2.2.3 Melanocortin 3 receptor

The human *MC3R* gene, the third MCR subtype to be cloned, encodes a peptide consisting of 361 amino acids. Located on chromosome 20q13.2-q13.3, MC3R is unique in that it lacks introns. The MC3R protein is the least selective among the MCR subtype, binding with equal affinity to ACTH as well as α -, β - and γ -MSH (Renquist et al., 2011). The *MC3R* gene is predominantly expressed in the hypothalamus but is also found in several peripheral tissues, including the heart, skeletal muscle, macrophages, and intestinal epithelial cells (Bertolini et al., 2009; Brzoska et al., 2008). In the hypothalamus, *MC3R* plays a crucial role in regulating energy homeostasis. *Mc3r*-deficient mice exhibit a distinctive obesity phenotype, characterized by increased fat mass, reduced lean mass, and no apparent hyperphagia (Marks et al., 2006). This phenotype is further exacerbated by high-fat diet feeding. While its primary function is in energy balance, recent studies have shown that MC3R is also involved in growth, puberty, and circadian rhythms (Yanik and Durhan, 2023). In leukocytes, particularly macrophages, *MC3R* has an anti-inflammatory effects (Getting et al., 1999), with similar immunomodulatory actions observed in the CNS (Muceniec et al., 2006). Additionally, *MC3R* is implicated in cardiovascular regulation, thermoregulation, and the neuroendocrine system (Roselli-Rehfuß et al., 1993).

2.2.4 Melanocortin 4 receptor

The human *MC4R* gene was independently discovered by the research groups of Gantz and Cone using degenerate polymerase chain reaction (PCR) and homology screening technique (Gantz et al., 1993; Mountjoy et al., 1994). It is the fourth *MCR* subtype to be cloned. The *MC4R* gene is intron-less, located on chromosome 18q21.3, and encodes a protein of 332 amino acid residues (Gantz et al., 1993; Magenis et al., 1994). Sequence homology analysis of MCRs revealed that MC4R shares the highest sequence similarity with MC3R, showing approximately 58% identity and 76% similarity. Similar to MC1R, MC4R binds to ACTH, α -MSH, and β -MSH with equal affinity, but has a lower affinity for γ -MSH (Yuan and Tao, 2022). MC4R is predominantly expressed in the CNS, with significant presence in the hypothalamus, thalamus, and hippocampus (Mountjoy et al., 1994). MC4R is known for its role in regulating food intake, energy expenditure, and sexual function (Cone, 2005). Activation of MC4R promotes satiety, increases energy expenditure, and contributes to weight loss, while its inactivation leads to increased food intake, energy conservation, and weight gain (Cone, 2005; Garfield et al., 2009), underscoring its central role in energy homeostasis. Consequently, mutations in the *MC4R* gene are associated with monogenetic obesity in humans (Cone, 2005). The critical role of MC4R in energy regulation has been further validated in animal

models, where targeted disruption of *Mc4r* in mice leads to severe obesity, insulin resistance, and hyperglycemia (Huszar et al., 1997; Ste Marie et al., 2000).

2.2.5 Melanocortin 5 receptor

The human *MC5R* gene was cloned via homology screening of human genomic DNA and was the last of the MCR subtype to be identified. MC5R has a high binding affinity for α -MSH and, to a lesser extent, ACTH, but it does not bind to γ -MSH (Catania et al., 2004). Located on chromosome 18p11.2, MC5R is widely expressed in exocrine glands. Unlike other MCR subtypes, MC5R is also ubiquitously expressed in various peripheral tissues, including the adrenal glands, white adipocytes, kidney, thymus, skin, testicular, ovarian, uterine, esophageal, duodenal, liver, and lung tissue (Xu et al., 2020). Additionally, MC5R is expressed in immune cells, where it plays a role in regulating immune responses. In mice, knockout of *Mc5r* gene leads to defects in exocrine gland function, impairing water expulsion and thermoregulation due to reduced production of sebaceous lipids (Chen et al., 1997). Activation of MC5R has also been shown to promote lipid mobilization in adipocytes (Ji et al., 2022) and glucose uptake in skeletal muscle (Enriori et al., 2016).

2.3 Synthetic ligands for melanocortin receptors

Targeting MCRs via rational peptide and peptidomimetic design is challenging due to the lack of characterization of their three-dimensional protein structures. Additionally, the high sequence homology among MCR subtypes challenges the development of highly selective and effective ligands. For example, MC1R and MC4R share structural similarities that can lead to off-target effects when developing ligands. This homology makes it hard to design peptides or peptidomimetics that are selective, meaning they only bind to one specific MCR subtype without affecting others. The lack of selectivity can result in unwanted side effects and limit the therapeutic potential of these compounds. Despite these challenges, there is a critical need to develop selective and stable synthetic ligands for MCRs. The natural ligands for MCRs, such as α -MSH, have several limitations. They degrade rapidly due to a short functional half-life, meaning they do not last long enough to provide sustained therapeutic effects (Diano, 2011). This rapid degradation makes endogenous ligands less effective as therapeutic agents for treating diseases like obesity, inflammation, and metabolic disorders, where prolonged receptor activation or inhibition is needed. Interestingly, MCRs are unique because they have both naturally occurring agonists and antagonists. This dual nature creates both challenges and opportunities for drug development. It complicates the design process due to the different binding

interactions and effects on receptor activity. However, it also opens possibilities for creating highly specialized drugs. By understanding the specific interactions of these natural ligands with different MCR subtypes, it is possible to design new molecules that selectively mimic or block these interactions, leading to targeted therapeutic effects with fewer side effects. Understanding of the flexibility of a molecule helps clarify the relationship between its structure and function. This knowledge can improve the selectivity, stability and bioavailability of the synthetic peptides compared to the natural peptides. However, predicting the most active and stable conformation of a molecule is challenging, so general strategies must be employed to address this issue (Hruby, 2002).

The very first synthetic analogue of α -MSH, [Nle⁴-d-Phe⁷]- α -MSH (NDP- α -MSH), was characterized in 1980 and is known as afamelanotide or melanotan-I (MT-I). It has a prolonged duration of action and high affinity and potency to all MCR subtypes (Sawyer et al., 1980). Another analog of α -MSH, known as melanotan-II (MT-II; Ac-Nle-cyclo[Asp-His-D-Phe-Arg-Trp-Lys]-NH₂), was developed later and displays high potency to MCR subtypes with improved half-life (Zhou and Cai, 2017). MT-II is a cyclic peptide that improves its metabolic stability and bioavailability. Moreover, the general structure of MT-II has been used as a model for further development of MCR subtype ligands, which has resulted in the discovery of selective agonists for MC1R and MC5R and antagonists for MC3R and MC4R (Doedens et al., 2010; Grieco et al., 2002). Interestingly, a highly selective agonist for MC1R, known as LD211, compound 28 in the original publication (Doedens et al., 2010), has been identified. This compound exhibits a strong binding affinity specifically for MC1R, demonstrating no activity on other MCR subtypes. Due to its biased agonism - meaning it preferentially activates specific signaling pathways and its pathway-selective properties, LD211 is considered a promising candidate for drug development targeting MC1R-related pathways. These properties make it of significant therapeutic interest, particularly for conditions where selective activation of MC1R could be beneficial. However, it is important to note that LD211 has only been tested in preclinical studies and has yet to be evaluated in human clinical trials, leaving its potential therapeutic applications still under investigation. Given the central role of MC4R in energy homeostasis, there has been particular interest to develop and characterize novel MC4R agonists with higher selectivity and greater efficacy. The first MC4R-targeted drug setmelanotide (Imcivree™, Rhythm Pharmaceuticals) was recently approved by FDA for use in the treatment of obesity resulting from POMC, proprotein convertase subtilisin/ kexin type 1 (PCSK1), or leptin receptor (LEPR) deficiency (Markham, 2021). Even though, it has high affinity for MC4R, but can activate also other MCR subtypes, demonstrating a need for the development of more selective MC4R agonists in the future.

The pursuit of highly selective, stable, and effective ligands for MCRs is complex yet vital endeavor. Overcoming the structural limitations, addressing the high sequence homology among receptor subtypes and enhancing the stability of synthetic ligands are crucial steps. Successfully tackling these obstacles will unlock the potential for innovative therapies targeting a wide range of MCR-mediated conditions, including metabolic disorders, skin diseases, and inflammatory conditions, offering new avenues for precise and effective treatment strategies.

2.4 Physiological functions and therapeutic potential of melanocortin 1 receptor

The *MC1R* gene is well-established for its central role in skin and hair pigmentation. Melanocytes in the epidermal layer of the skin produce two primary types of melanin: eumelanin and pheomelanin. Eumelanin, the darker pigment, is chemically inert and highly photoprotective, effectively absorbing ultraviolet (UV) radiation and thereby shielding the skin from UV-induced damage (Kaidbey et al., 1979). In contrast, pheomelanin, which imparts a red/yellow hue, is less efficient in UV filtering and can potentially contribute to UV-induced skin damage and oxidative stress by increasing free radical production (Mitra et al., 2012). Activation of MC1R promotes the synthesis of eumelanin and enhances the eumelanin-to-pheomelanin ratio (Fig. 2.7) (Hunt et al., 1995; Virador et al., 2002). The human *MC1R* gene exhibits considerable polymorphism, with several loss-of-function variants associated with the “red hair color” phenotype (Abdel-Malek et al., 2014; Valverde et al., 1995). Furthermore, *MC1R* polymorphism have been linked to various conditions beyond pigmentation, including major depressive disorder (MDD) (G.-S. Wu et al., 2011) and obesity (Gerhard et al., 2013) in certain Quebec families (Chagnon et al., 1997) via linkage studies. Interestingly, a recent study has also demonstrated a significant association between *MC1R* variants and type 2 diabetes (Amin et al., 2022).

Several studies have demonstrated that the expression and physiological functions of MC1R extend beyond melanocytes and pigmentation. Mounting evidence suggests that MC1R acts as a regulator of innate-immune responses, antioxidant defense, and DNA-repair mechanisms (Abdel-Malek et al., 2014; Li et al., 2021; Swope et al., 2014). MC1R has a wide expression profile in different cell types including endothelial cells, monocytes, macrophages, lymphocytes, neutrophils, intestinal epithelia, testicular, ovarian, placental, lung, and liver tissue (Brzoska et al., 2008; Schiöth et al., 1999). MC1R is also expressed in the central nervous system (CNS), although its expression is primarily localized to the periaqueductal grey matter of the midbrain, where it plays a key role in pain modulation (Mogil et al., 2003; Xia et al., 1995). In leukocytes, MC1R exerts anti-

inflammatory actions by suppressing the expression of pro-inflammatory markers, while simultaneously increasing the production of anti-inflammatory cytokines (Catania et al., 2004). Moreover, MC1R is expressed in fibroblasts, where it mediates anti-inflammatory, and antifibrotic effects. Therapeutic benefits of MC1R activation have been demonstrated in preclinical models of systemic sclerosis, where oral administration of a novel MC1R agonist, dersimelagon (MT-8117), exhibited disease-modifying effects (Kondo et al., 2022). MC1R activation has also been shown to be protective in animal models of intestinal and ocular inflammation, and in Parkinson's disease (Cai et al., 2022; Spana et al., 2019). A recent study revealed that the neuroprotective and anti-inflammatory effects of MC1R activation with the selective ligand BMS-470539 in a rat model of brain injury (Yu et al., 2021). Likewise, therapeutic potential of MC1R activation has been demonstrated in the treatment of melanoma, a highly aggressive and resistant skin cancer. Recent in vitro and in vivo mouse studies have revealed that overexpression of MC1R stimulates the DNA repair process and can overcome the traditional chemotherapy treatments for melanoma (Castejón-Griñán et al., 2018; Chen et al., 2017; Montero-Melendez et al., 2022). Furthermore, increased MC1R expression has been found in the adipose tissues of obese individuals as well as in mouse adipocytes, indicating a potential function also in lipid metabolism (Boston and Cone, 1996; Mountjoy and Wong, 1997). Indeed, a study by Richer and Schwandt demonstrated the lipolytic activity of MC1R in rabbit adipocytes (Richter and Schwandt, 1987). Additionally, in human preadipocytes, α -MSH has been shown to inhibit both proliferation and adipogenesis via MC1R activation (Smith et al., 2003). However, the precise lipolytic role of MC1R in murine and human adipocytes remains unclear.

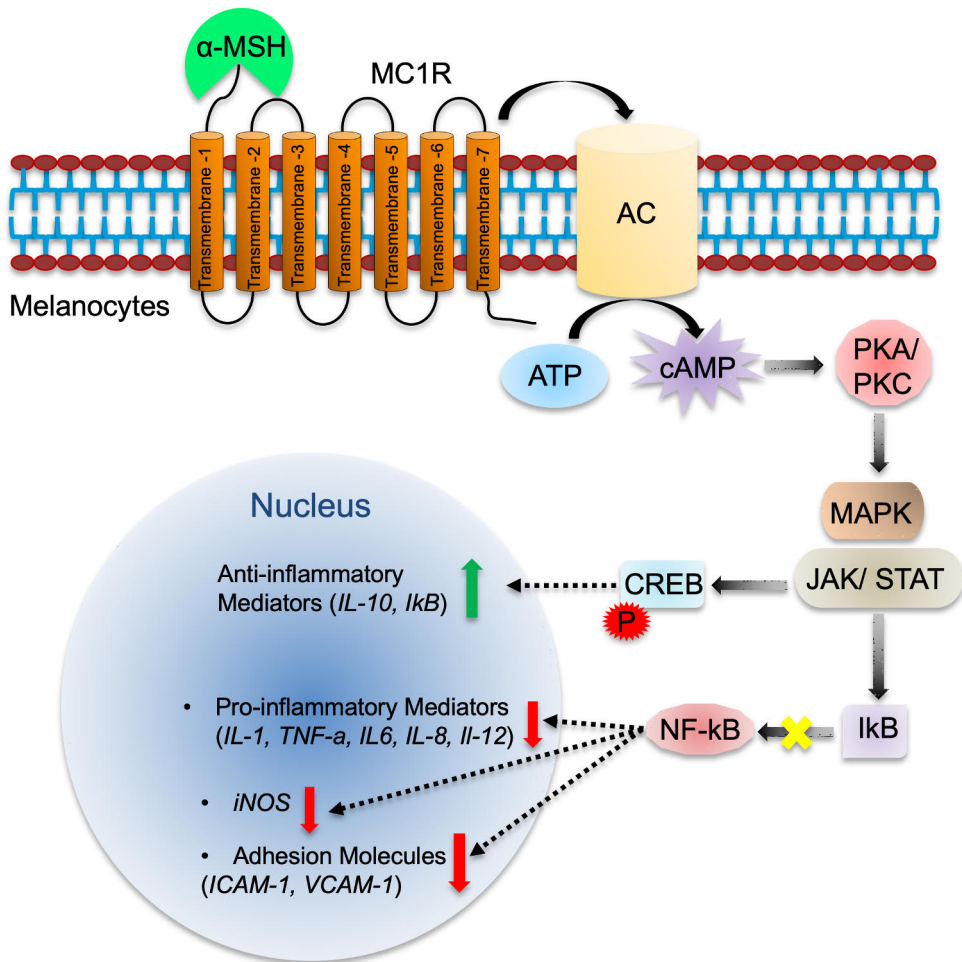


Figure 2.6. Anti-inflammatory effects melanocortin 1 receptor (MC1R). When α -MSH activates MC1R, it exerts an anti-inflammatory effect by increasing cyclic adenosine monophosphate (cAMP) production. Elevated cAMP activates protein kinase A (PKA) and protein kinase C (PKC), which in turn activate the MAPK and JAK/STAT signaling pathways. These pathways inhibit the degradation of I κ B, leading to a decrease in the expression of pro-inflammatory cytokines (IL-1, TNF- α , IL-6, IL-8, IL-12), inducible nitric oxide synthase (iNOS), and adhesion molecules (ICAM-1 and VCAM-1). Additionally, MC1R activation can phosphorylate cAMP response element-binding protein (CREB), which increases the expression of anti-inflammatory markers. Key abbreviations: AC – adenylyl cyclase; ATP – adenosine triphosphate; cAMP – cyclic adenosine monophosphate; PKA/PKC – protein kinase A/C; MAPK – mitogen-activated protein kinase; JAK/STAT – Janus kinase/signal transducer and activator of transcription; CREB – cAMP response element-binding protein; I κ B – I κ B kinase; NF- κ B – nuclear factor kappa B; IL-10 – interleukin-10; IL-1 – interleukin-1; TNF- α – tumor necrosis factor- α ; IL-6 – interleukin-6; IL-8 – interleukin-8; IL-12 – interleukin-12; iNOS – inducible nitric oxide synthase; ICAM-1 – intercellular adhesion molecule-1; VCAM-1 – vascular cell adhesion molecule-1. Figure adapted from (Mun et al., 2023).

The wide expression profile and diverse physiological functions of MC1R have generated significant interest in investigating its therapeutic potential across a broad range of diseases. As a key player in modulating immune responses, MC1R has been implicated in various inflammatory conditions, suggesting its promising role as a therapeutic target. Consequently, MC1R-targeted therapies are currently under investigation in both preclinical and clinical studies for the treatment of several challenging conditions, including multiple sclerosis, rheumatoid diseases, ulcerative colitis, and nephrotic syndrome (Montero-Melendez et al., 2022). These ongoing investigations highlight the receptor's potential to address unmet medical needs, offering new avenues for the treatment of diseases where inflammation plays a critical role in pathogenesis.

2.5 Melanocortin 1 receptor signaling pathways

Binding of α -MSH to MC1R activates adenylyl cyclase (AC), leading to an increase in cAMP production, a key second messenger that regulates a variety of cellular processes. In the downstream signaling cascade, cAMP activates either protein kinase A (PKA) or protein kinase C (PKC), which subsequently phosphorylates cAMP responsive element-binding protein (CREB). CREB is a transcription factor that plays a crucial role in the melanogenesis and the proliferation of melanocyte (Moscowitz et al., 2019). This signaling pathway is fundamental not only to pigmentation but also to the regulation of other cellular functions that are vital for skin homeostasis and response to external stimuli (Abdel-Malek et al., 2014; Kokot et al., 2009). In addition to the cAMP-dependent pathway, MC1R activation also engages a cAMP-independent pathway, which leads to the activation of extracellular signal-regulated protein kinase 1 and 2 (ERK1/2) via c-Kit signaling pathway (Fig. 2.7). This pathway provides an alternative mechanism for cellular response mediated by MC1R activation. Moreover, the c-Kit pathway may also activate AKT phosphorylation as a downstream effect of MC1R signaling, further contributing to various cellular processes such as survival, proliferation, and differentiation (Herraiz et al., 2011).

In terms of anti-inflammatory effects, MC1R signaling elevates the intracellular cAMP level, which activates PKA and PKC. These kinases then phosphorylate CREB, a transcription factor that plays a major role in inhibiting NF- κ B, a critical regulator of various inflammatory markers (Fig. 2.7) (Liu et al., 2017). Additionally, PKA activation suppresses p38 MAP kinase and TATA-binding protein (TBP) by inhibiting the phosphorylation of MAP kinase kinase kinase 1 (MEKKK1). This inhibition leads to the deactivation of c-JUN N-terminal kinase (JNK), further contributing to the anti-inflammatory response (Gonzalez-Rey et al., 2007; Kaneva,

2011). This complex signaling interactions underscore the potential function of MC1R signaling in modulating inflammatory processes.

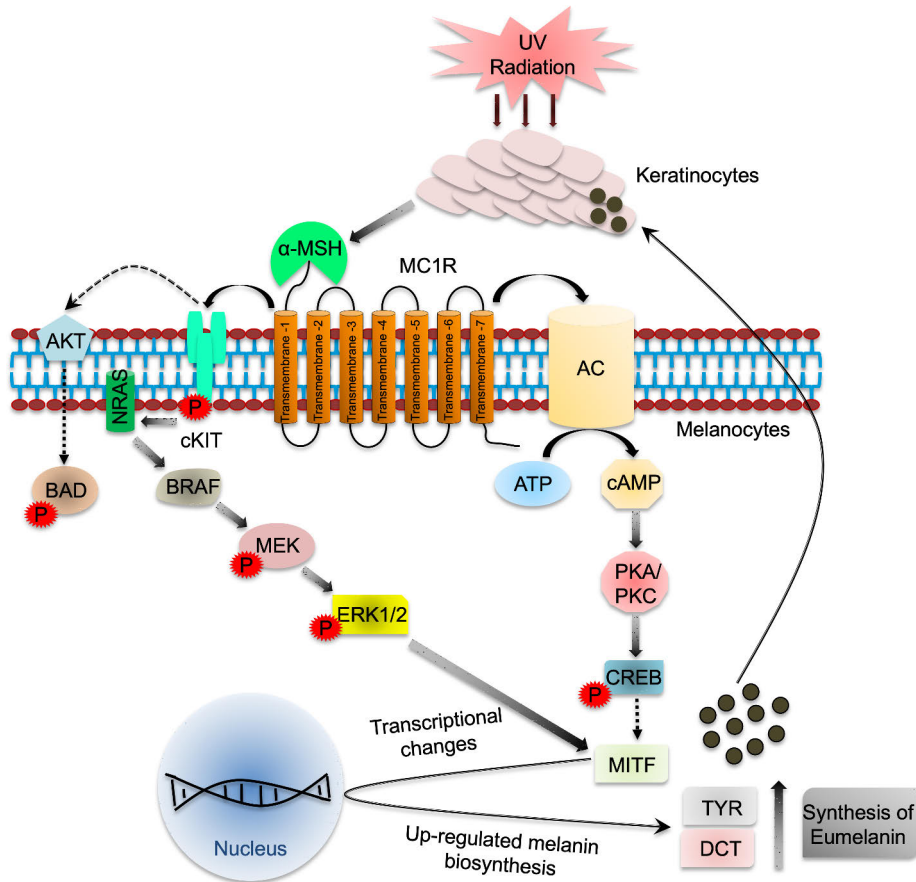


Figure 2.7. Melanocortin 1 Receptor (MC1R) triggered signaling pathways in melanocytes. UV exposure stimulates the production of α -MSH in the skin, which binds to MC1R, activating adenylate cyclase (AC) and increasing cyclic adenosine monophosphate (cAMP) levels. This leads to the activation of protein kinase A (PKA) and protein kinase C (PKC), which then activate cAMP response element-binding protein (CREB), promoting the expression of melanocyte-inducing transcription factor (MITF). Additionally, MC1R transactivates cKIT, which activates the NRAS-BRAF-MEK-ERK signaling cascade. Both pathways enhance eumelanin production, offering protection against UV radiation. Furthermore, this signaling improves DNA repair mechanisms, contributing to genomic stability in melanocytes. Key abbreviations: UV – ultraviolet; AC – adenylate cyclase; ATP – adenosine triphosphate; cAMP – cyclic adenosine monophosphate; PKA/PKC – protein kinase A/C; CREB – cAMP response element-binding protein; MITF – melanocyte-inducing transcription factor; TYR – tyrosinase; DCT – dopachrome tautomerase; cKIT – receptor tyrosine kinase; NRAS – neuroblastoma rat sarcoma; AKT – protein kinase B; BAD – B-cell leukemia/lymphoma 2-associated agonist of cell death; BRAF – B-Raf proto-oncogene; MEK – mitogen-activated protein kinase; ERK1/2 – extracellular signal-regulated kinase 1/2. Figure adapted from (Herraiz et al., 2011; Wolf Horrell et al., 2016).

2.6 The liver

2.6.1 Liver anatomy

The liver acts as a detoxifying organ and a key site for the synthesis, metabolism, storage and redistribution of carbohydrates, proteins, and lipids. In addition, the liver performs hundreds of other vital functions in the body including albumin production, bile production, blood filtration, amino acid regulation, and storage of vitamins and minerals. It is considered a part of the gastro-intestinal tract. The liver is the largest solid metabolic organ with a mass that amounts to approximately 2-5% of an adult's body weight and weights around 1.4-1.6 kilograms in men, and 1.2-1.4 kilograms in women. It is a reddish-brown cone-shaped organ located in the upper right-hand portion of the abdominal cavity, under the diaphragm, and on top of the right kidney, stomach, and intestines. According to the official International Anatomical Terminology (IAT), the human liver consists of four lobes: the larger right lobe and the left lobe and the smaller caudate lobe and the quadrate lobe (Gilloteaux, 1998). The caudate and quadrate lobes are well-defined units on the visceral aspect but have no representation on its ventral aspect. In practice, liver model with 8 segments has become the standard norm defined by Couinaud (Couinaud, 1957). Interestingly, humans have a non-lobated architecture, while rodents have a lobated liver consisting of 4 distinct lobes (Kruepunga et al., 2019).

2.6.2 The microscopic architecture and functions of the liver

On the microscopic scale, the liver is generally similar in all mammals and consists of lobules that are functional units of the liver (Fig. 2.8A). In these lobules, hepatocytes surround the central vein, while the terminal branches of the portal vein demarcate the periphery of the lobule (Kiernan, 1833). The portal tracts consist of the terminal branches of the portal vein, hepatic artery, and the bile duct, and form an isotropic three-dimensional network giving rise to classic hexagonal shape of the lobule with 3 portal tracts and 3 metabolic zones where the portal venules end (Fig. 2.8B). In each zone, hepatocytes have different metabolic gene expression and functionality. These zones are usually known as discrete areas and exist as a flexible spectrum. Zone 1 is the closest to the portal triad and receives highly oxygenated blood from the arterioles and nutrient-rich blood from the portal vein, and therefore, is responsible for oxidative metabolism such as β -oxidation, gluconeogenesis, bile formation, cholesterol formation, and break-down of amino acids. The oxygen and nutrient gradients decrease from zone 2 to zone 3, since the blood from portal triad flows towards the central vein (Trefths et al., 2017). Zone 2 is located between zone 1 and 3 and is a critical source of new hepatocytes during

homeostasis and regeneration. Zone 3 is known as the pericentral region of the hepatocytes and sits furthest away from the portal triad and has the lowest perfusion capability amongst all zones (Fig. 2.8D). Liver participates in the detoxification, ketogenesis, glycolysis, lipogenesis, and biotransformation of drugs (Kalra et al., 2024). It is the most vascularized organ with dual blood supply, i.e., the hepatic artery delivers approximately 25% of the blood and the remaining approximately 75% of the blood comes from the portal vein (Abdel-Misih and Bloomston, 2010).

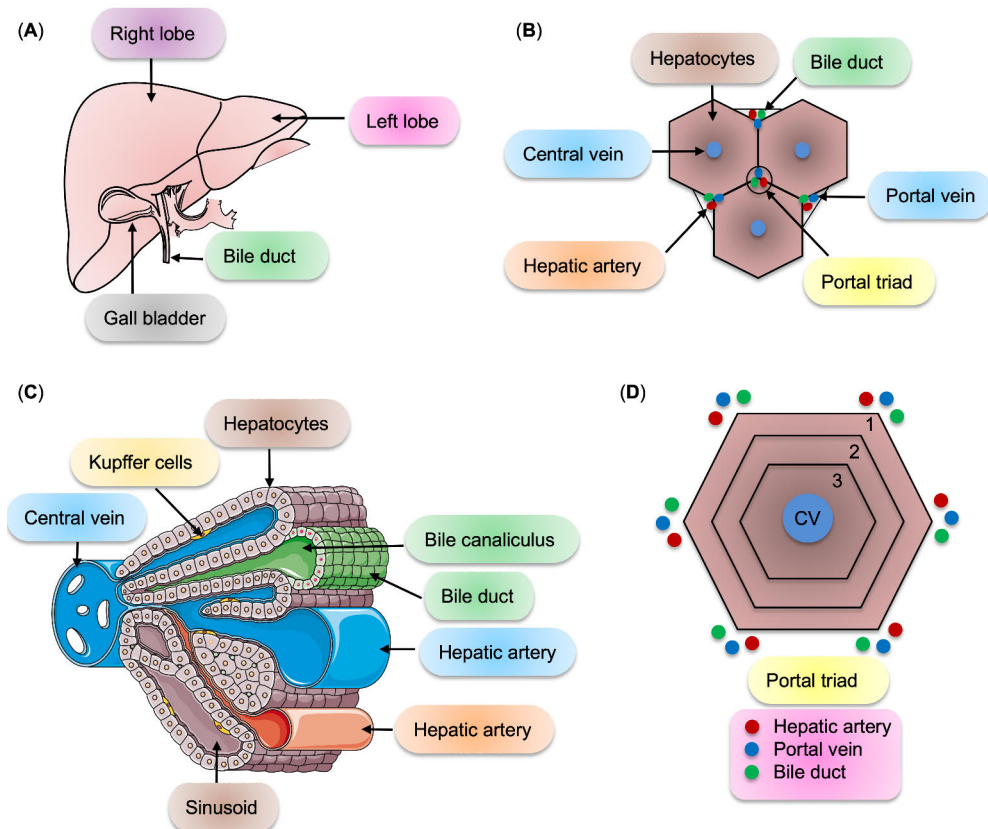


Figure 2.8. Anatomical and structural organization of the human liver. The liver is divided into lobes and lobules. (A) Graphical illustration of the anterior view (right and left lobes are only visible in this view) of the human liver. (B) Illustration of a hexagonal-shaped liver lobules, depicting the central vein, bile duct, hepatic arteries, and portal vein. (C) Detailed structure of a liver lobule, showing rows of hepatocytes radiating outwards from the central vein. (D) Zonal organization of liver lobules, divided into zones 1, 2 and 3, which reflect distinct metabolic functions. Parts of the figure was created using images from the Servier Medical Art, licensed under a Creative Commons Attribution 4.0 International License.

The liver consists of different cell types such as hepatocytes, biliary epithelial cells (also known as cholangiocytes), stellate cells, Kupffer cells, and liver sinusoidal endothelial cells. Hepatic functions are governed via the unique features of these different cell types. Most of the liver is comprised of hepatocytes and covers around 78% of the parenchymal volume, whereas 6% of the volume is occupied by the non-parenchymal cells and the remaining 16% is occupied by the extracellular space, including sinusoidal lumen, space of Disse, and biliary canaliculi (Ellias et al., 2021). Hepatocytes are epithelial cells with polygonal shape and have large centrally located nuclei and perform more metabolic functions than any other cell types in the body. These cells are organized to form a hepatic lobule with a central vein, sinusoids, and the portal triad consisting of a hepatic artery, a portal venule, and a bile duct (Fig. 2.8C). While hepatocytes play a pivotal roles in metabolism, detoxification, protein synthesis, and act as a principal site for metabolic regulatory pathways (Gong et al., 2023), the macrophagic Kupffer cells sit within the sinusoid walls and are mainly responsible for the production of inflammatory substances that could further influence the phenotypes of neighboring cells (Bilzer et al., 2006). Sinusoids are the smallest vessels composed of highly fenestrated channels. Hepatocytes contain organelles including endoplasmic reticulum (ER) and Golgi apparatus for the secretory functions and are enriched with high numbers of mitochondria, providing energy for various metabolic functions within the body. Hepatocytes are arranged in cords with layers of cells organized into the hexagonal lobules that build around a central vein and are separated by sinusoids, via which blood flows to the hepatic vein (Schulze et al., 2019). Hepatocytes store energy as glycogen and lipids and excrete salts and degraded proteins into canaliculi, which channel bile via the intrahepatic biliary tree. Cholangiocytes line this duct network, modifying bile as it flows to the gall bladder, where it is eventually released into the intestine during feeding (DiStefano et al., 2015).

Table 2.2. Liver cell types, their distribution, and essential functions. Table adapted from (Elias et al., 2021)

	Cell type	Percentage in liver	Major function	Location
Parenchymal cells (75-80%)	Hepatocytes	75-80%	Metabolism of lipids, protein, steroids, fats, bile secretion, sugar storage and detoxification of xenobiotics	Hepatic lobules
Non-Parenchymal cells (NPCs) (20-25%)	Sinusoidal endothelial cells	~44% of NPCs	Filtration and transport of nutrients from circulation, adhesion molecules for the leukocytes	Sinusoidal lining
	Kupffer cells (KC)	~33% of NPCs	Phagocytosis, cytokines responsible for inflammatory response and liver regeneration	Sinusoidal lumen
	Hepatic stellate cells (HSC)	~3-5% of NPCs	Fat-storing cells, maintains extracellular matrix, sinusoidal blood flow, and storage of vitamin A	Space of disse
	Mesenchymal cells	-	Tissue repair	Sinusoidal lumen
	Cholangiocytes	~3-5% of total liver cells	Bile secretion	Lining of interhepatic and extrahepatic duct system
	Dendritic cells	<1% of NPCs	Phagocytosis and antigen presenting function	Sinusoidal lumen
	Intrahepatic lymphocytes	20% of NPCs	Innate and adaptive immunity	Sinusoidal lumen

2.6.3 Liver energy metabolism

The liver performs various essential physiological processes such as nutrient metabolism, blood volume regulation, immune system support, lipid homeostasis, and biotransformation of xenobiotics (Trefts et al., 2017). The metabolic function of the liver is governed via the actions of insulin and metabolic hormones as well as other regulators such as substrate flux. The different functions of the liver can be categorized into metabolic, detoxification, and excretory. The most critical function of the liver is the processing, partitioning, and breakdown of the macronutrients to provide energy to the body. The ability of the liver to store glucose as glycogen and produce glucose via gluconeogenic pathways are immensely critical to maintain glucose homeostasis in the body. Different substances such as amino acids, monosaccharides, FA, and nutrients are delivered to the liver via circulation and further processed for the storage and production of energy. The liver also catabolizes

lipids to provide energy and secretes excess lipids for the storage in other peripheral tissues such as the adipose tissue (Kruepunga et al., 2019).

2.6.3.1 Hepatic lipid metabolism

The liver is a central metabolic organ responsible for regulating lipid metabolism throughout the body. It plays a critical role in the synthesis and breakdown of FA, managing their availability for energy production and storage. The liver facilitates FA synthesis (lipogenesis) to produce FA from excess carbohydrates and subsequently stores them as TG or directs them to other tissues. Additionally, the liver performs FA oxidation, breaking down FAs to generate energy, especially during fasting. The hepatic lipid metabolism involves several inter-dependent pathways and strictly controlled by three different mechanisms: (1) the activity of cellular molecules that accelerate acquisition of lipids including FA uptake and synthesis (de novo lipogenesis, DNL); (2) lipid storage including TG synthesis and formation of lipid droplets (LDs); (3) lipid consumption including β -oxidation and TG export via the secretion of very low-density lipoprotein (VLDL) (Bechmann et al., 2012). Therefore, lipid metabolism in the hepatocytes is crucial for maintaining whole-body lipid homeostasis. TG, a major source of energy, are primarily stored in adipose tissue and, to a lesser extent, in the liver. Disruption in this balance can impair insulin sensitivity and lead to excessive fat accumulation, particularly in the liver (Wang et al., 2015). Prolonged fat accumulation in hepatocytes predisposes individuals to steatotic liver diseases like MASLD, characterized by increased TG deposition in the liver cells.

2.6.3.1.1 Fatty acid metabolism in the liver

The liver regulates lipid metabolism by synthesizing and degrading FA to maintain lipid homeostasis. FA are stored and transported as TG, providing energy for most tissues except the brain and erythrocytes. FA are involved in several pivotal biological processes such as the synthesis of cellular membrane lipids and generation of lipid-containing messenger molecules involved in signal transduction (Eyster, 2007). Unlike limited glycogen stores, body fat can supply energy for extended periods. In fasting or prolonged exercise, FA provide most of the energy for tissues such as the liver, heart and skeletal muscle (Birkenfeld and Shulman, 2014).

FA are fundamental components of TG, phospholipids, glucolipids, and other lipids. They consist of a methyl group (omega; ω) at one end and a carboxyl group (C(=O) OH) at other end (Fig. 2.9). The alpha (α) carbon atom is present next to the carboxyl group and the subsequent carbon is known as beta (β) carbon. Letter ω (or

n) denotes the position of the double bond closest to the methyl end. FA are categorized into two types: saturated and unsaturated, based on the presence of double bonds. Saturated FA consist of unbranched, linear chains of methyl groups, typically ranging from 12 to 24 carbons in length; however, several biochemically significant FA also possess shorter chains. On the other hand, unsaturated FA contain one or more double bonds positioned at various locations along the carbon chain and like saturated FA, possess a terminal carboxylic group (Fig. 2.9). They are further divided into monounsaturated FA (MUFA), with a single carbon-carbon double bond and polyunsaturated FA (PUFA), which contain two or more carbon-carbon double bonds separated by a methylene group. Based on chain length, FA are also classified into short-chain FA (2-4 carbon atoms), medium-chain FA (6-10 carbon atoms), and long-chain FA (12-26 carbon atoms).

As mentioned previously, the major source of FA originates either from dietary or endogenous sources in the liver. Within the intestinal lumen, dietary TG are emulsified by bile acids following the hydrolysis by pancreatic lipase yielding sn-2-monoacylglycerols and free fatty acids (FFA) (Alves-Bezerra and Cohen, 2017). FFA are non-esterified FA (NEFA), that act as a major energy source and have a significant role in cell signaling (Tripathy et al., 2003). Enterocytes resynthesize lipid molecules into TG after the emulsification process and further pack them into chylomicrons (CM), which are transported to the lymphatic system and finally to the circulation. Lipoprotein lipase (LPL) localized in the endothelial cells adjacent to the muscle and adipose tissue absorbs most of the CM-associated TG and the remaining TG is delivered to the liver via receptor mediated endocytosis and FA are released during the lysosomal processing (Cohen and Fisher, 2013). Under normal conditions, the liver uses large amounts of FA daily and stores only a small fraction as TG. This occurs due to a balance between FA uptake and synthesis, and the processes of FA oxidation and secretion as TG-enriched VLDL. Any excess TG that is not secreted forms LDs in the liver (Nguyen et al., 2008).

however, in hepatic steatosis models and MASLD patients, CD36 mRNA levels increase and correlate positively with hepatic triglyceride content (Buqué et al., 2010; Miquilena-Colina et al., 2011). Nevertheless, the pathophysiological role of CD36 in the liver is still unclear. In vitro studies show that FABPpm facilitates FA uptake via protein-mediated transport ((Memon et al., 1999; Zhou et al., 1998), but its role in hepatic FA uptake in vivo is still unclear. FATP proteins are present in both plasma and intracellular membranes. Particularly, fatty acid transport protein-2 (FATP2) and fatty acid transport protein-5 (FATP5) are the dominant forms that are expressed in the liver (Chabowski et al., 2013; Doege et al., 2006). FATP2 is located in the ER and its overexpression is associated with the increased uptake of long-chain FA (Krammer et al., 2011), whereas FATP5 is located in the plasma membrane (Doege et al., 2006). Similarly, caveolae are small flask-shaped invaginations in the plasma membrane with a diameter of 50-100 nm and are involved in many different signal transduction processes and endocytosis processes (Parton and Simons, 2007). They are present in most of the cell types, especially in the endothelial cells, smooth muscle cells, fibroblasts and adipocytes, while they do not exist in red blood cells, platelets and lymphocytes (Parton and del Pozo, 2013). Caveolins are essential components of the caveolae, which are rich in proteins and lipids such as cholesterol, sphingolipids and saturated FA, and play a vital role in FA transport (Li et al., 2005). Within hepatocytes, FA are bound to fatty acid-binding protein-1 (FABP1) and sterol carrier protein-2 (SCP2), which control their cellular distribution in the cytosol. Likewise, FATP2, 4 and 5 as well as ACSL1, 3, and 5 regulate the activation of long-chain FA to acyl-CoA molecule and their channeling into metabolic pathways. The balance between FA and acyl-CoA within the hepatocytes in the cytosol might be controlled by Them1, 2 and 5, that counteract ACSL by catalyzing the hydrolysis of acyl-CoA molecules into FA and CoA. In the cytosol, Acyl-CoA are also bound acyl-CoA-binding protein (ACBP) or SCP2 (Alves-Bezerra and Cohen, 2017) (Fig. 2.10).

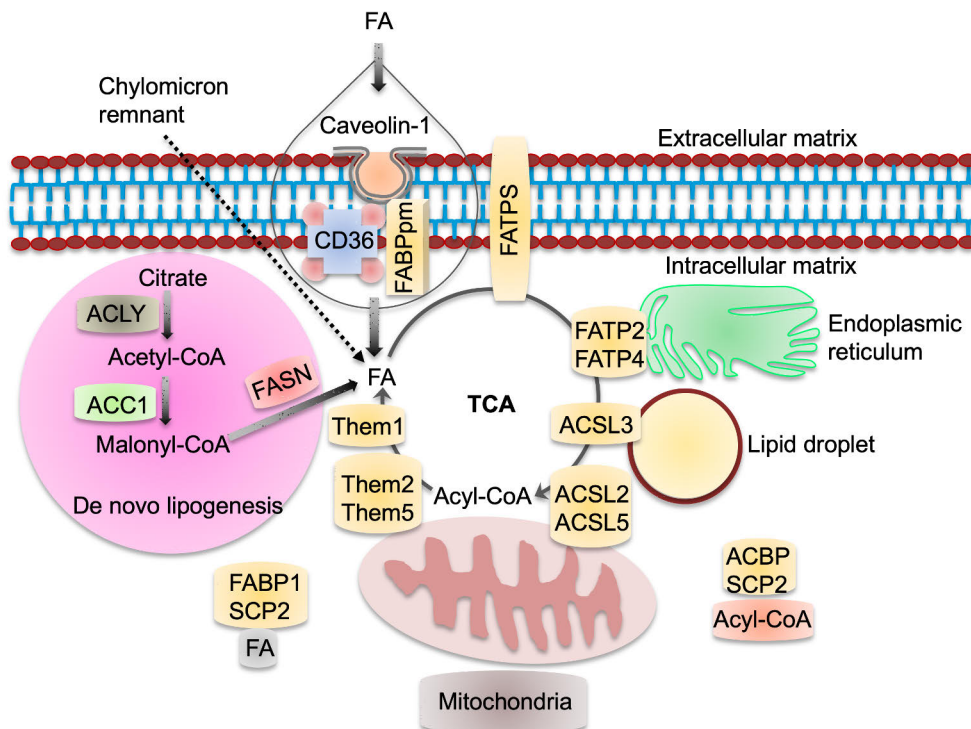


Figure 2.10. Pathways and enzymes involved in hepatic fatty acid (FA) uptake and metabolism. Hepatocytes obtain FA via two main routes: uptake of circulating FA via transporters such as FA translocase (CD36), plasma membrane FA-binding proteins (FABPpm), and Caveolin-1, or via de novo lipogenesis (DNL) involving enzymes like ATP-citrate lyase (ACLY), acetyl-CoA carboxylase (ACC), and fatty acid synthase (FASN). Intracellular FA localization is facilitated by fatty acid-binding protein-1 (FABP1) and sterol carrier protein-2 (SCP2). Long-chain FA activation to acyl-CoA is mediated by FA transport proteins (FATP2, 4, 5) and acyl-CoA synthetases (ACSL1, 3, 5), with the mitochondrial ACSL5 supporting triglyceride (TG) biosynthesis. Acyl-CoA thioesterases (ACOT) and thioesterase superfamily members (Them1, 2, 5) hydrolyze acyl-CoA to maintain a balance between the free FA (FFA) and acyl-CoA in hepatocytes. Figure adapted from (Alves-Bezerra and Cohen, 2017).

2.6.3.1.3 De novo lipogenesis

DNL is a crucial metabolic process that helps maintain the body's energy balance and tightly regulated by hormonal and nutritional signals. DNL accounts for about 5-10% of the total FA input in the liver. However, its activity increases significantly in conditions such as insulin resistance and metabolic diseases (Donnelly et al., 2005). In addition to the liver, adipocytes also robustly synthesize FA from carbohydrate via the DNL pathway. However, DNL in adipose tissue surprisingly contributes to only a small fraction (<2%) of the abundant TG stored in LDs. FA produced in the liver are incorporated into TG and packed into VLDL particles to

serve as an energy source for extrahepatic tissues. In contrast, DNL in adipose tissue directly contributes to local fat deposition and long-term energy storage. DNL is the process of synthesizing endogenous FA from acetyl-CoA subunits produced during glycolysis (Coleman and Lee, 2004; Smith and Tsai, 2007). Moreover, cytosolic acetyl-CoA can also serve as a source, apart from glycolysis, for the DNL process. In the presence of abundant glucose, hepatocytes convert glucose into FA, which are then processed into LDs and stored as TG. Furthermore, FA are oxidized, incorporated into structural lipids, or used for post-translational modifications within the cells. Depending on nutritional status, FA predominantly enter the liver as circulating FFA, TG lipoprotein remnants, or are endogenously produced via DNL. The essential role of DNL has been demonstrated in diverse conditions, including cancer, neurogenesis, and metabolic syndrome (Knobloch et al., 2013; Solinas et al., 2015; Svensson et al., 2016).

In mammalian cells, carbohydrates are essential macromolecules and serve as precursors for the DNL pathway. Initially, substrates like glucose, fructose, glucogenic amino acids and ethanol undergo glycolysis, ultimately producing citrate via the TCA cycle in the mitochondria (Alves-Bezerra and Cohen, 2017). Citrate is transported from the mitochondria to the cytosol, where ATP-citrate lyase (ACLY), a key enzyme in FA biosynthesis further converts citrate into acetyl-CoA (Pinkosky et al., 2017). FA biosynthesis is mediated by the cytosolic enzyme acetyl-CoA carboxylase (ACC), which catalyzes the transformation of acetyl-CoA into malonyl-CoA. Malonyl-CoA is further processed by FA synthase (FASN), which converts the substrate acyl chain into saturated 16 carbon FA (palmitic acid) in a stepwise process (Kawano and Cohen, 2013). Finally, the primary products of FASN can be further elongated and modified by the long chain fatty acid elongase 6 (ELOVL6) and stearoyl-CoA desaturase 1 (SCD1) in the ER and mitochondria to generate a diverse range of complex FA species. TG are ultimately synthesized by FA esterification of glycerol 3-phosphate (Fig. 2.11). As such, FA synthesis is a complex mechanism that relies on the synchronization of various enzymes and therefore, altering the activity of any of those enzymes could dysregulate the whole DNL process.

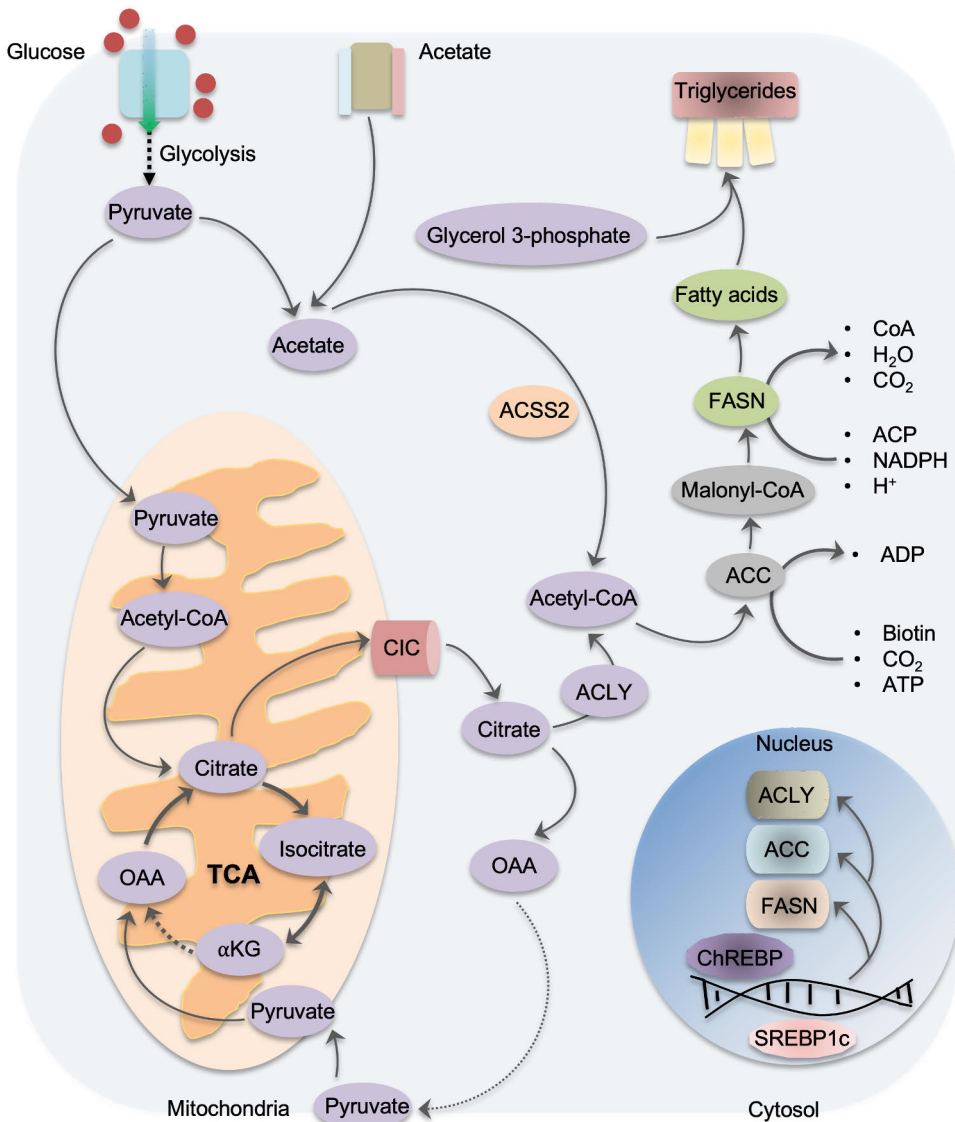


Figure 2.11. Hepatic de novo lipogenesis (DNL) pathways. DNL is a metabolic process in hepatocytes where glucose is taken up by transporters, via glycolysis to generate pyruvate, and then converted to acetyl-CoA. Acetyl-CoA enters the tricarboxylic acid (TCA) cycle, forming citrate, which exits the mitochondria. ATP-citrate lyase (ACLY) then converts citrate back to acetyl-CoA in the cytosol. Acetyl-CoA carboxylase (ACC) catalyzes the formation of malonyl-CoA, which is subsequently used by fatty acid synthase (FASN) to produce fatty acids like palmitate. Key abbreviations: ACC – acetyl-CoA carboxylase; ACLY – ATP-citrate lyase; ACSS2 – acetyl-CoA synthetase 2; ChREBP – carbohydrate response element-binding protein; CIC – citrate-isocitrate carrier; FASN – fatty acid synthase; α KG – alpha-ketoglutarate; OAA – oxaloacetic acid; SREBP1c – sterol regulatory element-binding protein-1c; TCA – tricarboxylic acid. Figure adapted from (Zhu et al., 2023).

During the postprandial period, when glucose uptake and insulin secretion are high in hepatocytes, expression of lipogenic genes are significantly upregulated (Ferré and Foufelle, 2007). The regulation of DNL primarily occurs at the transcriptional level and is mediated by multiple transcription factors, such as the upstream stimulatory factor (USF), the sterol regulatory element binding protein-1c (SREBP1c), the carbohydrate responsive element binding protein (ChREBP) and liver X receptors (LXRs). In contrast, a recent clinical study has demonstrated that increased substrate availability might be the cause of increased DNL rather than changes in transcriptional level due to glucose and insulin action. Nevertheless, transcriptional regulation of DNL pathway is controlled by the action of two major enzymes: SREBP1c and ChREBP and are induced by increased insulin and glucose concentrations respectively. SREBP1c promotes the expression of lipogenic genes such as FASN, ACC, SDC1, and lipin 1 (Csaki and Reue, 2010; Horton et al., 2002), and activated by insulin and liver X receptor (LXR) (Ferré and Foufelle, 2010). On the other hand, ChREBP is known to induce the liver-type pyruvate kinase expression, thus enhancing the accumulation of substrates for the synthesis of FA and TG (Uyeda and Repa, 2006). In addition, DNL is controlled via allosteric regulation of ACC (Kawano and Cohen, 2013; Oosterveer and Schoonjans, 2014). The two major isoforms of ACC in mammals are cytosolic ACC1 and mitochondrial ACC2 that enable the formation of two distinct pools of malonyl-CoA. ACC1 acts as the key DNL regulator and is expressed in major lipogenic tissues including the liver, WAT, and lactating mammary glands, whereas ACC2 is prevalent in skeletal and cardiac muscles (Bianchi et al., 1990). In the cytosol ACC1-generated malonyl-CoA in the cytosol is used by FASN for the synthesis of FA. Conversely, ACC2-generated malonyl-CoA prevents the β -oxidation by inhibiting the carnitine/palmitoyl-transferase 1 (CPT1) activity and the transfer of fatty acyl group to the mitochondria for β -oxidation (Wakil and Abu-Elheiga, 2009). Nonetheless, ACC1- and ACC2-generated malonyl-CoA do not mix within the cell and are hugely segregated from each other.

2.6.3.1.4 Fatty acid oxidation

Fatty acid oxidation (FAO) is a major pathway to produce energy during fasting and physiological stress. FAO provides energy for several extra-hepatic tissues including the heart and skeletal muscle. In this process, FA derived from different sources, such as hydrolysis of hepatic TG stores, circulating lipids, or from DNL in the liver, are broken down into acetyl-CoA, which can be further utilized to produce ATP or ketone bodies by multiple pathways. Short- (<C4), medium- (C4-C12), and long-chain (C12-C20) FA are oxidized in the mitochondria to generate acetyl-CoA, while β -oxidation of very long- (C20-C26) FA and branched-chain FA occurs in the peroxisomes (Alves-Bezerra and Cohen, 2017). Mitochondrial FAO is the primary pathway for FA

metabolism and can occur either completely or incompletely. FA oxidation is a crucial process for the production of both ATP (complete oxidation process) and ketone bodies (incomplete oxidation process) to the peripheral circulation (Eaton et al., 1996). In conditions of low blood glucose, ketone bodies derived from acetyl-CoA and acetoacetyl-CoA produced by β -oxidation of FA – serve as an important alternative fuel for the brain (which does not directly use FA for oxidative metabolism) and other highly oxidative extrahepatic tissues. Other FAO pathways such as α -oxidation and ω -oxidation are active in the ER and facilitated by cytochrome P450 4A family members (Lavoie and Gauthier, 2006; Musso et al., 2009).

Mitochondrial β -oxidation is the primary pathway for FAO in hepatocytes and involves a cyclical series of reactions that result in shortening of FA. In each cycle, two carbons are shortened, until the last cycle when two acetyl-CoA molecules are generated from the catabolism of four-carbon FA. FA are activated at the outer mitochondria membrane and transported by the activity of carnitine/palmitoyl-transferase 1 (CPT1), which produces acyl-carnitine from acyl-CoA and free carnitine. Further, acylcarnitine translocase transports acyl-carnitines to the inner mitochondrial membrane in exchange for free carnitine and eventually converts back to acyl-CoA by CPT2, which is found in the inner mitochondrial membranes. Acetyl-CoAs are synthesized by the breakdown of acyl-CoAs via the β -oxidation cycle in the mitochondrial matrix with the help of four different enzymes: acyl-CoA dehydrogenase, 2-enoyl-CoA hydratase, 3-hydroxyacyl-CoA dehydrogenase, and 3-oxoacyl-CoA thiolase. ATP is produced via the TCA cycle by the oxidation of acetyl-CoAs, which drives the electron transport chain reaction. In the presence of acetyl-CoA in mitochondria, ketone bodies (β -hydroxybutyrate, acetoacetate, and acetone) are produced by a series of reactions regulated by acetyl-CoA acetyltransferase (ACAT) 1, mitochondrial 3-hydroxy-3-methylglutaryl-CoA synthase (HMGCS) 2, HMG-CoA lyase (HMGCL), and β -hydroxybutyrate dehydrogenase (BDH) 1 (Stagg et al., 2021). The peroxisome proliferator-activated receptors (PPARs), particularly PPAR α , regulates the expression of FAO enzymes at the transcriptional level (Alves-Bezerra and Cohen, 2017). Although the peroxisomal and mitochondrial FAO pathways share a similar mechanism, there are significant differences between them. As an example, acetyl-CoA oxidase yields H₂O₂ in peroxisomal FAO route instead of NADH as in the mitochondrial β -oxidation pathway. Comparatively, peroxisomes lack an electron transport chain, thus generating less ATP-energy than mitochondrial FAO (Grum et al., 1994).

2.6.3.1.5 Lipoprotein metabolism and secretion

Lipoproteins are large, complex particles that transport insoluble TG and cholesterol in the bloodstream. They are classified based on their physical and chemical properties. The structure consists of a monolayer of amphipathic phospholipids and specialized

proteins called apolipoproteins, which surround a core of hydrophobic neutral lipids (Small, 1986) (Fig. 2.12). Phospholipids enable lipoproteins to interact with the aqueous environment, while apolipoproteins provide structural integrity and facilitate interactions with enzymes, lipid transport proteins, and cell surface receptors.

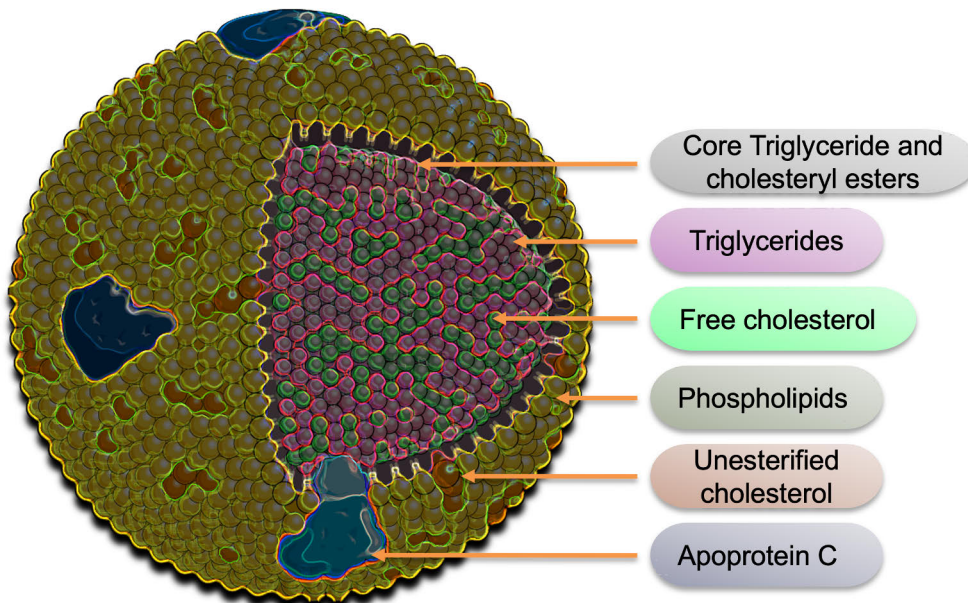


Figure 2.12. Schematic representation of a lipoprotein particle. The core of a lipoprotein particle contains triglycerides (TG) and cholesterol esters, which are surrounded by monolayer of phospholipids. Embedded within this layer are molecules of free cholesterol. Unesterified cholesterol, along with various apolipoproteins, including Apolipoprotein C, are present on the surface. This arrangement facilitates the transport of hydrophobic lipids in the aqueous environment of the bloodstream. Figure created using image from Servier Medical Art, licensed under a Creative Commons Attribution 4.0 International License.

Lipoproteins are classified based on their density, size, composition, and function. They vary in size from 5 to over 1000 nm and are grouped into five major families based on their density: CM, VLDL, intermediate-density lipoproteins (IDL), LDL, and HDL (Mach et al., 2020). HDL are the smallest and densest lipoprotein particles, primarily composed of proteins with a low lipid content, while CM are large, lipid-rich particles (Table 2.3). Apolipoproteins, the surface proteins of lipoproteins, facilitate particle transport, help solubilize the lipid core, and regulate metabolic functions by acting as receptor ligands and promoting lipoprotein metabolism in the plasma (Öörni et al., 2019). The most important apolipoprotein is apolipoprotein B (ApoB), a large particle with unique amphipathic properties that is essential for the assembly of VLDL in the liver.

Lipoproteins perform two primary functions: 1) Transporting TG from the liver and intestine to muscle and fat tissue via CM (apoB48) and VLDL (apoB100). VLDL releases TG and is converted into LDL, which delivers cholesterol to peripheral tissues. 2) Facilitating reverse cholesterol transport, where HDL carries excess cholesterol from tissues back to the liver, reducing arterial cholesterol buildup and atherosclerosis risk (Feingold, 2000). HDL also exhibits antioxidant, anti-inflammatory, and anti-apoptotic properties (Tall and Yvan-Charvet, 2015). Conversely, LDL, with a low protein-to-fat ratio, transports cholesterol, phospholipids and TG (Feingold, 2000). Elevated VLDL levels correlate with hypertriglyceridemia, low HDL levels, obesity, and atherosclerosis (Feingold, 2000; Libby, 2021). Particularly, the small dense LDL particles are atherogenic in nature due to their low affinity for LDL receptor (Berneis and Krauss, 2002). Small dense LDL particles easily penetrate the arterial walls and bind to proteoglycans in the subendothelial space, where they are retained. This retention makes them susceptible to oxidation, which increases their uptake by macrophages, leading to inflammation and the development of atherosclerosis (Matsuura et al., 2008).

Table 2.3. Basic characteristics of plasma lipoproteins. Table adapted from (Cohen and Fisher, 2013).

	Chylomicrons (CM)	Very low- density lipoprotein (VLDL)	Intermediate- density lipoprotein (IDL)	Low-density lipoprotein (LDL)	High-density lipoprotein (HDL)
Density (g/mL)	<0.9	0.95-1.006	1.006-1.019	1.019-1.063	1.063-1.210
Diameter (mm)	75-1200	30-80	25-35	18-25	5-12
Major Lipids	Triglycerides	Triglycerides	Triglycerides, Cholesterol	Triglycerides	Triglycerides, Cholesterol
Total Lipid (% wt)	98	90	82	75	67
Major Apoproteins	Apo B-48, Apo C, Apo E, Apo A-I, A-II, A-IV	Apo B-100, Apo E, Apo C	Apo B-100, Apo E, Apo C	Apo B-100	Apo A-I, Apo A-II, Apo C, Apo E

2.6.3.1.6 Triglyceride metabolism

TG, also known as triacylglycerol, are the most common type of fat, consisting of three FA bound to a glycerol backbone. Metabolic energy in human body is primarily derived from TG. The major sources of hepatic TG are dietary lipids, FA derived from adipose tissue, and FA produced via DNL. Endogenous TG synthesis

predominantly takes place in the liver and adipose tissue. Excess dietary carbohydrates and proteins are converted into FA via DNL in the liver. These diet-derived and de novo synthesized FA are then esterified with glycerol to form TG. Similarly, FA and glycerol taken from the bloodstream are used for the synthesis of TG in adipose tissue. The major source of energy in the body comes from the TG stored in adipose tissue, especially during periods of energy deficit or increased energy demand (Ahmadian et al., 2007). FA and glycerol are produced via TG hydrolysis, a process regulated by hormones such as glucagon and adrenaline. This metabolic process, also known as lipolysis, is most prominent in adipose tissue. After being released into the bloodstream, FA and glycerol are transported to other tissues, where they are utilized for energy production, a process that is especially crucial during fasting (Jaworski et al., 2007).

There are three major lipases involved in the hydrolysis of intracellular TG: adipose triglyceride lipase (ATGL), hormone-sensitive lipase (HSL), and monoglyceride lipase (MGL). ATGL, also known as palatin-like phospholipase domain-containing protein 2 (PNPLA2), performs the first and rate-limiting step of TG hydrolysis in adipocytes by generating diacylglycerol (DG) and one FA. The resulting DG molecules are then further hydrolyzed by HSL (second step) into monoacylglycerol (MG) and one FA. MGL is selective for MG and finally produces glycerol and the third FA (Edwards and Mohiuddin, 2024). Several factors influence TG metabolism such as nutritional status, hormonal signaling, and genetic factors. ATGL acts as a key enzyme in the regulation of whole-body energy homeostasis via its central role in lipolysis, which provides crucial energy substrates and precursors for the synthesis of membrane lipids (Schreiber et al., 2019). Similarly, HSL mobilizes FA from TG in the adipose tissue and activated by glucagon and adrenaline (epinephrine) and inhibited by insulin. Reduced insulin sensitivity is strongly associated with hepatic fat accumulation in humans and other animals. The determination of hepatic fat accumulation solely based on insulin sensitivity is challenging due to the large variability in factors regulating insulin sensitivity including overall obesity, body fat distribution, or circulating adipokines. Excess lipids can be stored for short term in ectopic tissues in the least toxic form, i.e., TG. FA storage in the form of TG protects against lipotoxicity, however, overwhelmed compensatory mechanism of high TG accumulation might cause damage to the cells as well as metabolic stress and dysfunction. In most mammalian cell types, TG obtained from the diet are broken down into several small lipid globules (emulsification) by bile acids in the intestinal lumen following their hydrolysis by pancreatic lipase into sn-2-monoacylglycerols and FFA. After the emulsification process, enterocytes resynthesize those lipid molecules into TG and assemble them into CM, which are then secreted into the lymphatic system and finally into the circulation (Hashimoto et al., 2000; Iqbal and Hussain, 2009). Under normal conditions, most FA are absorbed by adipose tissue and

muscle, while the remaining TG within the CM remnants are delivered to the liver, where FA are released during lysosomal processing (Cohen and Fisher, 2013).

2.6.3.1.7 Cholesterol metabolism

Cholesterol is a waxy, ubiquitous lipid found in all higher animals and is present in every tissue of the body. Chemically, it is an organic compound with 27 carbon atoms, consisting of a hydrocarbon tail, a central sterol nucleus composed of four hydrogen rings, and a hydroxyl group (Fig. 2.13). As a crucial component of animal cell membranes, cholesterol also serves as a precursor for the synthesis of bile acids, vitamin D, several hormones, including sex hormones (estrogen, testosterone, progesterone) and corticosteroids (corticosterone, cortisol, cortisone, and aldosterone) (Dietschy, 1984). In most tissues, unesterified (free) cholesterol is an essential component of cell membranes. Esterification helps store cholesterol and prevents the toxicity associated with free cholesterol. Cholesterol can be either synthesized *de novo* or obtained from the diet. *De novo* cholesterol synthesis primarily occurs in the liver (accounting for 70-80%) and in the small intestine (approximately 10%). Cholesterol and TG are packaged together with the apolipoprotein in the liver and released into the circulation as VLDL particles. Due to high hydrophobic nature of cholesterol, apolipoproteins help to package and transport it in the bloodstream. The degradation of TG in VLDL leads to the formation of LDL particles, which are rich in cholesterol (Kawano and Cohen, 2013). Cholesterol-rich LDL particles are transported to the peripheral tissues and taken up by the LDL receptors (LDLR) via receptor-mediated endocytosis (Goldstein et al., 1982). The majority of LDL particles are cleared from the circulation by hepatocytes, which then convert excess cholesterol into bile acids or excrete it into the bile as free cholesterol via specific transporters. In addition to LDL particles, HDL particles transport cholesterol from extra-hepatic tissues to the liver, where they are taken up via scavenger receptor class B member I (SR-BI, encoded by the *SCARB1* gene) (Ouimet et al., 2019). Intracellular cholesterol homeostasis is tightly regulated via a negative feedback mechanism, where cholesterol or its metabolites inhibit the expression of genes involved in cholesterol biosynthesis and LDLR activity (Luo et al., 2020). Hypercholesterolemia, which is linked to various CVD and heart conditions, has become a major global health concern.

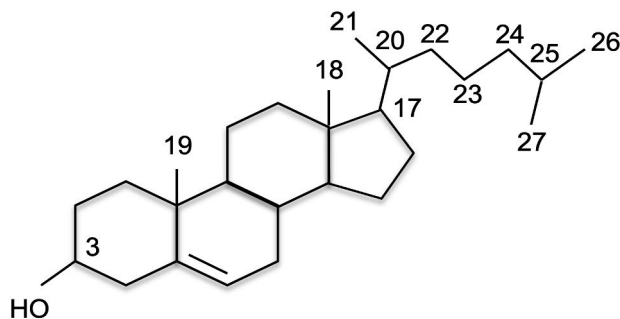


Figure 2.13. Structural formula of cholesterol. Cholesterol is a sterol lipid characterized by its distinct molecular structure, which includes a hydrocarbon tail, a central sterol nucleus composed of four interconnected hydrocarbon rings, and a single hydroxyl group (-OH).

Cholesterol biosynthesis is a complex and energy-intensive process that involves multiple enzymatic reactions. The rate-limiting step in this pathway is governed by HMG-CoA reductase, whose activation is regulated via various mechanisms (Craig et al., 2024). Classically, cholesterol levels are controlled by two main pathways at the transcriptional level. The first pathway is regulated by the transcription factors known as SREBPs, which regulate the expression of a cluster of cholesterol biosynthesis genes. In the setting of low intracellular cholesterol level, SREBPs are released from the ER and cleaved in the Golgi complex to produce an active fragment, which enters the nucleus to bind to the SRE (sterol regulatory element) and induces the transcription of the genes encoding HMG-CoA reductase and other enzymes. In contrast, in the setting of excess intracellular cholesterol, SREBPs are retained in the ER membranes and therefore, proteolytic cleavage of the active fragment of SREBPs and induction of cholesterol biosynthesis genes are inhibited (Istvan and Deisenhofer, 2001). The second pathway is regulated by the LXR/ RXR transcription factor family, which acts as cellular cholesterol sensors and protects the cells from cholesterol overload by controlling bile acid metabolism and cholesterol excretion by the liver. Additionally, several enzymes and proteins involved in cholesterol biosynthesis are regulated by small non-coding microRNAs, which play a role in the posttranscriptional control of gene expression (Bhattarai et al., 2021).

As previously mentioned, acetyl-CoA is a major precursor molecule in cholesterol synthesis. Once it exists the mitochondria, acetyl-CoA is converted into citrate and then back to acetyl-CoA by the ACLY enzyme in the cytosol. Acetyl-CoA can be derived from the oxidative decarboxylation of pyruvate from glycolysis, the oxidation of long-chain FA, or the oxidative degradation of certain amino acids (Shi and Tu, 2015). The first stage of cholesterol biosynthesis produces mevalonate as an intermediate, which represent the rate-limiting step in cholesterol synthesis (Fig. 2.14). In this process, two molecules of acetyl-CoA condense to form

acetoacetyl-CoA, which then combines with a third molecule of acetyl-CoA to generate HMG-CoA, a reaction catalyzed by the rate-determining enzyme HMG-CoA reductase. The subsequent steps are mostly unregulated, with mevalonate being used to synthesize isoprenoid units (five-carbon units). These units are then joined to form squalene (thirty-carbon units), which undergoes a cyclic reaction following epoxidation. Lastly, lanosterol, a cyclized product, undergoes several reactions to ultimately produce cholesterol as a final product (Cerqueira et al., 2016). Statins are the competitive inhibitors of HMG-CoA reductase and extensively used to reduce cholesterol levels in patients with hypercholesterolemia or other forms of dyslipidemia (Istvan and Deisenhofer, 2001; Keyomarsi et al., 1991; Menge et al., 2005; Shrivastava et al., 2010).

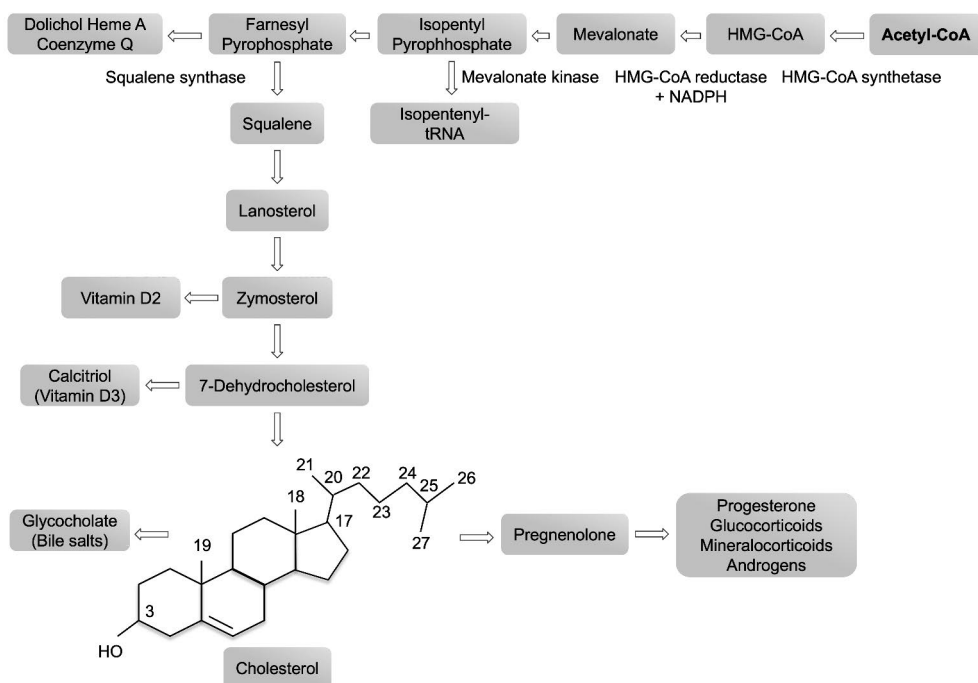


Figure 2.14. Major pathways involved in de novo cholesterol synthesis. Cholesterol is synthesized via the mevalonate pathway, a critical process that begins with the rate limiting step catalyzed by 3-hydroxy-3-methylglutaryl CoA reductase (HMG-CoA reductase), which converts HMG-CoA into mevalonate. This enzyme is key regulatory target for cholesterol-lowering drugs like statins. Mevalonate is subsequently phosphorylated using adenosine triphosphate (ATP), forming isoprenoid diphosphate, an active isoprenoid unit. Subsequent condensation reactions produce farnesyl diphosphate, which then condenses to form squalene. A series of reactions involving squalene epoxidase, lanosterol is generated in the endoplasmic reticulum (ER). Finally, via a series of complex reactions involving multiple enzymes, cholesterol is synthesized from lanosterol within the ER membrane. Figure adapted from (Bhattarai et al., 2021).

2.6.3.2 Bile acid metabolism

Cholesterol is broken down into amphipathic molecules called bile acids in the liver. In mammals, bile acids are mainly produced in pericentral hepatocytes, converted into bile salts, and then secreted into the bile ducts. These bile salts are stored in the gall bladder and released into the intestine after a meal (Li and Chiang, 2009). While cholesterol can be synthesized from acetyl-CoA in the liver, it cannot be broken down into smaller molecules or burned by the body. Therefore, bile acids are formed as part of cholesterol catabolism and are excreted into the feces. Besides their well-established role in aiding the absorption of fats and fat-soluble vitamins in the intestine, bile acids also participate in glucose metabolism and the secretion of glucoregulatory hormones (Hofmann, 2009). Moreover, bile acids act as bioactive signaling molecules, binding to receptors such as the farnesoid X receptor (FXR) and the GPCR-coupled bile acid receptor (Gpbar1 or TGR5) (Ahmad and Haeusler, 2019). Bile acids are conjugated with taurine or glycine and secreted into the bile after being synthesized in the hepatocytes. More than 90% of these bile acids are reabsorbed in the ileum (small intestine) via bile acid transporters, then travel back to the liver via the portal vein, where they are taken up and recycled. This exchange of bile acids between the liver and intestine is known as the enterohepatic circulation of bile. This process is crucial for maintaining liver function, excreting cholesterol, and facilitating the absorption of lipids and nutrients. However, some bile acids leak into the bloodstream or bypass the ileal uptake, where they are modified by intestinal microorganisms and later reabsorbed in the colon via passive diffusion (Dawson and Karpen, 2015). Bile acid concentrations are high in the liver, bile, and intestine, but low in the plasma, mainly due to incomplete reuptake by the hepatocytes.

In humans, bile acids are categorized into two distinct pools: primary bile acids, which are synthesized in the liver (cholic acid, CA, and chenodeoxycholic acid, CDCA) and secondary bile acids, which are produced from primary bile acids by gut microbiota (deoxycholic acid, DCA, and lithocholic acid, LCA) (Russell and Setchell, 1992). The synthesis of primary bile acids from cholesterol in the liver occurs via two main pathways: the classical pathway and the alternative pathway (Fig. 2.15) (Chiang, 2002). In the classical pathway, most of the bile acid intermediates are neutral sterols, earning it the name “neutral pathway”. This pathway produces equal amounts of CA and CDCA in humans and is considered the major bile acid biosynthesis route under normal physiological conditions. The alternative pathway, which produces acidic intermediates, is referred to as the “acidic pathway” (Axelson and Sjövall, 1990). Bile acids can be distinguished primarily by their hydroxylation sites and whether they are conjugated with amino acids. In rodents, bile acids are mostly conjugated with taurine, whereas in humans, the majority are conjugated with glycine.

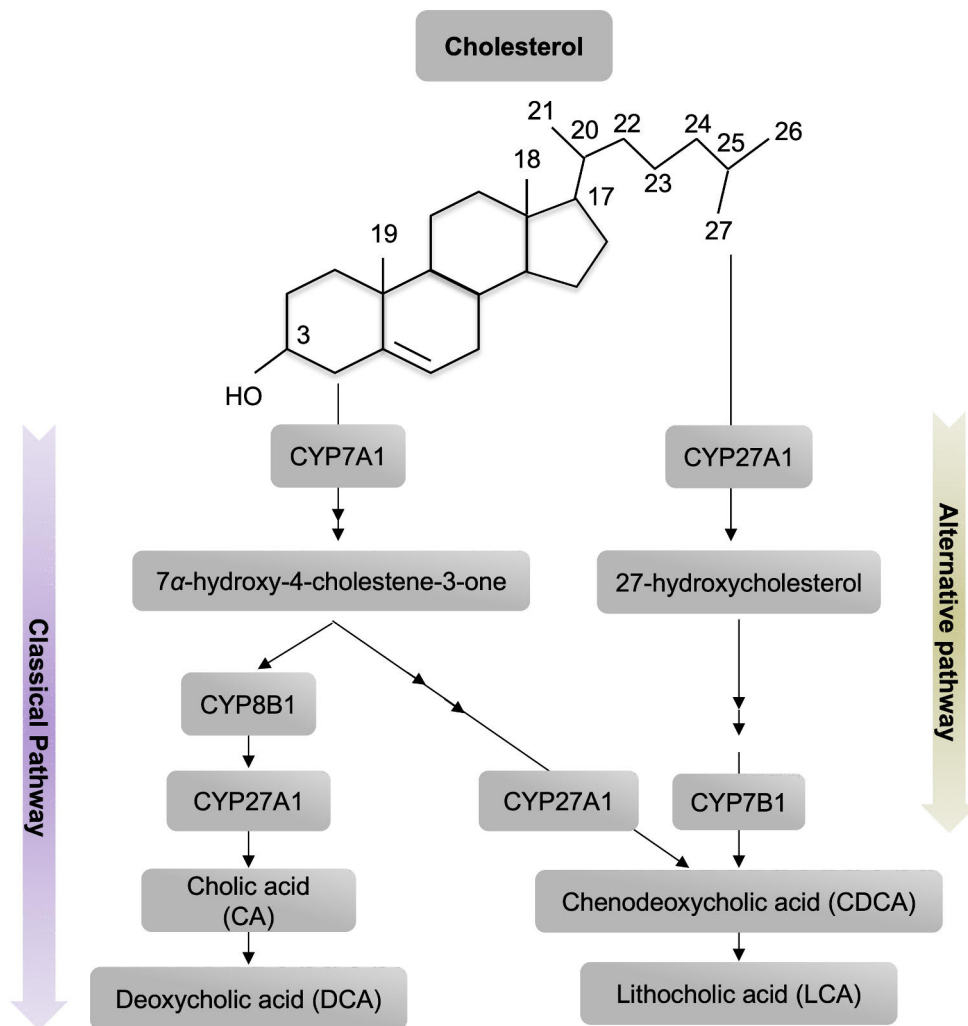


Figure 2.15. Bile acid synthesis and metabolism. Bile acid synthesis involves two main pathways: the classical (neutral) pathway and the alternative (acidic) pathway. The classical pathway takes place in the endoplasmic reticulum (ER) and is primarily regulated by the enzyme cholesterol 7 α -hydroxylase (CYP7A1), as indicated by the purple arrow. This pathway leads to the production of cholic acid (CA), with the enzyme sterol 12 α -hydroxylase (CYP8B1) playing a crucial role in its synthesis. In contrast, the alternative pathway begins in the mitochondria and is initiated by sterol 27-hydroxylase (CYP27A1), represented by the green arrow. This pathway contributes to the synthesis of chenodeoxycholic acid (CDCA) with the involvement of oxysterol 7 α -hydroxylase (CYP7B1). After their synthesis, primary bile acids (CA and CDCA) are secreted into the intestine, where gut microbiota further metabolize them into secondary bile acids, such as deoxycholic acid (DCA) and lithocholic acid (LCA), via dehydroxylation and other modifications. These processes are essential for bile acid recycling and maintaining cholesterol homeostasis. Figure adapted from (Li and Chiang, 2009).

2.6.3.3 Carbohydrate metabolism

The liver plays a critical role in the postprandial glucose homeostasis and disposes large portion of ingested glucose by restricting the acute increase in glucose and insulin levels in the bloodstream after feeding (Dimitriadis et al., 2021). The remaining glucose is further taken up by the other organs including skeletal muscle and non-insulin sensitive tissues such as the brain (Ferrannini et al., 1985). Regardless of the feeding or exercise state, liver significantly contributes to the regulation of blood glucose concentration by producing or consuming carbohydrates. Carbohydrate metabolism in the liver is strictly regulated and involves multiple processes such as glycolysis, glycogenesis, glycogenolysis, and gluconeogenesis. The hepatic glucose production is almost always active except in the fed state and is very important for maintaining the whole body glucose homeostasis (Burgess, 2015). Interestingly, the liver accounts for nearly 90% of the endogenous glucose production in the body (Ekberg et al., 1999; Moore et al., 2012).

2.6.3.3.1 Glucose uptake in the liver

In the postprandial state, blood glucose enters hepatocytes via glucose transporters located on the plasma membrane, which facilitates passive (energy-independent) glucose transport. In humans, the bidirectional glucose transport in hepatocytes is primarily mediated by glucose transporter-2 (GLUT2, also known as solute carrier family 2 member A2, SLC2A2), the main glucose transporter in the liver. GLUT2 has a low affinity but high capacity for glucose, allowing it to efficiently transport glucose from areas of higher to lower concentration, following its concentration gradient (Seyer et al., 2013). Once glucose is taken up by the hepatocytes, it is phosphorylated at the sixth carbon position by the enzyme glucokinase (GCK), forming glucose 6-phosphate (G6P). This phosphorylation reduces intracellular free glucose levels, enhancing further glucose uptake (Agius, 2008). G6P remains trapped inside hepatocytes since it cannot be transported by the glucose transporters. Depending on the body's metabolic state, G6P serves as a precursor for either glycolysis or glycogen synthesis (Fig. 2.16). Via glycolysis, G6P is converted into pyruvate in a ten-step process that produces a net gain of two ATP and NADH molecules per glucose molecule. Pyruvate then enters the mitochondria, where it is decarboxylated to form acetyl-CoA, which is further processed to generate ATP via the TCA cycle and oxidative phosphorylation. In the TCA cycle, acetyl-CoA combines with oxalacetate to form citrate, which can be transported to the cytoplasm. There, citrate is cleaved back into acetyl-CoA and oxaloacetate by ACL (Fig. 2.17). In the cytoplasm, acetyl-CoA can be used as a substrate for DNL and cholesterol synthesis (Rui, 2014).

Alternatively, lipogenesis utilizes pyruvate (produced by the hydrolysis of glucose via glycolysis) as a substrate molecule for FA synthesis (Fig. 2.17). The 3-carbon pyruvate molecule generated via glycolysis is decarboxylated to produce a

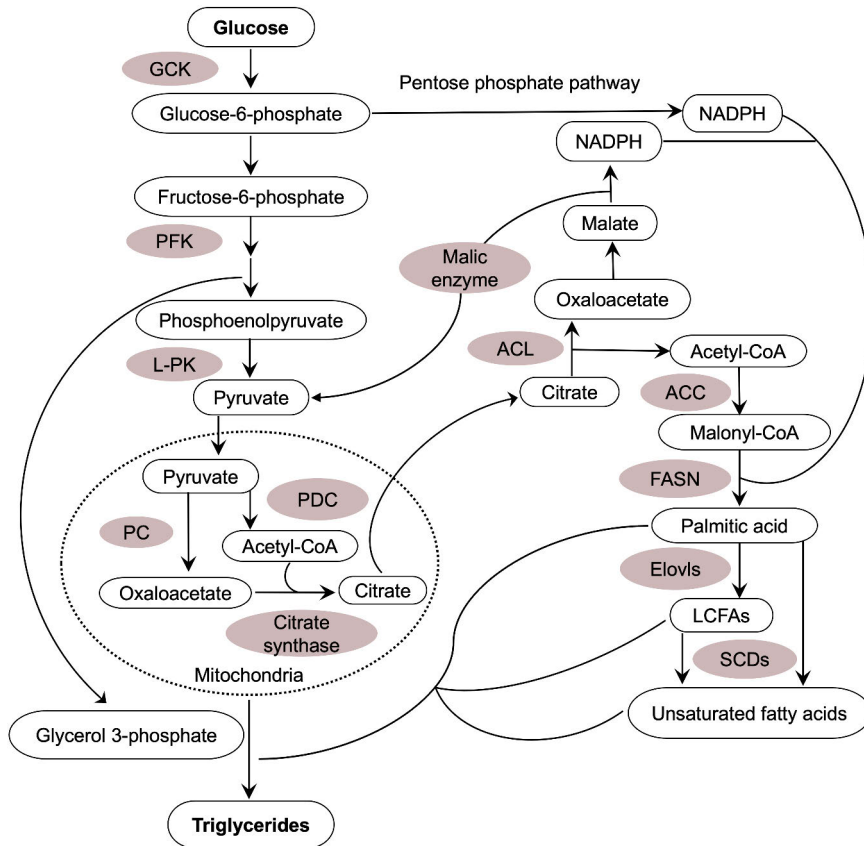


Figure 2.17. Schematic showing brief overview of lipogenic pathways. Pyruvate derived from glycolysis, enters the mitochondria and is converted to acetyl-CoA. Acetyl-CoA combines with oxaloacetate to form citrate via citrate synthase. In the cytoplasm, citrate is cleaved back into acetyl-CoA and oxaloacetate. Oxaloacetate is reduced to malate, generating NADPH, which is then converted back to pyruvate by the malic enzyme. Pyruvate re-enters the mitochondria for the tricarboxylic acid (TCA) cycle, contributing to citrate production. Acetyl-CoA is carboxylated by acetyl-CoA carboxylase (ACC) to form malonyl-CoA, a precursor for FA synthesis. Fatty acid synthase (FASN) uses malonyl-CoA to synthesize palmitic acid, utilizing NADPH. Long-chain fatty acids (LCFAs) are produced by elongating palmitic acid via fatty acyl-CoA elongase (Elovl) enzymes in the endoplasmic reticulum (ER). Stearoyl-CoA desaturases (SCDs) further desaturate LCFAs to form unsaturated FA. Finally, palmitic acid, LCFAs, and unsaturated FA combine with glycerol 3-phosphate to form TG in the cytoplasm. Acetyl-CoA serves as a key precursor in de novo synthesis and hepatic lipogenesis, contributing to TG production via a multi-step process. Enzymes responsible for lipogenesis are marked in pink color. Key abbreviations: ACL – ATP-citrate lyase; ACC – acetyl-CoA carboxylase; FASN – fatty acid synthase; Elovls – fatty acyl-CoA elongases; SCDs – stearoyl-CoA desaturases; TAG – triacylglycerol. Figure adapted from (Rui, 2014).

new, 2-carbon molecule i.e., acetyl CoA in the mitochondria. Acetyl CoA unit, which acts as a building block of FA is further converted into citrate in the TCA cycle before exiting the mitochondria to act as a substrate for lipogenesis. Nicotinamide adenine dinucleotide phosphate (NADPH) is generated by metabolizing G6P molecule via the pentose phosphate pathway. NADPH is an essential component for lipogenesis and biosynthesis of the bioactive molecules such as cholesterol biosynthesis. The dephosphorylation of glucose-6-phosphatase (G6Pase) occurs in the ER employing G6P to release glucose in the fed state (Rui, 2014).

2.6.3.3.2 Glycogen synthesis in the liver

Glycogen synthesis or glycogenesis is a multi-step process, which is initiated by the liver hexokinase enzyme to generate G6P. In the fed state, blood glucose level rises, and glucose enters the liver. The liver converts excess glucose into glycogen via glycogenesis. Glycogen is the most important storage form of glucose and makes up nearly 10% of the total liver weight in healthy individuals (Trefts et al., 2017). Glycogen synthesis continues via the conversion of G6P to glucose 1-phosphate (G1P) using phosphoglucomutase enzyme. The conversion of G1P to uridine diphosphate glucose (UDP-glucose) is mediated via UDP-glucose pyrophosphorylase and binding of UDP-glucose molecules to the carbon position 4 of glucose residues at the end of glycogen chains by glycogen synthase, an enzyme responsible for adding new glucose units to the chain. Glycogen molecule has a branched structure (polysaccharide of glucose) and is stored in the cytoplasm in the form of granules. In a state of lower glycogen availability, the rate of glycogen synthesis increases in the liver to ensure the replenishment of glycogen reserves (Guasch-Ferré et al., 2016). The build-up of hepatic glycogen is primarily activated by insulin, whereas glucagon and adrenaline inhibit hepatic glycogen synthesis (Pagliassotti et al., 1996).

2.6.3.3.3 Glycogenolysis in the liver

Glycogenolysis is not the reverse phenomenon of glycogenesis and occurs in the cytosol. It is the process by which glycogen is broken down into glucose to supply energy and maintain blood glucose levels in the fasted state or in highly intensive training periods. Glycogenolysis or the breakdown of glycogen is accomplished by coordinated actions of two key enzymes, namely glycogen phosphorylase and debranching enzyme. Glycogen phosphorylase utilizes phosphate (Pi) and PLP (pyridoxal phosphate) as cofactors to release G1P from a linear glycogen chain. On the other hand, a glycogen branching enzyme is required for the complete breakdown

of glycogen (Burwinkel et al., 1998). A somewhat similar action is carried out by the lysosomal enzyme acid α -glucosidase or acid maltase, which facilitates the breakdown of glycogen. G1P is derived from glycogen and isomerized into G6P and dephosphorylated to produce glucose by G6P in the cytosol. In the fasted state, when the blood glucose levels fall, the pancreas secretes glucagon, which is the primary hormone that stimulates glycogenolysis (Paredes-Flores et al., 2024). Glycogenolysis is also stimulated by adrenaline, while insulin is an inhibitory hormone for glycogenolysis.

2.6.3.3.4 Gluconeogenesis in the liver

In the fasted state, gluconeogenesis serves as a critical metabolic pathway in maintaining blood glucose homeostasis. This process is stimulated by glucagon and an increased availability of gluconeogenic substrates, while it is inhibited by insulin. However, in the context of insulin resistance, the suppression of hepatic gluconeogenesis by insulin becomes impaired, resulting in an increased rate of glucose production and contributing to hyperglycemia (Hirota and Fukamizu, 2010). Hepatic gluconeogenesis is a complex, genetically heterogenous and strictly regulated process that is initiated in response to changes in energy states and glucose availability (Petersen et al., 2017). Gluconeogenesis has a monumental significance to carnivores in the wild, where the availability of starch is virtually nonexistent. During gluconeogenesis, non-carbohydrate substrates including lactate, glucogenic amino acids, and glycerol are transformed into glucose (Fig. 2.18). Gluconeogenesis comprises several enzymatic steps, which are under the regulation of hormones, nutrient intake, and substrate concentrations. Substrates such as alanine and lactate are first converted into pyruvate and then subsequently to oxaloacetate (OAA) by the action of pyruvate carboxylase (PC) in the mitochondria. The major step in gluconeogenesis is regulated by phosphoenolpyruvate carboxy kinase (PEPCK) (Xiong et al., 2011). TCA cycle intermediates contribute to gluconeogenesis via the conversion of OAA to phosphoenolpyruvate (PEP) by PEPCK. Lastly, PEP enters into the gluconeogenic cycle (Petersen et al., 2017). After several steps of reverse glycolysis, the final step in gluconeogenesis is completed by G6P, which converts G6P to glucose via dephosphorylation. Thereafter, glucose exits the hepatocytes and enters to the circulation with the help of GLUT2 transporters (Fukumoto et al., 1988). Several hormones influence the expression of PEPCK including glucagon, epinephrine, insulin, and glucocorticoids (Chakravarty et al., 2005). Theoretically, glycolysis is the reverse process of gluconeogenesis. However, there are key irreversible glycolysis kinase reactions catalyzed by the action of glucokinase (GK), phosphofructokinase-1 (PFK-1), and pyruvate kinase (PK) (Pilkis and Granner, 1992).

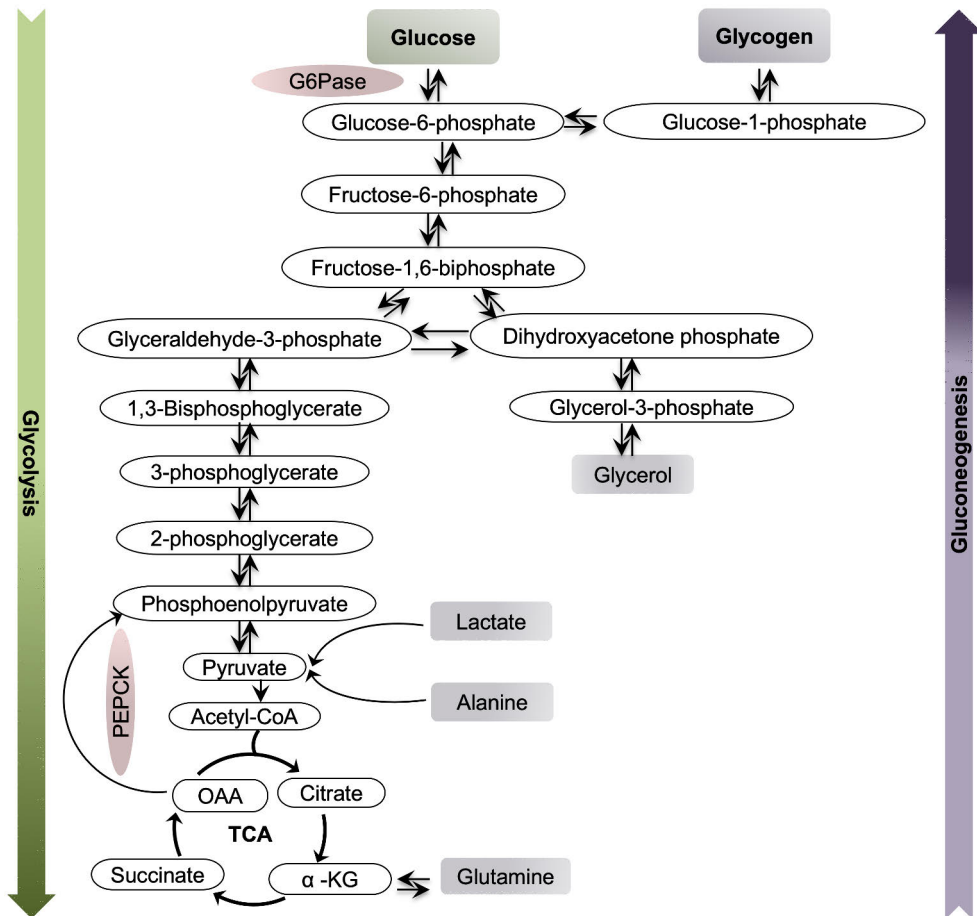


Figure 2.18. Diagram showing the overview of glucose metabolism in glycolysis and gluconeogenesis. Glycolysis is the anaerobic breakdown of glucose into two molecules of pyruvate via a series of 10 enzymatic steps (indicated by green arrow). This metabolic pathway involves the key rate-limiting enzymes including hexokinase (or glucokinase, depending on the tissue type), phosphofructokinase 1 (PFK1), and pyruvate kinase, which regulate the flow of glucose via glycolysis. In contrast, gluconeogenesis (depicted by purple up-arrow) is the anabolic process of synthesizing glucose from non-carbohydrate precursors, such as glucogenic amino acids, lactate, and glycerol. This pathway essentially reverses the glycolytic process, bypassing its irreversible steps via specific enzymes like glucose-6-phosphatase, fructose 1,6-biphosphatase and phosphoenolpyruvate carboxykinase (PEPCK). Key abbreviations: α -KG – α -ketoglutarate; G6Pase – glucose-6-phosphatase; OAA – oxaloacetate; PEPCK – phosphoenolpyruvate carboxykinase. Figure adapted from (Shah and Wondisford, 2020).

2.7 Liver diseases

Fat deposition in the liver depends on the amount of lipids the liver produces or absorbs from the bloodstream, as well as its ability to export lipids to other tissues or use them for energy. An imbalance in these processes results in the accumulation of LDs and can eventually lead to liver steatosis.

2.7.1 Metabolic dysfunction-associated steatotic liver disease

Liver diseases are classified into various categories based on their underlying pathology, clinical manifestations, and pathogenesis. One of the most prevalent forms of chronic liver disease is MASLD, which was previously known as non-alcoholic fatty liver disease (NAFLD). MASLD encompasses a wide range of liver conditions, from simple steatosis, where fat accumulates in the liver cells without significant inflammation or injury, to more advanced stages such as MASH. In MASH, there is considerable hepatocellular ballooning, inflammation, and fibrosis, which can further progress to cirrhosis. As cirrhosis advances, the liver becomes severely scarred, impairing its function and increasing the risk for complications such as liver failure, liver-related mortality, and liver cancer (Fig. 2.19). As the name indicates, MASLD can occur independently of alcohol consumption patterns or quantity. It is mainly characterized by abnormal accumulation of TG in the liver. Liver steatosis is histologically characterized by the presence of lipid macrovesicles in more than 5% of hepatocytes (Brunt et al., 1999). The accumulation of lipids in the liver is classified into mild (6-32%), moderate (33-66%) and severe (>60%) (Younossi et al., 2011). Even though most of the MASLD patients do not progress to MASH, the clinical and economic burden of this disease is significant due to its high prevalence. The prevalence of MASLD varies across different populations, but globally, it affects approximately 30% of individuals (Angulo et al., 2015). Many patients with MASLD could live with steatosis without experiencing significant liver damage. However, simple steatosis can progress to MASH, characterized by hepatocyte ballooning, a sign of cellular injury, along with inflammation and/or fibrosis. Patients with MASH are at a higher risk of developing cirrhosis, which can lead to liver-related mortality or the need for a liver transplant (Michelotti et al., 2013).

The gold standard for diagnosing MASLD used to be the liver biopsy, despite its limitations, such as sample variability, its invasive nature, and the high economic costs involved. Thus, liver biopsy is not recommended as a routine screening method for MASLD diagnosis in the general population. Other diagnostic approaches for MASLD, MASH, and advanced liver fibrosis include non-invasive biomarkers and imaging techniques. However, diagnosing MASALD remains challenging, as the

condition is often detected incidentally, either via elevated plasma liver enzyme levels or the identification of hepatic steatosis during an abdominal ultrasound (Wilkins et al., 2013).

The redefinition of NAFLD represents a significant shift in terminology, highlighting an expanded understanding of liver steatosis and its associated risk factors. MASLD reflects a broader context of metabolic syndrome, emphasizing the interplay between hepatic fat accumulation and systemic metabolic abnormalities (Boldys and Buldak, 2024). The high prevalence of MASLD is predominantly associated with obesity, particularly during childhood and adolescence (Younossi et al., 2018). The excess fat accumulation associated with obesity triggers cellular stress signaling and inflammatory pathways, which contribute to increase muscle insulin resistance, hepatic lipid accumulation and eventually result in organ damage (Hirosumi et al., 2002; Özcan et al., 2004; Yuan et al., 2001). MASLD is strongly associated with T2D, which has similarly emerged as a growing global pandemic. MASLD and T2D often coexist because they share a common underlying mechanism, such as insulin resistance, obesity and metabolic syndrome. However, the relationship between MASLD and T2D is complex and poorly understood, but it has become more evident that these conditions are inter-related and increase the risk for each other. Several studies indicate that an increasing number of patients are diagnosed with both T2D and MASLD. In fact, around 70% of the patients with T2D can have MASLD at the same time (Ciardullo et al., 2023; Younossi and Henry, 2024), indicating that steatotic liver is a common characteristic in T2D patients. Liver biopsies from patients with T2D and MASLD have also revealed that liver steatosis had progressed to MASH in majority of the cases and in some cases even to fibrosis and cirrhosis (Diehl and Choi, 2008), highlighting the contribution of liver diseases to the morbidity and mortality in T2D patients.

The degree of liver steatosis is determined by the flux of fat via hepatocytes (Claydon and Beynon, 2012). However, the size of LDs can vary significantly, with MASLD is primarily associated with macrovesicular steatosis, characterized by fewer but larger LDs. In MASLD, toxicity-induced steatosis or advanced liver injury is often marked by the build of large LDs within the hepatocytes, contributing to disease progression (Tandra et al., 2011). TG accumulation per se is not considered harmful in the liver and may be rather viewed as a protective mechanism against FFA-induced lipotoxicity. As such, the extent of hepatic steatosis may not necessarily correlate with the severity of MASLD or the state of hepatic injury (McClain et al., 2007). Hence, increased deposition of other types of toxic lipids such as FFA, diacylglycerols, free cholesterols, cholesterol ester, ceramide and phospholipids might rather denote the stage of disease progression (Cheung and Sanyal, 2008).

The precise mechanisms leading to MASLD remain unknown, nevertheless, it is known to be influenced by insulin resistance, increased expression of inflammatory cytokines, and oxidative stress. A key feature of MASLD is insulin resistance, that leads to increased DNL in the liver, reduced TG transportation from the liver as VLDL particles and enhanced lipolysis in the adipose tissue (Smith et al., 2020). In particular, increase in circulating FFA due to insulin resistance is the major cause of hepatic lipid buildup in MASLD patients (Donnelly et al., 2005). The stepwise progression of MASLD from a healthy liver to MASH has been explained by a recent “multiple parallel hits” hypothesis, in which hepatic steatosis and lipotoxicity as well as multiple factors outside the liver including adipose tissue inflammation and the gut microbiota contribute to the disease mechanisms (Tilg et al., 2021).

The first-line treatment of MASLD is weight loss by diet intervention and other lifestyle changes. Furthermore, associated risk factors such as hypertension, T2D and dyslipidemia need to be effectively treated with lifestyle changes and medication. However, there are only few specific medications available for MASLD that are recommended in treatment guidelines. For example, MASLD patients without T2D could benefit from taking vitamin E and pioglitazone, since the powerful antioxidant properties of vitamin E is believed to target the underlying oxidative stress, whereas pioglitazone is capable of ameliorating insulin resistance (Cusi, 2016; Sanyal et al., 2010). Additionally, the U.S. Food and Drug Administration (FDA) recently approved Rezdiffra (resmetirom) for the treatment of MASH with fibrosis (Vidal-Cevallos and Chávez-Tapia, 2024). Therefore, increasing our knowledge on the pathogenetic mechanisms of MASLD and the potential links between steatosis and liver damage (MASLD, MASH and cirrhosis) is essential to identify novel therapeutic targets for the treatment of a whole cluster of these diseases.

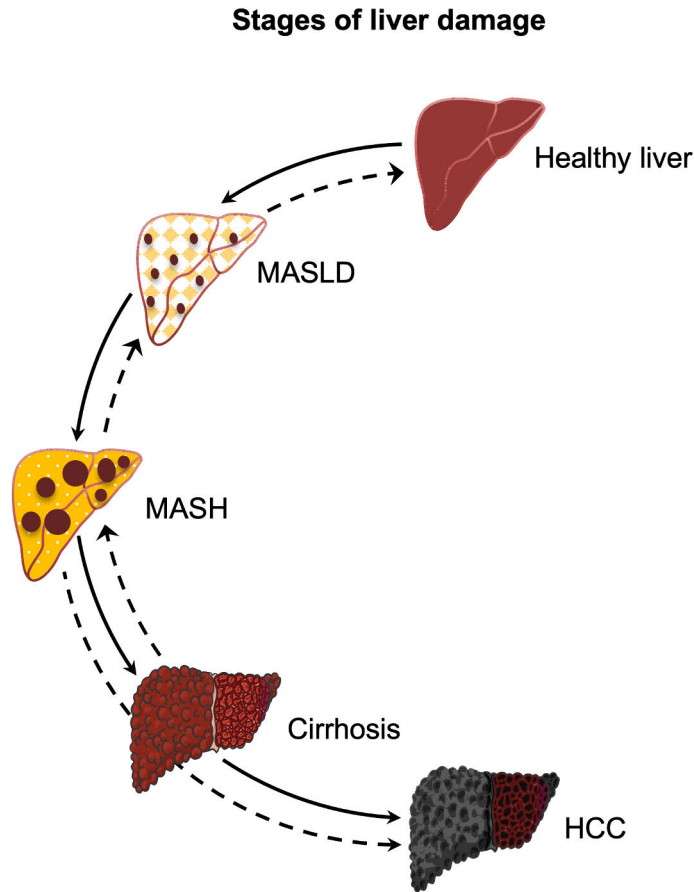


Figure 2.19. Stages of liver damage in the progression of metabolic dysfunction-associated steatotic liver disease (MASLD) to cirrhosis and hepatocellular carcinoma (HCC). The chronic liver disease progresses via four stages. The initial stage is simple steatosis, characterized by fat accumulation in the liver due to obesity and metabolic syndrome affecting 25-30% of the population. The disease can advance to metabolic dysfunction-associated steatohepatitis (MASH), marked by hepatic inflammation and apoptosis, seen in 7-30% of MASLD patients. Fibrosis, the next stage, impairs liver function and can progress to cirrhosis, which affects 4-14% of MASLD patients. The final stage is hepatocellular carcinoma (HCC), occurring in 0.2-0.5% of MASLD cases, and may develop from MASH with or without cirrhosis. HCC often results in liver failure, requires liver transplantation. The dotted arrow indicates potential reversibility if appropriate treatment is applied. Image adapted from (Engelmann and Tacke, 2022). Figure created using image from Servier Medical Art, licensed under a Creative Commons Attribution 4.0 International License.

2.7.1.1 Metabolic dysfunction-associated steatohepatitis

MASH is the updated term replacing non-alcoholic steatohepatitis (NASH), representing the more severe stage of MASLD. MASH is characterized by hepatocellular ballooning, a result of excessive fat accumulation in the liver cells.

This process is often accompanied by lobular inflammation, and in more advanced cases, can lead to liver fibrosis. If left unchecked, this condition can progress to cirrhosis or hepatocellular carcinoma. It is believed that around 10-25% of the patients with MASH could progress to cirrhosis (Matteoni et al., 1999). However, it is difficult to predict whether MASH patients eventually develop cirrhosis due to the complex multifactorial etiology of MASH contributed by sex, lifestyle, genetic polymorphisms, ethnicity, and health status. MASLD is becoming a dominant chronic liver disease in the developed world, while MASH is predicted to become the major cause of liver transplantation worldwide (Angulo et al., 2015). Amongst the many other causes, inflammation is the key factor in the development of MASH and involves Kupffer cells, infiltrating monocytes, T cells, and pro-inflammatory and anti-inflammatory macrophages. These cells respond to increased accumulation of TG by the secretion of cytokines and chemokines, and promote hepatic injury, apoptosis and tissue remodeling (Arrese et al., 2016; Jump et al., 2018, 2013). In addition, mitochondrial dysfunction because of hyperinsulinemia produces cytotoxic lipid species, which generate reactive oxygen species (ROS) in the hepatocytes. ROS stimulate the production of proinflammatory cytokines and participate in the progression of MASH (Buzzetti et al., 2016). Although there are not many options available for the treatment of MASH in the current market, a thyroid hormone receptor-beta (THR-beta) agonist also known as resmetirom has been recently shown to reduce hepatic fat content and to halt or even reverse the progression of fibrosis in patients with MASH (Harrison et al., 2024; Karim and Bansal, 2023). Moreover, drugs used for the treatment of T2D have shown promising effects and thereby could also be used for the treatment of MASH along with type 2 diabetes (Sumida and Yoneda, 2018). Currently, several drugs, including obeticholic acid, elafibranor, and selonertib, are being evaluated for their potential therapeutic benefits in treating MASH and liver fibrosis. If proven effective, these treatments could represent a groundbreaking advancement for patients suffering from these conditions.

2.7.1.2 Cirrhosis and hepatocellular carcinoma

Liver cirrhosis is defined as the late stage of the liver disease, in which a healthy liver is replaced with scar tissue, preventing it from working normally and causing permanent damage to the liver. Cirrhosis can be caused by multiple factors including chronic hepatitis B or C, but with the rising obesity epidemic, MASLD has become one of the main causes of cirrhosis. Liver fibrosis due to sustained injury can progress to a stage of advanced fibrosis and culminates in end-stage liver disease, e.g., liver cirrhosis, decompensated liver disease or hepatocellular carcinoma. Nevertheless, the development of liver fibrosis may take several years and is often asymptomatic in nature. Liver biopsy used to be the gold standard for diagnosing liver

fibrosis or cirrhosis in the past. However, with the invention of elastography, a non-invasive technique that measures liver stiffness, liver fibrosis can now be frequently examined without a biopsy. While elastography provides a reliable prediction of fibrosis severity, liver biopsies may still be necessary for cases requiring detailed histological information, even though they carry higher risks, requires significant resources and specialized expertise. Thus, performing a liver biopsy is not applicable in every clinical setting and is not appropriate for screening of the disease stage. Currently, there are no specific curative treatments for liver cirrhosis. However, managing the underlying condition that led to cirrhosis can slow disease progression and help prevent complications. Early intervention aiming at the root cause is of utmost important for mitigating further liver damage and improving patient prognosis.

2.8 Adipose tissue

Adipose tissue is the body's largest energy reservoir and a major source of metabolic fuel, functioning as an active endocrine organ with significant lipid metabolism. Most of the energy reserves in human are stored as TG within adipocytes. In the fed state, adipose tissue regulates lipid flux by increasing TG clearance from the plasma and by suppressing the release of FFA into circulation (Frayn, 2002). TG synthesis in adipocytes occurs via two primary pathways: first, via DNL, where non-lipid precursors, such as carbohydrates, are converted into FA; and second, via the uptake of circulating FA from lipoproteins like CM or VLDL. These FA are esterified into TG, contributing to lipid storage in adipose tissue. LPL, an enzyme produced by adipocytes, is transported to the luminal surface of endothelial cells, where it hydrolyzes TG in lipoprotein particles, releasing FFA for uptake by adipocytes. This LPL activity is essential for lipid storage and overall energy balance. Adipose tissue is classified into two primary types based on anatomical location: subcutaneous or visceral (Shen et al., 2003).

Adipose tissue is further categorized as either WAT or brown adipose tissue (BAT). WAT is the predominant form, acting as a fat reservoir between organs, providing insulation, and serving as an energy source during fasting or intense physical activity. WAT secretes adipokines, including adiponectin, leptin, interleukins (IL-6, IL-1 β), and TNF- α , which regulate glucose and lipid metabolism, inflammatory responses, blood pressure, and appetite (Galic et al., 2010; Guerre-Millo, 2004). In contrast, BAT, found primarily in new-born, plays a role in thermogenesis via the expression of uncoupling protein 1 (UCP1), which uncouples mitochondrial respiration and generates heat (Lee et al., 2013). Notably, thermogenically active BAT has also been identified in adult humans (Virtanen et al., 2009). The amount of BAT is inversely related to body mass index (BMI), and a

decrease or deficiency in BAT is associated with insulin resistance and obesity in animal models (Bartelt and Heeren, 2014). In humans, activating BAT via increased glucose uptake and energy expenditure has shown promise as a novel approach to combat obesity (Scheele and Nielsen, 2017).

Adipose tissue also protects against lipotoxicity by absorbing excess circulating FFA, thereby preventing ectopic deposition in organs that could lead to damage (Cusi, 2012; Frayn, 2002). It is composed of 50% adipocytes by cell number, with the remainder 50% consisting of various cell types, including immune and endothelial cells, which together form the stromal vascular fraction. Adipocytes secrete adipokines, while immune cells release cytokines such as IL6 and TNF- α (Gustafson and Smith, 2015). Adipose tissue has a remarkable ability to expand and store energy primarily as TG via two mechanisms: hypertrophy (increase in cell size) and hyperplasia (increase in cell number). However, there is a limit to this storage capacity, and once exceeded, lipids accumulate in ectopic tissues, leading to metabolic dysfunction and insulin resistance (Hardy et al., 2012; Virtue and Vidal-Puig, 2010). Excessive expansion of adipose tissue is associated with various metabolic consequences, including hepatic steatosis and inflammation. Although the precise links between obesity and metabolic diseases are not fully understood, they continue to be an area of active research.

2.8.1 The lipid droplets

LDs are highly dynamic organelles in the cytoplasm of adipocytes, playing key roles in cellular lipid metabolism, membrane trafficking, and cell signaling. They protect against lipotoxicity by storing excess lipids and essential for maintaining lipid homeostasis within the cell (Listenberger et al., 2003). The core of the LDs is composed primarily of neutral lipids such as TG and cholesterol esters, while a phospholipid/cholesterol monolayer surrounds the core, acting as a barrier to separate the hydrophobic lipids from the cytosol (Olzmann and Carvalho, 2019). LDs contain various lipids, including phosphatidylcholines (PC), phosphatidylethanolamines (PE), and phosphatidylinositol (PI), with PC being the most abundant in the LDs membrane (Bartz et al., 2007; Loizides-Mangold et al., 2014). The biogenesis of LDs occurs at the ER via three different biological processes: first, the synthesis of neutral lipids like TG and CE; second, the nucleation of these lipids along with perilipin proteins; and third, the release of LDs from the ER into the cytosol (Hsia et al., 2024). LDs are coated with various proteins that regulate lipid homeostasis in the cell by interacting with other organelles (Mak, 2012; Murphy, 2012). In adipocytes, the most abundant proteins on the surface of LDs are perilipins. Early studies have shown that perilipins inhibit lipolysis and contribute to lipid homeostasis (Brasaemle et al., 2000). Among the perilipins,

perilipin 1 (PLIN1) and perilipin 4 (PLIN4) are highly expressed in adipocytes, while perilipin 5 (PLIN5) is predominantly expressed in the heart (Greenberg et al., 1991). PLIN1 plays a critical role in regulating lipolysis via interaction with HSL and ATGL (Granneman et al., 2009). Perilipin 2 (PLIN2) is essential for the formation and stability of LDs (Xu et al., 2019), while perilipin 3 (PLIN3), though not directly involved in lipolysis, may contribute to the initiation of LDs biogenesis (Skinner et al., 2009). Additionally proteins such as comparative gene identification-58 (CGI-58) and others on the surface of LDs are also involved in regulating lipolysis in adipose tissue (Yu et al., 2020).

2.8.2 Adipose tissue lipolysis

Adipose tissue, functioning as an endocrine organ, plays a critical role in lipid homeostasis and inflammation. It serves as the primary energy reservoir for other organs by storing TG, which, when mobilized, release glycerol and FFA via lipolysis. Lipolysis is explicitly regulated by hormonal and biochemical signals in response to nutritional state. The major factors controlling lipolysis in humans are autonomic nervous system and insulin. Catecholamines stimulate and insulin suppresses lipolysis via PKA mediated phosphorylation of HSL and perilipins (Frühbeck et al., 2014). Multiple hormones such as growth hormone, ACTH, cortisol, thyroid hormones, and glucagon are also known to regulate lipolysis in the adipocytes. Amongst different hormones, insulin is quantitatively and qualitatively the most relevant as it inhibits lipolysis (Carey, 1998). In addition, several dietary nutrients such as calcium, ethanol, caffeine, and other methylxanthines have been found to regulate lipolysis (Duncan et al., 2007; Murosaki et al., 2007; Westerterp-Plantenga et al., 2005). On the other hand, the basal level of lipolysis is regulated by sex, age, physical activity, fat depot location, species, and genetic variance (Frühbeck and Gómez-Ambrosi, 2003; Langin et al., 2000). Additionally, lipolytic rate might be also influenced by genetic variation. In fact, variation in adrenoceptors has been widely investigated for its effect on lipolysis and associated obesity (Umekawa et al., 1999). Negative energy balance such as fasting or starvation, increases mobilization of FFA in response to catecholamines and reduces insulin production. In contrast, during energy deprivation states such as prolonged intensive training, plasma FFA increases in response to the elevated catecholamines and the reduced insulin production (Lange, 2004). Dysregulation of lipolysis and lipid metabolism has been shown to be implicated in a diverse range of metabolic disorders including obesity, T2D, and MASLD (Yang and Mottillo, 2020). Impaired lipolysis is often associated with obesity, which may increase the rate of basal lipolysis, reduce catecholamine-stimulated lipolysis and contribute to the development of insulin resistance (Large et al., 1999; Reynisdottir et al., 1995).

The basic function of adipose tissue is to store energy in the form of TG and release energy in the form of FFA. FA taken from circulation are esterified and stored as TG in the adipocytes. The hydrolysis of stored TG in adipocytes depends on demand. In case of active hydrolysis, FFA are released into the circulation and eventually delivered to the peripheral tissues for mitochondrial β -oxidation to generate ATP (Large et al., 2004). Lipolysis is the process of sequential hydrolysis of TG by three different enzymes (Nielsen et al., 2014). Within adipocytes, the first and the rate-limiting step in lipolysis is governed by ATGL, which produces DG via the hydrolysis of TG. In the second step, the newly formed DG are hydrolyzed by the HSL to yield MG. In the final step of lipolysis, MG molecule is cleaved into glycerol and FA by MGL (Edwards and Mohiuddin, 2024). Previous studies have described that ATGL is critical for TG lipolysis stored in LDs and controls the substrate availability for FAO as well as modulates the progression of hepato-steatosis (Ong et al., 2011; Reid et al., 2008; Wu et al., 2011). In addition, ATGL ablation in mice adipocytes has been shown to reduce lipolysis without increasing the overall fat mass and distribution (Schoiswohl et al., 2015). Furthermore, ATGL role in lipid homeostasis has been relatively well-reported in other tissues such as the heart, and skeletal muscle. Nevertheless, regulation of ATGL in the liver is poorly understood. In contrast to the adipose tissue, ATGL expression in the liver is relatively low, however, upregulated in the fasting state (Heier et al., 2015). Moreover, hepatic ATGL levels have been shown to be lower in MASLD patients (Kato et al., 2008). A key function of hepatic ATGL in lipid metabolism is further supported by the global deficiency of ATGL, which showed the reduced rate of mitochondrial β -oxidation indicating ATGL influence on hepatic energy metabolism (Ong et al., 2011). Similarly, progressive hepatic steatosis was observed in liver-specific ablation of the ATGL mouse model (Wu et al., 2011). Therefore, global and liver-specific loss of ATGL mouse models have strengthened our understanding of its tissue-specific roles in regulating hepatic lipid homeostasis and the progression of liver diseases (Missaglia et al., 2019; Schweiger et al., 2008; Zhou et al., 2016). While the specific roles of MGL and HSL in hepatocyte lipolysis remain unclear, studies in mice have shown that genetic ablation of *HSL* protects against diet-induced and genetic obesity (Harada et al., 2003; Sekiya et al., 2004).

2.8.3 Liver-adipose tissue crosstalk

Both the liver and adipose tissue play vital roles in regulating whole-body energy homeostasis, however, they are challenged by the persistent nutrient surplus as seen in the case of obesity. The prolonged metabolic stress triggers adipose tissue dysfunction, inflammation, and adipokine release leading to increased lipid flux to the liver (Azzu et al., 2020). After feeding, a small amount of dietary FA is

assembled into TG and stored in the form of LDs in the hepatocytes. The excess lipids are then exported into the circulation and further stored in adipose tissue and other extra-hepatic tissues as an energy reservoir (Angulo, 2002; Scheja and Heeren, 2016). In this context, liver acts as a pleiotropic endocrine organ to access nutrients first and then affects lipid metabolism in other organs. However, the exact mechanisms by which cell-specific signals from the liver modulate lipid metabolism in other organs have not been identified. Adipose tissue dysfunction has been shown to increase lipids and FFA levels in the serum, causing lipotoxicity and increased accumulation of ectopic fat, e.g., in the liver as in the case of MASLD (Virtue and Vidal-Puig, 2010). Similarly, the increased release of adipokines due to dysfunctional adipose tissue has been shown to induce chronic low-grade inflammation and the development of obesity-linked metabolic syndrome (Skurk et al., 2007). In addition, hepatic fat accumulation together with insulin-resistant state modulates hepatic lipid metabolism pathways, which results in the selective build-up of toxic lipid species, and aggravates inflammation, and fibrosis as seen in MASLD. The pathogenesis of the MASLD is critically determined by the enhanced lipolysis in the adipose tissue and the subsequent increase in circulating FFA and its flux to the liver. Increased FFA flux into the liver disturbs the insulin sensitivity and promotes hepatic DNL, which further predisposes to hepatic steatosis and lipotoxicity. Lipid overload causes redistribution of lipids among metabolic organs, including the liver, adipose tissue, and muscle. The pathophysiological mechanism of MASLD at the molecular level has not been completely identified yet. Thus, the crosstalk between liver and adipose tissue might play a crucial role for maintaining whole-body energy homeostasis and provide insights into the underlying mechanisms in the development of MASLD.

3 Aims

The aim of this thesis was to investigate the regulatory role of MC1R in hepatic cholesterol and FA metabolism using genetically modified mouse models for in vivo studies and liver cell culture models for in vitro experiments.

The specific objectives of this study were:

1. To determine the expression of MC1R in the liver and explore its regulation both in vivo and in vitro (Study I).
2. To examine the impact of hepatocyte-specific deletion of MC1R on cholesterol and bile acid metabolism in mice (Study I).
3. To elucidate the functional role of MC1R in the regulation of FA metabolism in vivo and in vitro (Study II).

4 Materials and Methods

4.1 Animals and animal models

All experimental procedures were conducted on adult female mice (Study I) and adult male mice (Study II). The mice were housed in groups with their littermates at the Central Animal Laboratory, University of Turku, under a 12-hour light/dark cycle, with controlled temperature ($21 \pm 1^\circ\text{C}$) and humidity ($50 \pm 5\%$). The number of mice used in each experiment is specified in the figure legends in the result section. Recessive yellow mice ($\text{Mc1r}^{\text{e/e}}$), which are homozygous for the Mc1r^{e} allele and lack functional MC1R due to a single base deletion mutation, along with their non-mutant littermate controls (WT), were obtained from the Jackson Laboratory (Strain # 000060, Bar Harbor, ME, USA). Both $\text{Mc1r}^{\text{e/e}}$ and WT mice were maintained on either a regular chow diet or Western-type diet (RD Western Diet, D12079B, Research Diets Inc, NJ, USA) for a total of 12 weeks, starting at eight weeks of age. The formulation of Western diet is provided in (Appendix Table 1). Hepatocyte-specific MC1R knock-out mice (Mc1r LKO) were generated by crossing mice homozygous for a floxed *Mc1r* allele ($\text{Mc1r}^{\text{fl/fl}}$, the Jackson Laboratory, strain #029239) (Takeo et al., 2016) with transgenic $\text{Alb}^{\text{Cre/+}}$ mice (B6N.Cg-Speer6-ps1Tg(Alb-cre)1MGn/J, the Jackson Laboratory, strain #018961) expressing Cre recombinase under the control of the albumin promoter ($\text{Alb}^{\text{Cre/+}}$) (Postic et al., 1999). These genetically modified mice were identified using earmarks and housed with same sex littermates, regardless of genotypes with 1-6 animals per cage. Age-matched $\text{Mc1r}^{\text{fl/fl}}$ and $\text{Mc1r}^{\text{fl/+}} \text{Alb}^{\text{Cre/+}}$ mice were used as controls. Mc1r LKO mice were fed either a regular chow-diet (Study I) or a cholesterol-rich Western-type diet (Study II). Efficient recombination of the loxP-flanked allele in Mc1r LKO mice was confirmed by genotyping liver samples for the recombined allele using the following primers: ACC ACT GCG TGC TAT CCT G (*Mc1r* 5' forward), ACC CCT TCC CTT GAG GAG T (*Mc1r* 5' reverse), and GAA CTC TGA GGT CAC TAT TTT CTG GAG A (*Mc1r* 3' reverse).

4.2 Ethical considerations

All animal procedures were approved by the local ethics committee (Animal Experiment Board in Finland, License Numbers: ESAVI/6280/04.10.07.2016 and ESAVI/1260/2020). The experiments were conducted in compliance with institutional and national guidelines for the care and use of laboratory animals. The studies were carefully designed following the ethical 3R principles (Replacement, Reduction and Refinement) to ensure ethical animal testing. In vivo experiments were replaced with in vitro experiments whenever possible to minimize animal use. The experiments were meticulously planned to minimize stress and suffering. Animals were closely monitored via regular assessments of food and water intake, body weight measurements, and observations of physical condition. For each experiment, mice were euthanized using CO₂ asphyxiation following a 4-hour fast, with efforts made to minimize external stress.

4.3 In vivo experiments

4.3.1 Body weight and body composition measurement

Body weight was measured weekly throughout the 12-week intervention period. Body composition (fat and lean mass) was assessed in vivo using quantitative nuclear magnetic resonance (NMR) scanning (EchoMRI-700, Echo Medical System, Houston, TX, USA). Measurements were taken from conscious mice either before the regular weight measurement period (Study I) or before the start of the dietary intervention (Study II), as well as at the end of the experiments (Study I and II). Each animal was scanned twice, and the average values for body fat mass, lean tissue mass, and relative fat and lean mass (% of the total body weight) were calculated from the two scans.

4.3.2 Food intake

Food intake was monitored weekly throughout the entire experimental period. Energy intake was calculated based on the caloric values of 3.82 kcal/g for the chow diet and 4.67 kcal/g for the Western diet (caloric values provided by Research Diets Inc). For group-housed mice, total food consumption per cage was calculated by subtracting the amount of food left (including any food spilled in the cage) from the initial amount provided, and then dividing the resulting value by the total number of mice per cage (2-6 mice/cage). Food consumption was expressed as average daily food intake or energy intake per mouse.

4.3.3 Glucose and insulin tolerance tests

Glucose sensitivity was assessed *in vivo* using a glucose tolerance test (GTT). For Mc1r^{ec} mice, GTT was performed once at the end of the experiment, while for Mc1r LKO mice, it was performed twice during the experimental period. The first GTT was conducted at week 4 of the diet intervention, and the second GTT was conducted at week 11, just before the end of the experiment. Mice were fasted for 4 hours prior to the GTT. They then received an intraperitoneal (i.p.) injection of glucose (1g/kg lean mass). Blood glucose levels were measured from the tail vein at 20-, 40-, 60-, and 90-minutes post injection using the Precision Xtra Glucose Monitoring Device (Abbott Diabetes Care, Abbott Park, CA, USA). Blood glucose was also measured immediately before glucose injection. In Study I, mice were additionally subjected to insulin tolerance test (ITT). After fasting for 4 hours, mice were injected with 0.75 IU/kg of insulin (Protaphane FlexPen, Novo Nordisk, Bagsvaerd, Denmark) via i.p. injection. Blood glucose levels were measured at 0-, 20-, 40-, 60-, and 90-minutes following insulin administration. Blood glucose was also measured just before the insulin injection. Additionally, blood glucose concentration was measured from the tail vein just before sacrifice after a 4-hour fast.

4.3.4 Feces collection for bile acid analysis

Female mice (n = 4-5 per genotype) were randomly selected for feces collection and individually housed in separate cages with minimum bedding material (Study I). Feces were collected over a 48-hour period, and body weight was measured before and after the collection period. Water and food consumption during this time were also measured. Separate tweezers were used to collect the feces from each individually housed mouse, and samples were stored into 50 mL falcon tubes. After collection, the mice were returned to their original cages. The specimens were then dried under airflow at 60°C for 48 hours, after which the dry weight was recorded. Fecal samples were stored at -80°C until they were assayed for bile acids.

4.3.5 Tissue collection

Mice were fasted for 4 hours and euthanized via CO₂ asphyxiation. Terminal blood (0.5-1.0 mL) was collected by cardiac puncture, centrifuged at 380 g for 20 minutes at 4°C, and plasma stored at -80°C for cholesterol and TG analysis. The entire liver was excised and weighed. In study II, the excised liver was also subjected to quantitative NMR scanning to measure liver composition. For histology analysis, a mid-section of the left lateral lobe was fixed in 10% formalin for 24 hours, dehydrated in 70% ethanol, and embedded in paraffin. Liver samples designated for RNA extraction, protein quantification, and lipid analysis were weighed, snap-frozen

and stored at -80°C . Samples of WAT from gonadal, subcutaneous, and retroperitoneal regions, as well as BAT, samples were collected, weighed, and snap-frozen, and stored at -80°C .

4.4 Ex vivo and in vitro assays

4.4.1 Blood parameters

Plasma samples were used to quantify total cholesterol and TG concentrations using enzymatic colorimetric assay kits (CHOD-PAP and GPO-PAP, mtDiagnosics, Idstein, Germany) according to the manufacturer's instructions. Plasma NEFA concentration was determined using the FFA Fluorometric Assay Kit (Item No. 700310, Cayman Chemicals, USA), following the manufacturer's instructions.

4.4.2 Hepatic lipid analysis

For hepatic lipid assessment, a ~ 100 mg piece of the liver from the left lobe was homogenized in $500\ \mu\text{L}$ of phosphate-buffered saline (PBS) containing 0.1% NP-40 (Abcam) using the Qiagen TissueLyser LT Bead Mill (QIAGEN, Venlo, Netherlands). The homogenate was then centrifuged to remove insoluble components. Cholesterol and TG concentrations in the liver homogenates were quantified using CHOD-PAP and GPO-PAP reagents, respectively. For hepatic lipid content analysis, a transverse piece of the left lobe was embedded in OCT compound (Tissue-Tek®, Sakura Finetek USA Inc, Torrance, CA, USA) and cryo-sectioned into $4\ \mu\text{m}$ -thick slices. The liver sections were stained with Oil-Red-O (ORO), counterstained with hematoxylin, and scanned using Panoramic 250 digital slide scanner (2DheHISTECH Kft, Budapest, Hungary).

4.4.3 Measurement of bile acids

Total and individual bile acids were measured in plasma, liver, and fecal samples. Feces were collected over 48 hours from individually housed mice. Total bile acids were extracted and analyzed using an ultra-high-performance liquid chromatography tandem-mass spectrometry method (UHPLC-MS/MS), as previously described (Jäntti et al., 2014).

4.4.4 Histology, immunohistochemistry, and immunofluorescence staining

To evaluate liver morphology and extent of hepatic fibrosis, 4 μm thick serial sections were prepared from paraffin-embedded liver tissues. Hematoxylin and eosin (H&E) staining and Picrosirius red staining (abcam, #ab150681) were performed according to manufacturer's protocols. For immunohistochemistry targeting MC1R, antigen retrieval was conducted using 10 mM sodium citrate buffer (pH 6.0). The sections were then quenched with 1% hydrogen peroxide (H_2O_2) and blocked using 5% normal horse serum with 1% bovine serum albumin (BSA). The liver sections were incubated overnight with a primary antibody against MC1R (Elabscience, Texas, USA, # E-AB-15765), followed by incubation with a biotinylated secondary antibody conjugated to horseradish peroxidase. The detection was performed using diaminobenzidine (DAB) as a chromogen (ABC kit, Vector Labs). For double immunofluorescence staining, the sections were incubated overnight with antibodies against MC1R (Elabscience), serum albumin (Bioss Antibodies, # BSM-0945M), and cytokeratin 19 (CK-19, Novus Biologicals, # NBP2-44827). The detection was carried out using fluorochrome-conjugated secondary antibodies, specifically anti-rabbit Alexa Fluor 647 and anti-mouse, anti-rat, or anti-goat Alexa Fluor 488 (Invitrogen). Image acquisition and analysis were performed using Panoramic/Caseviewer (3DHISTECH, Hungary) and ImageJ software (NIH, Bethesda, MD, USA).

4.4.5 Cell culture and treatment

An HepG2 cells (ATCC HB-8065), authenticated by STR profiling and confirmed to be free of mycoplasma contamination, were obtained from the American Type Culture Collection (Rockville, MD, USA). The cells were maintained in Dulbecco's modified Eagle's medium (DMEM, Sigma-Aldrich) supplemented with 10% (v/v) heat-inactivated fetal bovine serum (FBS, Gibco), 100 U/mL penicillin (Gibco), and 100 $\mu\text{g}/\text{mL}$ streptomycin (Gibco). Cultures were incubated at 37°C in a humidified atmosphere with 5% CO_2 . HepG2 cells were grown in 175 cm^2 culture flask with 15 mL of complete medium, and medium was refreshed as needed. Cells were maintained at approximately 75% confluence. For passaging, cells were rinsed twice with pre-warmed (37°C) phosphate-buffer saline (PBS), detached using 0.05% trypsin-EDTA solution, and neutralized with complete growth medium. Sub-culturing was performed at a 1:4 ratio every 3 days or a 1:8 ratio every 6 days. To investigate the regulation of MC1R expression, HepG2 cells were serum-deprived in medium containing 0.5% FBS for 16 hours. Cells were then treated with 200 $\mu\text{g}/\text{mL}$ of LDL (CliniSciences), 10 μM of atorvastatin (Sigma-Aldrich), or 500 μM of palmitic acid (Sigma-Aldrich) for 1, 3, 6, or 24 hours. For evaluating MC1R

activation effects, cells were similarly serum-deprived and treated with the endogenous MC1R agonist α -MSH (abcam, # ab120189) or the selective MC1R agonist LD211.

4.4.5.1 Primary mouse hepatocyte isolation and treatment

Primary mouse hepatocytes were isolated from 4-month-old male C57B1/6N mice to investigate the effects of MC1R activation. The peristaltic pump (ISMATEC instruments) was initially flushed with 70% ethanol, followed by pre-warmed distilled water and then pre-warmed perfusion medium (GIBCO #17701-038). Mice were anesthetized with ketamine (75 mg/kg, Ketaminol, Intervet Oy, Finland) and medetomidine (1 mg/kg, Cepetor, ScanVet Oy, Finland). The abdominal cavity was opened to expose the liver, portal vein, and inferior vena cava (IVC). A 24 G catheter was inserted into the IVC, and perfusion was initiated at a rate of 4.5 mL/min with perfusion medium, while the portal vein was immediately cut open to ensure adequate flow. Perfusion continued for approximately 5 minutes or until the effluent ran clear. Subsequently, the liver was perfused with 30 mL of digestion medium containing high-glucose DMEM, 1% Penicillin/Streptomycin (Thermo Fischer), 1 mg/mL collagenase IV, and 10 μ g/mL HEPES, 10% (v/v) FBS. The liver was excised, transferred to a petri dish containing 20 mL of cold wash medium (GIBCO #17704024), and kept on ice. The gall bladder was removed, and the liver tissue was gently disrupted using forceps. The resulting cell suspension was filtered via a 70 μ m strainer into a 50 mL tube. Additional wash medium was used to collect remaining cells from the dish. Cell suspension was centrifuged at 50 x g for 3 minutes at 4°C. The cell pellet was resuspended in 10 mL of cold wash medium and mixed with 40% Percoll solution (Sigma P1644). Subsequently, 10 mL of 90% Percoll-PBS solution was added, and the suspension was gently mixed by inversion approximately 20 times. The mixture was centrifuged at 300 x g for 10 minutes at 4°C. The viable hepatocyte pellet was resuspended in 20 mL of wash medium, followed by another centrifugation at 50 x g for 3 minutes at 4°C. Finally, the cell pellet was resuspended in maintenance medium; William's E medium (GlutaMAX Supplement, GIBCO #32551087) supplemented with 10% FBS and 1% Pen/Strep. Cells were plated in 12-well plates (2×10^5 cells/well) or 6-well plates (4×10^5 cells/well) and incubated at 37°C in a humidified 5% CO₂ atmosphere. Experiments were conducted approximately 12 hours after plating. For gene expression analysis, hepatocytes were treated with varying concentrations of the MC1R agonists α -MSH (0.1 nM, 10 nM, or 1 μ M) or LD211 for 3 hours at 37°C. For protein analysis, cells were treated with 1 μ M of α -MSH or LD211 for different time points (0, 5, 15, 30, or 60 minutes). In separate experiments, these treatments were extended to longer durations (0, 1, 3, 6, or 24 hours).

4.4.5.2 Cyclic AMP determination

Intracellular cAMP levels were measured in HepG2 cells. Cells were plated in 12-well plates (PhenoPlate, PerkinElmer) and serum-starved in DMEM containing 0.5% FBS for 18 hours. Following serum starvation, cells were pre-treated with 0.1 mM 3-isobutyl-1-methylxanthine (IBMX, Sigma-Aldrich) for 30 minutes to inhibit phosphodiesterase activity. Subsequently, cells were stimulated with either α -MSH or the selective MC1R agonist LD211 at concentrations of 0.1 nM, 10 nM, or 1 μ M for 30 minutes at 37°C. Forskolin (10 μ M, Sigma-Aldrich) was used as a positive control in separate wells. After incubation, cells were washed three times with cold PBS, lysed with 0.1 M HCl, and centrifuged at $600 \times g$ for 10 minutes at 4°C. The supernatant was collected for cAMP analysis using a Cyclic AMP Select ELISA kit (Cayman Chemical, #501040), following the manufacturer's instructions. cAMP levels were normalized to total protein concentrations determined by the Pierce BCA Protein Assay Kit (Thermo Fisher). The results were expressed as a percentage relative to control samples.

4.4.5.3 Fluorescently labelled LDL and HDL uptake assay

To assess the uptake of lipoproteins, HepG2 cells were seeded at a density of 40,000 cells per well in 96-well plates (PhenoPlate, PerkinElmer) and serum-starved in DMEM supplemented with 0.5% FBS for 18 hours. The cells were then treated with α -MSH or the selective MC1R agonist LD211 at concentrations of 0.1 nM, 10 nM, or 1 μ M for 18 hours at 37°C. Following treatment, cells were washed three times with pre-warmed PBS and incubated with fluorescently labeled HDL (DiI-HDL, 20 μ g/mL, CliniSciences) or LDL (DiI-LDL, 10 μ g/mL, CliniSciences) for 4 hours at 37°C. After the incubation period, the cells were washed three times with PBS to remove excess fluorescent probes. The fluorescence signal was measured using an EnSight Multimode Plate Reader (PerkinElmer) with excitation and emission wavelengths set to 549 nm and 565 nm, respectively. The results were normalized against cell confluency.

4.4.5.4 Filipin staining for cellular free cholesterol

To quantify intracellular free cholesterol, HepG2 cells were seeded at 40,000 cells per well in 96-well plates (PhenoPlate, PerkinElmer) and cultured until reaching 70% confluence. The cells were serum-starved in DMEM supplemented with 0.5% FBS for 16 hours before being treated with α -MSH or the selective MC1R agonist LD211 at concentrations of 0.1 nM, 10 nM, or 1 μ M for 24 hours. After treatment, the cells were washed three times with PBS and fixed with 4% paraformaldehyde (Sigma-Aldrich) for 15 minutes at room temperature. Following fixation, cells were

washed three more times with PBS and incubated with 1.5 mg/mL glycine (Sigma-Aldrich) for 10 minutes at room temperature to quench any residual paraformaldehyde. The cells were then washed again three times with PBS. For staining, the cells were incubated with 50 $\mu\text{g}/\text{mL}$ Filipin (Sigma-Aldrich, #F9765) for 1 hour at 37°C to visualize free cholesterol. After staining, cells were washed three times with PBS, and the fluorescence signal was measured using an EnSight Multimode Plate Reader (PerkinElmer) with excitation at 360 nm and emission at 480 nm. The results were normalized against cell confluency.

4.4.5.5 Enzyme-linked immunosorbent assay

To evaluate the activation of signaling pathways, HepG2 cells were seeded in 12-well plates (PhenoPlate, PerkinElmer) and cultured until reaching approximately 70% confluence. The cells were then serum-starved in DMEM supplemented with 0.5% FBS for 24 hours. Following serum starvation, cells were treated with α -MSH or the selective MC1R agonist LD211 at concentrations of 0.1 nM, 10 nM, or 1 μM for 10 minutes. After treatment, the cells were washed three times with ice-cold PBS to remove any residual media. Cells were then lysed using 150 μL of Lysis Buffer #6 (R&D Systems), and the lysates were analyzed for the expression of phosphorylated ERK1 (T202/Y204)/ERK2 (T185/Y187) and phosphorylated JNK (T183/Y185 for JNK1/2 and T221/Y223 for JNK3). Commercially available DuoSet IC ELISA kits (R&D Systems, #DYC1018B for ERK and #DYC1387B for JNK) were used following the manufacturer's instructions. Protein levels were normalized to total protein concentrations determined by the Pierce BCA Protein Assay Kit (Thermo Fisher).

4.4.5.6 Flow cytometry analysis of cell surface LDLR expression

To assess LDLR expression on the cell surface, HepG2 cells were seeded in 24-well plates at a density of 1 mL per well and cultured until reaching approximately 70% confluence. Cells were then serum-starved in DMEM medium supplemented with 0.5% FBS for 24 hours. Following serum starvation, cells were treated with 1 μM of α -MSH or the selective MC1R agonist LD211 for varying durations (0, 1, 3, 6, or 24 hours). After treatment, the cells were washed three times with ice-cold PBS and detached using 5 mM EDTA. For the detection of LDLR expression, cells were stained with a phycoerythrin (PE)-conjugated anti-human LDLR antibody (clone C7, BD Biosciences). The samples were analyzed using an LSR Fortessa flow cytometer (BD Biosciences), and data were processed using FlowJo software (FlowJo, LLC, Ashland, USA).

4.4.5.7 Gene expression analysis

Total RNA was extracted from HepG2 cells, primary mouse hepatocytes, liver tissue, and gonadal white adipose tissue (gWAT) using QIAzol Lysis Reagent (Qiagen). For HepG2 cells and primary hepatocytes, RNA isolation was performed using the Direct-zol RNA Miniprep kit (Zymo Research, CA, USA) according to the manufacturer's instructions. For liver and gWAT tissue samples, homogenization was carried out using metal beads in a Qiagen TissueLyser LT Bead Mill (QIAGEN, Venlo, Netherlands). Additionally, phase separation with chloroform was employed for gWAT samples. RNA extraction was performed using the Direct-zol RNA Miniprep columns and assessed for purity using a Nanodrop spectrophotometer (Thermo Fisher Scientific). Reverse transcription of total RNA into complementary DNA (cDNA) was performed with the PrimeScript RT Reagent Kit (Takara Clontech) following the manufacturer's instructions. Quantitative real-time PCR (qRT-PCR) was conducted using SYBR Green protocols (Kapa Biosystems, MA, USA). Each reaction was performed in duplicate, and the relative expression of target genes was normalized to the geometric mean of two housekeeping genes (ribosomal protein S29, PPIA, or β -actin) using the comparative delta-Ct ($2^{-\Delta\Delta Ct}$) method. Detailed primer sequences and qRT-PCR conditions are described in original publications (I and II). The results are presented as relative transcript levels.

4.4.5.8 Protein extraction and Western blot analysis

Protein lysates from HepG2 cells and primary mouse hepatocytes were prepared using ice-cold RIPA buffer (50 mM NaCl, 1% Triton X-100, 0.5% sodium deoxycholate, 0.1% SDS, pH 8.0) supplemented with a protease and phosphatase inhibitor cocktail (ThermoFisher, #A32961). For liver and gonadal white adipose tissue (gWAT) samples, homogenization was performed in ice-cold RIPA buffer using metal beads and Qiagen TissueLyser LT. Protein extracts were resolved via sodium dodecyl sulfate polyacrylamide gel electrophoresis (SDS-PAGE) using gels of varying concentrations (10%, 12%, 15%, or 4-20% gradient gels; Bio-Rad) and then transferred onto either nitrocellulose (GE Healthcare) or PVDF membranes (Bio-Rad). Blocking was performed in either 5% skimmed milk (Carl Roth) or 3% BSA (Tocris Bioscience) in TBS-T (Tris-Buffered Saline with 0.1% Tween® 20) for 1 hour at room temperature. Membranes were incubated overnight at 4°C with primary antibodies against specific targets, including: MC1R (Alomone Labs, #AMR-025), LDLR (Novus Biologicals, Littleton, CO, USA, #NBP1-06709), SR-BI (NovusBio, #NB400-104), SREBP2 (Novus Biologicals, #NB100-74543), HMGCR (Novus Biologicals, #NBP2-66888), DHCR7 (abcam, #ab103296), MRP4 (Cell Signaling Tech, Frankfurt, DE, #12857), StAR (Cell Signaling Tech, #8449), CYP8B1 (St John's Laboratory Ltd, #STJ92607), phospho-AMPK α (Cell Signaling

Tech, #2535), AMPK α (Cell Signaling Tech, #2532), SREBP1c (Novus Biologicals, #NBP600-582), HSL (Novus Biologicals, # NB110-37253), ATGL (Novus Biologicals, #NBP3-16567), CD36 (Abcam, #ab124515), FASN (Novus Biologicals, #NB400-114), pACC1 (Cell Signaling, #11811), PGC1a (Novus Biologicals, #NBP1-04676), MT2 (Abcam, #ab192385). The next day, membranes were washed in TBS-T and incubated with horseradish peroxidase (HRP)-conjugated secondary antibodies (Cell Signaling Technology) for 1 hour at room temperature. Protein bands were visualized using an enhanced chemiluminescence (ECL) detection kit (Millipore). The expression levels of target proteins were normalized to β -actin (Sigma-Aldrich, #2066) or vinculin (Bio-Rad, #MCA465GA) as loading controls. Band densities were quantified using ImageJ software (NIH, Bethesda, MD, USA).

4.5 Transcriptome analysis

RNA-sequencing (RNA-Seq) data was retrieved from the Gene Expression Omnibus (GSE120064) data repository to study MC1R expression in human liver biopsy samples from patients diagnosed with MASLD (n=51), MASH (n=155), and healthy obese control cases (n=10) without biochemical or histological evidence of MASLD (Govaere et al., 2020). The FIMM-RNAseq data analysis workflow (version 2.0.7) (Kangas et al., 2022) was used to process the raw data. The raw reads were pre-processed using Trim Galore software (version 0.6.6), then aligned to the human reference genome GRCh39 (release 93) from the Ensembl database. Gene count data was produced using Subreads (version 2.0.1) (Liao et al., 2013). Downstream data analysis was carried out using the R package edgeR (version 3.40.2) (Robinson et al., 2010). Low gene counts were removed using edgeR's default parameters, and the gene counts were normalized using the trimmed mean of M values (TMM) method, expressed as log₂ RPKM (reads per kilobase of exon per million reads mapped). Additionally, RNA was extracted from the liver of Western diet-fed control (n=4) and Mc1r LKO (n=4) mice for RNA-Seq analysis. The RNA-Seq was performed at the Finnish Functional Genomics Centre following Illumina protocols. The Illumina Novaseq 6000 produced binary base call (BCL) files, which were converted to FASTQ files using Illumina's bcl2fastq (version 2.18.0.12). The FASTQ files were processed using FIMM-RNAseq (Kangas et al., 2022) pipeline (version 3.0.0). The T overhang from the library preparation workflow was removed from both forward and reverse reads. Quality trimming and removal of adapter sequences were performed using the Trim-galore pipeline (Krueger et al., 2023, version 0.6.6). The reads were aligned to the mouse reference genome GRCh38 (release 102) from Ensembl using STAR (version 2.7.6a) (Dobin et al., 2012), and gene quantification was performed with Subread (version 2.0.1). Gene counts were

filtered using edgeR's (Robinson et al., 2010) filterByExpr function, applying default parameters. Normalization was performed using the TMM method. Differential gene expression analysis was conducted using DGA-quick in R, comparing expression profiles between control and Mc1r LKO mice. A total of 635 differentially expressed genes (DEGs) were identified, with a p-value cutoff of <0.05 and absolute log fold-change ≥ 0.25 . The DEGs were further analyzed for over-representation in Gene Ontology (GO) terms using topGO (Alexa and Rahnenfuhrer, 2023) (version 2.46.0), a Bioconductor R package. GO terms with an adjusted p-value (p_{adj}) ≤ 0.05 were considered significant.

4.6 Statistical analysis

All statistical analyses (except for RNA-Seq analysis) were performed using GraphPad Prism software (versions 9 or 10, La Jolla, CA, USA). Statistical significance between experimental groups was determined using a two-tailed, unpaired Student's t-test or one-way or two-way ANOVA followed by Bonferroni post hoc tests, as appropriate. The normality of the data was assessed using the D'Agostino, Pearson omnibus and Shapiro-Wilk normality test. Based on the results of the normality tests, statistical tests were selected. For data that were not normally distributed, or if the sample size was below $n < 8$ per group, nonparametric tests such as the Mann-Whitney U test or Kruskal-Wallis test were applied. Possible outliers were identified using the regression and outlier removal (ROUT) method with a Q-level of 1%. Data are presented as mean \pm standard error of the mean (SEM), unless otherwise stated. Results were considered statistically significant for p-values less than 0.05.

5 Results

5.1 The effects of MC1R on cholesterol and bile acid metabolism

5.1.1 MC1R expression in the liver

MC1R expression was first confirmed via immunohistochemical staining of the liver sections from chow-fed C57BL/6J mice, which showed strong and uniform MC1R expression throughout the liver (Fig 5.1A). Immunofluorescence staining further revealed the co-localization of MC1R with hepatocyte marker serum albumin and cholangiocyte marker cytokeratin 19 (CK19) (Fig. 5.1B and C). To investigate the effects of a high-fat diet on MC1R expression, mice were fed a Western-type diet for 12 weeks. Notably, both *Mclr* mRNA and protein levels were significantly reduced in the livers of Western diet-fed mice compared to chow diet-fed controls (Fig. 5.1D and E). Additionally, RNA sequencing of human liver biopsies indicated that *MC1R* expression was significantly downregulated in patients with MASLD or MASH relative to healthy control subjects (Fig. 5.1F).

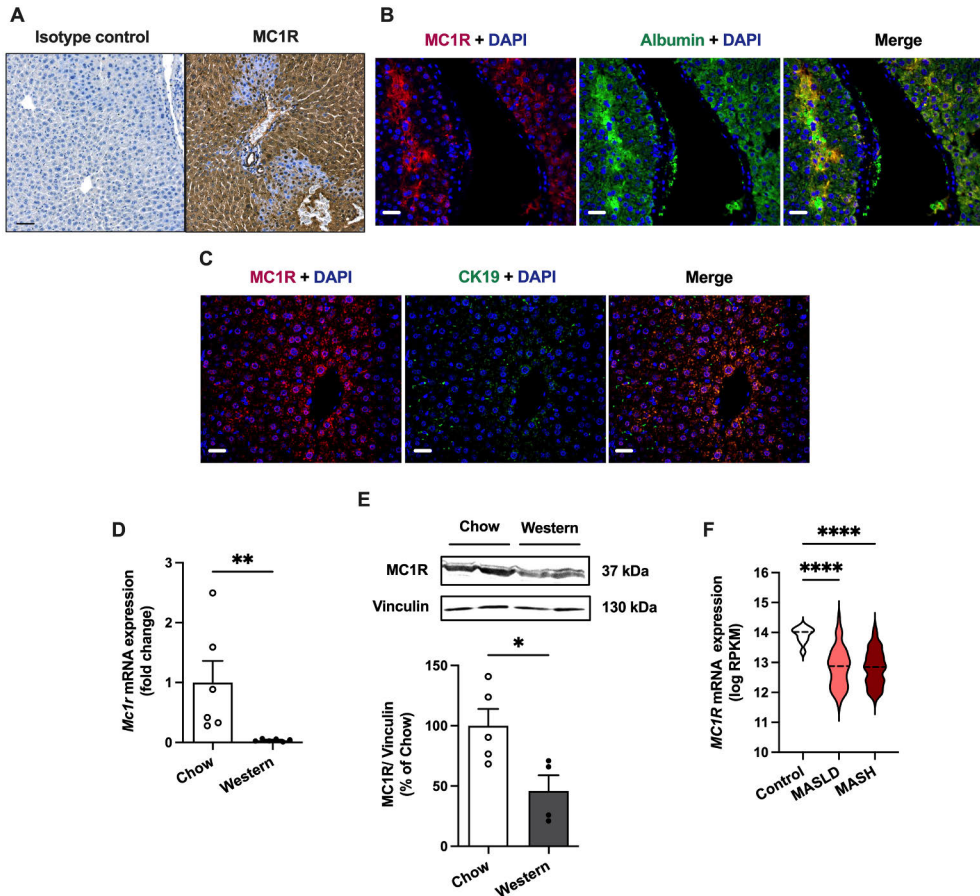


Figure 5.1. Expression of melanocortin 1 receptor (MC1R) in the mouse and human liver. (A) Immunostaining of MC1R in the liver of chow-fed C57BL/6J mice. Anti-MC1R antibody was replaced by purified normal rabbit IgG (isotype control) in the control section. Nuclei were stained with DAPI (blue). Scale bar: 50 μ m. (B) Immunofluorescence staining of MC1R (red) and hepatocyte marker serum albumin (green) in the liver of chow-fed C57BL/6J mice. (C) Immunofluorescence staining of MC1R (red) and hepatocyte marker serum albumin (green) in the liver of chow-fed C57BL/6J mice. Scale bar: 20 μ m. (D) Quantitative real-time PCR (qPCR) analysis of *Mc1r* mRNA expression in the liver of chow- and Western diet-fed mice. (E) Representative Western blots showing MC1R and β -actin (loading control) and quantification of MC1R protein levels in the livers of chow- and Western diet-fed mice. * $p < 0.05$ and ** $p < 0.01$ versus chow-fed mice (Student's *t*-test). (F) MC1R gene expression analysis in human liver biopsies from control cases ($n = 10$) and patients with metabolic dysfunction-associated steatotic liver disease (MASLD, $n = 51$) or metabolic dysfunction-associated steatohepatitis (MASH, $n = 155$). Violin plots show normalized log₂ RPKM values and medians (dashed line) for each sample group. The values are presented as mean \pm SEM, with $n = 5$ – 10 mice per group. * $p < 0.05$, ** $p < 0.01$, and **** $p < 0.0001$ for indicated comparisons (one-way ANOVA, Bonferroni post hoc tests). *Mc1r*: Melanocortin 1 Receptor.

5.1.2 Characterization of hepatocyte-specific MC1R knock-out mouse model

The regulatory role of hepatic MC1R was investigated by generating hepatocyte-specific MC1R knock-out mice ($Mclr^{fl/fl}Alb^{Cre/+}$; symbolized as Mc1r LKO) by crossing $Mclr$ floxed mice ($Mclr^{fl/fl}$) with transgenic mice expressing Cre recombinase under the control of the mouse albumin promoter ($Alb^{Cre/+}$). These mice were maintained on a normal chow diet, and body weight was monitored weekly from 8 to 16 weeks of age. Recombination efficacy was confirmed via PCR analysis of genomic DNA from the liver, demonstrating efficient recombination in Mc1r LKO mice (Appendix Fig. 1A). Correspondingly, $Mclr$ mRNA expression was significantly reduced in the livers of Mc1r LKO mice (Fig. 5.2A), and Western blotting revealed a marked decrease in MC1R protein levels in these mice compared to controls (Fig. 5.2B). Phenotypic analysis showed no significant differences in body weight between Mc1r LKO and control mice throughout the monitoring period (Appendix Fig. 1B), nor were there any changes in total fat or lean mass (Appendix Fig. 1C and D). However, Mc1r LKO mice exhibited significantly higher absolute liver weights and liver-to-body weight ratio compared to control mice (Fig. 5.2C and D).

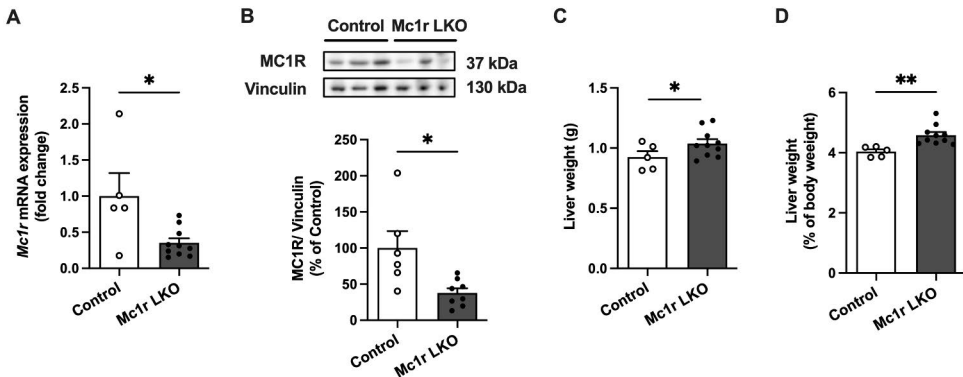


Figure 5.2. Low expression of melanocortin 1 receptor (MC1R) in the livers of hepatocyte-specific MC1R deficient mice. (A) Quantitative real-time polymerase chain reaction (qPCR) analysis of $Mclr$ expression in the liver of control and Mc1r LKO mice. (B) Representative Western blots and quantification of MC1R levels in the liver of Western diet-fed control and Mc1r LKO mice. (C and D) Absolute liver weights and liver-to-body weight ratio (expressed as a percentage of body weight) in chow-fed control and Mc1r LKO Mice. The values are presented as mean \pm SEM, $n=5-10$ mice per group. * $p<0.05$ versus control mice (Student's t-test). Mc1r LKO: hepatocyte-specific MC1R knockout.

5.1.3 The effects of hepatocyte-specific MC1R deficiency on cholesterol, triglycerides, fibrosis, and bile acids

To assess the effects of hepatocyte-specific MC1R deficiency on lipid accumulation, liver tissue samples from Mc1r LKO and control mice were stained with H&E and ORO, revealing a significant increase in intracellular LDs in Mc1r LKO mice (Fig. 5.3A). Lipid quantification in liver homogenates further confirmed a substantial increase in total cholesterol and TG levels in Mc1r LKO mice (Fig. 5.3B). Plasma cholesterol and TG levels were also elevated in Mc1r LKO mice (Fig. 5.3C). To explore potential mechanisms underlying these changes, mRNA expression levels of key genes involved in cholesterol synthesis and transport were analysed. Mc1r LKO mice exhibited increased hepatic expression of *Srebp2*, *Hmgcr*, *Dhcr7*, *Ldlr*, and ATP binding cassette subfamily A member 1 (*Abc1*) (Appendix Fig. 2A and B). Interestingly, while protein levels of both cleaved and precursor forms of SREBP2, a key regulator of cholesterol homeostasis, were unchanged, the ratio of mature to precursor SREBP2 was significantly reduced in the livers of Mc1r LKO mice (Fig. 5.3D and E). Protein levels of SREBP2 targets genes HMGCR and DHCR7 were reduced in Mc1r LKO mice liver (Fig. 5.3E and F). Histological analysis using Picosirius Red staining revealed increased fibrosis in Mc1r LKO liver, which corroborated by the upregulation of fibrotic genes (Fig 5.3G and H, Appendix Fig. 2C). However, no difference was observed between the genotypes in the mRNA expression of pro-inflammatory markers in the liver (Appendix Fig. 2D).

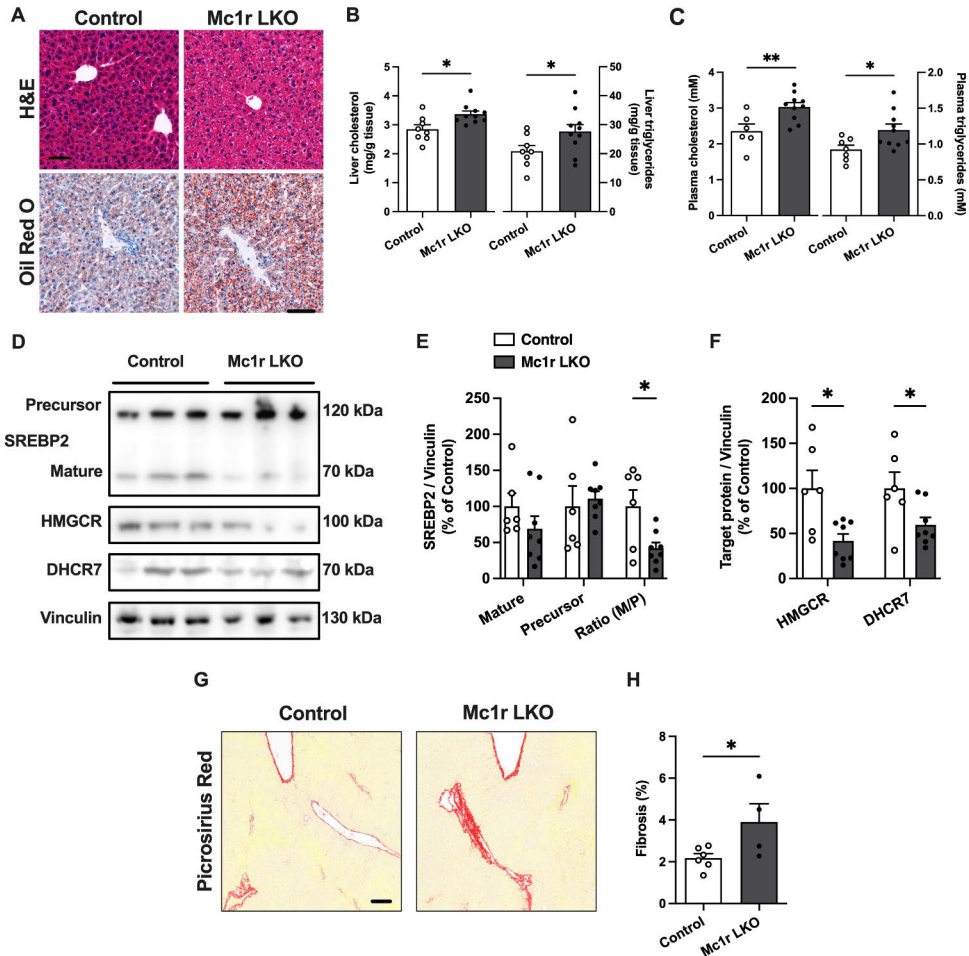


Figure 5.3. Loss of hepatic Melanocortin 1 receptor (MC1R) promotes cholesterol and triglycerides (TG) accumulation and enhances liver fibrosis. (A) Representative images of Hematoxylin and eosin (H&E) and Oil Red O (ORO)-stained liver sections from chow-fed control and Mc1r LKO mice. Scale bar: 50 μ m. (B and C) Quantification of total cholesterol and triglycerides (TG) levels in the liver and plasma of chow-fed control and Mc1r LKO mice. (D) Representative Western blots of SREBP2, HMGCR, DHCR7, and vinculin (loading control) expression in the liver of chow-fed control and Mc1r LKO mice. (E) Quantification of mature and precursor forms of SREBP2, and the precursor-to-mature SREBP2 ratio in the liver of chow-fed control and Mc1r LKO mice. (F) Quantification of HMGCR and DHCR7 protein levels in the liver of chow-fed control and Mc1r LKO mice. (G) Representative images of Picrosirius Red-stained liver sections from chow-fed control and Mc1r LKO mice. Scale bar: 100 μ m. (H) Quantification of fibrotic area (as a percentage of total tissue area) in the liver of chow-fed control and Mc1r LKO mice. The values are presented as mean \pm SEM, mice n=6–10 mice per group. * $p < 0.05$ and ** $p < 0.01$ versus control mice (Student's t-test). SREBP2: Sterol regulatory element-binding protein 2; HMGCR: 3-hydroxy-3-methylglutaryl-CoA reductase; DHCR7: 7-dehydrocholesterol reductase.

To investigate the potential causes of elevated cholesterol levels in the liver and plasma of Mc1r LKO mice, the levels of total and individual bile acids were measured in the liver, plasma, and feces using liquid chromatography-mass spectrometry. While hepatic bile acid levels did not differ significantly between genotypes (Fig. 5.4A), plasma bile acids were reduced, with a near-significant decrease in fecal bile acids ($p=0.06$) in Mc1r LKO mice. These changes in the bile acids pool were primarily attributed to a reduction in secondary bile acids (Fig 5.4B and C). Further analysis of individual bile acids revealed decreased levels of CA and UDCA, as well as secondary bile acids like DCA, HDCA, and ω -MCA in the plasma

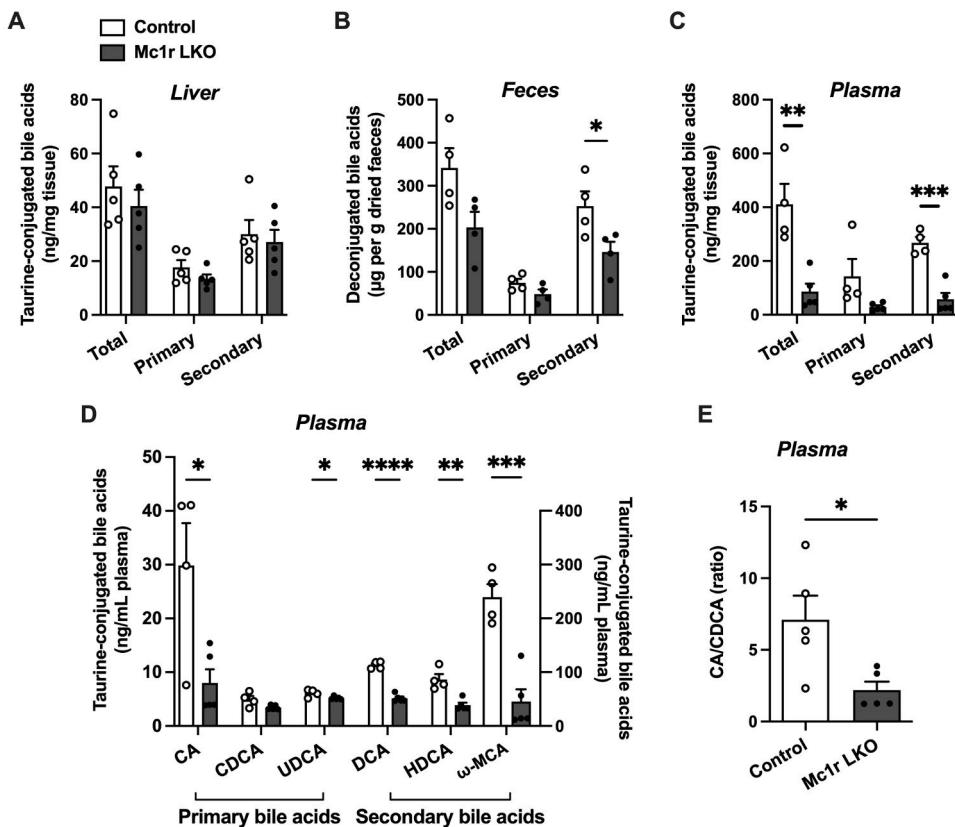


Figure 5.4. Reduction of bile acid levels due to loss of hepatocyte-specific melanocortin 1 receptor (MC1R) (A-C) Quantification of total, primary, and secondary bile acids in the liver, feces, and plasma samples of chow-fed control and Mc1r LKO mice. (D) Concentration of individual primary and secondary bile acids in the plasma of chow-fed control and Mc1r LKO mice. (E) Ratio of cholic acid (CA) to chenodeoxycholic acid (CDCA) in the plasma samples of chow-fed control and Mc1r LKO mice. The values are presented as mean \pm SEM, $n=4-5$ mice per group. * $p<0.05$, ** $p<0.01$, *** $p<0.001$, and **** $p<0.0001$ versus control mice (Student's t-test). Primary bile acids: cholic acid (CA), chenodeoxycholic acid (CDCA), ursodeoxycholic acid (UDCA); secondary bile acids: deoxycholic acid (DCA), hyodeoxycholic acid (HDCA), ω -muricholic acid (ω -MCA).

of Mc1r LKO mice (Fig. 5.4D). Additionally, DCA levels in the liver and HDCA, LCA, and 12-oxo LCA levels in the feces were reduced in Mc1r LKO mice (data not shown). Furthermore, the ratio of CA to CDCA in the plasma was lower in Mc1r LKO mice (Fig 5.4E).

To investigate the factors contributing to disrupted bile acid metabolism in Mc1r LKO mice, key enzymes regulating bile acid synthesis and transporters responsible for bile acid uptake and excretion were assessed in the liver. Mc1r LKO mice showed significant upregulation of sterol 12- α -hydroxylase (*Cyp8b1*) and sterol 27-hydroxylase (*Cyp27a1*), with no significant change in cholesterol 7 α -hydroxylase (*Cyp7a1*), the rate-limiting enzyme in bile acid synthesis (Fig. 5.5A). Conversely, the expression of steroidogenic acute regulatory protein 1 (*Stard1*), crucial for cholesterol transport to mitochondria in the alternative bile acid pathway, was downregulated. Among bile acid transporters Na⁺-taurocholate cotransport polypeptide (*Ntcp*) expression was elevated, while multidrug-associated protein 4

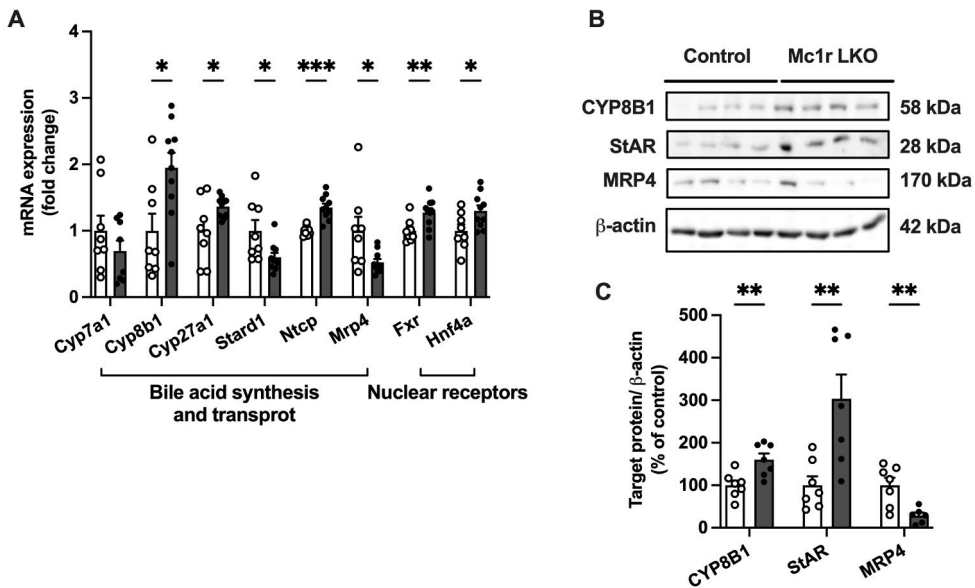


Figure 5.5. Impact of hepatocyte-specific melanocortin 1 receptor (MC1R) deficiency on a bile acid synthesis and transport gene expression. (A) Quantitative real time polymerase chain reaction (qPCR) analysis of bile acid synthesis, transport, and nuclear receptors genes in the liver of the chow-fed control and Mc1r LKO mice. (B and C) Representative Western blots and quantification of CYP8B1, StAR, and MRP4 protein levels in the liver of chow-fed control and Mc1r LKO mice. The values are presented as mean \pm SEM, n=7–10 mice per group. *p<0.05, **p<0.01, and ***p<0.001 versus control mice (Student’s t-test). Genes: Cyp7a1, cholesterol 7 α -hydroxylase; Cyp8b1, sterol 12- α -hydroxylase; Cyp27a1, sterol 27-hydroxylase; Stard1, steroidogenic acute regulatory protein; Ntcp, Na⁺-taurocholate cotransporting polypeptide; Mrp4, multidrug resistance-associated protein 4; Fxr, farnesoid X receptor; Hnf4a, hepatocyte nuclear factor 4 α .

(MRP4) was decreased in Mc1r LKO mice. Additionally, transcriptional regulators farnesoid X receptor (*Fxr*) and hepatocyte nuclear factor 4 alpha (*Hnf4a*) were significantly upregulated (Fig 5.5A). Protein analysis corroborated these findings, showing increased levels of CYP8B1 and decreased MRP4 in the liver of Mc1r LKO mice. Interestingly, the protein expression of StAR (*Stard1*) was increased, contrary to its downregulated gene expression profile (Fig. 5.5B and C).

5.1.4 The effects of MC1R activation on cholesterol and lipid handling in HepG2 cells

Given the observed hypercholesterolemia and increased TG levels in Mc1r LKO mice, the underlying mechanisms of MC1R activation on lipid metabolism in human hepatocytes (HepG2) was explored in vitro. Initially, MC1R expression was analyzed under the effect of saturated FA (palmitic acid), which led to a rapid and significantly downregulation of MC1R (Fig. 5.6A), mirroring the in vivo reduction in Western diet-fed mice. However, MC1R protein levels remained unchanged when HepG2 cells were treated with LDL cholesterol or atorvastatin (data not shown). To assess the impact of MC1R activation, we treated HepG2 cells with α -MSH or LD211. Both agonists significantly reduced intracellular free cholesterol levels in a dose-dependent manner, as demonstrated by filipin fluorescence staining (Fig. 5.6B). Additionally, MC1R enhanced the uptake of fluorescently labelled LDL and HDL particles (dil-LDL and dil-HDL) (Fig. 5.6C and D). Correspondingly, the mRNA levels of lipoprotein receptors, *LDLR* and HDL receptor *SR-BI* (*SCARB1*), were upregulated following treatment with MC1R agonists (Fig. 5.6E and F). Protein analysis revealed increased *LDLR* and *SR-BI* levels in α -MSH-treated cells, whereas no changes were observed with LD211 treatment (Appendix Fig. 3A and B). Enhanced surface expression of *LDLR* was confirmed by flow cytometry after treatment with MC1R agonists (data not shown). Despite the reduction in free cholesterol, MC1R activation did not alter the protein expression of key cholesterol biosynthesis enzymes, *HMGCR* or *DHCR7* (Appendix Fig. 3C and D). Lastly, treatment with LD211 led to downregulation of fibrosis-related genes, including *TGFBI*, *ACTA2*, and *COL1A1*, while similar but nonsignificant trends were observed with α -MSH-treatment (data not shown).

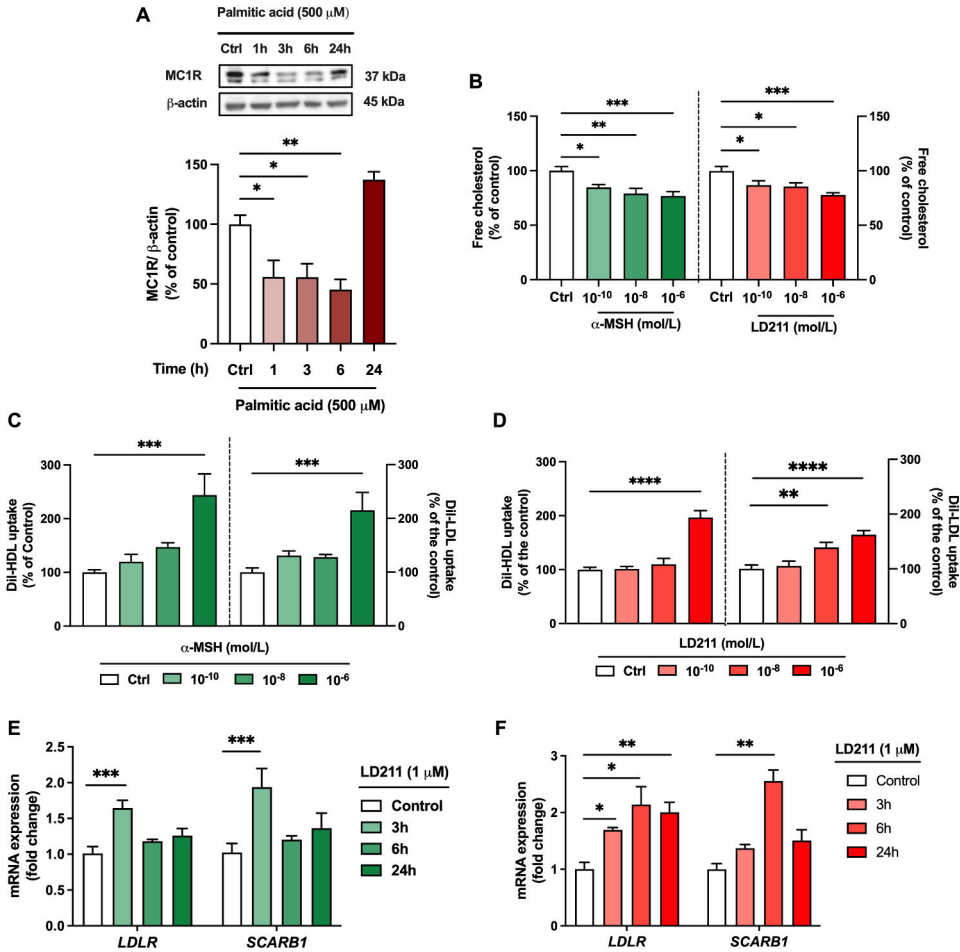


Figure 5.6. Effect of agonist-mediated melanocortin 1 receptor (MC1R) activation on cholesterol and lipoprotein uptake in HepG2 cells. (A) Representative Western blots and quantification of MC1R protein levels in HepG2 cells treated with palmitic acid (500 μ M) at different time points. (B) Quantification of free cholesterol content in HepG2 cells treated with α -MSH and LD211 (0.1 nM, 10 nM, or 1 μ M) for 24 hours. (C and D) Quantification of HDL and LDL uptake in HepG2 cells treated with α -MSH and LD211 (0.1 nM, 10 nM, or 1 μ M) for 24 hours. (E and F) Quantitative real-time polymerase chain reaction (qPCR) analysis of LDL receptor (*LDLR*) and scavenger receptor class B member 1 (*SCARB1*) expression in HepG2 cells treated with 1 μ M α -MSH and LD211 at different time points. The values are presented as mean \pm SEM, n=3–6 per group. *p<0.05, **p<0.01, ***p<0.001, and ****p<0.0001 by one-way ANOVA and Bonferroni *post hoc* tests.

In terms of bile acid metabolism, treatment of HepG2 cells with the MC1R agonist α -MSH led to an increase in CA levels without affecting CDCA levels (Fig. 5.7A). This resulted in a higher CA:CDCA ratio (Fig. 5.7B). Consistent with these

observations, α -MSH treatment increased the protein expression of CYP8B1, a crucial enzyme that regulates the CA:CDCA ratio (Fig. 5.7, C and D).

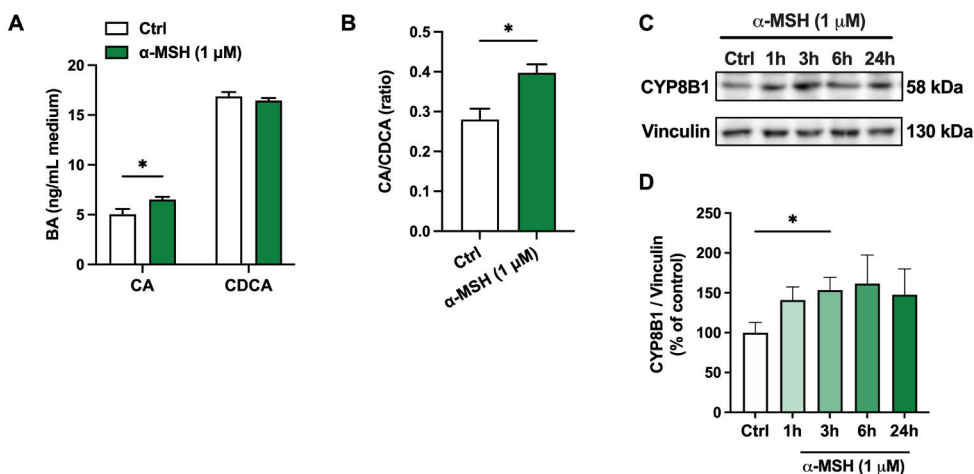


Figure 5.7. Effects of melanocortin 1 receptor (MC1R) activation by α -MSH on bile acid levels in HepG2 cells. (A) Quantification of cholic acid (CA) and chenodeoxycholic acid (CDCA) in HepG2 cells treated with 1 μ M α -MSH for 24 hours. (B) Ratio of CA to CDCA in HepG2 cells treated with 1 μ M α -MSH for 24 hr. (C and D) Representative Western blots and quantification of sterol 12-alpha-hydroxylase (CYP8B1) in HepG2 cells treated with 1 μ M α -MSH at different time points (0-, 1-, 3-, 6-, or 24-hours). The values are presented as mean \pm SEM, n=4-6 per group. *p<0.05 for the indicated comparisons by Student's t-test (A and B) or by one-way ANOVA and Bonferroni *post hoc* tests (D).

5.1.5 The effects of pharmacological activation of MC1R on intracellular signaling pathways in HepG2 cells

To evaluate the intracellular signaling pathways activated by MC1R in HepG2 cells, cells were treated with different concentrations of α -MSH or LD211. Surprisingly, neither α -MSH nor LD211 influenced cAMP levels (Fig. 5.8A and B). However, Western blot analysis revealed that both agonists decreased phosphorylation of extracellular-signal-regulated kinase (ERK) and c-Jun N-terminal kinase (JNK) (Fig. 5.8C-F). Additionally, both treatments induced rapid, transient phosphorylation of AMP-activated protein kinase (AMPK) (Fig. 5.8G and H). To determine if AMPK activation mediates the cholesterol-lowering effects of the agonists, HepG2 cells were treated with the AMPK inhibitor dorsomorphin. Notably, dorsomorphin increased cholesterol content and reversed the cholesterol-reducing effects of α -MSH, while the effects of LD211 was abolished by AMPK inhibition (Appendix 4A and B).

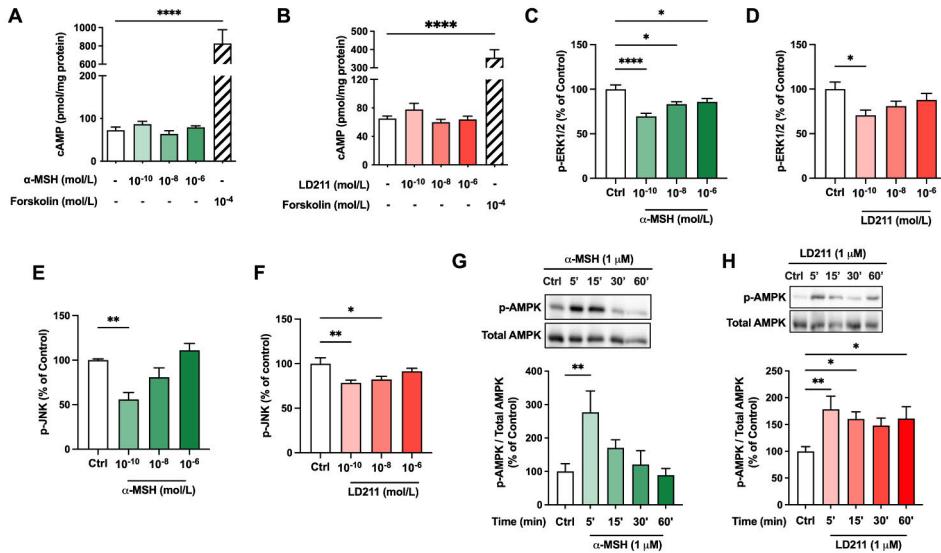


Figure 5.8. Effects of melanocortin 1 receptor (MC1R) activation on intracellular signaling in HepG2 cells. (A and B) Quantification of intracellular cyclic adenosine monophosphate (cAMP) levels in HepG2 cells treated with α -MSH and LD211 (0.1 nM, 10 nM, or 1 μ M) for 30 min. Forskolin used as a positive control. (C-F) Quantification of phosphorylated ERK1/2 and JNK by ELISA in HepG2 cells treated with α -MSH and LD211 (0.1 nM, 10 nM, or 1 μ M) for 10 minutes. (G and H) Representative Western blots and quantification of phosphorylated AMPK (p-AMPK) levels, normalized against total AMPK, in HepG2 cells treated with 1 μ M α -MSH and LD211 at different time points (5', 15', 30', or 60'-minutes). The values are presented as mean \pm SEM, n=3–6 per group. *p<0.05, **p<0.01, and ****p<0.0001 by one-way ANOVA with Bonferroni *post hoc* tests.

5.2 The effects of hepatocyte-specific MC1R deficiency on fatty acid metabolism

5.2.1 Adipose tissue and liver phenotype in global MC1R deficient mice

The impact of global MC1R deficiency on body weight and adiposity was assessed in *Mc1r^{e/c}* mice. Male *Mc1r^{e/c}* and WT mice were kept on either a chow or Western diet for 12 weeks. The body weight gain was monitored weekly for the whole experimental period. No significant differences in body weight or overall composition were observed between the genotypes on either diet (Appendix Fig. 5A-D). GTT also revealed no differences in fasting glucose levels between the genotypes (Appendix Fig. 5E-G). Despite similar body weights, *Mc1r^{e/c}* mice exhibited increased weights of gWAT, subcutaneous white adipose tissue (sWAT), and retroperitoneal white adipose tissue (rWAT) compared to WT mice on chow diet, with only gWAT significantly increased in Western diet-fed *Mc1r^{e/c}* mice (Fig. 5.9A

and B). Total WAT depot weight was significantly higher in $Mc1r^{e/e}$ mice across both diet groups (Fig. 5.9C). Histological analysis of gWAT showed larger adipocytes in $Mc1r^{e/e}$ mice, indicating adipocyte hypertrophy (Fig. 5.9D-G). Notably, food intake and physical activity levels were comparable between genotypes (data not shown), suggesting adipocyte hypertrophy was independent of these factors.

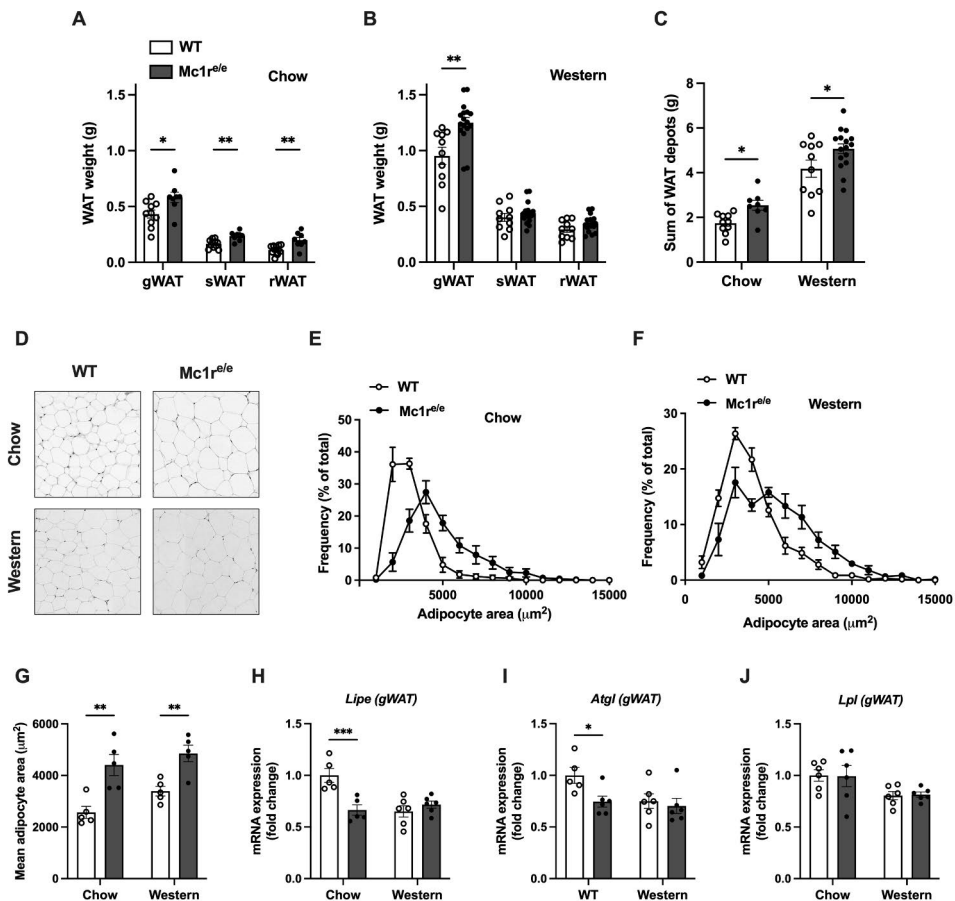


Figure 5.9. Increased adipocyte-hypertrophy in mice with global melanocortin 1 receptor (MC1R) deficiency (A-C) White adipose tissue (WAT) weights and the sum of WAT weights in chow- and Western diet-fed WT and $Mc1r^{e/e}$ mice. **(D)** Representative H&E-stained gWAT sections from chow- and Western diet-fed WT and $Mc1r^{e/e}$ mice. Scale bar: 100 μm . **(E and F)** Distribution of adipocyte size in gWAT samples from chow- and Western diet-fed WT and $Mc1r^{e/e}$ mice. **(G)** Mean adipocyte size in gWAT samples from chow- and Western diet-fed WT and $Mc1r^{e/e}$ mice. **(H-J)** Quantitative real-time-polymerase chain reaction (qPCR) analysis of *Lipe*, *Atgl*, and *Lpl* expression in gWAT samples. The values are presented as mean \pm SEM, $n=10-15$ mice per group. * $p<0.05$, ** $p<0.01$, and *** $p<0.001$ for the indicated comparisons by two-way ANOVA with Bonferroni post hoc tests. gWAT: gonadal white adipose tissue; *Lipe*: hormone-sensitive lipase; *Atgl*: adipose triglyceride lipase; *Lpl*: lipoprotein lipase.

To explore underlying mechanisms of adipocyte hypertrophy, the expression of key TG hydrolysis enzymes was examined in gWAT. $Mc1r^{e/e}$ mice on a chow diet showed reduced expression of *Lipe* and *Atgl*, while these differences were not present under a Western diet (Fig. 5.9H and I). Expression of *Lpl* (Fig. 5.9J) and other genes involved in TG hydrolysis, FA synthesis (e.g., *Fasn*, *Scd1*, *Accl*, *Dgat1*, *Dgat2*), and FAO (*Ppara*, *Acox1*) were not changed (data not shown). These findings indicate that global MC1R deficiency promotes adipocyte hypertrophy without affecting overall body weight or composition.

In addition to increased WAT mass, $Mc1r^{e/e}$ mice exhibited higher liver weights compared to WT mice in chow and Western diet groups (Fig. 5.9A). Plasma lipid analysis indicated elevated TG levels in $Mc1r^{e/e}$ mice on Western diet, while no differences were observed between genotypes on a chow diet (Fig. 5.9B). Gene expression profiling in the liver showed no significant differences in mRNA levels of *Srebp1c*, a primary transcription factor involved in lipogenesis. However, *Chrebp*, another major regulator of hepatic lipid synthesis, was significantly upregulated in

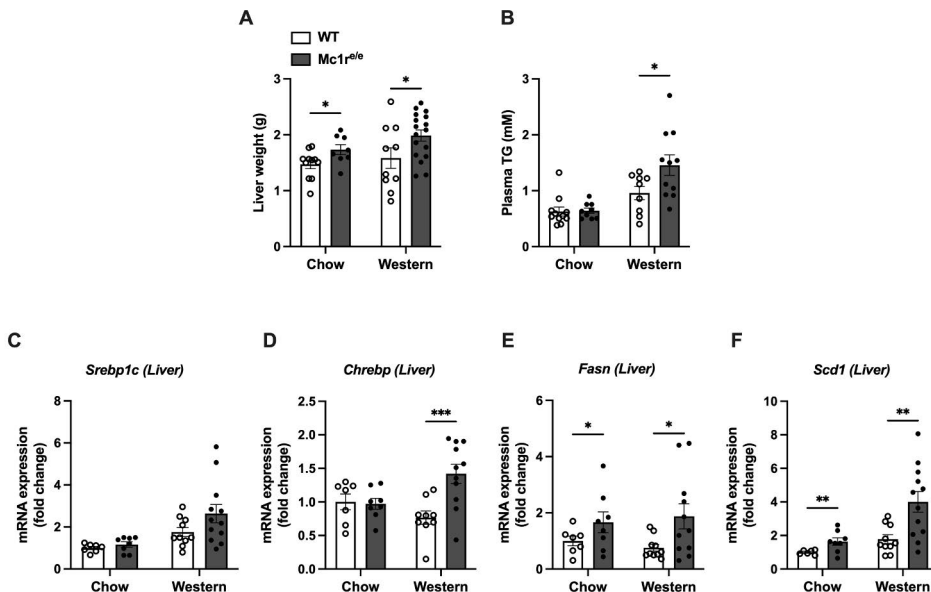


Figure 5.10. Increased liver weights and upregulation of lipogenesis-related genes in the livers of global melanocortin 1 receptor (MC1R) deficient mice (A) Liver weights of chow- and Western diet-fed WT and $Mc1r^{e/e}$ mice. **(B)** Quantification of plasma triglyceride (TG) concentrations in chow- and Western diet-fed WT and $Mc1r^{e/e}$ mice. **(C-F)** Quantitative real-time-polymerase chain reaction (qPCR) analysis of *Srebp1c*, *Chrebp*, *Fasn*, and *Scd1* mRNA expression levels in the liver. The values are presented as mean \pm SEM, n=10-15 mice per group. * p <0.05, ** p <0.01, and *** p <0.001 for the indicated comparisons by two-way ANOVA with Bonferroni *post hoc* tests. *Srebp1c*: sterol regulatory element-binding protein 1; *Chrebp*: carbohydrate response element-binding protein; *Fasn*: fatty acid synthase; *Scd1*: stearyl-CoA desaturase 1.

the livers of Western diet-fed $Mc1r^{e/c}$ mice (Fig. 5.9C and D). This upregulation corresponded with increased expression of *Chrebp* target genes, including *Fasn* and *Scd1*, which are key enzymes in FA synthesis (Fig. 5.9E and F). In summary, global MC1R deficiency led to increased liver weights and elevated plasma TG levels, alongside transcriptional changes in the liver indicative of enhanced hepatic DNL, particularly under a Western-type diet.

5.2.2 Liver and adipose tissue phenotype in Western diet-fed hepatocyte-specific MC1R deficient mice

Given the pronounced effects seen in Western diet-fed $Mc1r^{e/c}$ mice, $Mc1r$ LKO mice were subjected to Western diet for 12-weeks. In line with the $Mc1r^{e/c}$ mice, body weight gain and food intake remained similar between control and $Mc1r$ LKO mice throughout the intervention (Appendix Fig. 6A and B). Quantitative NMR scanning indicated no differences in total fat or lean mass at both the start and end of the diet period (Appendix Fig. 6C and D). However, $Mc1r$ LKO mice exhibited significantly increased liver weights compared to controls (Fig. 5.11A). Ex vivo quantitative NMR scanning revealed elevated relative fat mass and reduced relative lean mass in $Mc1r$ LKO mice (Fig. 5.11B and C). This was consistent with enhanced TG levels in the liver and elevated plasma TG levels, while plasma NEFA remained unchanged (Fig. 5.11D and E). GTT data showed no differences between genotypes (data not shown). Thus, hepatocyte-specific loss of MC1R led to increased liver weights and TG accumulation, resembling the liver phenotype seen in $Mc1r^{e/c}$ mice.

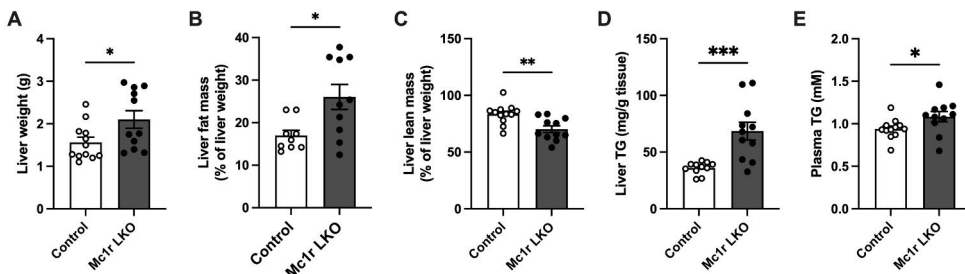


Figure 5.11. Hepatic loss of melanocortin 1 receptor (MC1R) increases liver weights and triglyceride (TG) accumulation (A) Liver weights measurement of control and $Mc1r$ LKO mice in Western diet. (B and C) Quantification of fat and lean mass in whole-liver samples of Western diet-fed WT and $Mc1r$ LKO mice using quantitative NMR scanning (D and E) Liver and plasma triglyceride (TG) levels in control and $Mc1r$ LKO mice on a Western diet. The values are presented as mean \pm SEM, $n=10-15$ mice per group. * $p<0.05$, ** $p<0.01$, and *** $p<0.001$ by unpaired two-tailed Student's t-test. $Mc1r$ LKO: hepatocyte-specific MC1R knockout mice; TG: triglycerides.

Consistent with the findings in *Mc1r^{e/e}* mice, *Mc1r* LKO mice exhibited significantly higher weights of gWAT, sWAT and rWAT depots as well as total WAT weight compared to controls (Fig. 5.12A, B). Histological analysis of H&E-stained gWAT increased adipocyte size, indicating hypertrophy in *Mc1r* LKO mice (Fig. 5.12C-E). To explore the mechanisms underlying this hypertrophy, key lipid metabolism genes were analyzed in gWAT samples. The expression of *Ppara*, a regulator of FAO, was reduced in *Mc1r* LKO mice, while *Srebp1c* and *Chrebp* levels

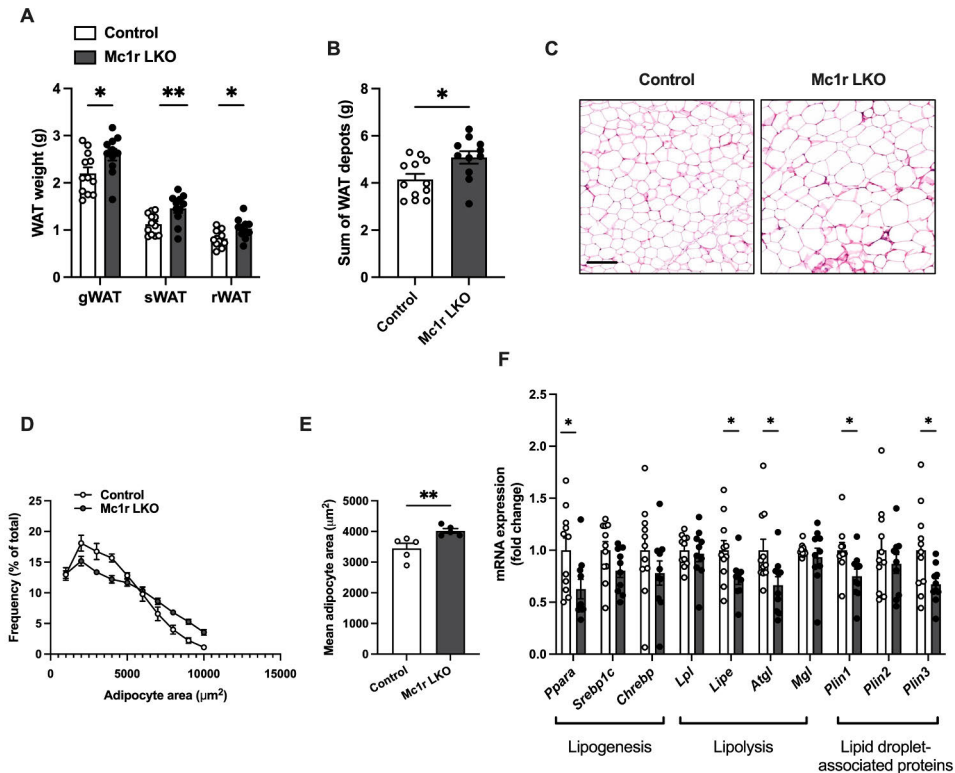


Figure 5.12. Hepatic loss of melanocortin 1 receptor (MC1R) increases adipocyte size and alters lipid metabolism in gWAT. (A and B) Absolute weight of different white adipose tissue (WAT) depots and total WAT mass in Western diet-fed control and *Mc1r* LKO mice. (C) Representative hematoxylin and eosin (H&E) stained gWAT sections from Western diet-fed control and *Mc1r* LKO mice. Scale bar: 100 µm. (D and E) Distribution of adipocyte sizes and average adipocyte volumes in gWAT of control and *Mc1r* LKO mice fed a Western diet. (F) Quantitative real-time-polymerase chain reaction (qPCR) analysis of genes involved in lipogenesis, lipolysis, and lipid droplet-associated proteins in gWAT of Western diet-fed control and *Mc1r* LKO mice. The values are presented as mean ± SEM, n = 10-15 mice per group. *p<0.05 and **p<0.01 by unpaired two-tailed Student's t-test. *Ppara*: peroxisome proliferator-activated receptor alpha; *Srebp1c*: sterol regulatory element-binding protein 1; *Chrebp*: carbohydrate response element-binding protein; *Lpl*: lipoprotein lipase; *Lipe*: hormone-sensitive lipase; *Atgl*: adipose triglyceride lipase; *Mgl*: monoglyceride lipase; *Plin1*: perilipin-1; *Plin2*: perilipin-2; *Plin3*: perilipin-3.

were unaffected (Fig. 5.12F). Lipolysis markers *Lipe* and *Atgl* showed reduced mRNA levels, whereas *Lpl* and *Mgl* were unchanged (Fig. 5.12F). Additionally, mRNA levels of lipid droplet-associated proteins *Plin 1* and *Plin 3* were lower in Mc1r LKO mice (Fig. 5.12F). Expression of other lipogenesis-related genes (*Fabp4*, *Cd36*, *Fasn*, *Acc1*, *Scd1*, *Dgat1*, *Dgat2* and *Gpat3*) and pro-inflammatory markers (*Il1b*, *Il6* and *Tnf-a*) did not differ between genotypes (Appendix Fig. 7A and B). Western blot analysis confirmed no change in the protein levels of lipogenesis (SREBP1c), lipolysis (HSL, ATGL) and lipid transport (CD36) markers in gWAT of Mc1r LKO mice (Appendix Fig. 7C and D). Overall, the loss of MC1R signaling in hepatocytes resulted in increased adipocyte size and alteration in lipid metabolism in gWAT. These changes suggest that MC1R plays a crucial role in maintaining normal adipocyte function and lipid homeostasis, highlighting its importance in metabolic regulation.

5.2.3 Hepatic transcriptome analysis of hepatocyte-specific MC1R deficient mice

To explore genome-wide transcriptomic changes in the liver of Mc1r LKO mice, a bulk RNA-Seq was conducted on liver samples from Western diet-fed control and Mc1r LKO mice (n=4 per genotype). Principal component analysis (PCA) showed a clustering between the genotypes (data not shown). RNA-Seq analysis identified 14,214 transcripts, with 635 being differentially expressed between Mc1r LKO and control mice, using an adjusted p-value < 0.05 and an absolute log fold change $\geq 0,25$. As shown in the volcano plot (Fig. 5.13A), 240 genes were upregulated, while 395 genes were downregulated in Mc1r LKO mice. Gene ontology (GO) enrichment analysis of 635 DEGs revealed significant associations with several biological processes. Enriched pathways included defense response to bacteria, cellular responses to lipopolysaccharide, interferon-gamma and -beta responses, and adaptive immune response (Fig. 5.13B). These findings indicate marked hepatic transcriptomic alterations in Mc1r LKO mice under Western diet. Overall, suggesting that the absence of MC1R in hepatocytes influences gene expression linked to lipid metabolism and inflammatory responses and this shift in gene expression may contribute to metabolic dysregulation in the context of high-fat diet.

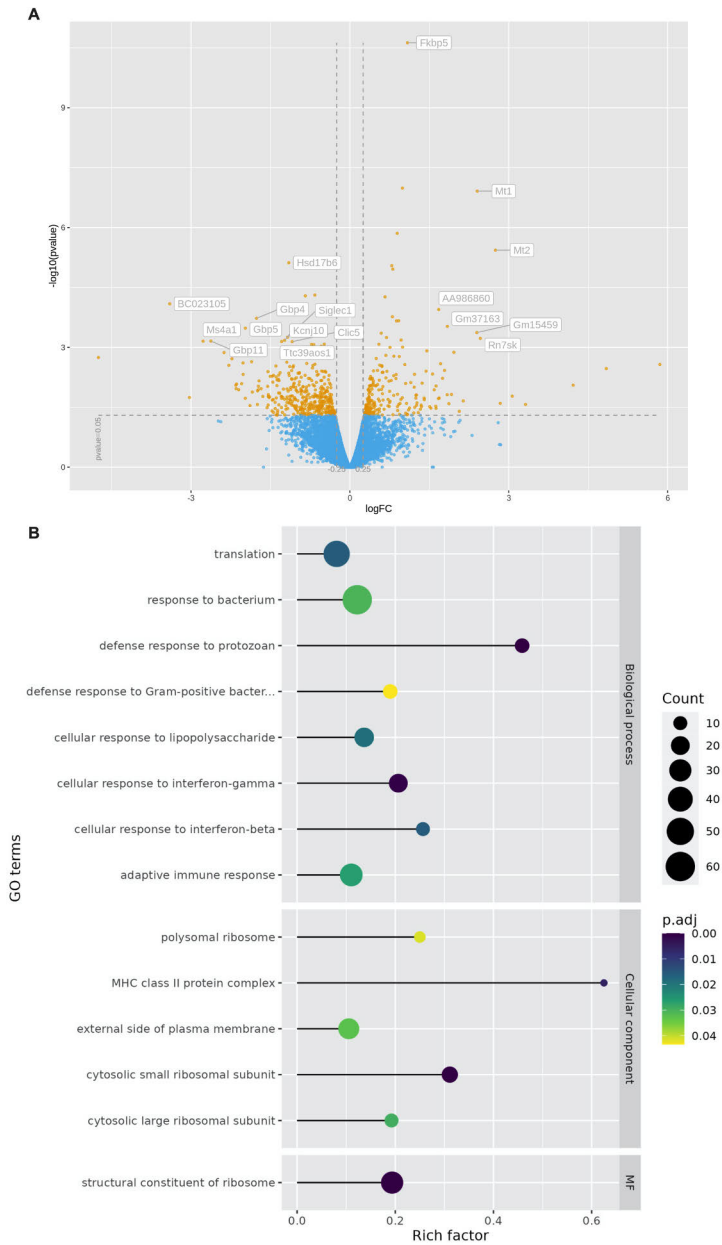


Figure 5.13. Hepatic transcriptomic difference between control and Mc1r LKO mice on Western diet. (A) Volcano plot showing upregulated and downregulated genes between control and Mc1r LKO mice. (B) Gene ontology (GO) terms associated with differentially expressed genes (DEGs) identified using topGO, a Bioconductor R package. The enriched pathways highlight significant alterations in inflammatory responses, adaptive immune responses, and cellular responses to lipopolysaccharide. The circle size represents the number of DEGs enriched in each pathway, while circle color indicates the degree of enrichment.

A few selected DEGs from RNA-Seq analysis were validated using qPCR on liver samples from control and Mc1r LKO mice. Consistent with the RNA-Seq analysis, top hit genes including metallothionein 1 (*Mt1*) and metallothionein 2 (*Mt2*) were significantly upregulated, while FK506 binding protein 5 (*Fkbp5*) showed a trend towards upregulation ($p=0.10$) in Mc1r LKO mice (Fig. 5.14A). Given the enrichment of inflammation-related GO terms among DEGs, the expression of pro-inflammatory cytokines was quantified. Mc1r LKO mice exhibited significant upregulation of interleukin 6 (*Il6*) and tumor necrosis factor alpha (*Tnf-a*), with a trend towards increased interleukin-1 beta (*Il1b*) expression ($p = 0.065$) (Fig. 5.14B). Additionally, there was an increase in the mRNA levels of 6-phosphofructo-2-kinase/fructose-2,6-biphosphatase 3 (*Pfkfb3*), a key glycolysis regulator associated with liver fibrosis (Zhou et al., 2021) (Fig. 5.14B). Histological analysis using Picrosirius Red staining

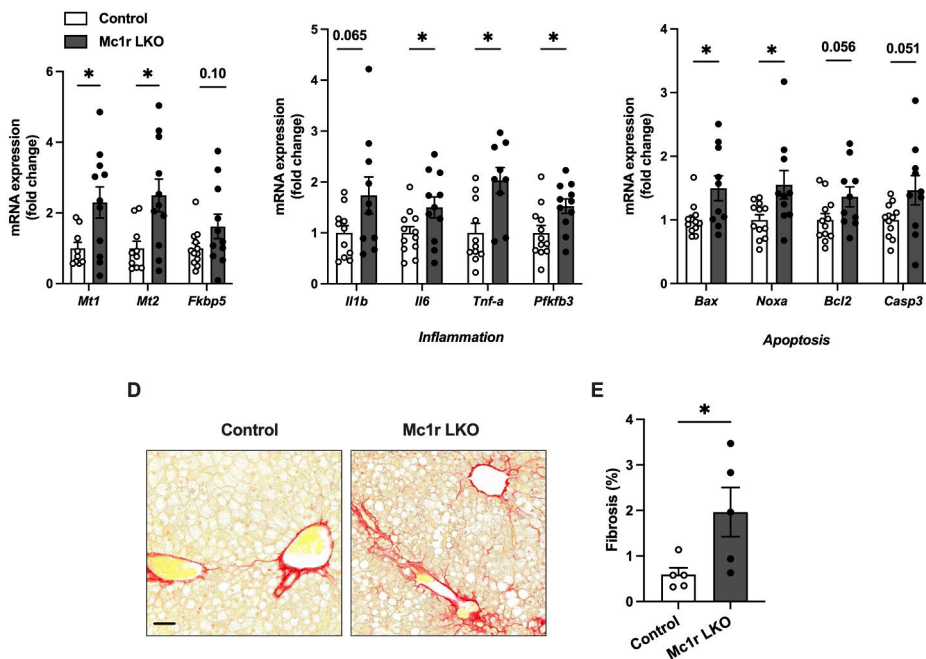


Figure 5.14. Hepatocyte-specific loss of melanocortin 1 receptor (MC1R) signaling induces inflammation, apoptosis, and fibrosis in the liver. (A) Validation of RNA-Seq data via quantitative real-time-polymerase chain reaction (qPCR) analysis of selected differentially expressed genes (DEGs). (B and C) qPCR analysis of pro-inflammatory cytokines and apoptosis markers in the liver of control and Mc1r LKO mice. (D) Representative Picrosirius Red-stained liver sections from Western diet-fed control and Mc1r LKO mice. Scale bar: 100 μm . (E) Quantification of liver fibrosis as percentage of total section area. The values are presented as mean \pm SEM, $n=5-10$ mice per group. * $p<0.05$ versus control mice by unpaired Student's t-test. Abbreviations: *Mt1*, metallothionein 1; *Mt2*, metallothionein 2; *Fkbp5*, FK506 binding protein 5; *Il1b*, interleukin-1 beta; *Il6*, interleukin 6; *Tnf-a*, tumor necrosis factor alpha; *Pfkfb3*, 6-phosphofructo-2-kinase/fructose-2,6-biphosphatase 3; *Bax*, Bcl2-associated X protein; *Noxa*, phorbol-12-myristate-13-acetate-induced protein 1; *Bcl2*, B-cell lymphoma 2; *Casp3*, caspase 3.

confirmed elevated fibrosis in Mc1r LKO mice (Fig. 5.14D and E). Markers of apoptosis were also examined, revealing significant upregulation of Bcl2-associated X protein (*Bax*) and phorbol-12-myristate-13-acetate-induced protein 1 (*Noxa*). There were also upward trends in B-cell lymphoma 2 (*Bcl2*) and caspase 3 (*Casp3*) expression levels (Fig. 5.14C). In summary, the hepatocyte-specific loss of MC1R signaling results in inflammation, apoptosis, and fibrosis in the liver. These findings underscore the critical role of MC1R in maintaining liver health, as its absence may drive pathological change leading to liver damage and dysfunction.

Enrichment analysis indicated that hepatocyte-specific MC1R deficiency may impact multiple nodes of the hepatic functions, including defense response to bacteria, cellular responses to lipopolysaccharide, interferon-gamma and -beta signaling, and adaptive immune response. Although the lipid metabolism pathway was not among the top significantly enriched GO terms, hepatic markers of lipogenesis, FAO and LDs were examined using qPCR. In line with the findings from Mc1r^{e/e} mice, *Srebp1c* mRNA expression remained unchanged in Mc1r LKO mice, whereas *Chrebp* was significantly upregulated (Fig. 5.15A). The upregulation of *Chrebp* was accompanied by increased expression of its target genes involved in DNL, such as *Acc1* and *Fasn*, with *Scd1* expression tented to be upregulated ($p=0.08$)

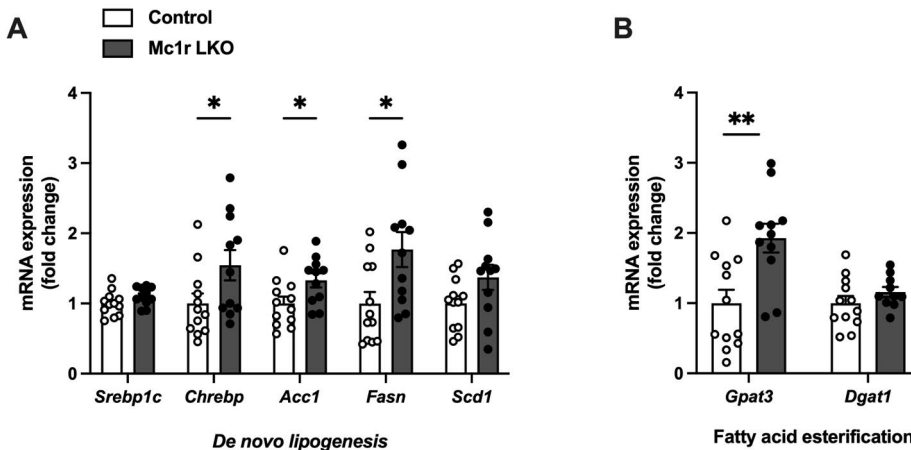


Figure 5.15. Hepatocyte-specific loss of melanocortin 1 receptor (MC1R) signaling increases expression of de novo lipogenesis (DNL) and fatty acid (FA) esterification genes in the liver. Quantitative real-time polymerase chain reaction (qPCR) analysis of: (A) Hepatic markers of de novo lipogenesis (DNL) in the liver of Western-diet fed control and Mc1r LKO mice. (B) Genes involved in FA esterification in the liver of Western diet fed control and Mc1r LKO mice. The values are presented as mean \pm SEM, $n=10-15$ mice per group. * $p<0.05$ and ** $p<0.01$ for the indicated comparisons by unpaired two-tailed Student's *t*-test. Abbreviations: *Srebp1c*, sterol regulatory element-binding protein 1; *Chrebp*, carbohydrate response element-binding protein; *Acc1*, acetyl-CoA carboxylase; *Fasn*, fatty acid synthase; *Scd1*, stearoyl-CoA desaturase 1; *Gpat3*, glycerol-3-phosphate acyltransferase 1; *Dgat1*, diglyceride acyltransferase.

in Mc1r LKO mice (Fig. 5.15A). However, there were no differences in the expression of genes related to lipid droplet-associated proteins, except for a notable downregulation of *Plin1* in Mc1r LKO mice (Appendix Fig. 8A and B). Additionally, genes involved in FA esterification were assessed. *Gpat1* expression was significantly upregulated, while *Dgat1* expression remained unchanged in the livers Mc1r LKO mice (Fig. 5.15B). In summary, the hepatocyte-specific loss of MC1R leads to increased expression of genes involved in DNL and FA esterification, suggesting that the loss of MC1R signaling disrupts normal hepatic metabolic regulation, promoting enhanced fat synthesis and storage.

5.2.4 The effects of pharmacological activation of MC1R in HepG2 cells and primary mouse hepatocytes

HepG2 cells and primary mouse hepatocytes were employed as an in vitro model to investigate whether pharmacological activation of MC1R signaling using α -MSH and LD211 could mitigate the expression of top DEGs and those involved in DNL observed in Mc1r LKO mice. The treatment with α -MSH significantly decreased the mRNA

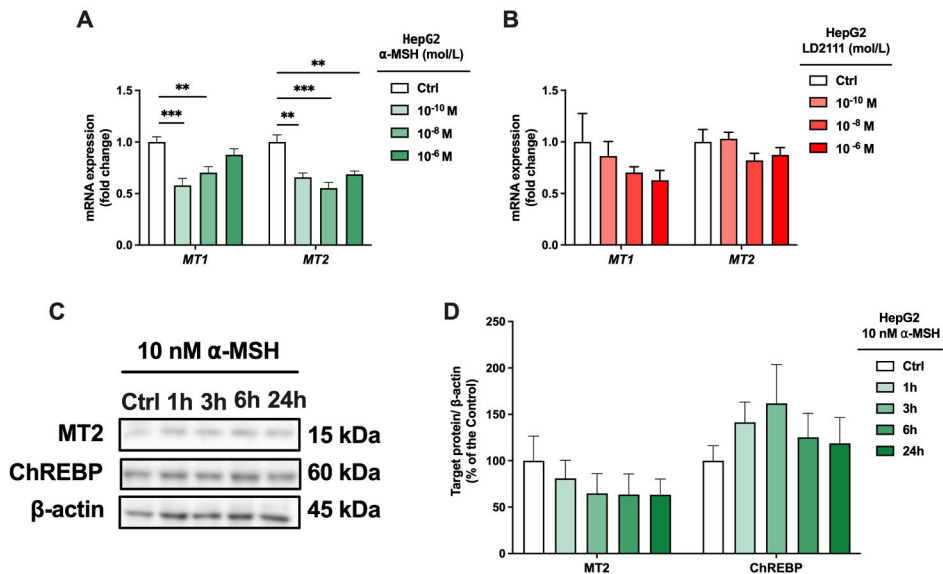


Figure 5.16. Pharmacological activation of melanocortin 1 receptor (MC1R) using α -MSH and LD211 results in variable responses in HepG2 cells (A and B) Quantitative real-time polymerase chain reaction (qPCR) analysis of metallothionein genes (*MT1* and *MT2*) in HepG2 treated with α -MSH and LD211 (0.1 nM, 10 nM, or 1 μ M). (C and D) Representative Western blots and quantification of MT2 and ChREBP protein levels in HepG2 cells treated with 10 nM α -MSH for different time points (1, 3, 6 and 24 hours). The values are presented as mean \pm SEM, n=3-6 per group. **p<0.01 and ***p<0.001 for the indicated comparisons by one-way ANOVA and Bonferroni *Post hoc* tests.

expression of stress-related proteins *MT1* and *MT2* (Fig. 5.16A), whereas LD211 showed no effect (Fig. 5.17B). Analysis of *ChREBP* gene expression, known to be upregulated in *Mc1r^{elc}* and *Mc1r* LKO mice, revealed no significant change in response to α -MSH (data not shown). Consistently, Western blot analysis showed no reduction in ChREBP or MT2 protein levels following α -MSH treatment (Fig. 5.16C and D). These results indicate that pharmacological activation of MC1R in HepG2 cells and did not consistently module MT2 and ChREBP expression at the protein level.

In contrast, primary mouse hepatocytes exhibited a different response profile. Treatment with α -MSH tended to lower *Mt1* and *Mt2* mRNA expression, though LD211 displayed inconsistent effects (Fig. 5.17A and B). Notably, both α -MSH and LD211 significantly reduced ChREBP protein expression in primary mouse hepatocytes (Fig. 5.17C and D). Additionally, LD211 decreased the expression of cleaved caspase 3, an apoptosis marker, while levels of BAX, BCL-2, and p53 remained unchanged (Appendix Fig.9B-D). To further explore the intracellular signaling pathways, primary hepatocytes were treated with α -MSH and LD211 for varying durations (5, 15, 30, and 60 minutes), and phosphorylation of c-Jun N-

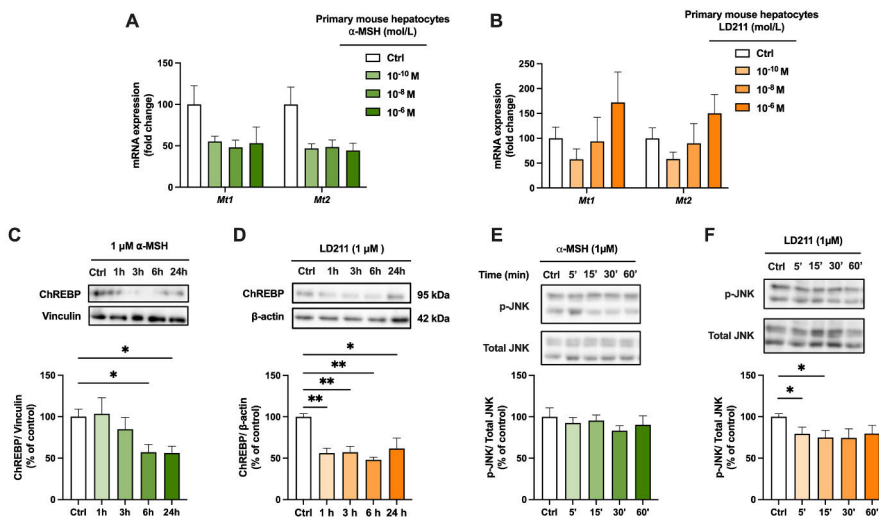


Figure 5.17. Selective pharmacological activation of melanocortin 1 receptor (MC1R) by LD211 reduces ChREBP and pJNK expression in primary mouse hepatocytes.

(A and B) Quantitative real-time polymerase chain reaction (qPCR) analysis of metallothionein genes (*Mt1* and *Mt2*) in primary mouse hepatocytes treated with α -MSH and LD211 (0.1 nM, 10 nM, or 1 μ M). (C and D) Representative Western blots and quantification of ChREBP protein levels in primary mouse hepatocytes treated with 1 μ M α -MSH for different time points (1, 3, 6 and 24 hours) (E and F) Representative Western blots and quantification of phosphorylated JNK protein levels in primary mouse hepatocytes treated with 1 μ M α -MSH and LD211 for different time points (5'-, 15'-, 30'- and 60'-minutes). The values are presented as mean \pm SEM, n=3-6 per group. * p <0.05 and ** p <0.01 for the indicated comparisons by one-way ANOVA and Bonferroni *Post hoc* tests.

terminal kinase (JNK) was assessed via Western blotting. Interestingly, LD211 rapidly reduced JNK phosphorylation, an effect not observed with α -MSH (Fig. 5.17E and F). In summary, these findings indicate that pharmacological activation of MC1R with LD211 effectively reduces ChREBP expression and apoptosis markers in primary mouse hepatocytes, highlighting the potential role in modulating hepatic metabolic and stress responses.

6 Discussion

The current understanding of the MC1R and its implication in the pathogenesis of obesity and obesity-related metabolic disorders remains limited. While MC1R is recognized for its established roles in pigmentation and inflammatory responses, its physiological functions in the regulation of cholesterol and FA metabolism have not been thoroughly investigated, leaving significant knowledge gaps in this area.

In this thesis, two distinct mouse models with MC1R deficiency were utilized: the recessive yellow mice ($Mc1r^{e/e}$) and hepatocyte-specific MC1R deficient mice (Mc1r LKO). These models were employed to elucidate the functional significance of MC1R signaling in the regulation of cholesterol and FA metabolism. Furthermore, the therapeutic potential of MC1R activation was explored via the application of two in vitro cell culture models: the human hepatocellular carcinoma (HepG2) cell line and freshly isolated primary mouse hepatocytes.

The findings presented in this thesis reveal the novel and significant role of MC1R signaling in the regulation of hepatic cholesterol, bile acids, and FA metabolism. This work not only advances our understanding of multifaceted functions of MC1R but also opens new avenues for potential therapeutic strategies targeting MC1R in the management of metabolic disorders.

6.1 Implication of MC1R signaling in the regulation of cholesterol and bile acid metabolism

One of the primary objectives of this thesis was to elucidate the regulatory role of MC1R in cholesterol and bile acid metabolism. Study I specifically investigated the biological consequences associated with the loss of hepatocyte-specific MC1R signaling by using female Mc1r LKO mice alongside control counterparts. Following a standard chow diet, MC1r LKO mice exhibited an increase in liver weights as well as elevated concentrations of total cholesterol and TG levels in both plasma and liver tissues. These observations are consistent with the results from the previous study that has demonstrated diet-induced hypercholesterolemia and enhanced hepatic lipid accumulation in *ApoE*^{-/-} mice with global MC1R deficiency (Rinne et al., 2018). This alignment of findings supports the hypothesis that the phenotypic characteristics observed in *ApoE*^{-/-} mice may be attributed to disturbance

in hepatocyte-specific MC1R signaling. Consequently, these results underscore the critical role of MC1R in maintaining lipid homeostasis and suggest a potential mechanistic link between disrupted MC1R signaling and the development of dyslipidemia. The exact mechanisms driving the increased hepatic cholesterol accumulation observed in Mc1r LKO mice are not fully understood. Under normal physiological conditions, *SREBP1c* predominantly activates genes involved in FA and TG biosynthesis, while *SREBP2* primarily regulates genes essential for cholesterol metabolism (Hua et al., 1993; Yokoyama et al., 1993). When intracellular cholesterol levels are elevated, the transcription activation of *SREBP2* are suppressed, resulting in decreased expression of its target genes, including *HMGCR* and *DHCR7*, which subsequently reduces cholesterol biosynthesis. Despite the increased hepatic cholesterol accumulation in Mc1r LKO mice, protein levels of HMGCR and DHCR7 were significantly lower, suggesting a disparity between cholesterol accumulation and *SREBP2* activity. This indicates that the elevated cholesterol in Mc1r LKO mice is unlikely due to upregulated DNL. Supporting this, in vitro experiments in HepG2 cells showed no change in HMGCR and DHCR7 levels following pharmacological activation of MC1R, signifying that MC1R signaling does not directly modulate the expression of SREBP2 or its target genes involved in cholesterol biosynthesis. These findings imply that MC1R signaling is not a direct regulator of hepatic cholesterol synthesis pathway. However, the hypercholesterolemia observed in Mc1r LKO mice may be partially linked to impaired cholesterol conversion into bile acids, which could contribute to the cholesterol accumulation. Further studies are needed to determine the specific pathways via which hepatic MC1R modulates cholesterol homeostasis, potentially identifying new regulatory mechanisms in cholesterol metabolism.

In Mc1r LKO mice, bile acid levels, particularly secondary bile acids, were reduced in both plasma and feces. This bile acid profile closely resembled that of *ApoE*^{-/-} mice with a global MC1R deficiency (Rinne et al., 2018). Notably, both models exhibited a decreased ratio of CA to CDCA, a ratio typically regulated by the activity of *Cyp8b1*, the enzyme responsible for CA synthesis (Chiang, 2004). Despite increased mRNA and protein levels of CYP8B1 in Mc1r LKO mice, the lower CA to CDCA ratio suggests dysfunctional *CYP8B1* activity, potentially disrupting the classical bile acid synthesis pathway. This disruption may lead to a compensatory increase in bile acid production via the alternative pathway, which has been reported to dominate in the liver diseases such as MASLD (Chiang, 2004; Crosignani et al., 2007; Lake et al., 2013). In humans, *CYP8B1* deficiency results in elevated plasma CDCA levels and reduced CA levels (Zhong et al., 2022). Similarly, genetic deletion of *Cyp8b1* in mice leads to decreased CA synthesis and subsequently lower levels of secondary bile acids derived from CA (Li-Hawkins et al., 2002). However, *Cyp8b1*-deficient mice maintain normal plasma cholesterol

levels and exhibit resistance to diet-induced obesity and liver steatosis (Bertaggia et al., 2017; Chevre et al., 2018). This suggests that hypercholesterolemic phenotype observed in Mc1r LKO mice is unlikely to be caused by *Cyp8b1* deficiency. The rate-limiting step of the classical bile acid synthesis pathway is regulated by *CYP7A1* (Russell and Setchell, 1992). While *Cyp7a1* knock-out models have shown variable effects on bile acid synthesis and cholesterol homeostasis (Dueland et al., 1993; Machleder et al., 1997; Schwarz et al., 2001, 1998), both human and murine *CYP7A1/Cyp7a1* deficiencies are associated with hypercholesterolemic (Erickson et al., 2003; Pullinger et al., 2002). Additionally, *Cyp7a1*-deficient mice show reduced hepatic *Ldlr* expression, increased intestinal cholesterol synthesis, and decreased fecal bile acid output, indicating a proatherogenic state (Erickson et al., 2003). Although no change in *Cyp7a1* expression was observed in Mc1r LKO mice, these findings imply that impaired bile acid synthesis could attribute to increased hepatic cholesterol levels.

Moreover, Mc1r LKO mice exhibited upregulation of *Stard1*, which facilitates mitochondrial cholesterol transport for substrate availability to *Cyp27a1*, a key enzyme in the alternative bile acid synthesis pathway (Ren et al., 2004). Overexpression studies in HepG2 cells have shown that increased *CYP27A1* enhances StAR expression, which in turn boosts bile acid synthesis via the alternative pathway (Hall et al., 2005). Elevated StAR expression has also been linked to MASH and MASH-driven HCC (Conde de la Rosa et al., 2021). Thus, the increased hepatic expression of StAR and *Cyp27a1* in Mc1r LKO mice may serve as markers of bile acid synthesis, suggesting a shift from classical to the alternative pathway as a compensatory mechanism. This shift is common in liver diseases such as MASLD, where the classical bile acid synthesis pathway is often compromised (Chiang, 2004; Crosignani et al., 2007; Lake et al., 2013). However, future studies are necessary to confirm this altered bile acid metabolism and its implication for cholesterol metabolism in Mc1r LKO mice. There was an increased expression of the bile acid transporter gene *Ntcp* and a decreased expression of another transporter, MRP4 in Mc1r LKO mice. These alterations are likely compensatory responses to disturbed bile acid synthesis. Upregulation of *Ntcp* may enhance bile salt uptake from the portal circulation, thereby promoting the enterohepatic recirculation of bile acids (Özvegy-Laczka et al., 2023). Conversely, the downregulation of MRP4 could reduce the efflux of bile acids into the circulation, preventing excessive spillover and thereby decreasing plasma bile acid levels (Zollner et al., 2006). This reduction in plasma bile acid levels may help to stabilize the hepatic bile acid pool despite of impaired bile acid synthesis in Mc1r LKO. These changes in bile acid transport suggest a compensatory mechanism aimed at maintaining bile acid homeostasis when its synthesis is disturbed. Given the well-documented interplay between steatotic liver diseases and bile acid dysregulation, it is unclear whether the altered

bile acid profile Mc1r LKO mice is a direct consequence of MC1R deficiency or an indirect effect of excessive hepatic lipid accumulation. However, *in vitro* studies with HepG2 cells support a direct role of MC1R in bile acid metabolism. Activation of MC1R signaling with α -MSH led to increased expression of *CYP8B1*, enhanced synthesis of CA, and CA:CDCA ratio. These findings indicate that hepatic MC1R signaling may play a direct role in regulating bile acid synthesis and composition in the liver. Further studies are needed to clarify the exact mechanisms and implications of this regulation in the context of liver health and disease.

Mc1r LKO mice displayed signs of liver fibrosis, potentially because of persistent hepatic cholesterol overload. Excessive cholesterol in the liver can exacerbate fibrosis by accumulating in hepatic stellate cells, which contributes to fibrogenic activation, as previously demonstrated in murine models (Teratani et al., 2012). As such, the fibrotic changes may be directly influenced by hepatocyte-specific MC1R deficiency. Contrary, MC1R activation has shown anti-fibrotic effects in various contexts, such as cultured fibroblasts and models of skin fibrosis and systemic sclerosis (Böhm and Stegemann, 2014; Kondo et al., 2022). Supporting this, *in vitro* experiments with HepG2 cells revealed a reduction in the expression of fibrotic markers upon MC1R activation with LD211. MC1R is widely recognized for its anti-inflammatory role, typically via the suppression of pro-inflammatory cytokine production (Böhm and Stegemann, 2014; Catania et al., 2004). However, in Study I, there was no direct evidence that MC1R signaling modulates inflammatory markers in the liver or cultured hepatocytes. Interestingly, Mc1r LKO mice displayed marked hepatic steatosis even when maintained on a standard chow diet, without accompanying signs of obesity or diabetes. Body weight gain and glucose homeostasis were comparable between Mc1r LKO and controls, indicating that the steatosis was not driven by systemic metabolic disturbances like obesity or insulin resistance. The precise mechanisms behind the onset of metabolic dysfunction in the liver, particularly in the form of MASLD, remain unclear. However, evidence from both human and animal studies suggest that, under normal caloric intake, MASLD may be linked to disturbed hepatic cholesterol metabolism (Kainuma et al., 2006; Min et al., 2012; Simonen et al., 2011). This dysregulation might precede or even contribute to the accumulation of TG in the liver. In Mc1r LKO mice, the increased hepatic TG content could therefore be a secondary consequence of elevated plasma and liver cholesterol levels, indicating a boarder disruption in lipid homeostasis.

Pharmacological activation of MC1R using the endogenous agonist α -MSH or the selective agonist LD211 led to the reduction in cellular cholesterol levels as well as enhanced uptake of both HDL and LDL particles in HepG2 cells. Typically, inhibition of cholesterol synthesis via statins decreases intracellular cholesterol levels in hepatocytes, which induces a compensatory increases in LDLR expression,

leading to lower plasma total and LDL cholesterol levels (Somers et al., 2023). The observed reduced in cholesterol following α -MSH-treatment could partially explain the upregulation of LDLR and the enhanced uptake of HDL and LDL particles in HepG2 cells. Interestingly, an upregulation of LDLR expression was detected as early as 1 hour after α -MSH treatment, even before any significant changes in intracellular cholesterol levels were evident. This suggests that MC1R activation directly stimulates LDLR expression rather than acting solely via feedback regulation due to lowered cholesterol. Similarly, MC1R activation rapidly increased SR-BI expression in HepG2 cells, which is consistent with the enhanced uptake of HDL particles. Previous studies have also shown increased LDLR expression and reduced plasma total cholesterol in atherosclerotic mice treated with a selective MC1R agonist (Rinne et al., 2017), underscoring the potential therapeutic benefits of MC1R activation in cholesterol regulation. Notably, while MC1R activation decreased cellular cholesterol levels in HepG2 cells, it did not alter the expression of key cholesterol biosynthetic enzymes HMGCR and DHCR7. This suggests that MC1R may reduce cholesterol synthesis via alternative mechanisms, possibly by regulating the phosphorylation state of HMGCR, which influences its enzymatic activity (Zhang et al., 2015). Additionally, increased cholesterol turnover into bile acids via elevated CYP8B1 expression and enhanced CA production could also contribute to the observed reduction in cellular cholesterol content following MC1R activation. However, further studies are needed to elucidate the exact molecular pathways via which MC1R activation reduces cholesterol levels in hepatocytes.

Classically, MC1R is coupled to the Gs protein, leading to the activation of AC and subsequent production of cAMP. In HepG2 cells, however, activation of MC1R with α -MSH or LD211 resulted in phosphorylation of AMPK and inhibition of ERK1/2 and JNK pathway, without altering cAMP levels. Mechanistically, inhibition of AMPK using dorsomorphin partially reversed the reduction in cellular cholesterol level in α -MSH-treated HepG2 cells. Despite this, the cholesterol-lowering effects α -MSH were still evident at lower concentrations even in the presence of dorsomorphin, indicating that the reduction in cholesterol levels is mediated via multiple signaling pathways, including AMPK and potentially MAPK pathways. In contrast, the cholesterol-lowering effect of LD211 was entirely dependent on AMPK phosphorylation, as dorsomorphin treatment completely reversed this effect. Previous studies have shown that AMPK activation reduces cholesterol synthesis, whereas its inhibition increases cholesterol synthesis in the liver (Clarke and Hardie, 1990; Loh et al., 2018; Steinberg and Kemp, 2009). The relationship between cholesterol metabolism and MAPK signaling is less understood. However, mechanistic study in HepG2 cells has demonstrated that ERK1/2 phosphorylation can enhance cholesterol synthesis via SREBP2, which regulates the transcription of *HMGCR* (Kotzka et al., 2004). The role of JNK

signaling pathway in cholesterol metabolism is even less explored, although it has been shown to contribute to hepatic steatosis and disturbance in bile acid metabolism (Manieri et al., 2020; Vernia et al., 2014). Therefore, it is plausible that MC1R activation by α -MSH modulates cholesterol metabolism in hepatocytes by inducing AMPK phosphorylation and inhibiting ERK1/2 and JNK signaling pathways.

In conclusion, hepatocyte-specific MC1R deficiency has been implicated in increasing cholesterol levels and disrupting bile acid metabolism in the liver. Conversely, activation of MC1R in hepatocytes led to the phenotype characterized by reduced cholesterol content. These findings suggest that targeting MC1R signaling, particularly within hepatic tissue, could serve as a promising therapeutic approach for managing MASLD and hypercholesterolemia. By modulating the MC1R signaling pathway, it may be possible to restore lipid homeostasis, thereby alleviating the adverse effects of MASLD. This therapeutic strategy could open new avenues for addressing conditions marked by elevated cholesterol levels and impaired bile acid metabolism, eventually improving liver health and overall metabolic functions of the liver.

6.2 Liver and adipose tissue phenotype of global and hepatocyte-specific MC1R deficient mouse models

The main objective of Study II was to investigate the regulatory role of MC1R signaling in FA metabolism in the liver and WAT. Mice with a global loss of MC1R ($Mc1r^{e/e}$) did not exhibit differences in body weight gain under a chow or a Western diet. However, these mice had significantly higher liver weights, plasma TG levels, and increased fat depot weights compared to control mice. Previous studies have shown that melanocortin receptors, including MC1R, are abundantly expressed in adipose tissue (Butler et al., 2000; Møller et al., 2015; Trevaskis et al., 2007; Zhang et al., 2005). MC1R expression has also been detected in both human and mouse adipocytes, where it has been implicated in regulating cell proliferation and inflammatory responses (Hoch et al., 2007; Møller et al., 2011). To further elucidate the functional role of MC1R in hepatocytes and adipocytes, the key enzymes involved in lipogenesis and FA hydrolysis were quantified. Hepatic gene expression analysis revealed more pronounced and consistent changes in $Mc1r^{e/e}$ mice on a Western diet compared to those observed in gWAT samples. While the observed effects might initially seem to result from the loss of MC1R signaling in adipose tissue, the phenotypic similarities between $Mc1r^{e/e}$ and $Mc1r$ LKO mice suggest otherwise. It is plausible that the increased adiposity and altered lipid metabolism in $Mc1r^{e/e}$ mice are primarily driven by the loss of MC1R signaling in the liver. This hypothesis is further supported by a previous study on cultured adipocytes, which

indicated that MC1R signaling in adipocyte does not directly influence lipid metabolism (Hoch et al., 2008). The functional role of MC1R in the liver was previously demonstrated in Study I, where hepatic MC1R signaling found to regulate cholesterol and bile acid metabolism. Hepatocyte-specific Mc1R deficient mice on a Western diet exhibited a similar phenotype, characterized by increased liver weights, elevated plasma and liver TG concentrations, as well as higher WAT weights. These findings underscore the critical role of hepatic MC1R signaling in regulating lipid metabolism and suggest that its loss contribute significantly to adipocyte hypertrophy and disrupted lipid homeostasis, particularly under high-fat diet conditions.

The increased expression of *Chrebp* and its target genes, along with elevated TG accumulation in the livers of Mc1R^{e/e} and Mc1R LKO mice, occurred without transcriptional changes in genes involved in FAO oxidation or export. The link between hepatocellular fat accumulation and an imbalance in FA uptake, DNL, FA oxidation, and lipid export is well-documented (Chao et al., 2019). The major transcriptional regulators, such as *ChREBP* and *SREBP1c*, control lipogenesis by modulating the expression of key lipogenic enzymes like *ACCI* and *FASN* (Wang et al., 2021). Despite their overlapping functions, *ChREBP* and *SREBP1c* have distinct roles in lipid metabolism, particularly in regulating genes involved in desaturation and elongation of FA (Linden et al., 2018). Interestingly, *Chrebp* was upregulated in the livers of Mc1R^{e/e} and Mc1R LKO mice, while *Srebp1c* remained unchanged. Given that *Chrebp* expression is typically regulated by glucose levels and that Mc1R^{e/e} and Mc1R LKO mice exhibited similar blood glucose levels, it is plausible that the loss of MC1R signaling directly induces *Chrebp* expression. The crucial role of *Chrebp* in glucose and lipid metabolism has been well-established; genetic ablation of *Chrebp* in rodents reduces the expression of key lipogenic and glycolytic enzymes necessary for the synthesis of FA and TG (Iizuka et al., 2004). In mouse model of genetic obesity, such as *ob/ob* mice, *Chrebp* deficiency led to a reduction in DNL in the liver and provided protected against obesity and adiposity (Iizuka et al., 2006). Conversely, *Chrebp* overexpression in mice has been shown to increase the expression of hepatic lipogenesis and FA esterification genes, elevate TG concentrations, and induce steatosis (Benhamed et al., 2012). However, these mice exhibited improved glucose tolerance, enhanced insulin sensitivity, and lower gWAT compared to wild-type controls following a Western diet, along with the reduced blood glucose and plasma TG levels (Iizuka et al., 2018). In contrast, Western diet-fed Mc1R^{e/e} and Mc1R LKO mice had showed increased WAT weights without changes in glucose homeostasis, exhibiting a phenotype distinct from that observed in *Chrebp* gain-of-function models. This discrepancy suggest that *Chrebp* upregulation alone may not account for the increased adiposity observed in Mc1R^{e/e} and Mc1R LKO mice. Therefore, it is likely that the loss of hepatocyte-specific

MC1R signaling disturbs additional, yet unidentified metabolic pathways involved in maintaining whole-body lipid homeostasis.

Mouse models deficient in MC1R signaling exhibited adipocyte hypertrophy, despite showing no significant differences in overall body weight gain. Additionally, these mice had comparable food intake and physical activity levels between genotypes, suggesting that the differences in energy intake or expenditure do not account for the increased fat mass. Thus, it is likely that increased adipocyte size in MC1R-deficient mice represents a compensatory mechanism to store more fat in gWAT in response to enhanced DNL in the liver. The ability of adipose tissue to expand and store extra fat has been shown to protect against diabetes (Kim et al., 2007). However, prolonged fat storage can lead to increased adipokine release, triggering metabolic disturbances that result in adipose tissue dysfunction, inflammation, and enhanced lipid flux to the liver (Pellegrinelli et al., 2016). Interestingly, *Mc1r^{e/e}* and *Mc1r* LKO mice exhibited reduced expression of adipose *Atgl* and *Lipe*, which are key enzymes involved in TG hydrolysis and FA mobilization. Previous studies have shown that the deletion of *Atgl* is associated with reduced lipolysis in adipocytes (Schoiswohl et al., 2015), while genetic ablation of *Hsl* protects against diet-induced and genetic obesity in mice (Harada et al., 2003; Sekiya et al., 2004). Given that the downregulation of *Lipe* and *Atgl* was only observed under chow diet conditions, it is unlikely that the increased fat mass in *Mc1r^{e/e}* mice is primarily due to the reduced expression of these lipolytic enzymes. In *Mc1r* LKO mice, there was a reduction in perilipins level, which play a crucial role in adipose tissue biology by regulating LDs stability and suppressing lipolysis (Brasaemle et al., 2000). The observed transcriptional alterations in *Lipe*, *Atgl*, and *Plin1* may indicate a compensatory mechanism aimed at suppressing lipolysis and consequently reducing FA flux to the liver. Despite increased adiposity, plasma FFA levels remained unchanged in MC1R-deficient mouse models, suggesting that lipolysis in adipose tissue is adequately controlled. These findings imply the involvement of alternative mechanisms, such as increased TG re-esterification, reduced VLDL export, or decreased FA oxidation, contributing to enhanced TG accumulation in the livers of *Mc1r* LKO mice. Additionally, the expression of *Ppara*, a key regulator of FAO and gluconeogenesis, was reduced in the gWAT of *Mc1r* LKO mice. This reduction may represent an adaptive response to lower FA oxidation process, facilitating the storage of excess TG sourced from the liver. In MASLD, insulin resistance in WAT plays a critical role in enhancing lipolysis, increasing FA flux to the liver, and promoting hepatic TG accumulation (Donnelly et al., 2005). Interestingly, *Mc1r* KO mice did not exhibit signs of insulin resistance or adipose tissue inflammation. These observations were supported by the unchanged plasma FFA levels and the absence of pro-inflammatory markers in the gWAT. Thus, it remains to be seen whether prolonged feeding with a Western diet or a diet with

higher fat content could potentially exceed the adipose tissue's capacity to store excess fat in Mc1r LKO mice. Such a scenario could lead to adipose tissue dysfunction, characterized by impaired lipid storage, inflammation, and exacerbation of metabolic disturbance.

The impact of loss of hepatocyte-specific MC1R signaling on various biological pathways was further investigated using RNA-Seq analysis. DEGs data indicated an upregulation of stress response proteins, specially metallothioneins (*Mt1* and *Mt2*), in the liver of Mc1r LKO mice. Under normal physiological conditions, metallothioneins maintain high zinc levels in the liver and release zinc during oxidative stress, thereby exerting potential antioxidant effects within the cells (Ruttkay-Nedecky et al., 2013). Metallothionein expression has been documented in several organs, including the liver, pancreas, intestine, and kidney. Notably, high-fat diet-induced liver anomalies in C57BL/6J mice have been associated with reduced hepatic expression of *Mt1* and *Mt2* (Waller-Evans et al., 2013). Interestingly, disruption of *Mt1* and *Mt2* genes increases susceptibility to diet-induced obesity, highlighting their potential role in regulating energy balance (Beattie et al., 1998; Kawakami et al., 2019). Conversely, overexpression of metallothioneins has been shown to protect hepatocytes from palmitate-induced lipotoxicity (Li et al., 2022). Thus, the observed increase in metallothioneins expression in the liver of Mc1r LKO mice is likely a consequence of elevated hepatic TG accumulation rather than a direct effect of MC1R deficiency. This hypothesis was confirmed in HepG2 and primary mouse hepatocytes. While activation of MC1R with α -MSH reduced the expression of *MT1* and *MT2* in HepG2 cells, similar effects were not observed with LD211 activation. Additionally, neither α -MSH nor LD211 mediated activation of MC1R altered metallothionein expression in primary mouse hepatocytes. Along with the increased hepatic TG accumulation, there was a significant upregulation of genes related to fibrosis, inflammation, and apoptosis in the liver of Mc1r LKO mice. This finding is intriguing, given that in Study I, selective activation of MC1R did not affect inflammatory markers in HepG2 cells. However, in Study II, MC1R activation had direct effects on apoptotic markers in primary mouse hepatocytes, suggesting that the loss of hepatic MC1R signaling may contribute to liver fibrosis and apoptosis. It remains unclear whether the increased TG accumulation in the livers of Mc1r LKO mice predisposes them to the pathological hallmarks of MASLD—such as apoptosis, inflammation, and fibrosis—or whether this hepatic TG buildup is a direct consequence of the impaired MC1R signaling in the liver. Further studies are needed to delineate these mechanisms and their implications for MASLD progression.

In vitro experiments demonstrated that MC1R activation reduced the protein expression of ChREBP in primary mouse hepatocytes, an effect not observed in HepG2 cells. While, HepG2 cells have been shown to share some biological characteristics with human primary hepatocytes (Rowe et al., 2013), significant

discrepancies exist between hepatoma cell lines and primary hepatocytes regarding DNL and gluconeogenesis (Calvisi et al., 2011; Molinaro et al., 2020). Comparative studies on lipid and glucose metabolism have revealed a marked reduction in DNL activity in HepG2 cells compared to primary hepatocytes (Nagarajan et al., 2019). Thus, differences in the regulation of metabolic pathways for glucose, FA, and cholesterol metabolism between primary hepatocytes and HepG2 cell lines explain why MC1R activation reduced ChREBP expression only in primary mouse hepatocytes.

In terms of intracellular signaling, MC1R activation increased AMPK phosphorylation and reduced JNK phosphorylation in HepG2 cells (Study I). Similarly, JNK phosphorylation was reduced in primary mouse hepatocytes following MC1R activation (Study II). AMPK serves as a master cellular energy sensor, responding to ATP depletion and maintaining energy homeostasis (Spaulding and Yan, 2022). AMPK activation is known to reduce the risk of MASLD by inhibiting hepatic DNL, promoting FAO in the liver, and enhancing mitochondrial integrity in adipose tissue (Smith et al., 2016). Moreover, AMPK inhibits ChREBP activity via phosphorylation, providing a mechanistic link between MC1R activation and reduced lipogenesis (Kawaguchi et al., 2002; Sato et al., 2016). The role of JNK signaling in FA metabolism is even less understood, but increased JNK activity has been observed in the livers of diet-induced and genetic mouse models (Hirosumi et al., 2002). Hence, it is plausible that both AMPK and JNK pathways mediate the effects of MC1R activation on FA metabolism. Given its central role in energy homeostasis, AMPK is a promising therapeutic target for various metabolic disorders. For example, metformin, an AMPK activator, effectively controls blood glucose levels in patients with T2D, particularly in the presence of obesity or metabolic syndrome (Cheang et al., 2014; Coughlan et al., 2014; Tong et al., 2022). Targeting MC1R to induce AMPK phosphorylation or modulating its signaling network could provide a novel approach for treating metabolic disorders. However, further research is needed to explore the broader implication of MC1R signaling in liver metabolism and its therapeutic potential.

In conclusion, Study II demonstrates how the hepatocyte-specific MC1R deficiency contributes to fat accumulation in the liver and adipose tissue, posing a significant metabolic risk. Specifically, the impairment of hepatic MC1R led to the upregulation of lipogenesis-related genes, indicating enhanced hepatic DNL, accompanied by fibrosis, inflammation, and signs of apoptosis. Conversely, pharmacological activation of MC1R reduced ChREBP expression in primary hepatocytes, suggesting a protective role against lipid overload. These findings suggest that targeting MC1R signaling could be a promising therapeutic strategy for treating metabolic disorders like MASLD.

6.3 Study limitations

While this study provides valuable insights into the role of hepatic MC1R in lipid metabolism, it has some limitations. First, the *in vitro* experiments primarily relied on HepG2 cells, with limited use of freshly isolated primary mouse hepatocytes, which are considered the gold standard for physiologically relevant liver models. The use of HepG2 cells was mainly due to the challenges of culturing primary hepatocyte, which are phenotypically unstable, have short lifespan and require a labor-intensive process. Another limitation is the lack of specificity in the *in vitro* studies, where cells were treated with the endogenous MC1R agonist α -MSH. Since α -MSH activates all MCR subtypes, except MC2R, some observed effects may not have been mediated by MC1R alone, potentially explaining differences between α -MSH and the selective MC1R agonist LD211. Although studies on the expression of MCR subtypes in the liver are limited, MC4R and MC5R have been detected in the human and rat liver (Bitto et al., 2011; Malik et al., 2012; Moscovitz et al., 2019). Thus, the effects of α -MSH should be interpreted with caution. Additionally, the absence of other selective MC1R agonists limits the interpretation of the findings. While LD211 shows selectivity for MC1R, testing additional MC1R agonists in both *in vitro* and *in vivo* studies could have validated LD211's effects and provided a more comprehensive understanding of MC1R signaling.

Regarding *in vivo* studies, the lack of gain-of-function models (either via drug intervention or genetic manipulation) is a limitation, as such studies would offer greater insights into the therapeutic potential of targeting MC1R in liver diseases like MASLD. Additionally, the lack of lipidomic profiling in Mc1r LKO mice limited the understanding of differentially expressed lipids in the livers, which could have complemented the hepatic transcriptomic analysis. Furthermore, *in vivo* studies did not include functional assays to determine whether MC1R affects rates of cholesterol synthesis or measurement of DNL flux in the liver. Although measurement of cholesterol synthesis and DNL or FAO is methodologically challenging, these assays would have validated the molecular mechanisms driving altered hepatic FA metabolism in Mc1r LKO mice. Additionally, this study lacked validation methods for liver fibrosis. While histological imaging is accurate, it is subject to sample variability and only assesses a limited liver area. Using assays that detect fibrotic markers like collagen, alpha smooth muscle actin (α -SMA), and transforming growth factor beta (TGF- β), could have provided a more precise and consistent assessment of liver fibrosis. Finally, while animal models offer valuable insights into human metabolic diseases, there are notable physiological differences between mice and humans that must be considered when interpreting these results. Recognizing these disparities is crucial for accurately translating findings from this study into potential therapeutic strategies for human metabolic syndrome.

6.4 Therapeutic perspectives

The future direction of this thesis is to conduct interventional studies to evaluate the therapeutic potential of hepatic MC1R signaling in the treatment of dyslipidemia and associated liver diseases, particularly MASLD. Given the current lack of treatment strategies to address the underlying pathogenic mechanisms of MASLD, there is an unmet need to explore innovative therapeutic approaches that could effectively halt disease progression. This research could contribute significantly to the development of novel therapies for conditions characterized by metabolic dysregulation and hepatic impairment. Recent advancements in understanding MCRs have generated significant interest in their therapeutic potential across various inflammatory, metabolic and CVD (Cai et al., 2009). MC1R's anti-inflammatory properties are well-established in multiple cell types (Catania et al., 2004), and its activation has shown anti-fibrotic effects, offering protection against skin fibrosis and systemic sclerosis (Böhm and Stegemann, 2014; Kondo et al., 2022). The therapeutic benefits of MC1R activation are increasingly recognized, warranting further exploration into its broader applications. This thesis identifies hepatic MC1R activation as a promising therapeutic strategy for targeting the underlying pathophysiological mechanisms of MASLD. Notably, afamelanotide (marketed as SCENESSE), a MC1R agonist, is approved for treating erythropoietic protoporphyria (EPP), demonstrating enhanced light tolerance with mild adverse effects (Wu and Cotliar, 2021). MC1R agonists currently in clinical trials primarily focus on chronic inflammatory conditions, including systemic sclerosis, neuroinflammation, and rheumatoid arthritis. Amongst these, Dersimelagon (MT-7117), a highly selective MC1R agonist (has much higher selectivity for MC1R than afamelanotide), has shown promise in increasing light tolerance in patients with EPP, as indicated by Phase 2 trial data (Balwani et al., 2020). MC1R agonists are generally well tolerated, with mild to moderate adverse effects such as injection site reactions, headaches, and gastrointestinal disturbances. However, further research is needed to fully assess their long-term safety and effectiveness across diverse populations.

This thesis demonstrated that the hepatocyte-specific MC1R deficiency leads to increased cholesterol and TG accumulation in the liver. In contrast, activation of hepatic MC1R reduces cellular cholesterol levels and enhances the uptake of HDL and LDL particles in cultured hepatocytes. While the cholesterol-lowering effects of MC1R activation may appear similar to those of statins, which reduces cholesterol synthesis, MC1R likely regulates multiple distinct pathways. For example, MC1R signaling appears to directly induce LDLR expression, whereas statins increase LDLR expression as a secondary effect of reduced cholesterol synthesis. Supporting this, selective MC1R agonist treatment in atherosclerotic mice reduced plasma total cholesterol and increased hepatic expression of LDLR, highlighting the therapeutic potential of MC1R activation in cholesterol management (Rinne et al., 2017).

Furthermore, Mc1r LKO mice exhibited increased TG accumulation and upregulation of *Chrebp*, a key regulator of hepatic DNL. MC1R activation reduced ChREBP expression in hepatocytes, suggesting an additional role in regulating hepatic DNL. Consistent with previous findings of MC1R's anti-fibrotic effects, MC1R activation downregulated fibrotic gene expression in hepatocytes, while Mc1r LKO mice showed enhanced liver fibrosis (Böhm and Stegemann, 2014). Additionally, MC1R activation influenced the expression of apoptotic markers in primary mouse hepatocytes.

In the light of the 'multiple parallel hits' -hypothesis of MASLD, the findings from this thesis suggest that MC1R activation could target multiple key pathways involved in the progression from steatosis to MASH. Specifically, targeting hepatic MC1R may help reduce hepatic TG and cholesterol accumulation while also mitigating fibrosis, inflammation, and apoptosis—critical pathological hallmarks of MASLD progression. Although this approach may not exceed the efficacy of current lipid-lowering drugs like statins, the ability of MC1R activation in the hepatocytes could simultaneously target multiple pathogenic mechanisms of MASLD highlights its therapeutic potential, warranting further investigation in future studies.

In conclusion, this thesis uncovers a novel role for hepatic MC1R signaling in the regulation of cholesterol, bile acid, and FA metabolism. Despite these promising insights, substantial research is needed to develop highly selective MC1R ligands and evaluate their pharmacological properties and therapeutic efficacy in liver diseases. The recent structural resolution of MC1R-Gs complexes via cryo-electron microscopy (Ma et al., 2021) provides a framework for designing melanocortin-targeted molecules, particularly using advanced in-silico drug discovery techniques (Sela et al., 2010). This structural insight enables precise modeling and targeting MC1R interactions to enhance selectivity and efficacy. Although promising drugs targeting the MCR family are in clinical trials for chronic diseases like systemic sclerosis, neuroinflammation, and rheumatoid arthritis, designing MC1R-selective ligands for metabolic conditions remain complex. Therefore, extensive preclinical and clinical studies are essential to identify optimal MC1R-targeted compounds and fully evaluate their therapeutic benefits in managing metabolic disorders such as, MASLD.

7 Summary/Conclusions

The main aim of this study was to investigate the functional role of MC1R in the regulation of cholesterol, bile acid, and FA metabolism in the liver. The key findings and conclusions of this thesis were as follows:

1. MC1R expression was downregulated in the livers of mice fed a cholesterol-rich Western-type diet. Similarly, decreased *MC1R* levels were observed in the liver biopsies from MASLD and MASH patients. In vitro, palmitic acid treatment of cultured HepG2 cells led to a reduction in MC1R protein levels. These findings indicate that MC1R is expressed in the hepatocytes and that its expression reduces in response to lipid overload.
2. Hepatocyte-specific MC1R deficiency led to increased accumulation of cholesterol and TG in the liver and circulation, along with disturbed bile acid metabolism. *Mc1r* LKO mice showed signs of hepatic steatosis and fibrosis. In contrast, pharmacological activation of MC1R signaling reduced intracellular cholesterol levels and enhanced the uptake of HDL and LDL particles in cultured HepG2 cells.
3. Global MC1R-deficient mice displayed hyperlipidemia, expanded WAT depots, and increased adipocyte hypertrophy. This phenotype was recapitulated in hepatocyte-specific MC1R deficient mice, suggesting that these effects were driven by impaired MC1R signaling in the liver. Hepatic transcriptomic analysis revealed upregulation of genes associated with DNL and FA esterification in *Mc1r* LKO mice. Furthermore, hepatocyte-specific MC1R deficiency was associated with increased signs of inflammation, fibrosis, and apoptosis in the liver.

In conclusion, hepatocyte-specific MC1R deficient mouse model exhibited key features of MASLD, including hepatic steatosis, dyslipidemia, inflammation, and fibrosis. These findings underscore the role of hepatic MC1R signaling in lipid metabolism and liver pathology, providing insight into the molecular mechanisms driving MASLD progression.

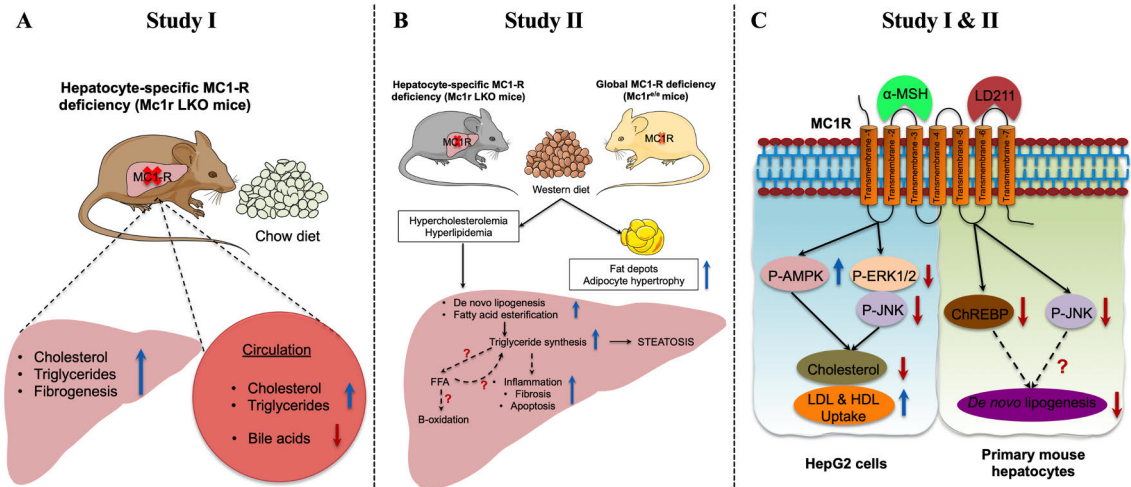


Figure 7.1. Schematic summary of the effects of hepatic MC1R signaling in vivo and in vitro.

(A) Loss of hepatocyte-specific MC1R signaling (Study I): The loss of hepatocyte-specific MC1R signaling enhances the accumulation of cholesterol and triglycerides (TG) in the liver, promotes fibrogenesis, and disrupts bile acid metabolism. This study illustrates the role of hepatic MC1R in regulating cholesterol and bile acid metabolism.

(B) Loss of global and hepatocyte-specific MC1R signaling (Study II): The loss of MC1R signaling, both globally and in hepatocytes, leads to increased fat depots, adipocyte hypertrophy, as well as elevated liver fibrosis, inflammation, and apoptosis.

(C) Pharmacological activation of MC1R signaling (Study I & II): Activation of MC1R in HepG2 cells and primary mouse hepatocytes by endogenous agonist α -MSH or synthetic agonist LD211 reduces cellular cholesterol content and enhances the uptake of low-density lipoprotein (LDL) and high-density lipoprotein (HDL) in HepG2 cells. In primary mouse hepatocytes, MC1R activation reduces ChREBP and p-JNK protein levels, likely inhibiting de novo lipogenesis (DNL). In summary, hepatic MC1R activation offers therapeutic potential for managing hypercholesterolemia and hyperlipidemia. Blue arrows indicate upregulation, red arrows indicate downregulation and the dashed arrows with red question mark suggest possible mechanisms, but these were not evaluated in this study. Key terms: MC1R: melanocortin 1 receptor; p-AMPK: phosphorylated AMP-activated protein kinase; p-ERK1/2: phosphorylated extracellular-signal-regulated kinase 1/2; p-JNK: phosphorylated c-Jun N-terminal kinase; ChREBP: carbohydrate response element binding protein. Parts of the figure was created using images from the Servier Medical Art, licensed under a Creative Commons Attribution 4.0 International License.

Acknowledgements

This thesis was conducted at the Department of Integrative Physiology and Pharmacology, Institute of Biomedicine, University of Turku. I extend my gratitude to Professor Pekka Hänninen, Dean of the Faculty and Professor Eriika Savontaus, Vice Dean of the Faculty as well as Professor Ullamari Pesonen, Director of the Drug Research Doctoral Programme (DRDP) for providing an excellent research facilities and resources. I also appreciate the educational support from the DRDP and its former coordinator Eeva Valve and current coordinator Marja Peura. Special thanks to the chief academic officer Outi Irjala for her unwavering support during the final stages of this thesis. This work was supported by grants from the Finnish Cultural Foundation, Turku University Foundation, DRDP, Finnish Atherosclerosis Society and the Academy of Finland.

I am profoundly grateful to my supervisor, Docent Petteri Rinne for his unwavering guidance, encouragements, and invaluable advice. From our very first conversation, I knew I had found an exceptional mentor. Your always-open office door provided comfort during times of confusion and struggle. I appreciate the freedom you allowed me to conduct my experiments while remaining readily available for support, fostering my growth and independence as a researcher. Your encouragement, especially during the manuscript preparation and thesis writing process has significantly enriched my academic writing skills and overall knowledge. I also wish to express my sincere gratitude to my co-supervisor, Professor Eriika Savontaus for her continuous support, inspiration, and fresh perspectives on my research. Her insightful suggestions have been instrumental in refining and aligning my ideas as I finalized this thesis. I also want to thank the follow-up committee members, Professor Eriika Savontaus and Docent Suvi Ruohonen, for the inspiring discussions and invaluable feedback.

I would like to express my sincere gratitude to the official examiners of this thesis, Docent Kaija Autio and Docent Panu Luukkonen. Your expertise and constructive feedback have greatly enhanced the quality of my thesis and expanded my knowledge in the field. I am also grateful to Professor Jukka Hakkola for graciously accepting the invitation to serve as my opponent during the public

examination of my thesis. Especial thanks to Elizabeth Nyman for her invaluable proofreading and insightful suggestions.

I would like to extend my heartfelt gratitude to all the members of the melanocortin family. I especially want to thank my wonderful colleagues Anni and Jamal; it has been a true pleasure to share a workspace with you. Our productive journal club sessions and regular group meetings have been both inspiring and fruitful. I also cherish the enjoyable moments we've shared, both in and out of the workplace. I would also like to extend my gratitude to all the past members of the melanocortin family: Iida Pennanen, Karla Saukkonen, Liisa Jokinen, Guillem Saldo Rubio and Johanna Jukkala. Your constant support and friendly nature have had a profound impact on my thesis. I sincerely value your contributions and assistance.

This thesis would not have been complete without the guidance and encouragement of many individuals. I would like to take this opportunity to express my sincere gratitude to all the former and current members of MedC6 "Farmis": Kim Eerola, Sanna Soini, Jonne Laurila, Ali Benkherouf, Mikko Uusi-Oukari, Hanna Haukkala, Elina Kahra, Marika Iljamo, Arto Liljebblad, Katri Lundell, Virpi Aaltonen, all the members of Alekski Tornio's group and Olli Pentikäinen's group, for fostering such a warm and professional work environment. I am especially thankful to Sanna Bastman for her skillful technical assistance and readiness to help, which have been invaluable throughout the process. To all my co-authors and collaborators, thank you for your insightful comments, suggestion, and generous time. Your contributions have been instrumental to the success of this thesis.

Heartfelt thanks to all my incredible friends especially to Kisun, for our journey since 2005. Thank you for keeping of the spirit alive and making every moment vibrant. I am grateful for your support in times of need, for all the laughter and for being a lifelong friend. Our friendship continues to grow strong together - now with our children joining the party. A big thank you to Bishwa for your thoughtful gesture. I am so grateful for your generosity and willingness to lend a hand. You have a unique gift for making everything feel just a bit easier and lighter. I truly cherish our unforgettable fishing trips; those moments will stay with me for a long time. To Pravin, thank you for the incredible years of friendship and for becoming like family. Thank you, Ciaran, for the joyful moments and effortless conversations. I appreciate your patience with my endless chatter, even from afar. Your friendship means a lot to me. Warmest thanks to Marjut and Uokku for your unwavering support and friendship. I treasure our late-night talks and the unforgettable memories we've shared together. Our epic trip to Koli always brings a smile to my face. A special thanks to Kaisa, Juri, Daniel, Aura, and Jussi for your unwavering support. A big shout-out to Daniel for organizing such a wonderful annual cray-fish party - it's an event I eagerly anticipate each year. It's been amazing to share those fun and joyful moments with all of you. I'm thrilled to have you as friends.

I would like to extend my heartfelt and special thanks to Päivi, Matti and Joel for their unwavering support throughout the years. Päivi, words cannot express the depth of my gratitude for everything you have done and continue to do for us. Thank you for embracing me like family, treating me with warmth and kindness that I truly feel loved and cherished. Your nurturing spirit has created a warmth that I hold dear, and I am endlessly thankful for the love and care you have shown us. Without a doubt, you are the world's best Mumma, and we all love you dearly.

I owe my deepest gratitude to my family for their unwavering support throughout my life. To my mother, I am eternally grateful for your boundless love, guidance, and endless support. Your nurturing spirit has shaped me into the person I am today. To my father, who left us far too soon, I carry your memory in my heart. To my sisters, I am incredibly thankful for your endless love and support. You have always been there for me, supporting me and sharing countless moments of joy and laughter. Your presence in my life has been a source of strength and comfort.

To my dearest sons, Aaron and Edvin, you are my greatest achievement. Since the moment you came into my life, you have brought overwhelming joy and happiness that I never knew was possible. Watching you grow and discover the world gives me such immense satisfaction and fills my heart with love that is beyond words. You have reshaped my life; you are my priority. You are my everything!

Finally, to my beloved Ilona - words can never fully express the depth of gratitude and love I have for you. Over these thirteen unforgettable years, we've built a life together, filled with love, laughter and memories that will forever fill my heart. From the moment our paths crossed, you have been my guiding light and my greatest source of strengths. Your unwavering belief in me has been a powerful force inspiring me to believe that no goal is too ambitious, and no dream is too distant. This journey, often unpredictable and challenging, would have been impossible without you by my side. You've walked with me through every peak and valley, sacrificing, reshaping your own dreams, and adapting your life to support mine. I am endlessly grateful—not only for your love and support, but also for the warmth and joy you bring into our home. Your care and devotion in raising our boys make you an extraordinary mother. Thank you for believing in me, for lifting me when I stumbled, and for always reminding me that together, we can overcome anything. You are the love of my life, and I cherish every moment we share. I love you beyond words, and beyond measure!

Turku, November 2024



Keshav Thapa

References

- Abdel-Malek, Z.A., Swope, V.B., Starner, R.J., Koikov, L., Cassidy, P., Leachman, S., 2014. Melanocortins and the melanocortin 1 receptor, moving translationally towards melanoma prevention. *Arch. Biochem. Biophys.* 563, 4–12. <https://doi.org/10.1016/j.abb.2014.07.002>
- Abdel-Misih, S.R.Z., Bloomston, M., 2010. Liver anatomy. *Surg. Clin. North Am.* 90, 643–653. <https://doi.org/10.1016/j.suc.2010.04.017>
- Agius, L., 2008. Glucokinase and molecular aspects of liver glycogen metabolism. *Biochem. J.* 414, 1–18. <https://doi.org/10.1042/BJ20080595>
- Ahmad, T.R., Haeusler, R.A., 2019. Bile acids in glucose metabolism and insulin signalling - mechanisms and research needs. *Nat. Rev. Endocrinol.* 15, 701–712. <https://doi.org/10.1038/s41574-019-0266-7>
- Ahmadian, M., Duncan, R.E., Jaworski, K., Sarkadi-Nagy, E., Sul, H.S., 2007. Triacylglycerol metabolism in adipose tissue. *Future Lipidol.* 2, 229–237. <https://doi.org/10.2217/17460875.2.2.229>
- Alves-Bezerra, M., Cohen, D.E., 2017. Triglyceride metabolism in the liver. *Compr. Physiol.* 8, 1. <https://doi.org/10.1002/cphy.c170012>
- Amin, M., Ott, J., Wu, R., Postolache, T.T., Gagnoli, C., 2022. Implication of Melanocortin Receptor Genes in the Familial Comorbidity of Type 2 Diabetes and Depression. *Int. J. Mol. Sci.* 23, 8350. <https://doi.org/10.3390/ijms23158350>
- Angulo, P., 2002. Nonalcoholic fatty liver disease. *N. Engl. J. Med.* 346, 1221–1231. <https://doi.org/10.1056/NEJMra011775>
- Angulo, P., Kleiner, D.E., Dam-Larsen, S., Adams, L.A., Bjornsson, E.S., Charatcharoenwitthaya, P., Mills, P.R., Keach, J.C., Lafferty, H.D., Stahler, A., Haflidadottir, S., Bendtsen, F., 2015. Liver Fibrosis, but No Other Histologic Features, Is Associated With Long-term Outcomes of Patients With Nonalcoholic Fatty Liver Disease. *Gastroenterology* 149, 389–397.e10. <https://doi.org/10.1053/j.gastro.2015.04.043>
- Arrese, M., Cabrera, D., Kalergis, A.M., Feldstein, A.E., 2016. Innate Immunity and Inflammation in NAFLD/NASH. *Dig. Dis. Sci.* 61, 1294–1303. <https://doi.org/10.1007/s10620-016-4049-x>
- Axelsson, M., Sjövall, J., 1990. Potential bile acid precursors in plasma—possible indicators of biosynthetic pathways to cholic and chenodeoxycholic acids in man. *J. Steroid Biochem.* 36, 631–640. [https://doi.org/10.1016/0022-4731\(90\)90182-r](https://doi.org/10.1016/0022-4731(90)90182-r)
- Azzu, V., Vacca, M., Virtue, S., Allison, M., Vidal-Puig, A., 2020. Adipose Tissue-Liver Cross Talk in the Control of Whole-Body Metabolism: Implications in Nonalcoholic Fatty Liver Disease. *Gastroenterology* 158, 1899–1912. <https://doi.org/10.1053/j.gastro.2019.12.054>
- Balwani, M., Bonkovsky, H.L., Belongie, K.J., Anderson, K.E., Takahashi, F., Irizarry, A., Amster, M., Bissell, D.M., Wang, B., Hazan, L., Parker, C.J., Cordasco, E., Levy, C., Desnick, R.J., 2020. Erythropoietic Protoporphyrin: Phase 2 Clinical Trial Results Evaluating the Safety and Effectiveness of Dersimelagon (MT-7117), an Oral MC1R Agonist. *Blood* 136, 51. <https://doi.org/10.1182/blood-2020-142467>
- Bartelt, A., Heeren, J., 2014. Adipose tissue browning and metabolic health. *Nat. Rev. Endocrinol.* 10, 24–36. <https://doi.org/10.1038/nrendo.2013.204>

- Bartz, R., Li, W.-H., Venables, B., Zehmer, J.K., Roth, M.R., Welti, R., Anderson, R.G.W., Liu, P., Chapman, K.D., 2007. Lipidomics reveals that adiposomes store ether lipids and mediate phospholipid traffic. *J. Lipid Res.* 48, 837–847. <https://doi.org/10.1194/jlr.M600413-JLR200>
- Beattie, J.H., Wood, A.M., Newman, A.M., Bremner, I., Choo, K.H., Michalska, A.E., Duncan, J.S., Trayhurn, P., 1998. Obesity and hyperleptinemia in metallothionein (-I and -II) null mice. *Proc. Natl. Acad. Sci. U. S. A.* 95, 358–363. <https://doi.org/10.1073/pnas.95.1.358>
- Becher, E., Mahnke, K., Brzoska, T., Kalden, D.H., Grabbe, S., Luger, T.A., 1999. Human peripheral blood-derived dendritic cells express functional melanocortin receptor MC-1R. *Ann. N. Y. Acad. Sci.* 885, 188–195. <https://doi.org/10.1111/J.1749-6632.1999.TB08676.X>
- Bechmann, L.P., Hannivoort, R.A., Gerken, G., Hotamisligil, G.S., Trauner, M., Canbay, A., 2012. The interaction of hepatic lipid and glucose metabolism in liver diseases. *J. Hepatol.* 56, 952–964. <https://doi.org/10.1016/j.jhep.2011.08.025>
- Benhamed, F., Denechaud, P.-D., Lemoine, M., Robichon, C., Moldes, M., Bertrand-Michel, J., Ratziu, V., Serfaty, L., Housset, C., Capeau, J., Girard, J., Guillou, H., Postic, C., 2012. The lipogenic transcription factor ChREBP dissociates hepatic steatosis from insulin resistance in mice and humans. *J. Clin. Invest.* 122, 2176–2194. <https://doi.org/10.1172/JCI41636>
- Bennett, H.P.J., 1986. Biosynthetic fate of the amino-terminal fragment of pro-opiomelanocortin within the intermediate lobe of the mouse pituitary. *Peptides* 7, 615–622. [https://doi.org/10.1016/0196-9781\(86\)90036-7](https://doi.org/10.1016/0196-9781(86)90036-7)
- Berneis, K.K., Krauss, R.M., 2002. Metabolic origins and clinical significance of LDL heterogeneity. *J. Lipid Res.* 43, 1363–1379. <https://doi.org/10.1194/jlr.r200004-jlr200>
- Bertaggia, E., Jensen, K.K., Castro-Perez, J., Xu, Y., Di Paolo, G., Chan, R.B., Wang, L., Haesler, R.A., 2017. Cyp8b1 ablation prevents Western diet-induced weight gain and hepatic steatosis because of impaired fat absorption. *Am. J. Physiol. - Endocrinol. Metab.* 313, E121–E133. <https://doi.org/10.1152/ajpendo.00409.2016>
- Bertolini, A., Tacchi, R., Vergoni, A.V., 2009. Brain effects of melanocortins. *Pharmacol. Res.* 59, 13–47. <https://doi.org/10.1016/j.phrs.2008.10.005>
- Bessone, F., Razoni, M.V., Roma, M.G., 2018. Molecular pathways of nonalcoholic fatty liver disease development and progression. *Cell. Mol. Life Sci. CMLS* 76, 99–128. <https://doi.org/10.1007/s00018-018-2947-0>
- Bhattarai, A., Likos, E.M., Weyman, C.M., Shukla, G.C., 2021. Regulation of cholesterol biosynthesis and lipid metabolism: A microRNA management perspective. *Steroids* 173, 108878. <https://doi.org/10.1016/j.steroids.2021.108878>
- Bianchi, A., Evans, J.L., Iverson, A.J., Nordlund, A.C., Watts, T.D., Witters, L.A., 1990. Identification of an isozymic form of acetyl-CoA carboxylase. *J. Biol. Chem.* 265, 1502–1509. [https://doi.org/10.1016/S0021-9258\(19\)40045-8](https://doi.org/10.1016/S0021-9258(19)40045-8)
- Bilzer, M., Roggel, F., Gerbes, A.L., 2006. Role of Kupffer cells in host defense and liver disease. *Liver Int.* 26, 1175–1186. <https://doi.org/10.1111/j.1478-3231.2006.01342.x>
- Birkenfeld, A.L., Shulman, G.I., 2014. Nonalcoholic fatty liver disease, hepatic insulin resistance, and type 2 diabetes. *Hepatol. Baltim. Md* 59, 713–723. <https://doi.org/10.1002/hep.26672>
- Bitto, A., Polito, F., Altavilla, D., Irrera, N., Giuliani, D., Ottani, A., Minutoli, L., Spaccapelo, L., Galantucci, M., Lodi, R., Guzzo, G., Guarini, S., Squadrito, F., 2011. Melanocortins protect against multiple organ dysfunction syndrome in mice. *Br. J. Pharmacol.* 162, 917–928. <https://doi.org/10.1111/j.1476-5381.2010.01098.x>
- Böhm, M., Stegemann, A., 2014. Bleomycin-induced fibrosis in MC1 signalling-deficient C57BL/6J-Mc1r(e/e) mice further supports a modulating role for melanocortins in collagen synthesis of the skin. *Exp. Dermatol.* 23, 431–433. <https://doi.org/10.1111/EXD.12409>
- Boldys, A., Buldak, L., 2024. Metabolic dysfunction-associated steatotic liver disease: Navigating terminological evolution, diagnostic frontiers and therapeutic horizon-an editorial exploration. *World J. Gastroenterol.* 30, 2387. <https://doi.org/10.3748/wjg.v30.i18.2387>

- Boston, B.A., Cone, R.D., 1996. Characterization of melanocortin receptor subtype expression in murine adipose tissues and in the 3T3-L1 cell line. *Endocrinology* 137, 2043–2050. <https://doi.org/2016092613411100918>
- Bradbury, M.W., 2006. Lipid Metabolism and Liver Inflammation. I. Hepatic fatty acid uptake: possible role in steatosis. *Am. J. Physiol.-Gastrointest. Liver Physiol.* 290, G194–G198. <https://doi.org/10.1152/ajpgi.00413.2005>
- Brasaemle, D.L., Rubin, B., Harten, I.A., Gruia-Gray, J., Kimmel, A.R., Londos, C., 2000. Perilipin A Increases Triacylglycerol Storage by Decreasing the Rate of Triacylglycerol Hydrolysis*. *J. Biol. Chem.* 275, 38486–38493. <https://doi.org/10.1074/jbc.M007322200>
- Brunt, E.M., Janney, C.G., Di Bisceglie, A.M., Neuschwander-Tetri, B.A., Bacon, B.R., 1999. Nonalcoholic steatohepatitis: a proposal for grading and staging the histological lesions. *Am. J. Gastroenterol.* 94, 2467–2474. <https://doi.org/10.1111/j.1572-0241.1999.01377.x>
- Brzoska, T., Luger, T.A., Maaser, C., Abels, C., Böhm, M., 2008. α -Melanocyte-Stimulating Hormone and Related Tripeptides: Biochemistry, Antiinflammatory and Protective Effects in Vitro and in Vivo, and Future Perspectives for the Treatment of Immune-Mediated Inflammatory Diseases. *Endocr. Rev.* 29, 581–602. <https://doi.org/2019041121385292900>
- Bumaschny, V.F., de Souza, F.S.J., López Leal, R.A., Santangelo, A.M., Baetscher, M., Levi, D.H., Low, M.J., Rubinstein, M., 2007. Transcriptional Regulation of Pituitary POMC Is Conserved at the Vertebrate Extremes Despite Great Promoter Sequence Divergence. *Mol. Endocrinol.* 21, 2738–2749. <https://doi.org/2019041201004909600>
- Buqué, X., Martínez, M.J., Cano, A., Miquilena-Colina, M.E., García-Monzón, C., Aspichueta, P., Ochoa, B., 2010. A subset of dysregulated metabolic and survival genes is associated with severity of hepatic steatosis in obese Zucker rats. *J. Lipid Res.* 51, 500–513. <https://doi.org/10.1194/jlr.M001966>
- Burgess, S.C., 2015. Regulation of glucose metabolism in liver, in: *International Textbook of Diabetes Mellitus*. John Wiley & Sons, Ltd, pp. 193–210. <https://doi.org/10.1002/9781118387658.ch13>
- Burwinkel, B., Bakker, H.D., Herschkovitz, E., Moses, S.W., Shin, Y.S., Kilimann, M.W., 1998. Mutations in the liver glycogen phosphorylase gene (PYGL) underlying glycogenosis type VI. *Am. J. Hum. Genet.* 62, 785–791. <https://doi.org/10.1086/301790>
- Butler, A.A., Kesterson, R.A., Khong, K., Cullen, M.J., Pellemounter, M.A., Dekoning, J., Baetscher, M., Cone, R.D., 2000. A unique metabolic syndrome causes obesity in the melanocortin-3 receptor-deficient mouse. *Endocrinology* 141, 3518–3521. <https://doi.org/10.1210/endo.141.9.7791>
- Buzzetti, E., Pinzani, M., Tsochatzis, E.A., 2016. The multiple-hit pathogenesis of non-alcoholic fatty liver disease (NAFLD). *Metabolism.* 65, 1038–1048. <https://doi.org/10.1016/j.metabol.2015.12.012>
- Cai, M., Nyberg, J., Hruby, V.J., 2009. Melanotropins as Drugs for the Treatment of Obesity and Other Feeding Disorders: Potential and Problems. *Curr. Top. Med. Chem.* 9, 554–563.
- Cai, W., Srivastava, P., Feng, D., Lin, Y., Vanderburg, C.R., Xu, Y., Mclean, P., Frosch, M.P., Fisher, D.E., Schwarzschild, M.A., Chen, X., 2022. Melanocortin 1 receptor activation protects against alpha-synuclein pathologies in models of Parkinson's disease. *Mol. Neurodegener.* 17, 16. <https://doi.org/10.1186/s13024-022-00520-4>
- Calvisi, D.F., Wang, C., Ho, C., Ladu, S., Lee, S.A., Mattu, S., Destefanis, G., Delogu, S., Zimmermann, A., Ericsson, J., Brozzetti, S., Staniscia, T., Chen, X., Dombrowski, F., Evert, M., 2011. Increased lipogenesis, induced by AKT-mTORC1-RPS6 signaling, promotes development of human hepatocellular carcinoma. *Gastroenterology* 140, 1071–1083. <https://doi.org/10.1053/j.gastro.2010.12.006>
- Carey, G.B., 1998. Mechanisms regulating adipocyte lipolysis. *Adv. Exp. Med. Biol.* 441, 157–170. https://doi.org/10.1007/978-1-4899-1928-1_15
- Castejón-Griñán, M., Herraiz, C., Olivares, C., Jiménez-Cervantes, C., García-Borrón, J.C., 2018. cAMP-independent non-pigmentary actions of variant melanocortin 1 receptor: AKT-mediated activation of protective responses to oxidative DNA damage. *Oncogene* 37, 3631–3646. <https://doi.org/10.1038/s41388-018-0216-1>

- Catania, A., 2007. The melanocortin system in leukocyte biology. *J. Leukoc. Biol.* 81, 383–392. <https://doi.org/10.1189/jlb.0706426>
- Catania, A., Cutuli, M., Garofalo, L., Carlin, A., Airaghi, L., Barcellini, W., Lipton, J.M., 2000. The Neuropeptide α -MSH in Host Defense. *Ann. N. Y. Acad. Sci.* 917, 227–231. <https://doi.org/10.1111/j.1749-6632.2000.tb05387.x>
- Catania, A., Gatti, S., Colombo, G., Lipton, J.M., 2004. Targeting Melanocortin Receptors as a Novel Strategy to Control Inflammation. *Pharmacol. Rev.* 56, 1–29. <https://doi.org/10.1124/pr.56.1.1>
- Catania, A., Rajora, N., Capsoni, F., Minonzio, F., Star, R.A., Lipton, J.M., 1996. The neuropeptide alpha-MSH has specific receptors on neutrophils and reduces chemotaxis in vitro. *Peptides* 17, 675–679. [https://doi.org/10.1016/0196-9781\(96\)00037-X](https://doi.org/10.1016/0196-9781(96)00037-X)
- Cerqueira, N.M.F.S.A., Oliveira, E.F., Gesto, D.S., Santos-Martins, D., Moreira, C., Moorthy, H.N., Ramos, M.J., Fernandes, P.A., 2016. Cholesterol Biosynthesis: A Mechanistic Overview. *Biochemistry* 55, 5483–5506. <https://doi.org/10.1021/acs.biochem.6b00342>
- Chabowski, A., Żendzian-Piotrowska, M., Konstantynowicz, K., Pankiewicz, W., Mikłosz, A., Łukaszuk, B., Górski, J., 2013. Fatty acid transporters involved in the palmitate and oleate induced insulin resistance in primary rat hepatocytes. *Acta Physiol.* 207, 346–357. <https://doi.org/10.1111/apha.12022>
- Chagnon, Y.C., Chen, W.J., PÃ©russe, L., Chagnon, M., Nadeau, A., Wilkison, W.O., Bouchard, C., 1997. Linkage and association studies between the melanocortin receptors 4 and 5 genes and obesity-related phenotypes in the QuÃ©bec Family Study. *Mol. Med.* 3, 663.
- Chai, B., Li, J.-Y., Zhang, W., Ammori, J.B., Mulholland, M.W., 2007. Melanocortin-3 receptor activates MAP kinase via PI3 kinase. *Regul. Pept.* 139, 115–121. <https://doi.org/10.1016/j.regpep.2006.11.003>
- Chakravarty, K., Cassuto, H., Reshef, L., Hanson, R.W., 2005. Factors That Control the Tissue-Specific Transcription of the Gene for Phosphoenolpyruvate Carboxykinase-C. *Crit. Rev. Biochem. Mol. Biol.* 40, 129–154. <https://doi.org/10.1080/10409230590935479>
- Chao, H.-W., Chao, S.-W., Lin, H., Ku, H.-C., Cheng, C.-F., 2019. Homeostasis of Glucose and Lipid in Non-Alcoholic Fatty Liver Disease. *Int. J. Mol. Sci.* 20, 298. <https://doi.org/10.3390/ijms20020298>
- Cheang, W.S., Tian, X.Y., Wong, W.T., Lau, C.W., Lee, S.S.-T., Chen, Z.Y., Yao, X., Wang, N., Huang, Y., 2014. Metformin Protects Endothelial Function in Diet-Induced Obese Mice by Inhibition of Endoplasmic Reticulum Stress Through 5' Adenosine Monophosphate-Activated Protein Kinase-Peroxisome Proliferator-Activated Receptor δ Pathway. *Arterioscler. Thromb. Vasc. Biol.* 34, 830–836. <https://doi.org/10.1161/ATVBAHA.113.301938>
- Chen, S., Zhu, B., Yin, C., Liu, W., Han, C., Chen, B., Liu, T., Li, X., Chen, X., Li, C., Hu, L., Zhou, J., Xu, Z.-X., Gao, X., Wu, X., Goding, C.R., Cui, R., 2017. Palmitoylation-dependent activation of MC1R prevents melanomagenesis. *Nature* 549, 399–403. <https://doi.org/10.1038/nature23887>
- Chen, W., Kelly, M.A., Opitz-Araya, X., Thomas, R.E., Low, M.J., Cone, R.D., 1997. Exocrine gland dysfunction in MC5-R-deficient mice: evidence for coordinated regulation of exocrine gland function by melanocortin peptides. *Cell* 91, 789–798. [https://doi.org/10.1016/s0092-8674\(00\)80467-5](https://doi.org/10.1016/s0092-8674(00)80467-5)
- Cheung, O., Sanyal, A.J., 2008. Abnormalities of lipid metabolism in nonalcoholic fatty liver disease. *Semin. Liver Dis.* 28, 351–359. <https://doi.org/10.1055/s-0028-1091979>
- Chevre, R., Trigueros-Motos, L., Castaño, D., Chua, T., Corliano, M., Patankar, J.V., Sng, L., Sim, L., Juin, T.L., Carissimo, G., Ng, L.F.P., Yi, C.N.J., Eliathamby, C.C., Groen, A.K., Hayden, M.R., Singaraja, R.R., 2018. Therapeutic modulation of the bile acid pool by Cyp8b1 knockdown protects against nonalcoholic fatty liver disease in mice. *FASEB J.* 32, 3792–3802. <https://doi.org/10.1096/fj.201701084RR>
- Chhajlani, V., Wikberg, J.E., 1992. Molecular cloning and expression of the human melanocyte stimulating hormone receptor cDNA. *FEBS Lett.* 309, 417–420. [https://doi.org/10.1016/0014-5793\(92\)80820-7](https://doi.org/10.1016/0014-5793(92)80820-7)

- Chiang, J.Y.L., 2004. Regulation of bile acid synthesis: Pathways, nuclear receptors, and mechanisms. *J. Hepatol.* 40, 539–551. <https://doi.org/10.1016/j.jhep.2003.11.006>
- Chiang, J.Y.L., 2002. Bile acid regulation of gene expression: roles of nuclear hormone receptors. *Endocr. Rev.* 23, 443–463. <https://doi.org/10.1210/er.2000-0035>
- Chrétien, M., Benjannet, S., Gossard, F., Gianoulakis, C., Crine, P., Lis, M., Seidah, N.G., 1979. From beta-lipotropin to beta-endorphin and “pro-opio-melanocortin.” *Can. J. Biochem.* 57, 1111–1121. <https://doi.org/10.1139/o79-143>
- Ciardullo, S., Vergani, M., Perseghin, G., 2023. Nonalcoholic Fatty Liver Disease in Patients with Type 2 Diabetes: Screening, Diagnosis, and Treatment. *J. Clin. Med.* 12, 5597. <https://doi.org/10.3390/jcm12175597>
- Clarke, P.R., Hardie, D.G., 1990. Regulation of HMG-CoA reductase: identification of the site phosphorylated by the AMP-activated protein kinase in vitro and in intact rat liver. *EMBO J.* 9, 2439–2446. <https://doi.org/10.1002/J.1460-2075.1990.TB07420.X>
- Claydon, A.J., Beynon, R., 2012. Proteome dynamics: revisiting turnover with a global perspective. *Mol. Cell. Proteomics MCP* 11, 1551–1565. <https://doi.org/10.1074/mcp.O112.022186>
- Cohen, D.E., Fisher, E.A., 2013. Lipoprotein Metabolism, Dyslipidemia and Nonalcoholic Fatty Liver Disease. *Semin. Liver Dis.* 33, 380–388. <https://doi.org/10.1055/s-0033-1358519>
- Coleman, R.A., Lee, D.P., 2004. Enzymes of triacylglycerol synthesis and their regulation. *Prog. Lipid Res.* 43, 134–176. [https://doi.org/10.1016/S0163-7827\(03\)00051-1](https://doi.org/10.1016/S0163-7827(03)00051-1)
- Colombo, G., Buffa, R., Bardella, M.T., Garofalo, L., Carlin, A., Lipton, J.M., Catania, A., 2002. Anti-inflammatory effects of alpha-melanocyte-stimulating hormone in celiac intestinal mucosa. *Neuroimmunomodulation* 10, 208–216. <https://doi.org/10.1159/000068323>
- Conde de la Rosa, L., Garcia-Ruiz, C., Vallejo, C., Baulies, A., Nuñez, S., Monte, M.J., Marin, J.J.G., Baila-Rueda, L., Cénarro, A., Civeira, F., Fuster, J., Garcia-Valdecasas, J.C., Ferrer, J., Karin, M., Ribas, V., Fernandez-Checa, J.C., 2021. STARD1 promotes NASH-driven HCC by sustaining the generation of bile acids through the alternative mitochondrial pathway. *J. Hepatol.* 74, 1429–1441. <https://doi.org/10.1016/J.JHEP.2021.01.028>
- Cone, R.D., 2006. Studies on the Physiological Functions of the Melanocortin System. *Endocr. Rev.* 27, 736–749. <https://doi.org/2019041123291956600>
- Cone, R.D., 2005. Anatomy and regulation of the central melanocortin system. *Nat. Neurosci.* 8, 571–578. <https://doi.org/10.1038/nn1455>
- Cone, R.D., 1999. The Central Melanocortin System and Energy Homeostasis. *Trends Endocrinol. Metab.* 10, 211–216. [https://doi.org/10.1016/S1043-2760\(99\)00153-8](https://doi.org/10.1016/S1043-2760(99)00153-8)
- Cone, R.D., Lu, D., Koppula, S., Vage, D.I., Klungland, H., Boston, B., Chen, W., Orth, D.N., Pouton, C., Kesterson, R.A., 1996. The melanocortin receptors: agonists, antagonists, and the hormonal control of pigmentation. *Recent Prog. Horm. Res.* 51, 287–317; discussion 318.
- Coughlan, K.A., Valentine, R.J., Ruderman, N.B., Saha, A.K., 2014. AMPK activation: a therapeutic target for type 2 diabetes? *Diabetes Metab. Syndr. Obes. Targets Ther.* 7, 241–253. <https://doi.org/10.2147/DMSO.S43731>
- Couinaud, C., 1957. *Le foie: études anatomiques et chirurgicales.* Masson.
- Craig, M., Yarrarapu, S.N.S., Dimri, M., 2024. *Biochemistry, Cholesterol*, in: StatPearls. StatPearls Publishing, Treasure Island (FL).
- Crosignani, A., Del Puppo, M., Longo, M., De Fabiani, E., Caruso, D., Zuin, M., Podda, M., Javitt, N.B., Kienle, M.G., 2007. Changes in classic and alternative pathways of bile acid synthesis in chronic liver disease. *Clin. Chim. Acta Int. J. Clin. Chem.* 382, 82–88. <https://doi.org/10.1016/J.CCA.2007.03.025>
- Csaki, L.S., Reue, K., 2010. Lipins: multifunctional lipid metabolism proteins. *Annu. Rev. Nutr.* 30, 257–272. <https://doi.org/10.1146/annurev.nutr.012809.104729>
- Cusi, K., 2016. Treatment of patients with type 2 diabetes and non-alcoholic fatty liver disease: current approaches and future directions. *Diabetologia* 59, 1112–1120. <https://doi.org/10.1007/s00125-016-3952-1>

- Cusi, K., 2012. Role of obesity and lipotoxicity in the development of nonalcoholic steatohepatitis: pathophysiology and clinical implications. *Gastroenterology* 142, 711–725.e6. <https://doi.org/10.1053/j.gastro.2012.02.003>
- Dawson, P.A., Karpen, S.J., 2015. Intestinal transport and metabolism of bile acids. *J. Lipid Res.* 56, 1085–1099. <https://doi.org/10.1194/jlr.R054114>
- Diano, S., 2011. New aspects of melanocortin signaling: A role for PRCP in α -MSH degradation. *Front. Neuroendocrinol.* 32, 70–83. <https://doi.org/10.1016/j.yfrne.2010.09.001>
- Diehl, A.M., Choi, S.S., 2008. The Liver in Type 2 Diabetes Mellitus, in: Feinglos, M.N., Bethel, M.A. (Eds.), *Type 2 Diabetes Mellitus: An Evidence-Based Approach to Practical Management*. Humana Press, Totowa, NJ, pp. 351–364. https://doi.org/10.1007/978-1-60327-043-4_21
- Dietschy, J.M., 1984. Regulation of cholesterol metabolism in man and in other species. *Klin. Wochenschr.* 62, 338–345. <https://doi.org/10.1007/BF01716251>
- Dimitriadis, G.D., Maratou, E., Kountouri, A., Board, M., Lambadiari, V., 2021. Regulation of Postabsorptive and Postprandial Glucose Metabolism by Insulin-Dependent and Insulin-Independent Mechanisms: An Integrative Approach. *Nutrients* 13, 159. <https://doi.org/10.3390/nu13010159>
- DiStefano, M.T., Danai, L.V., Roth Flach, R.J., Chawla, A., Pedersen, D.J., Guilherme, A., Czech, M.P., 2015. The Lipid Droplet Protein Hypoxia-inducible Gene 2 Promotes Hepatic Triglyceride Deposition by Inhibiting Lipolysis. *J. Biol. Chem.* 290, 15175–15184. <https://doi.org/10.1074/jbc.M115.650184>
- Do Carmo, J.M., da Silva, A.A., Rushing, J.S., Pace, B., Hall, J.E., 2013. Differential control of metabolic and cardiovascular functions by melanocortin-4 receptors in proopiomelanocortin neurons. *Am. J. Physiol. Regul. Integr. Comp. Physiol.* 305, R359–368. <https://doi.org/10.1152/ajpregu.00518.2012>
- Doedens, L., Opperer, F., Cai, M., Beck, J.G., Dedek, M., Palmer, E., Hruby, V.J., Kessler, H., 2010. Multiple N-methylation of MT-II backbone amide bonds leads to melanocortin receptor subtype hMC1R selectivity; pharmacological and conformational studies. *J. Am. Chem. Soc.* 132, 8115–8128. <https://doi.org/10.1021/ja101428m>
- Doege, H., Baillie, R.A., Ortegon, A.M., Tsang, B., Wu, Q., Punreddy, S., Hirsch, D., Watson, N., Gimeno, R.E., Stahl, A., 2006. Targeted Deletion of FATP5 Reveals Multiple Functions in Liver Metabolism: Alterations in Hepatic Lipid Homeostasis. *Gastroenterology* 130, 1245–1258. <https://doi.org/10.1053/j.gastro.2006.02.006>
- Donnelly, K.L., Smith, C.I., Schwarzenberg, S.J., Jessurun, J., Boldt, M.D., Parks, E.J., 2005. Sources of fatty acids stored in liver and secreted via lipoproteins in patients with nonalcoholic fatty liver disease. *J. Clin. Invest.* 115, 1343–1351. <https://doi.org/10.1172/JCI23621>
- Dueland, S., Drisko, J., Graf, L., Machleder, D., Lusi, A., Davis, R., 1993. Effect of dietary cholesterol and taurocholate on cholesterol 7 α -hydroxylase and hepatic LDL receptors in inbred mice. *J. Lipid Res.* 34, 923–931. [https://doi.org/10.1016/S0022-2275\(20\)39679-6](https://doi.org/10.1016/S0022-2275(20)39679-6)
- Duncan, R.E., Ahmadian, M., Jaworski, K., Sarkadi-Nagy, E., Sul, H.S., 2007. Regulation of Lipolysis in Adipocytes. *Annu. Rev. Nutr.* 27, 79–101. <https://doi.org/10.1146/annurev.nutr.27.061406.093734>
- Eaton, S., Bartlett, K., Pourfarzam, M., 1996. Mammalian mitochondrial beta-oxidation. *Biochem. J.* 320, 345–357.
- Edwards, M., Mohiuddin, S.S., 2024. *Biochemistry, Lipolysis*, in: StatPearls. StatPearls Publishing, Treasure Island (FL).
- Ekberg, K., Landau, B.R., Wajngot, A., Chandramouli, V., Efendic, S., Brunengraber, H., Wahren, J., 1999. Contributions by kidney and liver to glucose production in the postabsorptive state and after 60 h of fasting. *Diabetes* 48, 292–298. <https://doi.org/10.2337/diabetes.48.2.292>
- Ellias, S.D., Larson, E.L., Taner, T., Nyberg, S.L., 2021. Cell-Mediated Therapies to Facilitate Operational Tolerance in Liver Transplantation. *Int. J. Mol. Sci.* 22, 4016. <https://doi.org/10.3390/ijms22084016>

- Engelmann, C., Tacke, F., 2022. The Potential Role of Cellular Senescence in Non-Alcoholic Fatty Liver Disease. *Int. J. Mol. Sci.* 23, 652. <https://doi.org/10.3390/ijms23020652>
- Enriori, P.J., Chen, W., Garcia-Rudaz, M.C., Grayson, B.E., Evans, A.E., Comstock, S.M., Gebhardt, U., Müller, H.L., Reinehr, T., Henry, B.A., Brown, R.D., Bruce, C.R., Simonds, S.E., Litwak, S.A., McGee, S.L., Luquet, S., Martinez, S., Jastroch, M., Tschöp, M.H., Watt, M.J., Clarke, I.J., Roth, C.L., Grove, K.L., Cowley, M.A., 2016. α -Melanocyte stimulating hormone promotes muscle glucose uptake via melanocortin 5 receptors. *Mol. Metab.* 5, 807–822. <https://doi.org/10.1016/j.molmet.2016.07.009>
- Erickson, S.K., Lear, S.R., Deane, S., Dubrac, S., Huling, S.L., Nguyen, L., Bollineni, J.S., Shefer, S., Hyogo, H., Cohen, D.E., Shneider, B., Sehayek, E., Ananthanarayanan, M., Balasubramaniyan, N., Suchy, F.J., Batta, A.K., Salen, G., 2003. Hypercholesterolemia and changes in lipid and bile acid metabolism in male and female cyp7A1-deficient mice. *J. Lipid Res.* 44, 1001–1009. <https://doi.org/10.1194/JLR.M200489-JLR200>
- Eves, P., Haycock, J., Layton, C., Wagner, M., Kemp, H., Szabo, M., Morandini, R., Ghanem, G., García-Borrón, J.C., Jiménez-Cervantes, C., Neil, S.M., 2003. Anti-inflammatory and anti-invasive effects of α -melanocyte-stimulating hormone in human melanoma cells. *Br. J. Cancer* 89, 2004. <https://doi.org/10.1038/sj.bjc.6601349>
- Eyster, K.M., 2007. The membrane and lipids as integral participants in signal transduction: lipid signal transduction for the non-lipid biochemist. *Adv. Physiol. Educ.* 31, 5–16. <https://doi.org/10.1152/advan.00088.2006>
- Fan, W., Boston, B.A., Kesterson, R.A., Hruby, V.J., Cone, R.D., 1997. Role of melanocortinergic neurons in feeding and the agouti obesity syndrome. *Nature* 385, 165–168. <https://doi.org/10.1038/385165a0>
- Feingold, K.R., 2000. Introduction to Lipids and Lipoproteins, in: Feingold, K.R., Anawalt, B., Blackman, M.R., Boyce, A., Chrousos, G., Corpas, E., de Herder, W.W., Dhariya, K., Dungan, K., Hofland, J., Kalra, S., Kalsas, G., Kapoor, N., Koch, C., Kopp, P., Korbonits, M., Kovacs, C.S., Kuohung, W., Laferrère, B., Levy, M., McGee, E.A., McLachlan, R., New, M., Purnell, J., Sahay, R., Shah, A.S., Singer, F., Sperling, M.A., Stratakis, C.A., Trencé, D.L., Wilson, D.P. (Eds.), *Endotext*. MDText.com, Inc., South Dartmouth (MA).
- Ferrannini, E., Bjorkman, O., Reichard, G.A., Jr, Pilo, A., Olsson, M., Wahren, J., DeFronzo, R.A., 1985. The Disposal of an Oral Glucose Load in Healthy Subjects: A Quantitative Study. *Diabetes* 34, 580–588. <https://doi.org/10.2337/diab.34.6.580>
- Ferré, P., Fofelle, F., 2010. Hepatic steatosis: a role for de novo lipogenesis and the transcription factor SREBP-1c. *Diabetes Obes. Metab.* 12, 83–92. <https://doi.org/10.1111/j.1463-1326.2010.01275.x>
- Ferré, P., Fofelle, F., 2007. SREBP-1c Transcription Factor and Lipid Homeostasis: Clinical Perspective. *Horm. Res.* 68, 72–82. <https://doi.org/10.1159/000100426>
- Frayn, K., 2002. Adipose tissue as a buffer for daily lipid flux. *Diabetologia* 45, 1201–1210. <https://doi.org/10.1007/s00125-002-0873-y>
- Frühbeck, G., Gómez-Ambrosi, J., 2003. Control of body weight: a physiologic and transgenic perspective. *Diabetologia* 46, 143–172. <https://doi.org/10.1007/s00125-003-1053-4>
- Frühbeck, G., Méndez-Giménez, L., Fernández-Formoso, J.-A., Fernández, S., Rodríguez, A., 2014. Regulation of adipocyte lipolysis. *Nutr. Res. Rev.* 27, 63–93. <https://doi.org/10.1017/S095442241400002X>
- Fukumoto, H., Seino, S., Imura, H., Seino, Y., Eddy, R.L., Fukushima, Y., Byers, M.G., Shows, T.B., Bell, G.I., 1988. Sequence, tissue distribution, and chromosomal localization of mRNA encoding a human glucose transporter-like protein. *Proc. Natl. Acad. Sci. U. S. A.* 85, 5434–5438. <https://doi.org/10.1073/pnas.85.15.5434>
- Galic, S., Oakhill, J.S., Steinberg, G.R., 2010. Adipose tissue as an endocrine organ. *Mol. Cell. Endocrinol.* 316, 129–139. <https://doi.org/10.1016/j.mce.2009.08.018>

- Gantz, I., Miwa, H., Konda, Y., Shimoto, Y., Tashiro, T., Watson, S.J., DelValle, J., Yamada, T., 1993. Molecular cloning, expression, and gene localization of a fourth melanocortin receptor. *J. Biol. Chem.* 268, 15174–15179.
- Gantz, I., Yamada, T., Tashiro, T., Konda, Y., Shimoto, Y., Miwa, H., Trent, J.M., 1994. Mapping of the gene encoding the melanocortin-1 (alpha-melanocyte stimulating hormone) receptor (MC1R) to human chromosome 16q24.3 by Fluorescence in situ hybridization. *Genomics* 19, 394–395. <https://doi.org/10.1006/geno.1994.1080>
- Garfield, A.S., Lam, D.D., Marston, O.J., Przydzial, M.J., Heisler, L.K., 2009. Role of central melanocortin pathways in energy homeostasis. *Trends Endocrinol. Metab.* 20, 203–215. <https://doi.org/10.1016/j.tem.2009.02.002>
- Gatti, S., Colombo, G., Turcatti, F., Lonati, C., Sordi, A., Bonino, F., Lipton, J.M., Catania, A., 2006. Reduced expression of the melanocortin-1 receptor in human liver during brain death. *Neuroimmunomodulation* 13, 51–55. <https://doi.org/10.1159/000094513>
- Gerhard, G.S., Chu, X., Wood, G.C., Gerhard, G.M., Benotti, P., Petrick, A.T., Gabrielsen, J., Strodel, W.E., Still, C.D., Argyropoulos, G., 2013. Next-Generation Sequence Analysis of Genes Associated with Obesity and Nonalcoholic Fatty Liver Disease-Related Cirrhosis in Extreme Obesity. *Hum. Hered.* 75, 144. <https://doi.org/10.1159/000351719>
- Gether, U., 2000. Uncovering molecular mechanisms involved in activation of G protein-coupled receptors. *Endocr. Rev.* 21, 90–113. <https://doi.org/2019041122083272700>
- Getting, S.J., Gibbs, L., Clark, A.J., Flower, R.J., Perretti, M., 1999. POMC gene-derived peptides activate melanocortin type 3 receptor on murine macrophages, suppress cytokine release, and inhibit neutrophil migration in acute experimental inflammation. *J. Immunol. Baltim. Md 1950* 162, 7446–7453.
- Gilloteaux, J., 1998. Terminologia anatomica. International anatomical terminology. Georg Thieme Verlag.
- Goldstein, J.L., Anderson, R.G., Brown, M.S., 1982. Receptor-mediated endocytosis and the cellular uptake of low density lipoprotein. *Ciba Found. Symp.* 77–95. <https://doi.org/10.1002/9780470720745.ch5>
- Gong, J., Tu, W., Liu, J., Tian, D., 2023. Hepatocytes: A key role in liver inflammation. *Front. Immunol.* 13, 1083780. <https://doi.org/10.3389/fimmu.2022.1083780>
- Gong, R., 2014. Leveraging melanocortin pathways to treat glomerular diseases. *Adv. Chronic Kidney Dis.* 21, 134–151. <https://doi.org/10.1053/j.ackd.2013.09.004>
- Gonzalez-Rey, E., Chorny, A., Delgado, M., 2007. Regulation of immune tolerance by anti-inflammatory neuropeptides. *Nat. Rev. Immunol.* 7, 52–63. <https://doi.org/10.1038/nri1984>
- Granneman, J.G., Moore, H.-P.H., Krishnamoorthy, R., Rathod, M., 2009. Perilipin controls lipolysis by regulating the interactions of AB-hydrolase containing 5 (Abhd5) and adipose triglyceride lipase (Atgl). *J. Biol. Chem.* 284, 34538–34544. <https://doi.org/10.1074/jbc.M109.068478>
- Greenberg, A.S., Egan, J.J., Wek, S.A., Garty, N.B., Blanchette-Mackie, E.J., Londos, C., 1991. Perilipin, a major hormonally regulated adipocyte-specific phosphoprotein associated with the periphery of lipid storage droplets. *J. Biol. Chem.* 266, 11341–11346.
- Grieco, P., Han, G., Weinberg, D., Van der Ploeg, L.H.T., Hruby, V.J., 2002. Design and synthesis of highly potent and selective melanotropin analogues of SHU9119 modified at position 6. *Biochem. Biophys. Res. Commun.* 292, 1075–1080. <https://doi.org/10.1006/bbrc.2002.6739>
- Grum, D.E., Hansen, L.R., Drackley, J.K., 1994. Peroxisomal β -oxidation of fatty acids in bovine and rat liver. *Comp. Biochem. Physiol. Part B Comp. Biochem.* 109, 281–292. [https://doi.org/10.1016/0305-0491\(94\)90012-4](https://doi.org/10.1016/0305-0491(94)90012-4)
- Guasch-Ferré, M., Hruby, A., Toledo, E., Clish, C.B., Martínez-González, M.A., Salas-Salvadó, J., Hu, F.B., 2016. Metabolomics in Prediabetes and Diabetes: A Systematic Review and Meta-analysis. *Diabetes Care* 39, 833–846. <https://doi.org/10.2337/dc15-2251>
- Guerre-Millo, M., 2004. Adipose tissue and adipokines: for better or worse. *Diabetes Metab.* 30, 13–19. [https://doi.org/10.1016/s1262-3636\(07\)70084-8](https://doi.org/10.1016/s1262-3636(07)70084-8)

- Gustafson, B., Smith, U., 2015. Regulation of white adipogenesis and its relation to ectopic fat accumulation and cardiovascular risk. *Atherosclerosis* 241, 27–35. <https://doi.org/10.1016/j.atherosclerosis.2015.04.812>
- Hadley, M.E., 2005. Discovery that a melanocortin regulates sexual functions in male and female humans. *Peptides* 26, 1687–1689. <https://doi.org/10.1016/j.peptides.2005.01.023>
- Hall, E.A., Ren, S., Hylemon, P.B., Rodriguez-Agudo, D., Redford, K., Marques, D., Kang, D., Gil, G., Pandak, W.M., 2005. Detection of the steroidogenic acute regulatory protein, StAR, in human liver cells. *Biochim. Biophys. Acta* 1733, 111–119. <https://doi.org/10.1016/j.bbali.2005.01.004>
- Harada, K., Shen, W.-J., Patel, S., Natu, V., Wang, J., Osuga, J., Ishibashi, S., Kraemer, F.B., 2003. Resistance to high-fat diet-induced obesity and altered expression of adipose-specific genes in HSL-deficient mice. *Am. J. Physiol.-Endocrinol. Metab.* 285, E1182–E1195. <https://doi.org/10.1152/ajpendo.00259.2003>
- Hardy, O.T., Czech, M.P., Corvera, S., 2012. What causes the insulin resistance underlying obesity? *Curr. Opin. Endocrinol. Diabetes Obes.* 19, 81–87. <https://doi.org/10.1097/MED.0b013e3283514e13>
- Harrison, S.A., Bedossa, P., Guy, C.D., Schattenberg, J.M., Loomba, R., Taub, R., Labriola, D., Moussa, S.E., Neff, G.W., Rinella, M.E., Anstee, Q.M., Abdelmalek, M.F., Younossi, Z., Baum, S.J., Francque, S., Charlton, M.R., Newsome, P.N., Lanthier, N., Schiefke, I., Mangia, A., Pericàs, J.M., Patil, R., Sanyal, A.J., Noureddin, M., Bansal, M.B., Alkhouiri, N., Castera, L., Rudraraju, M., Ratziu, V., MAESTRO-NASH Investigators, 2024. A Phase 3, Randomized, Controlled Trial of Resmetirom in NASH with Liver Fibrosis. *N. Engl. J. Med.* 390, 497–509. <https://doi.org/10.1056/NEJMoa2309000>
- Hartmeyer, M., Scholzen, T., Becher, E., Bhardwaj, R.S., Schwarz, T., Luger, T.A., 1997. Human dermal microvascular endothelial cells express the melanocortin receptor type 1 and produce increased levels of IL-8 upon stimulation with alpha-melanocyte-stimulating hormone. *J. Immunol. Baltim. Md* 159, 1930–7.
- Hashimoto, T., Cook, W.S., Qi, C., Yeldandi, A.V., Reddy, J.K., Rao, M.S., 2000. Defect in Peroxisome Proliferator-activated Receptor α -inducible Fatty Acid Oxidation Determines the Severity of Hepatic Steatosis in Response to Fasting*. *J. Biol. Chem.* 275, 28918–28928. <https://doi.org/10.1074/jbc.M910350199>
- Heier, C., Radner, F.P.W., Moustafa, T., Schreiber, R., Grond, S., Eichmann, T.O., Schweiger, M., Schmidt, A., Cerk, I.K., Oberer, M., Theussl, H.-C., Wojciechowski, J., Penninger, J.M., Zimmermann, R., Zechner, R., 2015. G0/G1 Switch Gene 2 Regulates Cardiac Lipolysis. *J. Biol. Chem.* 290, 26141–26150. <https://doi.org/10.1074/jbc.M115.671842>
- Herraiz, C., Journé, F., Abdel-Malek, Z., Ghanem, G., Jiménez-Cervantes, C., García-Borrón, J.C., 2011. Signaling from the Human Melanocortin 1 Receptor to ERK1 and ERK2 Mitogen-Activated Protein Kinases Involves Transactivation of cKIT. *Mol. Endocrinol.* 25, 138–156. <https://doi.org/10.1093/mend/25.2.138>
- Heyens, L.J.M., Busschots, D., Koek, G.H., Robaey, G., Francque, S., 2021. Liver Fibrosis in Non-alcoholic Fatty Liver Disease: From Liver Biopsy to Non-invasive Biomarkers in Diagnosis and Treatment. *Front. Med.* 8. <https://doi.org/10.3389/fmed.2021.615978>
- Hirosumi, J., Tuncman, G., Chang, L., Görgün, C.Z., Uysal, K.T., Maeda, K., Karin, M., Hotamisligil, G.S., 2002. A central role for JNK in obesity and insulin resistance. *Nature* 420, 333–336. <https://doi.org/10.1038/nature01137>
- Hirota, K., Fukamizu, A., 2010. Transcriptional regulation of energy metabolism in the liver. *J. Recept. Signal Transduct.* 30, 403–409. <https://doi.org/10.1093/jrecept/30.3.403>
- Hoch, M., Eberle, A.N., Wagner, U., Bussmann, C., Peters, T., Peterli, R., 2007. Expression and Localization of Melanocortin-1 Receptor in Human Adipose Tissues of Severely Obese Patients. *Obesity* 15, 40–49. <https://doi.org/10.1038/oby.2007.525>
- Hoch, M., Hirzel, E., Lindinger, P., Eberle, A.N., Linscheid, P., Martin, I., Peters, T., Peterli, R., 2008. Weak Functional Coupling of the Melanocortin-1 Receptor Expressed in Human Adipocytes. *J. Recept. Signal Transduct.* 28, 485–504. <https://doi.org/10.1080/10799890802442622>

- Hofmann, A.F., 2009. The enterohepatic circulation of bile acids in mammals: form and functions. *Front. Biosci. Landmark Ed.* 14, 2584–2598. <https://doi.org/10.2741/3399>
- Horton, J.D., Goldstein, J.L., Brown, M.S., 2002. SREBPs: activators of the complete program of cholesterol and fatty acid synthesis in the liver. *J. Clin. Invest.* 109, 1125–1131. <https://doi.org/10.1172/JCI15593>
- Hruby, V.J., 2002. Designing peptide receptor agonists and antagonists. *Nat. Rev. Drug Discov.* 1, 847–858. <https://doi.org/10.1038/nrd939>
- Hsia, J.Z., Liu, D., Haynes, L., Cruz-Cosme, R., Tang, Q., 2024. Lipid Droplets: Formation, Degradation, and Their Role in Cellular Responses to Flavivirus Infections. *Microorganisms* 12, 647. <https://doi.org/10.3390/microorganisms12040647>
- Hua, X., Yokoyama, C., Wu, J., Briggs, M.R., Brown, M.S., Goldstein, J.L., Wang, X., 1993. SREBP-2, a second basic-helix-loop-helix-leucine zipper protein that stimulates transcription by binding to a sterol regulatory element. *Proc. Natl. Acad. Sci. U. S. A.* 90, 11603. <https://doi.org/10.1073/PNAS.90.24.11603>
- Humphreys, M.H., 2004. γ -MSH, sodium metabolism, and salt-sensitive hypertension. *Am. J. Physiol.-Regul. Integr. Comp. Physiol.* 286, R417–R430. <https://doi.org/10.1152/ajpregu.00365.2003>
- Hunt, G., Kyne, S., Wakamatsu, K., Ito, S., Thody, A.J., 1995. Nle4DPhe7 alpha-melanocyte-stimulating hormone increases the eumelanin:phaeomelanin ratio in cultured human melanocytes. *J. Invest. Dermatol.* 104, 83–85. <https://doi.org/10.1111/1523-1747.ep12613565>
- Huszar, D., Lynch, C.A., Fairchild-Huntress, V., Dunmore, J.H., Fang, Q., Berkemeier, L.R., Gu, W., Kesterson, R.A., Boston, B.A., Cone, R.D., Smith, F.J., Campfield, L.A., Burn, P., Lee, F., 1997. Targeted disruption of the melanocortin-4 receptor results in obesity in mice. *Cell* 88, 131–141. [https://doi.org/10.1016/s0092-8674\(00\)81865-6](https://doi.org/10.1016/s0092-8674(00)81865-6)
- Iizuka, K., Bruick, R.K., Liang, G., Horton, J.D., Uyeda, K., 2004. Deficiency of carbohydrate response element-binding protein (ChREBP) reduces lipogenesis as well as glycolysis. *Proc. Natl. Acad. Sci. U. S. A.* 101, 7281–7286. <https://doi.org/10.1073/pnas.0401516101>
- Iizuka, K., Miller, B., Uyeda, K., 2006. Deficiency of carbohydrate-activated transcription factor ChREBP prevents obesity and improves plasma glucose control in leptin-deficient (ob/ob) mice. *Am. J. Physiol.-Endocrinol. Metab.* 291, E358–E364. <https://doi.org/10.1152/ajpendo.00027.2006>
- Iizuka, K., Takao, K., Kato, T., Horikawa, Y., Takeda, J., 2018. ChREBP Reciprocally Regulates Liver and Plasma Triacylglycerol Levels in Different Manners. *Nutrients* 10, 1699. <https://doi.org/10.3390/nu10111699>
- Iqbal, J., Hussain, M.M., 2009. Intestinal lipid absorption. *Am. J. Physiol. Endocrinol. Metab.* 296, E1183–1194. <https://doi.org/10.1152/ajpendo.90899.2008>
- Israeli, H., Degtjarik, O., Fierro, F., Chunilal, V., Gill, A.K., Roth, N.J., Botta, J., Prabakar, V., Peleg, Y., Chan, L.F., Ben-Zvi, D., McCormick, P.J., Niv, M.Y., Shalev-Benami, M., 2021. Structure reveals the activation mechanism of the MC4 receptor to initiate satiation signaling. *Science* 372, 808–814. <https://doi.org/10.1126/science.abf7958>
- Istvan, E.S., Deisenhofer, J., 2001. Structural Mechanism for Statin Inhibition of HMG-CoA Reductase. *Science* 292, 1160–1164. <https://doi.org/10.1126/science.1059344>
- Jackson, I.J., Budd, P.S., Keighren, M., McKie, L., 2007. Humanized MC1R transgenic mice reveal human specific receptor function. *Hum. Mol. Genet.* 16, 2341–2348. <https://doi.org/10.1093/hmg/ddm191>
- Jääntti, S.E., Kivilompolo, M., Öhrnberg, L., Pietiläinen, K.H., Nygren, H., Orešič, M., Hyötyläinen, T., 2014. Quantitative profiling of bile acids in blood, adipose tissue, intestine, and gall bladder samples using ultra high performance liquid chromatography-tandem mass spectrometry. *Anal. Bioanal. Chem.* 406, 7799–7815. <https://doi.org/10.1007/S00216-014-8230-9>
- Jaworski, K., Sarkadi-Nagy, E., Duncan, R.E., Ahmadian, M., Sul, H.S., 2007. Regulation of Triglyceride Metabolism. IV. Hormonal regulation of lipolysis in adipose tissue. *Am. J. Physiol. Gastrointest. Liver Physiol.* 293, G1–G4. <https://doi.org/10.1152/ajpgi.00554.2006>

- Ji, L.-Q., Hong, Y., Tao, Y.-X., 2022. Melanocortin-5 Receptor: Pharmacology and Its Regulation of Energy Metabolism. *Int. J. Mol. Sci.* 23, 8727. <https://doi.org/10.3390/ijms23158727>
- Jump, D.B., Lytle, K.A., Depner, C.M., Tripathy, S., 2018. Omega-3 polyunsaturated fatty acids as a treatment strategy for nonalcoholic fatty liver disease. *Pharmacol. Ther.* 181, 108–125. <https://doi.org/10.1016/j.pharmthera.2017.07.007>
- Jump, D.B., Tripathy, S., Depner, C.M., 2013. Fatty acid-regulated transcription factors in the liver. *Annu. Rev. Nutr.* 33, 249–269. <https://doi.org/10.1146/annurev-nutr-071812-161139>
- Kaidbey, K.H., Grove, K.H., Kligman, A.M., 1979. The influence of longwave ultraviolet radiation on sunburn cell production by UVB. *J. Invest. Dermatol.* 73, 743–745. <https://doi.org/10.1111/1523-1747.ep12514324>
- Kainuma, M., Fujimoto, M., Sekiya, N., Tsuneyama, K., Cheng, C., Takano, Y., Terasawa, K., Shimada, Y., 2006. Cholesterol-fed rabbit as a unique model of nonalcoholic, nonobese, non-insulin-resistant fatty liver disease with characteristic fibrosis. *J. Gastroenterol.* 41, 971–980. <https://doi.org/10.1007/S00535-006-1883-1>
- Kalra, A., Yetiskul, E., Wehrle, C.J., Tuma, F., 2024. Physiology, Liver, in: StatPearls. StatPearls Publishing, Treasure Island (FL).
- Kaneva, M., 2011. Investigation into the immuno-therapeutic potential of melanocortin peptides on activated chondrocytes (doctoral). *Eng. Life Sci.* University of Westminster. <https://doi.org/10.34737/8zyw6>
- Karim, G., Bansal, M.B., 2023. Resmetirom: An Orally Administered, Smallmolecule, Liver-directed, β -selective THR Agonist for the Treatment of Non-alcoholic Fatty Liver Disease and Non-alcoholic Steatohepatitis. *TouchREVIEWS Endocrinol.* 19, 60–70. <https://doi.org/10.17925/EE.2023.19.1.60>
- Kato, M., Higuchi, N., Enjoji, M., 2008. Reduced hepatic expression of adipose tissue triglyceride lipase and CGI-58 may contribute to the development of non-alcoholic fatty liver disease in patients with insulin resistance. *Scand. J. Gastroenterol.* 43, 1018–1019. <https://doi.org/10.1080/00365520802008140>
- Kawaguchi, T., Osatomi, K., Yamashita, H., Kabashima, T., Uyeda, K., 2002. Mechanism for Fatty Acid “Sparing” Effect on Glucose-induced Transcription: REGULATION OF CARBOHYDRATE-RESPONSIVE ELEMENT-BINDING PROTEIN BY AMP-ACTIVATED PROTEIN KINASE *. *J. Biol. Chem.* 277, 3829–3835. <https://doi.org/10.1074/jbc.M107895200>
- Kawakami, T., Takasaki, S., Kadota, Y., Fukuoka, D., Sato, M., Suzuki, S., 2019. Regulatory role of metallothionein-1/2 on development of sex differences in a high-fat diet-induced obesity. *Life Sci.* 226, 12–21. <https://doi.org/10.1016/j.lfs.2019.04.012>
- Kawano, Y., Cohen, D.E., 2013. Mechanisms of hepatic triglyceride accumulation in non-alcoholic fatty liver disease. *J. Gastroenterol.* 48, 434–441. <https://doi.org/10.1007/s00535-013-0758-5>
- Keyomarsi, K., Sandoval, L., Band, V., Pardee, A.B., 1991. Synchronization of tumor and normal cells from G1 to multiple cell cycles by lovastatin. *Cancer Res.* 51, 3602–3609.
- Kiernan, F., 1833. XXIX. The anatomy and physiology of the liver. *Philos. Trans. R. Soc. Lond.* 711–770.
- Kim, C.S., Lee, S.H., Kim, R.Y., Kim, B.J., Li, S.Z., Lee, I.H., Lee, E.J., Lim, S.K., Bae, Y.S., Lee, W., Baik, J.H., 2002. Identification of domains directing specificity of coupling to G-proteins for the melanocortin MC3 and MC4 receptors. *J. Biol. Chem.* 277, 31310–31317. <https://doi.org/10.1074/JBC.M112085200>
- Kim, J.-Y., van de Wall, E., Laplante, M., Azzara, A., Trujillo, M.E., Hofmann, S.M., Schraw, T., Durand, J.L., Li, H., Li, G., Jeliciks, L.A., Mehler, M.F., Hui, D.Y., Deshaies, Y., Shulman, G.I., Schwartz, G.J., Scherer, P.E., 2007. Obesity-associated improvements in metabolic profile through expansion of adipose tissue. *J. Clin. Invest.* 117, 2621–2637. <https://doi.org/10.1172/JCI31021>
- Kim, M.S., Small, C.J., Stanley, S.A., Morgan, D.G., Seal, L.J., Kong, W.M., Edwards, C.M., Abusnana, S., Sunter, D., Ghatei, M.A., Bloom, S.R., 2000. The central melanocortin system

- affects the hypothalamo-pituitary thyroid axis and may mediate the effect of leptin. *J. Clin. Invest.* 105, 1005–1011. <https://doi.org/10.1172/JCI8857>
- Knobloch, M., Braun, S.M.G., Zurkirchen, L., von Schoultz, C., Zamboni, N., Araúzo-Bravo, M.J., Kovacs, W.J., Karalay, Ö., Suter, U., Machado, R.A.C., Roccio, M., Lutolf, M.P., Semenkovich, C.F., Jessberger, S., 2013. Metabolic control of adult neural stem cell activity by Fasn-dependent lipogenesis. *Nature* 493, 226–230. <https://doi.org/10.1038/nature11689>
- Kokot, A., Metzke, D., Mouchet, N., Galibert, M.-D., Schiller, M., Luger, T.A., Böhm, M., 2009. Alpha-melanocyte-stimulating hormone counteracts the suppressive effect of UVB on Nrf2 and Nrf-dependent gene expression in human skin. *Endocrinology* 150, 3197–3206. <https://doi.org/2020071612385662500>
- Konda, Y., Gantz, I., DelValle, J., Shimoto, Y., Miwa, H., Yamada, T., 1994. Interaction of dual intracellular signaling pathways activated by the melanocortin-3 receptor. *J. Biol. Chem.* 269, 13162–13166. [https://doi.org/10.1016/S0021-9258\(17\)36813-8](https://doi.org/10.1016/S0021-9258(17)36813-8)
- Kondo, M., Suzuki, T., Kawano, Y., Kojima, S., Miyashiro, M., Matsumoto, A., Kania, G., Blyszczuk, P., Ross, R.L., Mulipa, P., Del Galdo, F., Zhang, Y., Distler, J.H.W., 2022. Dersimelagon, a novel oral melanocortin 1 receptor agonist, demonstrates disease-modifying effects in preclinical models of systemic sclerosis. *Arthritis Res. Ther.* 24, 210. <https://doi.org/10.1186/s13075-022-02899-3>
- Kotzka, J., Lehr, S., Roth, G., Avci, H., Knebel, B., Muller-Wieland, D., 2004. Insulin-activated Erk-mitogen-activated protein kinases phosphorylate sterol regulatory element-binding Protein-2 at serine residues 432 and 455 in vivo. *J. Biol. Chem.* 279, 22404–22411. <https://doi.org/10.1074/JBC.M401198200>
- Krammer, J., Digel, M., Ehehalt, F., Stremmel, W., Füllekrug, J., Ehehalt, R., 2011. Overexpression of CD36 and acyl-CoA synthetases FATP2, FATP4 and ACSL1 increases fatty acid uptake in human hepatoma cells. *Int. J. Med. Sci.* 8, 599–614. <https://doi.org/10.7150/ijms.8.599>
- Kruepunga, N., Hakvoort, T.B.M., Hikspoors, J.P.J.M., Köhler, S.E., Lamers, W.H., 2019. Anatomy of rodent and human livers: What are the differences? *Biochim. Biophys. Acta BBA - Mol. Basis Dis., Animal Models in Liver Disease* 1865, 869–878. <https://doi.org/10.1016/j.bbadis.2018.05.019>
- Lake, A.D., Novak, P., Shipkova, P., Aranibar, N., Robertson, D., Reily, M.D., Lu, Z., Lehman-McKeeman, L.D., Cherrington, N.J., 2013. Decreased hepatotoxic bile acid composition and altered synthesis in progressive human nonalcoholic fatty liver disease. *Toxicol. Appl. Pharmacol.* 268, 132–140. <https://doi.org/10.1016/J.TAAP.2013.01.022>
- Lange, K.H.W., 2004. Fat metabolism in exercise – with special reference to training and growth hormone administration. *Scand. J. Med. Sci. Sports* 14, 74–99. <https://doi.org/10.1111/j.1600-0838.2004.381.x>
- Langin, D., Lucas, S., Lafontan, M., 2000. Millennium fat-cell lipolysis reveals unsuspected novel tracks. *Horm. Metab. Res. Horm. Stoffwechselforschung Horm. Metab.* 32, 443–452. <https://doi.org/10.1055/s-2007-978670>
- Large, V., Peroni, O., Leticier, D., Ray, H., Beylot, M., 2004. Metabolism of lipids in human white adipocyte. *Diabetes Metab.* 30, 294–309. [https://doi.org/10.1016/s1262-3636\(07\)70121-0](https://doi.org/10.1016/s1262-3636(07)70121-0)
- Large, V., Reynisdottir, S., Langin, D., Fredby, K., Klannemark, M., Holm, C., Arner, P., 1999. Decreased expression and function of adipocyte hormone-sensitive lipase in subcutaneous fat cells of obese subjects. *J. Lipid Res.* 40, 2059–2066.
- Lavoie, J.-M., Gauthier, M.-S., 2006. Regulation of fat metabolism in the liver: link to non-alcoholic hepatic steatosis and impact of physical exercise. *Cell. Mol. Life Sci. CMLS* 63, 1393–1409. <https://doi.org/10.1007/s00018-006-6600-y>
- Lee, P., Swarbrick, M.M., Ho, K.K.Y., 2013. Brown adipose tissue in adult humans: a metabolic renaissance. *Endocr. Rev.* 34, 413–438. <https://doi.org/2019041201441866400>
- Li, T., Chiang, J.Y.L., 2009. Regulation of Bile Acid and Cholesterol Metabolism by PPARs. *PPAR Res.* 2009, 501739. <https://doi.org/10.1155/2009/501739>

- Li, X., Zhong, S., Sun, Y., Huang, X., Li, Y., Wang, L., Wu, Y., Yang, M., Yuan, H.-X., Liu, J., Zang, S., 2022. Integration analysis identifies the role of metallothionein in the progression from hepatic steatosis to steatohepatitis. *Front. Endocrinol.* 13, 951093. <https://doi.org/10.3389/fendo.2022.951093>
- Li, X., Zou, H., Tang, M., Wang, Y., Tang, X., Tian, C., 2021. Optimization analysis of linear compressor using R290 for capacity-modulation performance improvement. *Int. J. Refrig.* 127, 111–119. <https://doi.org/10.1016/j.ijrefrig.2021.01.010>
- Li, X.-A., Everson, W.V., Smart, E.J., 2005. Caveolae, Lipid Rafts, and Vascular Disease. *Trends Cardiovasc. Med.* 15, 92–96. <https://doi.org/10.1016/j.tcm.2005.04.001>
- Libby, P., 2021. The changing landscape of atherosclerosis. *Nature* 592, 524–533. <https://doi.org/10.1038/s41586-021-03392-8>
- Li-Hawkins, J., Gåfvæls, M., Olin, M., Lund, E.G., Andersson, U., Schuster, G., Björkhem, I., Russell, D.W., Eggertsen, G., 2002. Cholic acid mediates negative feedback regulation of bile acid synthesis in mice. *J. Clin. Invest.* 110, 1191–1200. <https://doi.org/10.1172/JCI16309>
- Lin, L., Hindmarsh, P.C., Metherell, L.A., Alzyoud, M., Al-Ali, M., Brain, C.E., Clark, A.J.L., Dattani, M.T., Achermann, J.C., 2007. Severe loss-of-function mutations in the adrenocorticotropin receptor (ACTHR, MC2R) can be found in patients diagnosed with salt-losing adrenal hypoplasia. *Clin. Endocrinol. (Oxf.)* 66, 205–210. <https://doi.org/10.1111/j.1365-2265.2006.02709.x>
- Linden, A.G., Li, S., Choi, H.Y., Fang, F., Fukasawa, M., Uyeda, K., Hammer, R.E., Horton, J.D., Engelking, L.J., Liang, G., 2018. Interplay between ChREBP and SREBP-1c coordinates postprandial glycolysis and lipogenesis in livers of mice. *J. Lipid Res.* 59, 475–487. <https://doi.org/10.1194/jlr.M081836>
- Listenberger, L.L., Han, X., Lewis, S.E., Cases, S., Farese, R.V., Ory, D.S., Schaffer, J.E., 2003. Triglyceride accumulation protects against fatty acid-induced lipotoxicity. *Proc. Natl. Acad. Sci. U. S. A.* 100, 3077–3082. <https://doi.org/10.1073/pnas.0630588100>
- Liu, T., Zhang, L., Joo, D., Sun, S.-C., 2017. NF- κ B signaling in inflammation. *Signal Transduct. Target. Ther.* 2, 1–9. <https://doi.org/10.1038/sigtrans.2017.23>
- Loh, K., Tam, S., Murray-Segal, L., Huynh, K., Meikle, P.J., Scott, J.W., van Denderen, B., Chen, Z., Steel, R., LeBlond, N.D., Burkovsky, L.A., O'Dwyer, C., Nunes, J.R.C., Steinberg, G.R., Fullerton, M.D., Galic, S., Kemp, B.E., 2018. Inhibition of Adenosine Monophosphate-Activated Protein Kinase-3-Hydroxy-3-Methylglutaryl Coenzyme A Reductase Signaling Leads to Hypercholesterolemia and Promotes Hepatic Steatosis and Insulin Resistance. *Hepatol. Commun.* 3, 84–98. <https://doi.org/10.1002/HEP4.1279>
- Loizides-Mangold, U., Clément, S., Alfonso-Garcia, A., Branche, E., Conzelmann, S., Parisot, C., Potma, E.O., Riezman, H., Negro, F., 2014. HCV 3a Core Protein Increases Lipid Droplet Cholesteryl Ester Content via a Mechanism Dependent on Sphingolipid Biosynthesis. *PLoS ONE* 9, e115309. <https://doi.org/10.1371/journal.pone.0115309>
- Luo, J., Yang, H., Song, B.-L., 2020. Mechanisms and regulation of cholesterol homeostasis. *Nat. Rev. Mol. Cell Biol.* 21, 225–245. <https://doi.org/10.1038/s41580-019-0190-7>
- Ma, S., Chen, Y., Dai, A., Yin, W., Guo, J., Yang, D., Zhou, F., Jiang, Y., Wang, M.-W., Xu, H.E., 2021. Structural mechanism of calcium-mediated hormone recognition and G β interaction by the human melanocortin-1 receptor. *Cell Res.* 31, 1061–1071. <https://doi.org/10.1038/s41422-021-00557-y>
- Maaser, C., Kannengiesser, K., Specht, C., Lügering, A., Brzoska, T., Luger, T.A., Domschke, W., Kucharzik, T., 2006. Crucial role of the melanocortin receptor MC1R in experimental colitis. *Gut* 55, 1415. <https://doi.org/10.1136/gut.2005.083634>
- Mach, F., Baigent, C., Catapano, A.L., Koskinas, K.C., Casula, M., Badimon, L., Chapman, M.J., De Backer, G.G., Delgado, V., Ference, B.A., Graham, I.M., Halliday, A., Landmesser, U., Mihaylova, B., Pedersen, T.R., Riccardi, G., Richter, D.J., Sabatine, M.S., Taskinen, M.-R., Tokgozoglul, L., Wiklund, O., ESC Scientific Document Group, 2020. 2019 ESC/EAS Guidelines for the management of dyslipidaemias: lipid modification to reduce cardiovascular risk: The Task

- Force for the management of dyslipidaemias of the European Society of Cardiology (ESC) and European Atherosclerosis Society (EAS). *Eur. Heart J.* 41, 111–188. <https://doi.org/10.1093/eurheartj/ehz455>
- Machleder, D., Ivandic, B., Welch, C., Castellani, L., Reue, K., Lusis, A.J., 1997. Complex genetic control of HDL levels in mice in response to an atherogenic diet. Coordinate regulation of HDL levels and bile acid metabolism. *J. Clin. Invest.* 99, 1406–1419. <https://doi.org/10.1172/JCI119300>
- Magee, N., Zou, A., Zhang, Y., 2016. Pathogenesis of Nonalcoholic Steatohepatitis: Interactions between Liver Parenchymal and Nonparenchymal Cells. *BioMed Res. Int.* 2016, 5170402. <https://doi.org/10.1155/2016/5170402>
- Magenis, R.E., Smith, L., Nadeau, J.H., Johnson, K.R., Mountjoy, K.G., Cone, R.D., 1994. Mapping of the ACTH, MSH, and neural (MC3 and MC4) melanocortin receptors in the mouse and human. *Mamm. Genome Off. J. Int. Mamm. Genome Soc.* 5, 503–508. <https://doi.org/10.1007/BF00369320>
- Mak, H.Y., 2012. Lipid droplets as fat storage organelles in *Caenorhabditis elegans*: Thematic Review Series: Lipid Droplet Synthesis and Metabolism: from Yeast to Man. *J. Lipid Res.* 53, 28–33. <https://doi.org/10.1194/jlr.R021006>
- Malik, I.A., Triebel, J., Posselt, J., Khan, S., Ramadori, P., Raddatz, D., Ramadori, G., 2012. Melanocortin receptors in rat liver cells: change of gene expression and intracellular localization during acute-phase response. *Histochem. Cell Biol.* 137, 279. <https://doi.org/10.1007/S00418-011-0899-7>
- Manieri, E., Folgueira, C., Rodríguez, M.E., Leiva-Vega, L., Esteban-Lafuente, L., Chen, C., Cubero, F.J., Barrett, T., Cavanagh-Kyros, J., Seruggia, D., Rosell, A., Sanchez-Cabo, F., Gómez, M.J., Monte, M.J., Marin, J.J.G., Davis, R.J., Mora, A., Sabio, G., 2020. JNK-mediated disruption of bile acid homeostasis promotes intrahepatic cholangiocarcinoma. *Proc. Natl. Acad. Sci. U. S. A.* 117, 16492–16499. <https://doi.org/10.1073/PNAS.2002672117>
- Markham, A., 2021. Setmelanotide: First Approval. *Drugs* 81, 397–403. <https://doi.org/10.1007/s40265-021-01470-9>
- Marks, D.L., Hruby, V., Brookhart, G., Cone, R.D., 2006. The regulation of food intake by selective stimulation of the type 3 melanocortin receptor (MC3R). *Peptides* 27, 259–264. <https://doi.org/10.1016/j.peptides.2005.01.025>
- Matsuura, E., Hughes, G.R.V., Khamashta, M.A., 2008. Oxidation of LDL and its clinical implication. *Autoimmun. Rev., Redox and Autoimmunity* 7, 558–566. <https://doi.org/10.1016/j.autrev.2008.04.018>
- Matteoni, C.A., Younossi, Z.M., Gramlich, T., Boparai, N., Liu, Y.C., McCullough, A.J., 1999. Nonalcoholic fatty liver disease: a spectrum of clinical and pathological severity. *Gastroenterology* 116, 1413–1419. [https://doi.org/10.1016/s0016-5085\(99\)70506-8](https://doi.org/10.1016/s0016-5085(99)70506-8)
- McClain, C.J., Barve, S., Deaciuc, I., 2007. Good fat/bad fat. *Hepatol. Baltim. Md* 45, 1343–1346. <https://doi.org/10.1002/hep.21788>
- Memon, R.A., Fuller, J., Moser, A.H., Smith, P.J., Grunfeld, C., Feingold, K.R., 1999. Regulation of putative fatty acid transporters and Acyl-CoA synthetase in liver and adipose tissue in ob/ob mice. *Diabetes* 48, 121–127. <https://doi.org/10.2337/diabetes.48.1.121>
- Menge, T., Hartung, H.-P., Stüve, O., 2005. Statins--a cure-all for the brain? *Nat. Rev. Neurosci.* 6, 325–331. <https://doi.org/10.1038/nrn1652>
- Michelotti, G.A., Machado, M.V., Diehl, A.M., 2013. NAFLD, NASH and liver cancer. *Nat. Rev. Gastroenterol. Hepatol.* 10, 656–665. <https://doi.org/10.1038/nrgastro.2013.183>
- Min, H.K., Kapoor, A., Fuchs, M., Mirshahi, F., Zhou, H., Maher, J., Kellum, J., Warnick, R., Contos, M.J., Sanyal, A.J., 2012. Increased hepatic synthesis and dysregulation of cholesterol metabolism is associated with the severity of nonalcoholic fatty liver disease. *Cell Metab.* 15, 665–674. <https://doi.org/10.1016/j.cmet.2012.04.004>
- Miquilena-Colina, M.E., Lima-Cabello, E., Sánchez-Campos, S., García-Mediavilla, M.V., Fernández-Bermejo, M., Lozano-Rodríguez, T., Vargas-Castrillón, J., Buqué, X., Ochoa, B., Aspichueta, P.,

- González-Gallego, J., García-Monzón, C., 2011. Hepatic fatty acid translocase CD36 upregulation is associated with insulin resistance, hyperinsulinaemia and increased steatosis in non-alcoholic steatohepatitis and chronic hepatitis C. *Gut* 60, 1394–1402. <https://doi.org/10.1136/gut.2010.222844>
- Missaglia, S., Coleman, R.A., Mordente, A., Tavian, D., 2019. Neutral Lipid Storage Diseases as Cellular Model to Study Lipid Droplet Function. *Cells* 8, 187. <https://doi.org/10.3390/cells8020187>
- Mitra, D., Luo, X., Morgan, A., Wang, J., Hoang, M.P., Lo, J., Guerrero, C.R., Lennerz, J.K., Mihm, M.C., Wargo, J.A., Robinson, K.C., Devi, S.P., Vanover, J.C., D’Orazio, J.A., McMahon, M., Bosenberg, M.W., Haigis, K.M., Haber, D.A., Wang, Y., Fisher, D.E., 2012. An ultraviolet-radiation-independent pathway to melanoma carcinogenesis in the red hair/fair skin background. *Nature* 491, 449–453. <https://doi.org/10.1038/nature11624>
- Mogil, J.S., Wilson, S.G., Chesler, E.J., Rankin, A.L., Nemmani, K.V.S., Lariviere, W.R., Groce, M.K., Wallace, M.R., Kaplan, L., Staud, R., Ness, T.J., Glover, T.L., Stankova, M., Mayorov, A., Hrubby, V.J., Grisel, J.E., Fillingim, R.B., 2003. The melanocortin-1 receptor gene mediates female-specific mechanisms of analgesia in mice and humans. *Proc. Natl. Acad. Sci.* 100, 4867–4872. <https://doi.org/10.1073/pnas.0730053100>
- Molinaro, A., Becattini, B., Solinas, G., 2020. Insulin signaling and glucose metabolism in different hepatoma cell lines deviate from hepatocyte physiology toward a convergent aberrant phenotype. *Sci. Rep.* 10, 12031. <https://doi.org/10.1038/s41598-020-68721-9>
- Møller, C.L., Pedersen, S.B., Richelsen, B., Conde-Frieboes, K.W., Raun, K., Grove, K.L., Wulff, B.S., 2015. Melanocortin agonists stimulate lipolysis in human adipose tissue explants but not in adipocytes. *BMC Res. Notes* 8, 559. <https://doi.org/10.1186/s13104-015-1539-4>
- Møller, C.L., Raun, K., Jacobsen, M.L., Pedersen, T.Å., Holst, B., Conde-Frieboes, K.W., Wulff, B.S., 2011. Characterization of murine melanocortin receptors mediating adipocyte lipolysis and examination of signalling pathways involved. *Mol. Cell. Endocrinol.* 341, 9–17. <https://doi.org/10.1016/j.mce.2011.03.010>
- Montero-Melendez, T., Boesen, T., Jonassen, T.E.N., 2022. Translational advances of melanocortin drugs: Integrating biology, chemistry and genetics. *Semin. Immunol.* 101603. <https://doi.org/10.1016/J.SMIM.2022.101603>
- Moore, M.C., Coate, K.C., Winnick, J.J., An, Z., Cherrington, A.D., 2012. Regulation of Hepatic Glucose Uptake and Storage In Vivo. *Adv. Nutr.* 3, 286–294. <https://doi.org/10.3945/an.112.002089>
- Moscowitz, A.E., Asif, H., Lindenmaier, L.B., Calzadilla, A., Zhang, C., Mirsaeidi, M., 2019. The Importance of Melanocortin Receptors and Their Agonists in Pulmonary Disease. *Front. Med.* 6. <https://doi.org/10.3389/fmed.2019.00145>
- Mountjoy, K.G., Mortrud, M.T., Low, M.J., Simerly, R.B., Cone, R.D., 1994. Localization of the melanocortin-4 receptor (MC4-R) in neuroendocrine and autonomic control circuits in the brain. *Mol. Endocrinol. Baltim. Md* 8, 1298–1308. <https://doi.org/2016092613593000056>
- Mountjoy, K.G., Robbins, L.S., Mortrud, M.T., Cone, R.D., 1992. The cloning of a family of genes that encode the melanocortin receptors. *Science* 257, 1248–1251. <https://doi.org/10.1126/science.1325670>
- Mountjoy, K.G., Wong, J., 1997. Obesity, Diabetes and Functions for Proopiomelanocortin-derived Peptides. *Mol. Cell. Endocrinol.* 128, 171–177. [https://doi.org/10.1016/S0303-7207\(96\)04017-8](https://doi.org/10.1016/S0303-7207(96)04017-8)
- Muceniece, R., Zvejniece, L., Liepinsh, E., Kirjanova, O., Bauman, L., Petrovska, R., Mutulis, F., Mutule, I., Kalvinsh, I., Wikberg, J.E.S., Dambrova, M., 2006. The MC3 receptor binding affinity of melanocortins correlates with the nitric oxide production inhibition in mice brain inflammation model. *Peptides* 27, 1443–1450. <https://doi.org/10.1016/j.peptides.2005.12.002>
- Mun, Y., Kim, W., Shin, D., 2023. Melanocortin 1 Receptor (MC1R): Pharmacological and Therapeutic Aspects. *Int. J. Mol. Sci.* 24, 12152. <https://doi.org/10.3390/ijms241512152>

- Murosaki, S., Lee, T.R., Muroyama, K., Shin, E.S., Cho, S.Y., Yamamoto, Y., Lee, S.J., 2007. A Combination of Caffeine, Arginine, Soy Isoflavones, and l-Carnitine Enhances Both Lipolysis and Fatty Acid Oxidation in 3T3-L1 and HepG2 Cells in Vitro and in KK Mice in Vivo. *J. Nutr.* 137, 2252–2257. <https://doi.org/10.1093/jn/137.10.2252>
- Murphy, D.J., 2012. The dynamic roles of intracellular lipid droplets: from archaea to mammals. *Protoplasma* 249, 541–585. <https://doi.org/10.1007/s00709-011-0329-7>
- Musso, G., Gambino, R., Cassader, M., 2009. Recent insights into hepatic lipid metabolism in non-alcoholic fatty liver disease (NAFLD). *Prog. Lipid Res.* 48, 1–26. <https://doi.org/10.1016/j.plipres.2008.08.001>
- Nagarajan, S.R., Paul-Heng, M., Krycer, J.R., Fazakerley, D.J., Sharland, A.F., Hoy, A.J., 2019. Lipid and glucose metabolism in hepatocyte cell lines and primary mouse hepatocytes: a comprehensive resource for in vitro studies of hepatic metabolism. *Am. J. Physiol. Endocrinol. Metab.* 316, E578–E589. <https://doi.org/10.1152/ajpendo.00365.2018>
- Nagui, N.A., Mahmoud, S.B., Abdel Hay, R.M., Hassieb, M.M., Rashed, L.A., 2017. Assessment of gene expression levels of proopiomelanocortin (POMC) and melanocortin-1 receptor (MC1R) in vitiligo. *Australas. J. Dermatol.* 58, e36–e39. <https://doi.org/10.1111/ajd.12408>
- Nakanishi, S., Inoue, A., Kita, T., Nakamura, M., Chang, A.C., Cohen, S.N., Numa, S., 1979. Nucleotide sequence of cloned cDNA for bovine corticotropin-beta-lipotropin precursor. *Nature* 278, 423–427. <https://doi.org/10.1038/278423a0>
- Nguyen, P., Leray, V., Diez, M., Serisier, S., Bloc'h, J.L., Siliart, B., Dumon, H., 2008. Liver lipid metabolism. *J. Anim. Physiol. Anim. Nutr.* 92, 272–283. <https://doi.org/10.1111/j.1439-0396.2007.00752.x>
- Nielsen, T.S., Jessen, N., Jørgensen, J.O.L., Møller, N., Lund, S., 2014. Dissecting adipose tissue lipolysis: Molecular regulation and implications for metabolic disease. *J. Mol. Endocrinol.* 52, R199–R222. <https://doi.org/10.1530/JME-13-0277>
- Olzmann, J.A., Carvalho, P., 2019. Dynamics and functions of lipid droplets. *Nat. Rev. Mol. Cell Biol.* 20, 137–155. <https://doi.org/10.1038/s41580-018-0085-z>
- Ong, K.T., Mashek, M.T., Bu, S.Y., Greenberg, A.S., Mashek, D.G., 2011. Adipose triglyceride lipase is a major hepatic lipase that regulates triacylglycerol turnover and fatty acid signaling and partitioning. *Hepatology* 53, 116–126. <https://doi.org/10.1002/hep.24006>
- Öörni, K., Lehti, S., Sjövall, P., Kovanen, P.T., 2019. Triglyceride-Rich Lipoproteins as a Source of Proinflammatory Lipids in the Arterial Wall. *Curr. Med. Chem.* 26, 1701–1710. <https://doi.org/10.2174/0929867325666180530094819>
- Oosterveer, M.H., Schoonjans, K., 2014. Hepatic glucose sensing and integrative pathways in the liver. *Cell. Mol. Life Sci.* 71, 1453–1467. <https://doi.org/10.1007/s00018-013-1505-z>
- Ouimet, M., Barrett, T.J., Fisher, E.A., 2019. HDL and Reverse Cholesterol Transport. *Circ. Res.* 124, 1505–1518. <https://doi.org/10.1161/CIRCRESAHA.119.312617>
- Özcan, U., Cao, Q., Yilmaz, E., Lee, A.-H., Iwakoshi, N.N., Özdelen, E., Tuncman, G., Görgün, C., Glimcher, L.H., Hotamisligil, G.S., 2004. Endoplasmic Reticulum Stress Links Obesity, Insulin Action, and Type 2 Diabetes. *Science* 306, 457–461. <https://doi.org/10.1126/science.1103160>
- Özvegy-Laczka, C., Ungvári, O., Bakos, É., 2023. Fluorescence-based methods for studying activity and drug-drug interactions of hepatic solute carrier and ATP binding cassette proteins involved in ADME-Tox. *Biochem. Pharmacol.* 209, 115448. <https://doi.org/10.1016/j.bcp.2023.115448>
- Pagliassotti, M.J., Holste, L.C., Moore, M.C., Neal, D.W., Cherrington, A.D., 1996. Comparison of the time courses of insulin and the portal signal on hepatic glucose and glycogen metabolism in the conscious dog. *J. Clin. Invest.* 97, 81–91. <https://doi.org/10.1172/JCI118410>
- Palczewski, K., Kumasaka, T., Hori, T., Behnke, C.A., Motoshima, H., Fox, B.A., Le Trong, I., Teller, D.C., Okada, T., Stenkamp, R.E., Yamamoto, M., Miyano, M., 2000. Crystal structure of rhodopsin: A G protein-coupled receptor. *Science* 289, 739–745. <https://doi.org/10.1126/science.289.5480.739>

- Paredes-Flores, M.A., Rahimi, N., Mohiuddin, S.S., 2024. Biochemistry, Glycogenolysis, in: StatPearls. StatPearls Publishing, Treasure Island (FL).
- Park, J., Jeong, D., Jang, B., Oh, E.-S., 2019. The melanocortin-1 receptor reversely regulates the melanin synthesis and migration of melanoma cells via dimerization-induced conformational changes. *Biochem. Biophys. Res. Commun.* 518, 739–745. <https://doi.org/10.1016/j.bbrc.2019.08.123>
- Parton, R.G., del Pozo, M.A., 2013. Caveolae as plasma membrane sensors, protectors and organizers. *Nat. Rev. Mol. Cell Biol.* 14, 98–112. <https://doi.org/10.1038/nrm3512>
- Parton, R.G., Simons, K., 2007. The multiple faces of caveolae. *Nat. Rev. Mol. Cell Biol.* 8, 185–194. <https://doi.org/10.1038/nrm2122>
- Pellegrinelli, V., Carobbio, S., Vidal-Puig, A., 2016. Adipose tissue plasticity: how fat depots respond differently to pathophysiological cues. *Diabetologia* 59, 1075–1088. <https://doi.org/10.1007/s00125-016-3933-4>
- Petersen, M.C., Vatner, D.F., Shulman, G.I., 2017. Regulation of hepatic glucose metabolism in health and disease. *Nat. Rev. Endocrinol.* 13, 572–587. <https://doi.org/10.1038/nrendo.2017.80>
- Pilkis, S.J., Granner, D.K., 1992. Molecular physiology of the regulation of hepatic gluconeogenesis and glycolysis. *Annu. Rev. Physiol.* 54, 885–909. <https://doi.org/10.1146/annurev.ph.54.030192.004321>
- Pinkosky, S.L., Groot, P.H.E., Lalwani, N.D., Steinberg, G.R., 2017. Targeting ATP-Citrate Lyase in Hyperlipidemia and Metabolic Disorders. *Trends Mol. Med.* 23, 1047–1063. <https://doi.org/10.1016/j.molmed.2017.09.001>
- Postic, C., Shiota, M., Niswender, K.D., Jetton, T.L., Chen, Y., Moates, J.M., Shelton, K.D., Lindner, J., Cherrington, A.D., Magnuson, M.A., 1999. Dual roles for glucokinase in glucose homeostasis as determined by liver and pancreatic beta cell-specific gene knock-outs using Cre recombinase. *J. Biol. Chem.* 274, 305–315. <https://doi.org/10.1074/JBC.274.1.305>
- Pullinger, C.R., Eng, C., Salen, G., Shefer, S., Batta, A.K., Erickson, S.K., Verhagen, A., Rivera, C.R., Mulvihill, S.J., Malloy, M.J., Kane, J.P., 2002. Human cholesterol 7 α -hydroxylase (CYP7A1) deficiency has a hypercholesterolemic phenotype. *J. Clin. Invest.* 110, 109–117. <https://doi.org/10.1172/JCI15387>
- Reichrath, J.J., Girdt, M., Tilgen, Wolfgang, Querings, K., Lehmann, B., Knuschke, P., Meurer, M., Seifert, M., Diesel, B., Meese, E., Tilgen, W., Reichrath, J., Printed, B.M., Denmark, I., 2005. Expression and functional relevance of melatonin receptors in hair follicle biology. *Exp. Dermatol.* 14, 157–157. <https://doi.org/10.1111/J.0906-6705.2005.0266P.X>
- Reid, B.N., Ables, G.P., Otlivanchik, O.A., Schoiswohl, G., Zechner, R., Blaner, W.S., Goldberg, I.J., Schwabe, R.F., Chua, S.C., Huang, L.-S., 2008. Hepatic overexpression of hormone-sensitive lipase and adipose triglyceride lipase promotes fatty acid oxidation, stimulates direct release of free fatty acids, and ameliorates steatosis. *J. Biol. Chem.* 283, 13087–13099. <https://doi.org/10.1074/jbc.M800533200>
- Ren, S., Hylemon, P.B., Marques, D., Gurley, E., Bodhan, P., Hall, E., Redford, K., Gil, G., Pandak, W.M., 2004. Overexpression of cholesterol transporter StAR increases in vivo rates of bile acid synthesis in the rat and mouse. *Hepatology* 40, 910–917. <https://doi.org/10.1002/hep.20382>
- Renquist, B.J., Lippert, R., Sebag, J.A., Ellacott, K.L.J., Cone, R.D., 2011. Physiological roles of the melanocortin MC3 receptor. *Eur. J. Pharmacol.* 660, 13–20. <https://doi.org/10.1016/j.ejphar.2010.12.025>
- Reynisdottir, S., Langin, D., Carlström, K., Holm, C., Rössner, S., Arner, P., 1995. Effects of weight reduction on the regulation of lipolysis in adipocytes of women with upper-body obesity. *Clin. Sci. Lond. Engl.* 1979 89, 421–429. <https://doi.org/10.1042/cs0890421>
- Richter, W.O., Schwandt, P., 1987. Lipolytic potency of proopiomelanocorticotropin peptides in vitro. *Neuropeptides* 9, 59–74. [https://doi.org/10.1016/0143-4179\(87\)90033-3](https://doi.org/10.1016/0143-4179(87)90033-3)

- Rinne, P., Kadiri, J.J., Velasco-Delgado, M., Nuutinen, S., Viitala, M., Hollmén, M., Rami, M., Savontaus, E., Steffens, S., 2018. Melanocortin 1 Receptor Deficiency Promotes Atherosclerosis in Apolipoprotein E $-/-$ Mice. *Arterioscler. Thromb. Vasc. Biol.* 38, 313–323. <https://doi.org/10.1161/ATVBAHA.117.310418>
- Rinne, P., Rami, M., Nuutinen, S., Santovito, D., van der Vorst, E.P.C., Guillaumat-Prats, R., Lyytikäinen, L.-P.P., Raitoharju, E., Oksala, N., Ring, L., Cai, M., Hruby, V.J., Lehtimäki, T., Weber, C., Steffens, S., 2017. Melanocortin 1 Receptor Signaling Regulates Cholesterol Transport in Macrophages. *Circulation* 136, 83–97. <https://doi.org/10.1161/CIRCULATIONAHA.116.025889>
- Roberts, J.L., Eberwine, J.H., Gee, C.E., 1983. Analysis of POMC gene expression by transcription assay and in situ hybridization histochemistry. *Cold Spring Harb. Symp. Quant. Biol.* 48 Pt 1, 385–391. <https://doi.org/10.1101/sqb.1983.048.01.042>
- Roselli-Rehfuß, L., Mountjoy, K.G., Robbins, L.S., Mortrud, M.T., Low, M.J., Tatro, J.B., Entwistle, M.L., Simerly, R.B., Cone, R.D., 1993. Identification of a receptor for gamma melanotropin and other proopiomelanocortin peptides in the hypothalamus and limbic system. *Proc. Natl. Acad. Sci.* 90, 8856–8860. <https://doi.org/10.1073/pnas.90.19.8856>
- Rowe, C., Gerrard, D.T., Jenkins, R., Berry, A., Durkin, K., Sundstrom, L., Goldring, C.E., Park, B.K., Kitteringham, N.R., Hanley, K.P., Hanley, N.A., 2013. Proteome-wide analyses of human hepatocytes during differentiation and dedifferentiation. *Hepatology* 58, 799–809. <https://doi.org/10.1002/hep.26414>
- Ruggiero, C., Lalli, E., 2016. Impact of ACTH Signaling on Transcriptional Regulation of Steroidogenic Genes. *Front. Endocrinol.* 7. <https://doi.org/10.3389/fendo.2016.00024>
- Rui, L., 2014. Energy Metabolism in the Liver. *Compr. Physiol.* 4, 177–197. <https://doi.org/10.1002/cphy.c130024>
- Russell, D.W., Setchell, K.D.R., 1992. Bile acid biosynthesis. *Biochemistry* 31, 4737–4749. <https://doi.org/10.1021/bi00135a001>
- Ruttikay-Nedecky, B., Nejdil, L., Gumulec, J., Zitka, O., Masarik, M., Eckschlager, T., Stiborova, M., Adam, V., Kizek, R., 2013. The Role of Metallothionein in Oxidative Stress. *Int. J. Mol. Sci.* 14, 6044–6066. <https://doi.org/10.3390/ijms14036044>
- Sanyal, A.J., Chalasani, N., Kowdley, K.V., McCullough, A., Diehl, A.M., Bass, N.M., Neuschwander-Tetri, B.A., Lavine, J.E., Tonascia, J., Unalp, A., Van Natta, M., Clark, J., Brunt, E.M., Kleiner, D.E., Hoofnagle, J.H., Robuck, P.R., NASH CRN, 2010. Pioglitazone, vitamin E, or placebo for nonalcoholic steatohepatitis. *N. Engl. J. Med.* 362, 1675–1685. <https://doi.org/10.1056/NEJMoa0907929>
- Sato, S., Jung, H., Nakagawa, T., Pawlosky, R., Takeshima, T., Lee, W.-R., Sakiyama, H., Laxman, S., Wynn, R.M., Tu, B.P., MacMillan, J.B., Brabander, J.K.D., Veech, R.L., Uyeda, K., 2016. Metabolite Regulation of Nuclear Localization of Carbohydrate-response Element-binding Protein (ChREBP): ROLE OF AMP AS AN ALLOSTERIC INHIBITOR *. *J. Biol. Chem.* 291, 10515–10527. <https://doi.org/10.1074/jbc.M115.708982>
- Sawyer, T.K., Sanfilippo, P.J., Hruby, V.J., Engel, M.H., Heward, C.B., Burnett, J.B., Hadley, M.E., 1980. 4-Norleucine, 7-D-phenylalanine-alpha-melanocyte-stimulating hormone: a highly potent alpha-melanotropin with ultralong biological activity. *Proc. Natl. Acad. Sci. U. S. A.* 77, 5754–5758. <https://doi.org/10.1073/pnas.77.10.5754>
- Scheele, C., Nielsen, S., 2017. Metabolic regulation and the anti-obesity perspectives of human brown fat. *Redox Biol.* 12, 770–775. <https://doi.org/10.1016/j.redox.2017.04.011>
- Scheja, L., Heeren, J., 2016. Metabolic interplay between white, beige, brown adipocytes and the liver. *J. Hepatol.* 64, 1176–1186. <https://doi.org/10.1016/j.jhep.2016.01.025>
- Schiöth, H.B., 2001. The physiological role of melanocortin receptors. *Vitam. Horm.* 63, 195–232. [https://doi.org/10.1016/s0083-6729\(01\)63007-3](https://doi.org/10.1016/s0083-6729(01)63007-3)

- Schiöth, H.B., Phillips, S.R., Rudzish, R., Birch-Machin, M.A., Wikberg, J.E., Rees, J.L., 1999. Loss of function mutations of the human melanocortin 1 receptor are common and are associated with red hair. *Biochem. Biophys. Res. Commun.* 260, 488–491. <https://doi.org/10.1006/bbrc.1999.0935>
- Schoiswohl, G., Stefanovic-Racic, M., Menke, M.N., Wills, R.C., Surlow, B.A., Basantani, M.K., Sitnick, M.T., Cai, L., Yazbeck, C.F., Stolz, D.B., Pulinilkunnil, T., O'Doherty, R.M., Kershaw, E.E., 2015. Impact of Reduced ATGL-Mediated Adipocyte Lipolysis on Obesity-Associated Insulin Resistance and Inflammation in Male Mice. *Endocrinology* 156, 3610–3624. <https://doi.org/2020071612505236600>
- Schreiber, R., Xie, H., Schweiger, M., 2019. Of mice and men: The physiological role of adipose triglyceride lipase (ATGL). *Biochim. Biophys. Acta Mol. Cell Biol. Lipids* 1864, 880–899. <https://doi.org/10.1016/j.bbalip.2018.10.008>
- Schulze, R.J., Schott, M.B., Casey, C.A., Tuma, P.L., McNiven, M.A., 2019. The cell biology of the hepatocyte: A membrane trafficking machine. *J. Cell Biol.* 218, 2096–2112. <https://doi.org/10.1083/jcb.201903090>
- Schwarz, M., Russell, D.W., Dietschy, J.M., Turley, S.D., 2001. Alternate pathways of bile acid synthesis in the cholesterol 7 α -hydroxylase knockout mouse are not upregulated by either cholesterol or cholestyramine feeding. *J. Lipid Res.* 42, 1594–1603. [https://doi.org/10.1016/S0022-2275\(20\)32213-6](https://doi.org/10.1016/S0022-2275(20)32213-6)
- Schwarz, M., Russell, D.W., Dietschy, J.M., Turley, S.D., 1998. Marked reduction in bile acid synthesis in cholesterol 7 α -hydroxylase-deficient mice does not lead to diminished tissue cholesterol turnover or to hypercholesterolemia. *J. Lipid Res.* 39, 1833–1843. [https://doi.org/10.1016/S0022-2275\(20\)32171-4](https://doi.org/10.1016/S0022-2275(20)32171-4)
- Schweiger, M., Schoiswohl, G., Lass, A., Radner, F.P.W., Haemmerle, G., Malli, R., Graier, W., Cornaciu, I., Oberer, M., Salvayre, R., Fischer, J., Zechner, R., Zimmermann, R., 2008. The C-terminal region of human adipose triglyceride lipase affects enzyme activity and lipid droplet binding. *J. Biol. Chem.* 283, 17211–17220. <https://doi.org/10.1074/jbc.M710566200>
- Sekiya, M., Osuga, J., Okazaki, H., Yahagi, N., Harada, K., Shen, W.-J., Tamura, Y., Tomita, S., Iizuka, Y., Ohashi, K., Okazaki, M., Sata, M., Nagai, R., Fujita, T., Shimano, H., Kraemer, F.B., Yamada, N., Ishibashi, S., 2004. Absence of hormone-sensitive lipase inhibits obesity and adipogenesis in Lep ob/ob mice. *J. Biol. Chem.* 279, 15084–15090. <https://doi.org/10.1074/jbc.M310985200>
- Sela, I., Golan, G., Strajbl, M., Rivenzon-Segal, D., Bar-Haim, S., Bloch, I., Inbal, B., Shitrit, A., Ben-Zeev, E., Fichman, M., Markus, Y., Marantz, Y., Senderowitz, H., Kalid, O., 2010. G Protein Coupled Receptors - In Silico Drug Discovery and Design. *Curr. Top. Med. Chem.* 10, 638–656. <https://doi.org/10.2174/156802610791111498>
- Seyer, P., Vallois, D., Poiry-Yamate, C., Schütz, F., Metref, S., Tarussio, D., Maechler, P., Staels, B., Lanz, B., Grueter, R., Decaris, J., Turner, S., da Costa, A., Preitner, F., Minehira, K., Foretz, M., Thorens, B., 2013. Hepatic glucose sensing is required to preserve β cell glucose competence. *J. Clin. Invest.* 123, 1662–1676. <https://doi.org/10.1172/JCI65538>
- Shah, A.M., Wondisford, F.E., 2020. Tracking the carbons supplying gluconeogenesis. *J. Biol. Chem.* 295, 14419–14429. <https://doi.org/10.1074/jbc.REV120.012758>
- Shen, W., Wang, Z., Punyanita, M., Lei, J., Sinav, A., Kral, J.G., Imielinska, C., Ross, R., Heymsfield, S.B., 2003. Adipose Tissue Quantification by Imaging Methods: A Proposed Classification. *Obes. Res.* 11, 5–16. <https://doi.org/10.1038/oby.2003.3>
- Shi, L., Tu, B.P., 2015. Acetyl-CoA and the Regulation of Metabolism: Mechanisms and Consequences. *Curr. Opin. Cell Biol.* 33, 125. <https://doi.org/10.1016/j.ceb.2015.02.003>
- Shrivastava, S., Pucadyil, T.J., Paila, Y.D., Ganguly, S., Chattopadhyay, A., 2010. Chronic cholesterol depletion using statin impairs the function and dynamics of human serotonin(1A) receptors. *Biochemistry* 49, 5426–5435. <https://doi.org/10.1021/bi100276b>
- Simonen, P., Kotronen, A., Hallikainen, M., Sevastianova, K., Makkonen, J., Hakkarainen, A., Lundbom, N., Miettinen, T.A., Gylling, H., Yki-Järvinen, H., 2011. Cholesterol synthesis is

- increased and absorption decreased in non-alcoholic fatty liver disease independent of obesity. *J. Hepatol.* 54, 153–159. <https://doi.org/10.1016/J.JHEP.2010.05.037>
- Skinner, J.R., Shew, T.M., Schwartz, D.M., Tzekov, A., Lepus, C.M., Abumrad, N.A., Wolins, N.E., 2009. Diacylglycerol enrichment of endoplasmic reticulum or lipid droplets recruits perilipin 3/TIP47 during lipid storage and mobilization. *J. Biol. Chem.* 284, 30941–30948. <https://doi.org/10.1074/jbc.M109.013995>
- Skurk, T., Alberti-Huber, C., Herder, C., Hauner, H., 2007. Relationship between adipocyte size and adipokine expression and secretion. *J. Clin. Endocrinol. Metab.* 92, 1023–1033. <https://doi.org/10.1210/jc.2006-1055>
- Small, D.M., 1986. The physical chemistry of lipids. No Title.
- Smith, A.I., Funder, J.W., 1988. Proopiomelanocortin processing in the pituitary, central nervous system, and peripheral tissues. *Endocr. Rev.* 9, 159–179. <https://doi.org/10.1210/EDRV-9-1-159>
- Smith, B.K., Marcinko, K., Desjardins, E.M., Lally, J.S., Ford, R.J., Steinberg, G.R., 2016. Treatment of nonalcoholic fatty liver disease: role of AMPK. *Am. J. Physiol.-Endocrinol. Metab.* 311, E730–E740. <https://doi.org/10.1152/ajpendo.00225.2016>
- Smith, G.I., Shankaran, M., Yoshino, M., Schweitzer, G.G., Chondronikola, M., Beals, J.W., Okunade, A.L., Patterson, B.W., Nyangau, E., Field, T., Sirlin, C.B., Talukdar, S., Hellerstein, M.K., Klein, S., 2020. Insulin resistance drives hepatic de novo lipogenesis in nonalcoholic fatty liver disease. *J. Clin. Invest.* 130, 1453–1460. <https://doi.org/10.1172/JCI134165>
- Smith, S., Tsai, S.-C., 2007. The type I fatty acid and polyketide synthases: a tale of two megasynthases. *Nat. Prod. Rep.* 24, 1041–1072. <https://doi.org/10.1039/b603600g>
- Smith, S.R., Gawronska-Kozak, B., Janderová, L., Nguyen, T., Murrell, A., Stephens, J.M., Mynatt, R.L., 2003. Agouti Expression in Human Adipose Tissue: Functional Consequences and Increased Expression in Type 2 Diabetes. *Diabetes* 52, 2914–2922. <https://doi.org/10.2337/diabetes.52.12.2914>
- Solinas, G., Borén, J., Dulloo, A.G., 2015. De novo lipogenesis in metabolic homeostasis: More friend than foe? *Mol. Metab.* 4, 367–377. <https://doi.org/10.1016/j.molmet.2015.03.004>
- Somers, T., Siddiqi, S., Morshuis, W.J., Russel, F.G.M., Schirris, T.J.J., 2023. Statins and Cardiomyocyte Metabolism, Friend or Foe? *J. Cardiovasc. Dev. Dis.* 10, 417. <https://doi.org/10.3390/jcdd10100417>
- Spana, C., Taylor, A.W., Yee, D.G., Makhlina, M., Yang, W., Dodd, J., 2019. Probing the Role of Melanocortin Type 1 Receptor Agonists in Diverse Immunological Diseases. *Front. Pharmacol.* 9. <https://doi.org/10.3389/fphar.2018.01535>
- Spaulding, H.R., Yan, Z., 2022. AMPK and the Adaptation to Exercise. *Annu. Rev. Physiol.* 84, 209–227. <https://doi.org/10.1146/annurev-physiol-060721-095517>
- Stagg, D.B., Gillingham, J.R., Nelson, A.B., Lengfeld, J.E., d’Avignon, D.A., Puchalska, P., Crawford, P.A., 2021. Diminished ketone interconversion, hepatic TCA cycle flux, and glucose production in D-β-hydroxybutyrate dehydrogenase hepatocyte-deficient mice. *Mol. Metab.* 53, 101269. <https://doi.org/10.1016/j.molmet.2021.101269>
- Star, R.A., Rajora, N., Huang, J., Stock, R.C., Catania, A., Lipton, J.M., 1995. Evidence of autocrine modulation of macrophage nitric oxide synthase by alpha-melanocyte-stimulating hormone. *Proc. Natl. Acad. Sci. U. S. A.* 92, 8016–8020. <https://doi.org/10.1073/PNAS.92.17.8016>
- Ste Marie, L., Miura, G.I., Marsh, D.J., Yagaloff, K., Palmiter, R.D., 2000. A metabolic defect promotes obesity in mice lacking melanocortin-4 receptors. *Proc. Natl. Acad. Sci. U. S. A.* 97, 12339–12344. <https://doi.org/10.1073/pnas.220409497>
- Steinberg, G.R., Kemp, B.E., 2009. AMPK in Health and Disease. *Physiol. Rev.* 89, 1025–1078. <https://doi.org/10.1152/PHYSREV.00011.2008>
- Subramaniam, S., Henderson, R., 1999. Electron crystallography of bacteriorhodopsin with millisecond time resolution. *J. Struct. Biol.* 128, 19–25. <https://doi.org/10.1006/jsbi.1999.4178>
- Sumida, Y., Yoneda, M., 2018. Current and future pharmacological therapies for NAFLD/NASH. *J. Gastroenterol.* 53, 362–376. <https://doi.org/10.1007/s00535-017-1415-1>

- Svensson, R.U., Parker, S.J., Eichner, L.J., Kolar, M.J., Wallace, M., Brun, S.N., Lombardo, P.S., Van Nostrand, J.L., Hutchins, A., Vera, L., Gerken, L., Greenwood, J., Bhat, S., Harriman, G., Westlin, W.F., Harwood, H.J., Saghatelian, A., Kapeller, R., Metallo, C.M., Shaw, R.J., 2016. Inhibition of acetyl-CoA carboxylase suppresses fatty acid synthesis and tumor growth of non-small-cell lung cancer in preclinical models. *Nat. Med.* 22, 1108–1119. <https://doi.org/10.1038/nm.4181>
- Swope, V., Alexander, C., Starner, R., Schwemberger, S., Babcock, G., Abdel-Malek, Z.A., 2014. Significance of the melanocortin 1 receptor in the DNA damage response of human melanocytes to ultraviolet radiation. *Pigment Cell Melanoma Res.* 27, 601–610. <https://doi.org/10.1111/pcmr.12252>
- Takeo, M., Lee, W., Rabbani, P., Sun, Q., Hu, H., Lim, C.H., Manga, P., Ito, M., 2016. EdnrB Governs Regenerative Response of Melanocyte Stem Cells by Crosstalk with Wnt Signaling. *Cell Rep.* 15, 1291–1302. <https://doi.org/10.1016/J.CELREP.2016.04.006>
- Tall, A.R., Yvan-Charvet, L., 2015. Cholesterol, inflammation and innate immunity. *Nat. Rev. Immunol.* 15, 104–116. <https://doi.org/10.1038/nri3793>
- Tandra, S., Yeh, M.M., Brunt, E.M., Vuppalanchi, R., Cummings, O.W., Ünalp-Arida, A., Wilson, L.A., Chalasani, N., 2011. Presence and significance of microvesicular steatosis in nonalcoholic fatty liver disease. *J. Hepatol.* 55, 654–659. <https://doi.org/10.1016/j.jhep.2010.11.021>
- Tao, Y.-X., 2017. Melanocortin receptors. *Biochim. Biophys. Acta Mol. Basis Dis.* 1863, 2411–2413. <https://doi.org/10.1016/j.bbadis.2017.08.001>
- Targher, G., Byrne, C.D., Tilg, H., 2024. MASLD: a systemic metabolic disorder with cardiovascular and malignant complications. *Gut* 73, 691–702. <https://doi.org/10.1136/gutjnl-2023-330595>
- Tatro, J.B., 1996. Receptor biology of the melanocortins, a family of neuroimmunomodulatory peptides. *Neuroimmunomodulation* 3, 259–284. <https://doi.org/10.1159/000097281>
- Teratani, T., Tomita, K., Suzuki, T., Oshikawa, T., Yokoyama, H., Shimamura, K., Tominaga, S., Hiroi, S., Irie, R., Okada, Y., Kurihara, C., Ebinuma, H., Saito, H., Hokari, R., Sugiyama, K., Kanai, T., Miura, S., Hibi, T., 2012. A High-Cholesterol Diet Exacerbates Liver Fibrosis in Mice via Accumulation of Free Cholesterol in Hepatic Stellate Cells. *Gastroenterology* 142, 152-164.e10. <https://doi.org/10.1053/j.gastro.2011.09.049>
- Than, N.N., Newsome, P.N., 2015. A concise review of non-alcoholic fatty liver disease. *Atherosclerosis*. <https://doi.org/10.1016/J.ATHEROSCLEROSIS.2015.01.001>
- Thompson, B.R., Lobo, S., Bernlohr, D.A., 2010. Fatty acid flux in adipocytes: the in's and out's of fat cell lipid trafficking. *Mol. Cell. Endocrinol.* 318, 24–33. <https://doi.org/10.1016/j.mce.2009.08.015>
- Tilg, H., Adolph, T.E., Moschen, A.R., 2021. Multiple Parallel Hits Hypothesis in Nonalcoholic Fatty Liver Disease: Revisited After a Decade. *Hepatol. Baltim. Md* 73, 833–842. <https://doi.org/10.1002/hep.31518>
- Tong, D., Schiattarella, G.G., Jiang, N., Daou, D., Luo, Y., Link, M.S., Lavandro, S., Gillette, T.G., Hill, J.A., 2022. Impaired AMP-Activated Protein Kinase Signaling in Heart Failure With Preserved Ejection Fraction-Associated Atrial Fibrillation. *Circulation* 146, 73–76. <https://doi.org/10.1161/CIRCULATIONAHA.121.058301>
- Trefts, E., Gannon, M., Wasserman, D.H., 2017. The liver. *Curr. Biol.* CB 27, R1147–R1151. <https://doi.org/10.1016/j.cub.2017.09.019>
- Trevaskis, J.L., Gawronska-Kozak, B., Sutton, G.M., McNeil, M., Stephens, J.M., Smith, S.R., Butler, A.A., 2007. Role of adiponectin and inflammation in insulin resistance of Mc3r and Mc4r knockout mice. *Obes. Silver Spring Md* 15, 2664–2672. <https://doi.org/10.1038/oby.2007.318>
- Tripathy, D., Mohanty, P., Dhindsa, S., Syed, T., Ghanim, H., Aljada, A., Dandona, P., 2003. Elevation of free fatty acids induces inflammation and impairs vascular reactivity in healthy subjects. *Diabetes* 52, 2882–2887. <https://doi.org/10.2337/diabetes.52.12.2882>
- Umekawa, T., Yoshida, T., Sakane, N., Kogure, A., Kondo, M., Honjyo, H., 1999. Trp64Arg mutation of beta3-adrenoceptor gene deteriorates lipolysis induced by beta3-adrenoceptor agonist in human omental adipocytes. *Diabetes* 48, 117–120. <https://doi.org/10.2337/diabetes.48.1.117>

- Uyeda, K., Repa, J.J., 2006. Carbohydrate response element binding protein, ChREBP, a transcription factor coupling hepatic glucose utilization and lipid synthesis. *Cell Metab.* 4, 107–110. <https://doi.org/10.1016/j.cmet.2006.06.008>
- Valverde, P., Healy, E., Jackson, I., Rees, J.L., Thody, A.J., 1995. Variants of the melanocyte-stimulating hormone receptor gene are associated with red hair and fair skin in humans. *Nat. Genet.* 11, 328–330. <https://doi.org/10.1038/ng1195-328>
- Vernia, S., Cavanagh-Kyros, J., Garcia-Haro, L., Sabio, G., Barrett, T., Jung, D.Y., Kim, J.K., Xu, J., Shulha, H.P., Garber, M., Gao, G., Davis, R.J., 2014. The PPAR α -FGF21 hormone axis contributes to metabolic regulation by the hepatic JNK signaling pathway. *Cell Metab.* 20, 512–525. <https://doi.org/10.1016/J.CMET.2014.06.010>
- Vidal-Cevallos, P., Chávez-Tapia, N., 2024. Resmetirom, the long-awaited first treatment for metabolic dysfunction-associated steatohepatitis and liver fibrosis? *Med N. Y. N* 5, 375–376. <https://doi.org/10.1016/j.medj.2024.03.013>
- Virador, V.M., Muller, J., Wu, X., Abdel-Malek, Z.A., Yu, Z.-X., Ferrans, V.J., Kobayashi, N., Wakamatsu, K., Ito, S., Hammer, J.A., Hearing, V.J., 2002. Influence of alpha-melanocyte-stimulating hormone and ultraviolet radiation on the transfer of melanosomes to keratinocytes. *FASEB J. Off. Publ. Fed. Am. Soc. Exp. Biol.* 16, 105–107. <https://doi.org/10.1096/fj.01-0518fje>
- Virtanen, K.A., Lidell, M.E., Orava, J., Heglind, M., Westergren, R., Niemi, T., Taittonen, M., Laine, J., Savisto, N.-J., Enerbäck, S., Nuutila, P., 2009. Functional brown adipose tissue in healthy adults. *N. Engl. J. Med.* 360, 1518–1525. <https://doi.org/10.1056/NEJMoa0808949>
- Virtue, S., Vidal-Puig, A., 2010. Adipose tissue expandability, lipotoxicity and the Metabolic Syndrome — An allostatic perspective. *Biochim. Biophys. Acta BBA - Mol. Cell Biol. Lipids, Lipotoxicity* 1801, 338–349. <https://doi.org/10.1016/j.bbalip.2009.12.006>
- Wakil, S.J., Abu-Elheiga, L.A., 2009. Fatty acid metabolism: target for metabolic syndrome. *J. Lipid Res.* 50 Suppl, S138-143. <https://doi.org/10.1194/jlr.R800079-JLR200>
- Waller-Evans, H., Hue, C., Fearnside, J., Rothwell, A.R., Lockstone, H.E., Caldérari, S., Wilder, S.P., Cazier, J.-B., Scott, J., Gauguier, D., 2013. Nutrigenomics of High Fat Diet Induced Obesity in Mice Suggests Relationships between Susceptibility to Fatty Liver Disease and the Proteasome. *PLoS ONE* 8, e82825. <https://doi.org/10.1371/journal.pone.0082825>
- Wallingford, N., Perroud, B., Gao, Q., Coppola, A., Gyengesi, E., Liu, Z.-W., Gao, X.-B., Diament, A., Haus, K.A., Shariat-Madar, Z., Mahdi, F., Wardlaw, S.L., Schmaier, A.H., Warden, C.H., Diano, S., 2009. Prolylcarboxypeptidase regulates food intake by inactivating α -MSH in rodents. *J. Clin. Invest.* 119, 2291. <https://doi.org/10.1172/JCI37209>
- Wang, W., Guo, D.-Y., Lin, Y.-J., Tao, Y.-X., 2019. Melanocortin Regulation of Inflammation. *Front. Endocrinol.* 10, 683. <https://doi.org/10.3389/fendo.2019.00683>
- Wang, X., Rao, H., Liu, F., Wei, L., Li, H., Wu, C., 2021. Recent Advances in Adipose Tissue Dysfunction and Its Role in the Pathogenesis of Non-Alcoholic Fatty Liver Disease. *Cells* 10, 3300. <https://doi.org/10.3390/cells10123300>
- Wang, Y., Viscarra, J., Kim, S.-J., Sul, H.S., 2015. Transcriptional Regulation of Hepatic Lipogenesis. *Nat. Rev. Mol. Cell Biol.* 16, 678–689. <https://doi.org/10.1038/nrm4074>
- Wardlaw, S.L., 2011. Hypothalamic proopiomelanocortin processing and the regulation of energy balance. *Eur. J. Pharmacol.* 660, 213–219. <https://doi.org/10.1016/j.ejphar.2010.10.107>
- Westerterp-Plantenga, M.S., Lejeune, M.P.G.M., Kovacs, E.M.R., 2005. Body Weight Loss and Weight Maintenance in Relation to Habitual Caffeine Intake and Green Tea Supplementation. *Obes. Res.* 13, 1195–1204. <https://doi.org/10.1038/oby.2005.142>
- Wilkins, T., Tadkod, A., Hepburn, I., Schade, R.R., 2013. Nonalcoholic Fatty Liver Disease: Diagnosis and Management. *Am. Fam. Physician* 88, 35–42.
- Wolf Horrell, E.M., Boulanger, M.C., D’Orazio, J.A., 2016. Melanocortin 1 Receptor: Structure, Function, and Regulation. *Front. Genet.* 7, 95. <https://doi.org/10.3389/fgene.2016.00095>
- Wu, J., Cotliar, R., 2021. Afamelanotide: An Orphan Drug with Potential for Broad Dermatologic Applications. *J. Drugs Dermatol. JDD* 20, 290–294. <https://doi.org/10.36849/JDD.5526>

- Wu, J.W., Wang, S.P., Alvarez, F., Casavant, S., Gauthier, N., Abed, L., Soni, K.G., Yang, G., Mitchell, G.A., 2011. Deficiency of liver adipose triglyceride lipase in mice causes progressive hepatic steatosis. *Hepatology* 54, 122–132. <https://doi.org/10.1002/hep.24338>
- Xia, Y., Wikberg, J.E., Chhajlani, V., 1995. Expression of melanocortin 1 receptor in periaqueductal gray matter. *Neuroreport* 6, 2193–2196. <https://doi.org/10.1097/00001756-199511000-00022>
- Xiong, Y., Lei, Q.-Y., Zhao, S., Guan, K.-L., 2011. Regulation of Glycolysis and Gluconeogenesis by Acetylation of PKM and PEPCK. *Cold Spring Harb. Symp. Quant. Biol.* 76, 285–289. <https://doi.org/10.1101/sqb.2011.76.010942>
- Xu, S., Zou, F., Diao, Z., Zhang, S., Deng, Y., Zhu, X., Cui, L., Yu, J., Zhang, Z., Bamigbade, A.T., Zhang, H., Wei, X., Zhang, X., Liang, B., Liu, P., 2019. Perilipin 2 and lipid droplets provide reciprocal stabilization. *Biophys. Rep.* 5, 145–160. <https://doi.org/10.1007/s41048-019-0091-5>
- Xu, Y., Guan, X., Zhou, R., Gong, R., 2020. Melanocortin 5 receptor signaling pathway in health and disease. *Cell. Mol. Life Sci.* 77, 3831–3840. <https://doi.org/10.1007/s00018-020-03511-0>
- Yang, A., Mottillo, E.P., 2020. Adipocyte Lipolysis: from molecular mechanisms of regulation to disease and therapeutics. *Biochem. J.* 477, 985–1008. <https://doi.org/10.1042/BCJ20190468>
- Yang, Y., 2011. Structure, function and regulation of the melanocortin receptors. *Eur. J. Pharmacol.* 660, 125–130. <https://doi.org/10.1016/j.ejphar.2010.12.020>
- Yanik, T., Durhan, S.T., 2023. Specific Functions of Melanocortin 3 Receptor (MC3R). *J. Clin. Res. Pediatr. Endocrinol.* 15, 1–6. <https://doi.org/10.4274/jcrpe.galenos.2022.2022-5-21>
- Yokoyama, C., Wang, X., Briggs, M.R., Admon, A., Wu, J., Hua, X., Goldstein, J.L., Brown, M.S., 1993. SREBP-1, a basic-helix-loop-helix-leucine zipper protein that controls transcription of the low density lipoprotein receptor gene. *Cell* 75, 187–197. [https://doi.org/10.1016/S0092-8674\(05\)80095-9](https://doi.org/10.1016/S0092-8674(05)80095-9)
- Younossi, Z., Anstee, Q.M., Marietti, M., Hardy, T., Henry, L., Eslam, M., George, J., Bugianesi, E., 2018. Global burden of NAFLD and NASH: trends, predictions, risk factors and prevention. *Nat. Rev. Gastroenterol. Hepatol.* 15, 11–20. <https://doi.org/10.1038/nrgastro.2017.109>
- Younossi, Z.M., Henry, L., 2024. Understanding the Burden of Nonalcoholic Fatty Liver Disease: Time for Action. *Diabetes Spectr.* 37, 9–19. <https://doi.org/10.2337/ds123-0010>
- Younossi, Z.M., Stepanova, M., Rafiq, N., Makhlof, H., Younoszai, Z., Agrawal, R., Goodman, Z., 2011. Pathologic criteria for nonalcoholic steatohepatitis: Interprotocol agreement and ability to predict liver-related mortality. *Hepatology* 53, 1874–1882. <https://doi.org/10.1002/hep.24268>
- Yu, J., Marsh, S., Hu, J., Feng, W., Wu, C., 2016. The Pathogenesis of Nonalcoholic Fatty Liver Disease: Interplay between Diet, Gut Microbiota, and Genetic Background. *Gastroenterol. Res. Pract.* 2016, 2862173. <https://doi.org/10.1155/2016/2862173>
- Yu, L., Li, Y., Grisé, A., Wang, H., 2020. CGI-58: Versatile Regulator of Intracellular Lipid Droplet Homeostasis. *Adv. Exp. Med. Biol.* 1276, 197–222. https://doi.org/10.1007/978-981-15-6082-8_13
- Yu, S., Doycheva, D.M., Gamdzyk, M., Yang, Y., Lenahan, C., Li, G., Li, D., Lian, L., Tang, J., Lu, J., Zhang, J.H., 2021. Activation of MC1R with BMS-470539 attenuates neuroinflammation via cAMP/PKA/Nurr1 pathway after neonatal hypoxic-ischemic brain injury in rats. *J. Neuroinflammation* 18, 26. <https://doi.org/10.1186/s12974-021-02078-2>
- Yuan, M., Konstantopoulos, N., Lee, J., Hansen, L., Li, Z.-W., Karin, M., Shoelson, S.E., 2001. Reversal of Obesity- and Diet-Induced Insulin Resistance with Salicylates or Targeted Disruption of Ikk β . *Science* 293, 1673–1677. <https://doi.org/10.1126/science.1061620>
- Yuan, X.-C., Tao, Y.-X., 2022. Ligands for Melanocortin Receptors: Beyond Melanocyte-Stimulating Hormones and Adrenocorticotropin. *Biomolecules* 12, 1407. <https://doi.org/10.3390/biom12101407>
- Zhang, X., Song, Y., Feng, M., Zhou, X., Lu, Y., Gao, L., Yu, C., Jiang, X., Zhao, J., 2015. Thyroid-stimulating hormone decreases HMG-CoA reductase phosphorylation via AMP-activated protein kinase in the liver. *J. Lipid Res.* 56, 963–971. <https://doi.org/10.1194/jlr.M047654>

- Zhang, Y., Kilroy, G.E., Henagan, T.M., Prpic-Uhing, V., Richards, W.G., Bannon, A.W., Mynatt, R.L., Gettys, T.W., 2005. Targeted deletion of melanocortin receptor subtypes 3 and 4, but not CART, alters nutrient partitioning and compromises behavioral and metabolic responses to leptin. *FASEB J. Off. Publ. Fed. Am. Soc. Exp. Biol.* 19, 1482–1491. <https://doi.org/10.1096/fj.05-3851com>
- Zhong, S., Chèvre, R., Mayan, D.C., Corliano, M., Cochran, B.J., Sem, K.P., Dijk, T.H. van, Peng, J., Tan, L.J., Hartimath, S.V., Ramasamy, B., Cheng, P., Groen, A.K., Kuipers, F., Goggi, J.L., Drum, C., Dam, R.M. van, Tan, R.S., Rye, K.-A., Hayden, M.R., Cheng, C.-Y., Chacko, S., Flannick, J., Sim, X., Tan, H.C., Singaraja, R.R., 2022. Haploinsufficiency of *CYP8B1* associates with increased insulin sensitivity in humans. *J. Clin. Invest.* 132. <https://doi.org/10.1172/JCI1152961>
- Zhou, M., Zhao, X., Huang, T., Zou, G., Hu, R.-H., Cheng, M., 2021. PFKFB3 Promotes Liver Fibrosis by Regulating Aerobic Glycolysis of Hepatic Stellate Cells. *Hepat. Mon.* 21. <https://doi.org/10.5812/hepatmon.113968>
- Zhou, S.L., Gordon, R.E., Bradbury, M., Stump, D., Kiang, C.L., Berk, P.D., 1998. Ethanol up-regulates fatty acid uptake and plasma membrane expression and export of mitochondrial aspartate aminotransferase in HepG2 cells. *Hepatology. Baltim. Md* 27, 1064–1074. <https://doi.org/10.1002/hep.510270423>
- Zhou, Y., Cai, M., 2017. Novel approaches to the design of bioavailable melanotropins. *Expert Opin. Drug Discov.* 12, 1023–1030. <https://doi.org/10.1080/17460441.2017.1351940>
- Zhou, Z., Xu, M.-J., Gao, B., 2016. Hepatocytes: a key cell type for innate immunity. *Cell. Mol. Immunol.* 13, 301–315. <https://doi.org/10.1038/cmi.2015.97>
- Zhu, Z., Zhang, X., Pan, Q., Zhang, L., Chai, J., 2023. In-depth analysis of *de novo* lipogenesis in non-alcoholic fatty liver disease: Mechanism and pharmacological interventions. *Liver Res.* 7, 285–295. <https://doi.org/10.1016/j.livres.2023.11.003>
- Zollner, G., Marschall, H.-U., Wagner, M., Trauner, M., 2006. Role of nuclear receptors in the adaptive response to bile acids and cholestasis: pathogenetic and therapeutic considerations. *Mol. Pharm.* 3, 231–251. <https://doi.org/10.1021/mp060010s>

Appendices

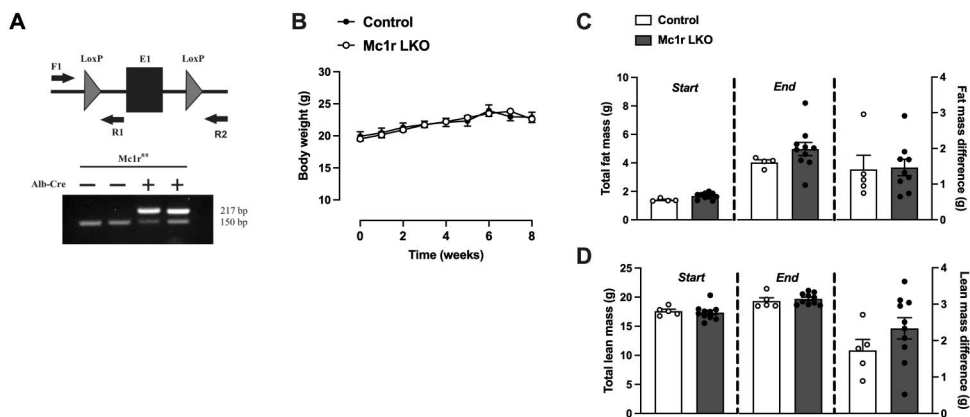


Figure 1. Hepatocyte-specific melanocortin 1 receptor (MC1R) deficiency does not impact body weight or composition in chow diet-fed mice. (A) Schematic representation of the loxP-flanked (floxed) *Mc1r* allele, with the positions of forward and reverse primers used for PCR genotyping. PCR analysis of DNA samples extracted from the liver of Alb-Cre-negative and -positive mice with homozygous for the *Mc1r* floxed allele (*Mc1r^{fl/fl}*) confirmed recombination, with the recombined allele size being approximately 217 bp. (B) Weekly body weight gain curves for chow-fed control and *Mc1r* LKO mice. (C and D) Total fat and lean mass, as well as the difference between fat and lean mass, measured at the start and end of the experimental period in chow-fed control and *Mc1r* LKO mice. The values are presented as mean \pm SEM, $n=5-10$ mice per group. *Mc1r* LKO: hepatocyte-specific MC1R knock-out mice.

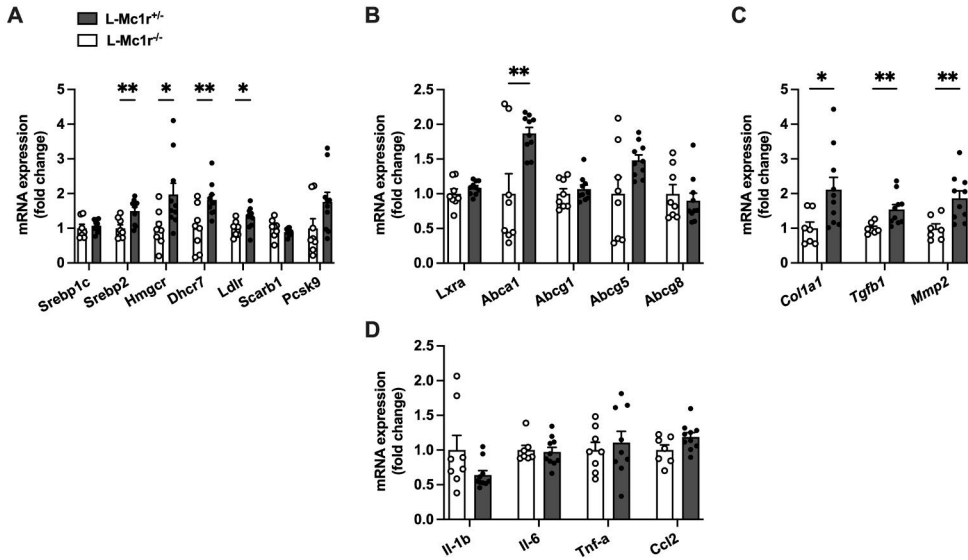


Figure 2. Hepatocyte-specific melanocortin 1 receptor (MC1R) deficiency alters the expression of markers related to cholesterol synthesis and fibrosis. Quantitative real-time polymerase chain reaction (qPCR) analysis was conducted on genes involved in cholesterol synthesis (**A**), transport (**B**), fibrosis (**C**), and pro-inflammatory processes (**D**) in the liver of chow-fed control and Mc1r LKO mice. The values are presented as mean \pm SEM, n=7–10 mice per group. *p<0.05 and **p<0.01 versus control mice by Student’s t-test. Key genes include *Srebp1c* (sterol regulatory element-binding protein 1), *Srebp2* (sterol regulatory element-binding protein 2), *Hmgcr* (3-hydroxy-3-methylglutaryl-CoA reductase), *Dhcr7* (7-dehydrocholesterol reductase), *Ldlr* (low-density lipoprotein receptor), *Scarb1* (scavenger receptor class B member 1), *Pcsk9* (proprotein convertase subtilisin/kexin type 9), and several ATP-binding cassette (ABC) transporters (*ABCA1*, *ABCG1*, *ABCG5*, *ABCG8*), along with fibrosis markers such as *Col1a1* (collagen type I alpha 1), *Tgf- β 1* (transforming growth factor beta-1), *Mmp2* (matrix metalloproteinase 2), and pro-inflammatory cytokines (*Il-1 β* , *Il-6*, *Tnf-a*, *Ccl2*).

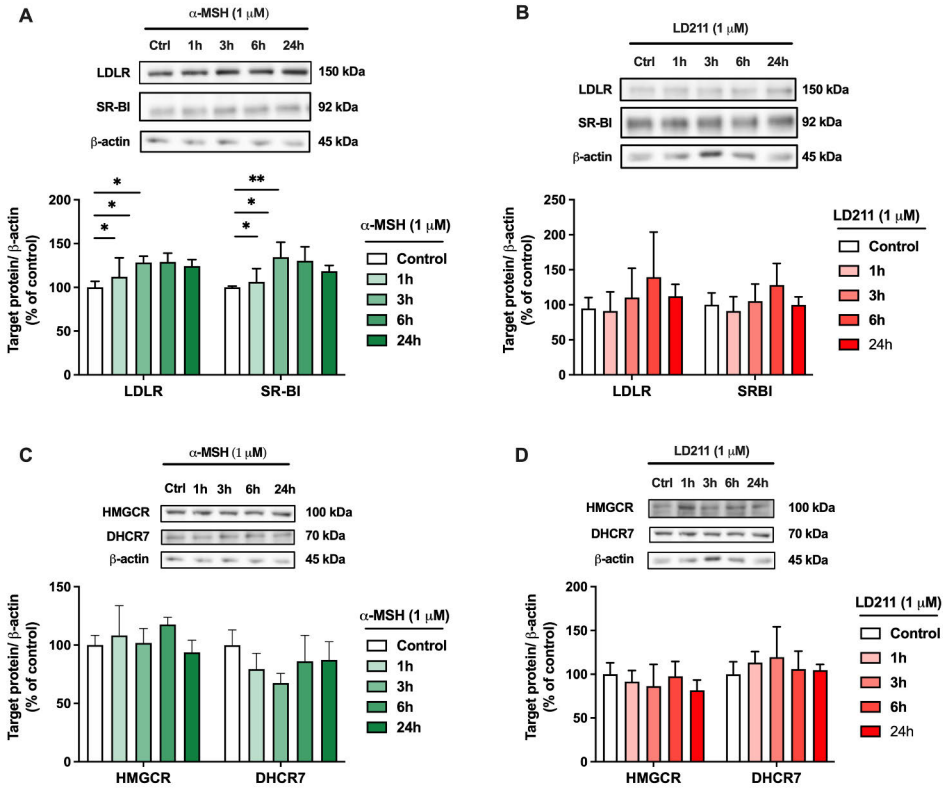


Figure 3. Agonists stimulated effects of melanocortin 1 receptor (MC1R) in protein expression in HepG2 cells. (A and B) Representative Western blots and quantification of LDLR and SRBI protein levels in HepG2 cells treated with 1 μ M α -MSH and LD211 for 1, 3, 6, or 24 hr. (C and D) HMGCR and DHCR7 proteins levels in HepG2 cells treated with 1 μ M α -MSH and LD211 for 1, 3, 6, or 24 hr. The values are mean \pm SEM, n=3–6 per group in each graph. * p <0.05 and ** p <0.01 for the indicated comparisons by one-way ANOVA and Bonferroni *post hoc* tests.

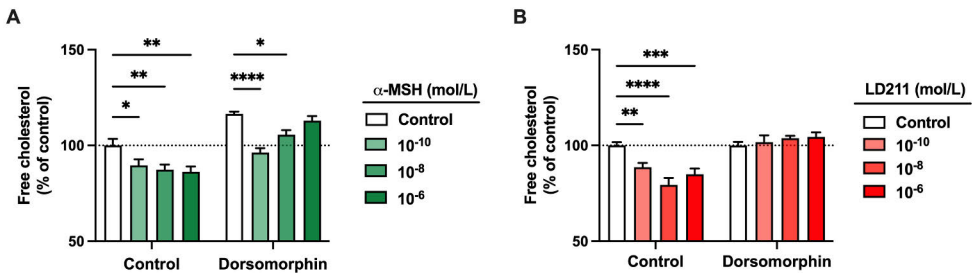


Figure 4. Melanocortin 1 receptor (MC1R) agonists reduce cholesterol content in the HepG2 cells. (A and B) Quantification of free cholesterol content was performed using filipin staining in HepG2 cells treated with α -MSH and LD211 (0.1 nM, 10 nM, or 1 μ M) with or without AMP-activated protein kinase (AMPK) inhibitor dorsomorphin (1 μ M) for 2h hr. The values are presented as mean \pm SEM, n=3–6 per group. * p <0.05, ** p <0.01, *** p <0.001, and **** p <0.0001 indicate statistical significance in comparisons made using one-way ANOVA and Bonferroni *post hoc* tests.

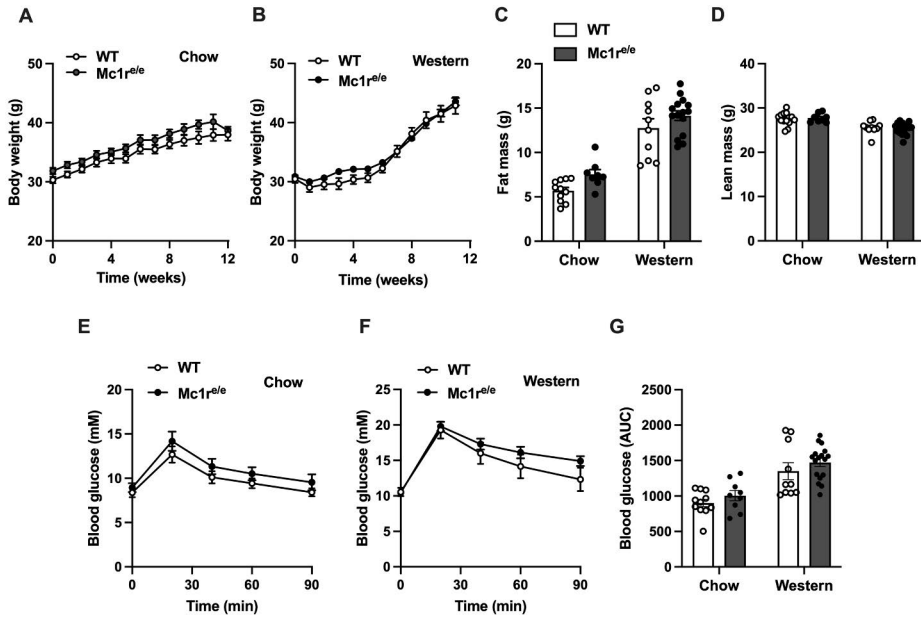


Figure 5. Global melanocortin 1 receptor (MC1R) deficiency does not impact body weight, body composition or glucose handling capacity in *Mc1r^{e/e}* mice on chow- and Western diets. (A and B) Body weight gain curves in chow- and Western diet-fed wild type (WT) and *Mc1r^{e/e}* mice. (C and D) Quantification of fat and lean mass using quantitative NMR scanning of whole-body composition in chow- and Western diet-fed WT and *Mc1r^{e/e}* mice. (E and F) Glucose tolerance test (GTT) performed at the end of a 12-week diet intervention in chow- and Western diet-fed WT and *Mc1r^{e/e}* mice. (G) Area under the blood glucose curves. The values are presented as mean \pm SEM, n = 9-17 mice.

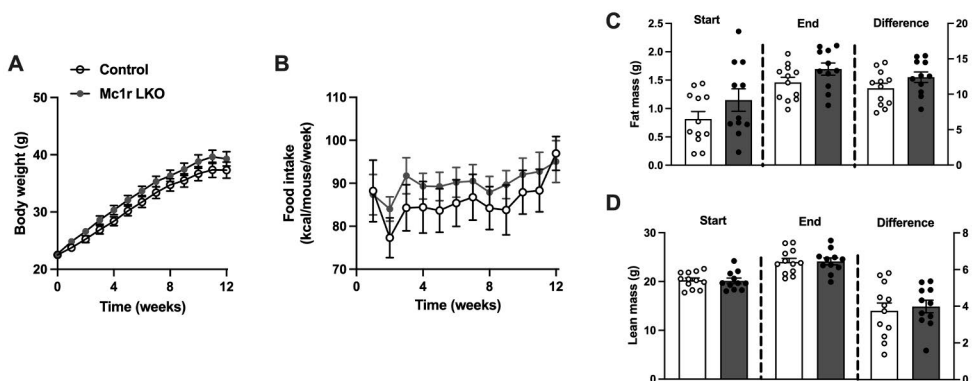


Figure 6. Hepatocyte-specific MC1R deficiency does not impact body weight gain, body composition, or food intake in Western diet-fed mice. (A and B) Body weight gain curves and food intake (g/week) in Western diet-fed control and *Mc1r* LKO mice. (C and D) Total fat and lean mass, as well as the difference between fat and lean mass, at the start and end of a 12-week diet intervention in control and *Mc1r* LKO mice. The values are presented as mean \pm SEM, n=10-12 mice per group.

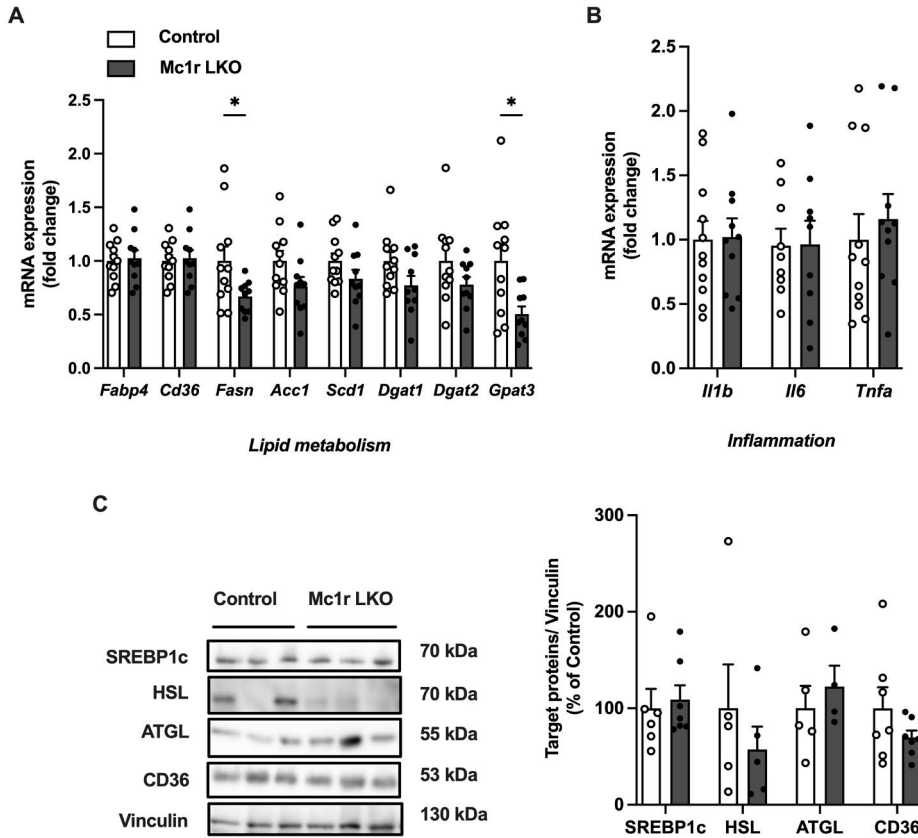


Figure 7. Hepatocyte-specific melanocortin 1 receptor (MC1R) deficiency does not impact lipid metabolism or inflammation in the gWAT of Mc1r LKO mice. (A) Quantitative real-time-polymerase chain reaction (qPCR) analysis of genes involved in lipid metabolism and (B) inflammation in the gWAT samples of Western diet-fed control and Mc1r LKO mice. (C) Representative Western blots and quantifications of SREBP1c, HSL, ATGL, CD36, and vinculin (loading control) protein levels in gWAT samples from Western diet-fed control and Mc1r LKO mice. The values are presented as mean \pm SEM, n = 10-15 mice per group. *p<0.05 for the indicated comparisons by unpaired two-tailed Student's t-test.

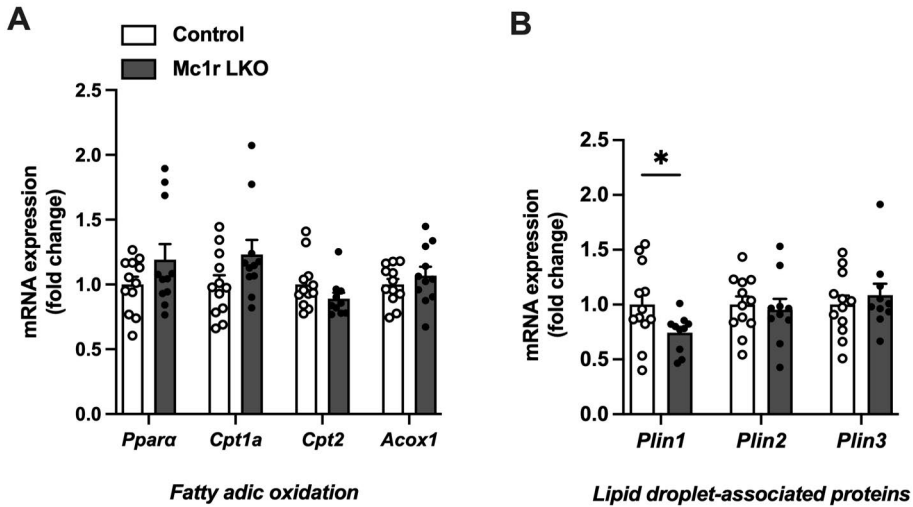


Figure 8. Hepatocyte-specific MC1R deficiency does not affect the expression of fatty acid oxidation (FAO) markers in the liver. (A) Quantitative real-time-polymerase chain reaction (qPCR) analysis of genes involved in FAO and **(B)** Lipid droplet-associated (LDs) proteins. The values are presented as mean \pm SEM, n = 10-15 mice per group. * $p < 0.05$ indicates statistically significant difference compared to control mice. Mc1r LKO: hepatocyte-specific MC1R knock-out mice. Key genes include *Ppara* (peroxisome proliferator-activated receptor), *Cpt1a* (carnitine O-palmitoyltransferase 1), *Acox1* (peroxisomal acyl-coenzyme A oxidase 1), *Plin1* (perilipin-1), *Plin2* (perilipin-2), and *Plin3* (perilipin-3).

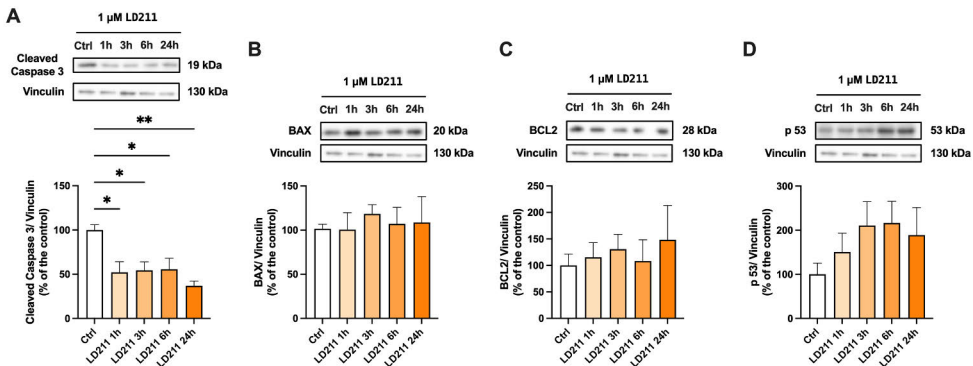


Figure 9. The effects of pharmacological activation of melanocortin 1 receptor (MC1R) with LD211 on protein expression levels in primary mouse hepatocytes. (A-D) Representative Western blots and quantification of Caspase 3, BAX, BCL2 and p53 protein levels in primary mouse hepatocytes treated with 1 μ M LD211 for different time points (1, 3, 6 and 24 hr). The values are presented as mean \pm SEM, n=3-6 per group. * $p < 0.05$ and ** $p < 0.01$ for the indicated comparisons by one-way ANOVA and Bonferroni post hoc tests."

Table 1. Calorie density of the Western diet (D12079B).

Product # D12079B	g%	kcal%
Protein	20	17
Carbohydrate	50	43
Fat	21	41
Total		100
kcal/g	4,7	
Ingredient	g	kcal
Casein, 80 Mesh	195	780
DL-Methionine	3	12
Corn Starch	50	200
Maltodextrin 10	100	400
Sucrose	341	1364
Cellulose	50	0
Milk Fat, Anhydrous *	200	1800
Corn Oil	10	90
Mineral Mix S10001	35	0
Calcium Carbonate	4	0
Vitamin Mix V1001	10	40
Choline Bitartrate	2	0
Cholesterol, USP*	1,5	0
Ethoxyquin	0,04	0
Total	1001,54	4686

*Anhydrous milk fat typically contains approximately 0.3% cholesterol. On this basis, D12079B contains approximately 0.21% cholesterol.



**TURUN
YLIOPISTO**
UNIVERSITY
OF TURKU

ISBN 978-951-29-9963-7 (PRINT)
ISBN 978-951-29-9964-4 (PDF)
ISSN 0355-9483 (Print)
ISSN 2343-3213 (Online)

